PYRUVATE CARBOXYLASE

A STRUCTURE AND FUNCTION STUDY USING MONOCLONAL ANTIBODIES AND MUTAGENESIS

By

Teerakul Arpornsuwan, B. Sc., M. Sc. (Biotech, Chulalongkorn)

A thesis submitted to the

University of Adelaide, South Australia

For the degree of Doctor of Philosophy

June, 2003

School of Molecular and Biomedical Science,

Discipline of Biochemistry,

University of Adelaide,

South Australia

TABLE OF CONTENTS

SUMMARY

Pyruvate carboxylase (PC)[EC 6.4.1.1] is a member of the biotin dependent family of enzymes found widely throughout nature. The comparison of primary structures has shown that PC from different species contains three functional domains ie. the biotin carboxylation domain (N-terminal region), the transcarboxylation domain (central region) and the biotin carboxyl carrier domain (C-terminal region). Because of its importance in the intermediary metabolism of both prokaryotes and eukaryotes, PC has been of particular interest to our research laboratory with respect to its reaction mechanism, its subunit structure, the relationship between its structure and activity, and the regulation of its catalytic activity.

I have investigated the structure and function of recombinantly expressed human pyruvate carboxylase (hPC) by epitope mapping, using three monoclonal antibodies raised against sheep PC (mAb6, 12 and 42) which display strong inhibitory effects towards the catalytic activity of hPC (91%, 89% and 90% inhibition) as do they similarly affect sheep PC activity (96%, 96% and 91% inhibition).

Using thioredoxin fusion protein technology, several hPC fragments were constructed and expressed in *E. coli* BL21. Six overlapping fusion proteins of hPC, viz BC (residues 1-488), F1 (residues 475-718), F2 (residues 711-954), F3 (residues 947-1178), TB1 (residues 947-1077) and TB2 (residues 1048-1178) covering the complete hPC sequence, were constructed using PCR and introduced into the pET32a (+) expression vector. Each fusion construct was expressed in *E. coli* BL21 and the cell lysates were subjected to SDS-PAGE followed by Western blot. The epitope of mAb6 resides in the fragment containing residues 947-1048 in the region between the transcarboxylation domain and the N-terminal end of the biotin carboxyl carrier domain. To further define the minimal residues for the epitope recognised by mAb6, five

overlapping fragments covering residues 947-1048 of hPC were generated and screened for interaction with mAb6. The results reveal that this linear epitope is the amino acid sequence LKDLPRV (residues 968-974).

To identify the critical residues that contribute to the immunoreactivity of this epitope to mAb6 and to the enzymatic activity of hPC, each was replaced singularly by alanine screening mutagenesis. The data obtained through mutational analysis of this epitope showed that when expressed both as a fusion protein fragment in *E. coli* and as full-length hPC in a mammalian cell line, only the D970A mutant showed a complete loss of binding to mAb6. In addition, the acetylCoA-dependent activity of the hPC mutein bearing the D970A mutation was significantly reduced to 50% compared to wild type activity.

The location of mAb6's epitope in the proline rich region at the junction between the transcarboxylation and the biotin carboxyl carrier domains may imply that mAb6 binding affects the mobility of the BCC domain in the catalytic reaction of PC.

Using six overlapping fusion proteins of hPC (BC, F1, F2, F3, TB1 and TB2), it was shown that mAb12 and 42 recognised only F3 and its derivative TB2 that includes the biotinylated K^{1144}, 35 residues from the C-terminus. To further define the minimal epitopes, which these antibodies recognised, various deletions of the TB2 fragment were constructed, resulting in proteins truncated at the C terminus. All these C-terminally truncated proteins failed to cross-react with antibodies 12 and 42 and with avidin alkaline phosphatase. Consequently, we further mapped these epitopes with N-terminal truncations of the hPC biotin carboxyl carrier domain fused to the C-terminus of thioredoxin. Two of these fragments encoding amino acids 1071-1178 (TB2 107n) and 1098-1178 (TB2 80n) cross-reacted with both antibodies, but none of the fragments encoding amino acids 1168-1178 (TB2 10n), 1158-1178 (TB2 20n) and 1118-1178 (TB2 60n) reacted with either antibody. The same pattern of reactivity was

seen with an avidin-alkaline phosphatase blot suggesting that all but fragments TB2 107n and TB2 80n had failed to fold to a conformation able to interact productively with biotin protein ligase. Accordingly the epitopes of mAb12 and 42 were revealed as discontinuous epitopes contained within the minimal C-terminal 80 residues of the biotin carboxyl carrier domain (BCC) of human PC. To further define these epitopes, measurements (Western blot) were made on a series of BCCs containing point mutations that were based not only on the sequence alignment of human PC, the BCC of yeast PC_1 and BCC of *E. coli* acetyl-CoA carboxylase but also on the predicted structure of this domain. As summarised in the accompanying figure, alanine substitution of Met^{1116}, Met^{1143}, Leu^{1168} and Glu^{1169} resulted in reduction of the binding of mAb12. Of these the most significant contributor to the binding of mAb12 is Met^{1143}. For mAb42, the alanine substitutions of Ser^{1141}, Met^{1143} and Leu^{1168} most significantly account for reduced binding while $Lys^{1119}$and Asp^{1165} also had modest effects. Therefore, mAb42 appears to bind to the BCC domain of hPC in an area that includes Leu^{1168} as well as Met^{1143}, Asp^{1165}, Lys^{1119} and Ser^{1141} which are close to the biotin moiety. However, mAb12's epitope appears to be on the opposite site of the biotin moiety, and includes Met^{1116}, Met^{1143}, Leu^{1168} and Glu^{1169}. Met^{1143} and Leu^{1168} may be part of the overlap of these epitopes.

Until now, hPC has been successfully expressed in a mammalian cell line, 293T and active hPC purified from a mitochondrial extract (Jitrapakdee *et al.*, 1999). I have attempted the expression of full-length hPC in bacterial systems in many ways to obtain functional hPC which can be used for kinetic and physicochemical studies. Attempts to express cDNA encoding full-length hPC in an *E. coli* expression using a T7-driven vector [pET32a (+)] and taking various measures to account for codon usage and the possible need for additional GroEL-GroES and DnaK-DnaJ chaperones resulted in only very low levels of expression. However, I have succeeded in expressing the hPC in *E.*

coli by changing the vector system to a T5 *lac*-driven vector (pQE system). Although the expression of hPC increased to detectable levels, the expressed hPC was inactive, presumably because it was unfolded or unable to assemble in the *E. coli* system. Expression of hPC in a *S. cerevisiae* system was not improved whether or not it had a mitochondrial targeting sequence. Thus future structure and function studies of hPC requiring substantial quantities of highly purified enzyme will first need to develop a readily available and sustainable source. Meanwhile, monoclonal antibodies and site-directed mutagenesis studies will provide sensitive probes of structure and function relationships albeit at lower resolution than we ultimately desire for this fascinating enzyme.

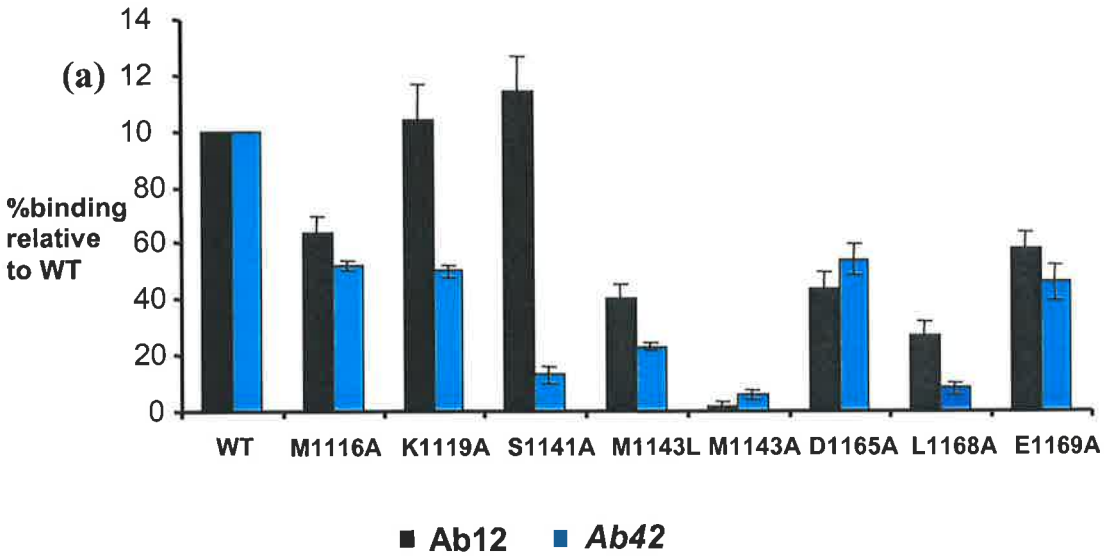

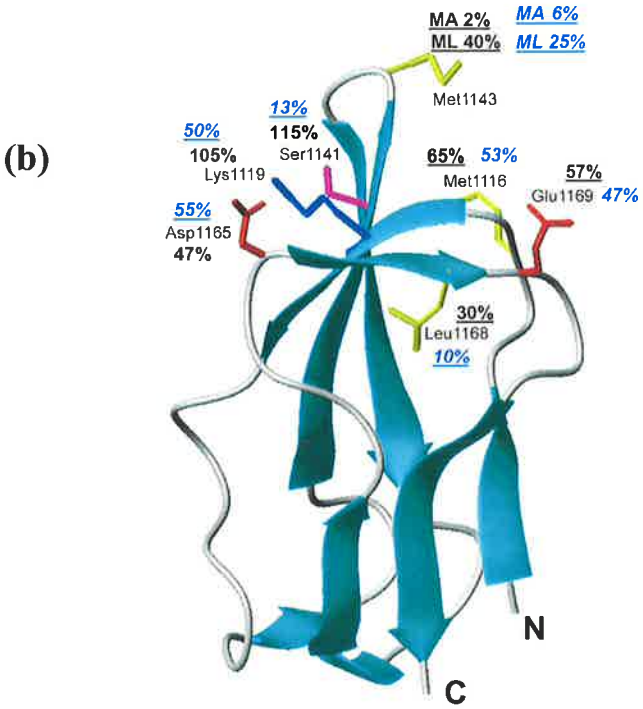

The percent relative binding of mAb12 and 42 with eight mutants of biotin carboxyl carrier domains (BCC) of hPC compared to wild type. (a) Eight mutants of BCC of hPC were expressed and lysates prepared for the binding with mAb12 and 42. The results were quantitated from the antibody blots and are shown as the mean of the measurement ± standard deviation (SD). The percent relative bindings compared with wild type (TB2 107n) were determined in triplicate. (b) The predicted three-dimensional structure of hPC BCC, with summarised results of percent bindings of mAb12 and 42 to eight mutants shown in black for mAb12 and in blue italics for mAb42. The reduction of binding by critical residues is shown in black or (italic) blue colour with underlining.

STATEMENT OF ORIGINALITY

This thesis contains no material that has been accepted for the award of any degree or diploma by any other University. To the best of my knowledge it contains no material that has previously been published by any other person, except where due reference has been made in the text. I consent to this thesis, when deposited in the University library, being available for photocopying and loan.

.....

Teerakul Arpornsuwan

ACKNOWLEDGEMENTS

I would like to thank Professor Peter Rathjen for giving me the opportunity to undertake a PhD program in the School of Molecular Biomedical Science (Biochemistry Discipline) of the University of Adelaide. I am very grateful to my supervisor, Professor John C. Wallace for his support, encouragement, helpful feedback and financial support during my study.

I would like to thank Dr. Keith Shearwin, Dr. Sarawut Jitrapakdee, Mark Nezic and Dr. Anne Chapman-Smith for their criticisms, helpful and useful suggestions, feedback and friendly advice. Thank you also to Cvetan Stojkoski for his help to generate the model for the biotin domain of human PC in Chapter 5. I would also like to convey my special appreciation to my friend Sittiruk Roytrakul, PhD student in the Netherland for his patience with me in an early morning discussion and also for his good suggestions throughout the 4 years.

In addition, I would like to thank the other members of the Wallace lab including Dr. Steven Polyak who was kind to help with my thesis, Dr. Briony Forbes, Kerrie McNeil, Melinda Lucic, Samantha Lien, Francine Carrick, Jan Cook, Carlie Delaine, Fiona Whelan, Mehrnaz Keyhanfar (especially be company for evening tea time) Zhihe Kuang (Wau), Adam Denley, Adam Charlton, Rachel Swift and Gemma Brierley for their friendship, helpful comments on my project, especially on my pronunciation to Adam Denley, Fiona Whelan, Rachel Swift and Gemma Brierley.

Finally, I would like to thank all of many people in this building for their support and being cheerful for all my study, for example, Grant Booker Lab; Sue Fowler, Rebecca Bilton, Anita Merkel; CSU, Ros Hammond, Judy Whittle (especially for 30 sterile flasks for my bacterial culture); Tissue culture lab, John Mackrill; Jan Soltys (always understanding and helpful for all things to be ordered for the lab) and Barrie Egan's Lab; Rachel Schubert and Benji Callen for all kindness to listen to my story in the late evening and weekend.

ABBREVIATIONS

In addition to those accepted for use in the *Journal of Biological Chemistry*, the following abbreviations are used in this thesis:

A600	Absorbance at $\lambda = 600$ nm
ACC	Acetyl-CoA carboxylase
ATP	Adenosine triphosphate
BCIP	5-bromo-4-chloro-3-indolyl-phosphate
BSA	Bovine serum albumin
DTT	Dithiothreitol
EDTA	Ethylenediaminetetra acetic acid
IPTG	Isopropyl β-D-thiogalactopyranoside
MCD	Multiple carboxylase deficiency
NADH	Nicotinamide adenine dinucleotide (reduced)
NiNTA	Nickel-nitriloacetic acid
NMR	Nuclear magnetic resonance
NOE	Nuclear overhauser effect
PAGE	Polyacrylamide gel electrophoresis
PBS	Phosphate buffer saline
PC	Pyruvate carboxylase
PEP	Phosphoenolpyruvate
Pi	Inorganic phosphate
PMSF	Phenylmethylsulphonyl fluoride
SDS	Sodium dodecyl sulfate
SH	Sulphydryl group
STD	Saturation transfer difference
TC	Transcarboxylase
TRNOE	Transferred nuclear overhauser effect
Tris	Tris-(hydroxymethyl)-methylamine
WT	Wild type

CHAPTER 1

Introduction and Literature Review

CHAPTER 1

1.1 BIOTIN DEPENDENT ENZYMES

Biotin plays a central role in all forms of life as a specialised carrier of single carbon groups in their most oxidised form, CO_2. It is a water-soluble molecule found in all organisms and functions as a cofactor of enzymes known as biotin-dependent carboxylases (Wood & Barden, 1977). The role of biotin in carboxylases is to act as a vector for carboxyl-group transfer between donor and acceptor molecules during carboxylation reactions (Pacheco-Alvarez *et al.*, 2002). Covalent addition of biotin to these proteins is catalysed by biotin protein ligase, which in prokaryotes is known as BirA protein and in eukaryotes as holocarboxylase synthetase (HCS) (Campeau & Gravel, 2001).

Until recently, the sole known function of biotin was to act as a cofactor of a large family of related enzymes that all utilise a biotin prosthetic group (Samols *et al.*, 1988). Although biotin dependent enzymes have diverse metabolic roles, all share several features in common. The catalytic reaction always occurs in two distinct steps, each carried out at separate subsites on the molecule. The role of biotin in these reactions is to act as a mobile shuttle system, passing CO_2 from the first to the second catalytic site.

Biotin dependent enzymes catalyse key reactions in gluconeogenesis, fatty acid synthesis, and amino acid catabolism. Because these enzymes play such an important role in intermediary metabolism, biotin starvation or deficiencies of one enzyme involved in biotin utilisation is potentially lethal (Pacheco-Alvarez *et al.*, 2002). It has been suggested in recent years that biotin may play a role in other cellular events in eukaryotic organisms such as transcriptional or translational regulation or activity

enhancement of different hepatic enzymes (Chauhan & Dakshinamurti, 1991; Spence & Koudelka, 1984).

Biotin dependent enzymes can be grouped into three distinct classes depending on the identity of the carboxyl donor and the carboxyl acceptor (Samols *et al.*, 1988; Wood & Barden, 1977).

Carboxylases (Class I)

Comparisons of the partial reactions of several biotin enzymes lead to the recognition that all Class I biotin dependent enzymes are composed of three basic functional elements. These are biotin carboxylase (BC) which is the site of biotin carboxylation, biotin carboxyl carrier protein (BCCP) where the biotin prosthetic group is covalently bound to the ε-amino group of a specific lysine residue via an amide bond (Chapman-Smith & Cronan, 1999a) and carboxyl transferase (CT) where the carboxyl group is transferred from biotin to the acceptor molecule.

All carboxylases convert bicarbonate to CO_2 in an ATP dependent reaction. This conversion of HCO_3^- to CO_2 is necessitated by the absence of significant amounts of free CO_2 in solution at neutral pH. The CO_2 is then transferred to the biotin moiety, which swings across to the second subsite where CO_2 is donated to the acceptor molecule. Extensive study has been undertaken to elucidate the mechanism of biotin carboxylation (Attwood, 1995; Knowles, 1989; Wood & Barden, 1977). All eukaryotic biotin-dependent enzymes belong to class I, and include pyruvate carboxylase (PC, EC 6.4.1.1), acetyl-CoA carboxylase (ACC, EC 6.4.1.2), propionyl-CoA carboxylase (PCC, EC 6.4.1.3), 3-methylcrotonyl-CoA carboxylase (MCC, EC 6.4.1.4), geranyl-CoA carboxylase (EC 6.4.1.5) and urea carboxylase (EC 6.3.4.4). In contrast, prokaryotes contain examples of enzymes from all three classes.

Decarboxylases (Class II)

Unlike the class I enzymes, all decarboxylases operate in an ATP-independent manner to catalyse the decarboxylation of a specific β-keto acid or acyl-CoA, coupled to sodium ion export against a concentration gradient (Dimroth & Thomer, 1992). Therefore, class II enzymes serve an important role as efficient energy transducers that operate without the use of ATP. Examples of class II enzymes include oxaloacetate decarboxylase (ODC, EC 4.1.1.3), glutaconyl-CoA decarboxylase (EC 4.1.1.70) and methylmalonyl-CoA decarboxylase (EC 4.1.1.41).

Transcarboxylases (Class III)

The only known example of class III is *Propionibacterium shermani* transcarboxylase (TC, EC 2.1.3.1) which catalyses the transfer of a carboxyl group from oxaloacetate to propionyl-CoA to form methylmalonyl-CoA (Samols et al., 1988).

1.2 PYRUVATE CARBOXYLASE

1.2.1 The metabolic role of PC

Pyruvate carboxylase (PC) is a class I biotin dependent enzyme which was first described by Utter and Keech (1960) during their studies of gluconeogenesis in chicken liver. PC was found to catalyse the carboxylation of pyruvate to form oxaloactate (Eqn 1.1). Further characterisation of the chicken enzyme followed, resulting in a more detailed description of its general properties and reactions (Keech & Utter, 1963; Utter & Keech, 1963).

$$\text{Pyruvate} + HCO_3^- + \text{ATP} \xrightleftharpoons{\text{Acetyl-CoA, } Mg^{2+}} \text{oxaloacetate} + \text{ADP} + \text{Pi}$$

.....Eqn (1.1)

It was found that PC in conjunction with phosphoenol pyruvate carboxykinase (PEPCK) was capable of forming phosphoenol pyruvate (PEP) from pyruvate, thus reversing the reaction catalysed by pyruvate kinase (Keech & Utter, 1963).

PC has since been identified in a wide range of vertebrates including human, sheep, chicken and rat as well as invertebrates and in many micro organisms (for a review, see Wallace, 1985). PC not only plays a key role in gluconegenesis from lactate and alanine, but also has an anaplerotic role in replenishing mitochondrial oxaloacetate utilised in the export of 2-C units for the synthesis of fatty acids and neurotransmitters as discussed below.

Among prokaryotes, PC has been found in *Pseudomonas* spp., *Rhodobacter* spp., *Bacillus* spp., *Rhizobium* spp., etc., but not in *Enterobacteriaceae* (Wallace, 1985). In bacteria, anaplerotic CO_2 fixation is critical for the maintenance of the oxaloacetate pool during growth on compounds that are utilised via pyruvate (Al-ssum & White, 1977). Although PC fulfils this function in many prokaryotes (Willison, 1988), enteric bacteria as well as some other groups convert phosphoenolpyruvate (PEP) to oxaloacetate in the reaction catalysed by PEP carboxylase (PPC) (McAlister *et al.*, 1981). These two pathways for oxaloacetate synthesis are not mutually exclusive, since some bacteria produce both PC and PPC (Encarnacion *et al.*, 1995; O'Brien *et al.*, 1977; Scrutton & Taylor, 1974). PC activity in *Rhizobium etli* is essential for growth with pyruvate or sugars as the sole carbon source, but not for symbiotic nitrogen fixation in common bean (Dunn *et al.*, 1997; Dunn *et al.*, 1996). Rhizobia (members of the gram-negative bacterial genera Rhizobium, Sinorhizobium, Mesorhizobium, Bradyrhizobium and Azorhizobium) use a variety of anaplerotic pathways to maintain tricarboxylic acid (TCA) cycle activity under different growth conditions; and some of these reactions are also required in symbiosis (Dunn, 1998; Dunn *et al.*, 2001).

In the yeast *Saccharomyces cerevisiae*, there are two primary anaplerotic pathways for replenishing the intermediates of the Krebs cycle that have been removed for biosynthesis. They are the glyoxylate cycle and the carboxylation of pyruvate to oxaloacetate, catalysed by two cytosolic isozymes of PC (Palmieri *et al.*, 1999). However, during growth in glucose, the glyoxylate cycle is suppressed therefore leaving PC as the only known means of replenishing the citric acid cycle in the presence of glucose (Gancedo, 1992). As a consequence of the anaplerotic role of yeast PC (yPC), yeasts lacking yPC enzyme activity cannot grow on minimal glucose media unless aspartate or glutamate is added, being amino acids that can be converted into oxaloacetate (Ozimek *et al.*, 2003). The two isozymes coded by different PC genes (PYC1 and PYC2) were found in the cytosol in yeast (Rohde *et al.*, 1986; Stucka *et al.*, 1991; Walker *et al.*, 1991). By analysing null mutants, these two isozymes were shown to be under discrete gene regulation and appear to have different metabolic functions (Brewster *et al.*, 1994). PYC1 is essential in the anaplerotic pathway for maintaining the fermentative growth and for the establishment of gluconeogenic growth, whereas, PYC2 may play a more specific role in the early stages of fermentative growth (Brewster *et al.*, 1994).

In methylotrophic yeast, *Hansenula polymorpha* and *Pichia pastoris*, yPC plays a dual role in that, beside its well-characterised metabolic function as an anaplerotic enzyme, the protein fulfils a specific role in the alcohol oxidase (AO) sorting and assembly process in peroxisomes, possibly by mediating FAD-binding to AO monomers (Ozimek *et al.*, 2003).

PC has been shown to be present in plants, but its exact role is uncertain (Wurtele & Nikolau, 1990). It has been suggested that plant PC functions as an

alternative gluconeogenic pathway additional to the process of photosynthesis (Wurtele & Nikolau, 1990).

In mammals, PC is a mitochondrial matrix enzyme which is encoded by a single nuclear gene, and is synthesized in the cytosol as a large precursor polypeptide with a cleavable amino terminal mitochondrial targeting sequence (Owen *et al.*, 1976). Vertebrate PC is expressed in a tissue specific manner, the activity being highest in the liver and kidney (gluconeogenic tissues), lactating mammary gland and adipose tissue (lipogenic tissues), moderate in heart, brain and adrenal gland and least in white blood cells and skin fibroblasts (Jitrapakdee *et al.*, 1996; Wallace, 1985; Wexler *et al.*, 1994). The metabolic roles of PC in these different tissues are described below.

Gluconeogenesis

Probably the most well established role of PC is to catalyse the first committed step in the gluconeogenic pathway, beginning from a pyruvate precursor. When the cell is at a state of high energy charge, pyruvate can be used to produce glucose. In the gluconeogenic pathway, pyruvate carboxylation is the first step in gluconeogenesis and PC is one of the key regulating enzymes in this pathway that occurs in the liver and kidney of vertebrates (Blackard & Clore, 1988). In certain tissue types (most notably brain and kidney medulla), glucose is required at relatively constant levels. During starvation or fasting, the gluconeogenic pathway is the primary source of endogenous glucose and studies have shown PC and other gluconeogenic enzymes [phosphoenolpyruvate carboxykinase (PEPCK), fructose 1, 6-bisphosphatase and glucose 6-phosphatase] to be elevated during these periods (Owen *et al.*, 1976).

Anaplerosis

PC has since been found to have several other roles. PC has an important anaplerotic function in replenishing oxaloacetate, which is an intermediate of the

tricarboxylic acid cycle (TCA) that has a variety of biosynthetic function purposes in addition to energy production. PC helps to maintain the concentration of TCA cycle intermediates to keep the TCA cycle at the required level of activity (Barritt, 1985).

The anaplerotic role of PC has also been proposed to be important for the maintenance of TCA cycle components used in the production of glutamine, the precursor of neurotransmitter substances, via the operation of the glutamate/glutamine cycle (Benjamin & Quastel, 1974). The nerve endings of neurones release glutamate, a neurotransmitter substance, which is converted into glutamine by astrocytic glutamine synthetase and secreted into the extracellular fluid. Glutamine is taken up by neurones for conversion into glutamate, aspartate and γ-aminobutyric acid (Shank *et al.*, 1993).

Lipogenesis

PC also plays a role in the fatty acid synthesis pathway in vertebrates because the 2-C moieties of acetyl-CoA produced by pyruvate dehydrogenase must be transported out of mitochondria as citrate to yield cytoplasmic acetyl-CoA and oxaloacetate through the citrate cleavage pathway. PC is involved in providing the mitochondrial oxaloacetate for fatty acid synthesis and was found to be expressed at a very high level during the differentiation of adipocytes (Mackall & Lane, 1977). Further work revealed that PC contributes to lipogenesis by providing a source of oxaloacetate, which is converted by malate dehydrogenase in a NADH-dependent reaction to malate for export to the cytosol where it is then decarboxylated to pyruvate by malic enzyme, generating NADPH in the process. Thus this reaction contributes a considerable proportion of the NADPH utilised in the fatty acid synthesis pathway (Ballard *et al.*, 1970).

Insulin release from pancreatic islets

The long term regulation of PC by hormones in response to nutritional and developmental parameters is not clearly defined, but is likely to involve changes in the levels of insulin, glucagon, thyroid hormones and glucocorticoids. The activities of two mitochondrial enzymes, pyruvate dehydrogenase and PC are elevated when pancreatic islets are grown in higher than physiological concentrations of glucose. This suggested that both enzymes are involved in the regulation of glucose-induced insulin release (MacDonald *et al.*, 1991). However, the precise metabolic signalling mechanism leading to insulin release remains unclear. It is known however that pancreatic islet cells have a relatively high concentration of PC but are lacking in PEPCK activity and its mRNA. This suggests that gluconeogenesis is not taking place since PEPCK is required for the formation of PEP in the gluconeogenesis pathway (MacDonald & Chang, 1985; MacDonald *et al.*, 1992).

The PC catalysed reaction is an important link between gluconeogenesis and other biochemical pathways. The metabolic roles of PC have recently been reviewed by Wallace *et al.* (1998) and are summarised in Figure 1.1 (Wallace *et al.*, 1998).

1.2.2 Role of PC in disease processes

PC deficiency is an autosomal recessive trait which has been seen widely in the world affecting approximately 1 in 250000 live births (Wallace *et al.*, 1998). PC deficiency ranges in severity from the Benign (Type C) form causing only mild recurrent episodes of lactic acidosis with normal neurological development (Arnold *et al.*, 2001; Crabtree *et al.*, 1972; Hamilton *et al.*, 1997), through the Simple (Type A) milder form in which the presenting features are lactic acidaemia and psychomotor retardation (Lee & Davis, 1979) to the Severe (Type B) form in which neonatal lactic acidosis, hyperammonaemia and abnormal redox states result in death at less than 3 months of

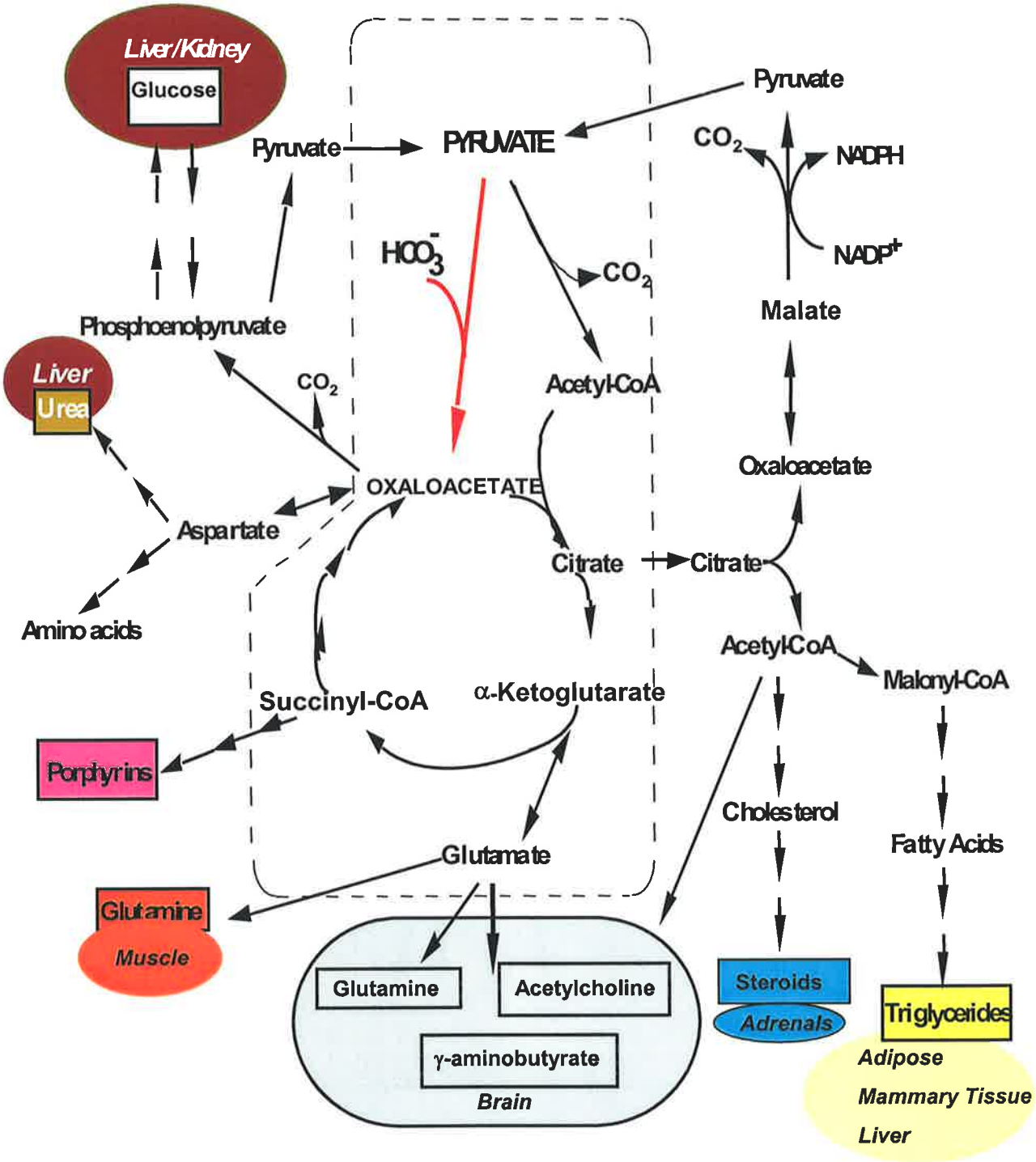

Figure 1.1 A schematic diagram illustrating the anaplerotic function of PC in replenishing oxaloacetate used for various biosynthetic purposes originating from the TCA in mammals. The highest activities of pathways in tissues are highlighted in colour. The dotted lines represent mitochondrial localisation of PC in the tissues of vertebrates (Wallace *et al.*, 1998).

age (Comte *et al.*, 1997; Robinson *et al.*, 1996). Recently, it has been reported that there have been four documented point mutations associated with Type A PC deficiency (Carbone *et al.*, 1998; Wexler *et al.*, 1998), two deletion mutations associated with Type B PC deficiency (Carbone *et al.*, 2002), and two point mutations associated with Type C PC deficiency (Carbone, M. A., Rahman, S., Besley, G.T.N., Clayton, P.T. and Robinson, B.H. unpublished work). The exact mechanism by which these mutations adversely affect PC activity remains unexplained (Carbone & Robinson, 2003).

Molecular characterisation of the A and B forms showed that those with Type A PC deficiency had detectable PC and its mRNA on Northern blotting. In these patients, the gene is expressed in the form of a biotin containing protein that possesses enough residual catalytic activity to sustain the anaplerotic role of PC (Carbone *et al.*, 2002). Those with Type B PC deficiency were completely missing PC and its mRNA or had low levels of PC protein and its mRNA (Robinson *et al.*, 1996; Robinson *et al.*, 1987). In the Type B PC deficiency patients, lack of intracellular aspartate and oxaloacetate compromises both the synthetic and anaplerotic pathways that require PC activity.

Another group of patients, who display PC deficiency, also appear to suffer from deficiency of all biotin containing enzymes, and this is called multiple carboxylase deficiency (Wolf, 1995). These patients show obvious developmental delay and lactic acidemia in addition to increased levels of organic acids, which are metabolites of acetyl-CoA, propionyl-CoA and β-methylcrotonyl-CoA. Not surprisingly patients with multiple carboxylase deficiency actually suffer from a defect in biotin processing metabolism, which effectively restricts or denies the essential biotin prosthetic group to all biotin dependent enzymes. In many patients the defect is in the biotin ligase which normally catalyses the reaction to covalently attach biotin to all biotin dependent

enzymes. It can be effectively treated in many cases of this disease by biotin supplements in the diet (Wolf, 1995).

1.3 MECHANISM OF PC REACTION

The overall reaction catalysed by PC, shown in equation 1.1, occurs as a multi step process (Knowles, 1989) which can be simplified to the carboxylation and decarboxylation of biotin, as shown in equation 1.2 and 1.3. The presence of the biotin prosthetic group is also a strict requirement for the reaction mechanism in that biotin acts as a shuttle system to carry CO_2 between the two partial reaction subsites. The first evidence for two distinct reaction sites came from work with isotopic exchange reactions with radioactive substrates or products used in isolation (Bais & Keech, 1972; McClure *et al.*, 1971; Scrutton *et al.*, 1964). It was shown that the substrates involved in each of the two subsites could undergo isotopic exchange independently of each other. Moreover, studies with the isolated carboxybiotin complex found that the binding of oxamate, an analogue of pyruvate, at the second subsite acted as a trigger for the dissociation of the carboxybiotin complex from the first subsite and its movement to the second subsite (Goodall *et al.*, 1981).

The reaction mechanism of PC has been extensively reviewed by Attwood (1995) and Attwood & Wallace (2002).

$$\text{Enzyme-biotin} + \text{ATP} + HCO_3^- \xrightleftharpoons{\text{Acetyl-CoA, } Mg^{2+}} \text{Enzyme-biotin-}CO_2 + \text{ADP} + \text{Pi}$$

.....Eqn (1.2)

$$\text{Enzyme-biotin-}CO_2 + \text{pyruvate} \rightleftharpoons \text{oxaloacetate} + \text{Enzyme-biotin}$$

.....Eqn (1.3)

The first partial reaction

The first partial reaction is known to involve the binding of Mg^{2+}, ATP and HCO_3^- to the first subsite. Biotin is then carboxylated, accompanied by the cleavage of ATP to ADP and Pi. The carboxylation of biotin is not a spontaneous process, it requires energy and this is provided by the cleavage of ATP. The mechanism of ATP cleavage to drive the reaction has not been revealed, but most likely involves phosphorylation of HCO_3^- by ATP to form a reactive carboxyphosphate intermediate (Knowles, 1989). The evidence to support this idea comes from a study of carbamoyl phosphate which is a structural analogue of carboxyphosphate, and which has been found to be capable of transferring its phosphate group to MgADP in reactions catalysed by acetyl-CoA carboxylase from *E. coli* (Polakis *et al.*, 1972), sheep kidney PC (Ashman & Keech, 1975) and chicken liver PC (Attwood & Graneri, 1991). Support for this proposed mechanism has yet to be provided by the isolation of this carboxyphosphate intermediate. The observed sequence similarity between carbamoyl-phosphate synthetase and the region in the N-terminal half of yeast PC identified as the probable ATP-binding domain (Lim *et al.*, 1988) also tends to support a mechanistic similarity in terms of the formation of a carboxyphosphate intermediate (Phillips *et al.*, 1992).

Magnesium ions are found to have at least two modes of action. Firstly, it is the MgATP complex that acts as a substrate for PC (Bais & Keech, 1972). Secondarily, it has been shown that the presence of additional Mg^{2+} ions is an essential cofactor for the catalytic activity as revealed by kinetic studies of PC. Studies by Bais and Keech (1972) revealed that MgATP cleavage would not proceed before Mg^{2+} is bound to the enzyme. Recently an X-ray crystallographic structure of carbamoyl phosphate synthetase (CPS) of *E. coli* complexed with ADP, Pi and Mn^{2+} has shown that the carboxyphosphate

synthetic domain of the large subunit has two Mn^{2+} ions bound (Waldrop *et al.*, 1994). One of the Mn^{2+} ions is also coordinated to the side-chain oxygens of Gln285 and Glu299, while the other is coordinated to the side-chain oxygens of Asn301 and Glu299 (Waldrop *et al.*, 1994). Attwood and Wallace (2002) suggest similar binding sites for Mg^{2+} in the biotin dependent enzymes since amino acids corresponding to Glu299 and Asn301 are highly conserved in not only CPS from other species but also across biotin dependent carboxylases. Several studies on PC have shown that the binding of Mg^{2+} to the enzyme may effect an allosteric change, resulting in an increase in the affinity of biotin for the first partial reaction site and allowing the carboxylation of biotin to occur (Attwood & Graneri, 1992; Branson & Attwood, 2000). Recently, a study by Werneburg & Ash (1997) using electron paramagnetic resonance (EPR) spectroscopy demonstrated that two equivalents of the divalent oxyvanadyl cation, VO^{2+} bind at the first subsite of PC. One of the VO^{2+} ions is involved in nucleotide substrate binding, while the other interacts strongly with bicarbonate. These authors have suggested that the role of this second extrinsic cation could include orientation of the bicarbonate for attack on the γ-phosphoryl group of ATP as well as minimising charge repulsion between these anionic substrate species.

In the first partial reaction, in which it is known that HCO_3^- binds to the first reaction site of PC, one possible mechanism is that the carboxyphosphate intermediate is directly responsible for the carboxylation of biotin (Kaziro *et al.*, 1962). However, it has been shown that CO_2 is a better target for nucleophilic attack than either carboxyphosphate or HCO_3^- (Sauers *et al.*, 1975). Therefore, the most likely reaction mechanism that has been proposed is that the first partial reaction involves the formation of carboxyphosphate from ATP and HCO_3^-, followed by decarboxylation to form CO_2 which then electrophilically attacks the 1′-nitrogen on biotin (Knowles, 1989).

In studies on the catalysis of oxaloacetate decarboxylation by chicken liver PC, pH profile data showed the presence of several ionisable groups in the first partial reaction site. Several of these ionisable groups might be involved in the tautomerisation of biotin (Attwood & Cleland, 1986). It was shown that there was a large inverse solvent isotope effect in the reaction catalysed by biotin carboxylase, which suggests a sulphydryl group is involved in a proton transfer (Tipton & Cleland, 1988 a). Participation of an active-site cysteine residue in catalysis by biotin carboxylase was further supported by the observation that *N*-ethylmaleimide inactivated the enzyme while the substrates protected against the inactivation (Tipton & Cleland, 1988 b). Studies by Werneburg & Ash (1993) with sulphydryl modification showed that chicken liver PC activity was abolished by cross-linking of a cysteine-lysine ion pair in the first partial reaction site by *o*-phthalaldehyde, suggesting these modified ion pair residues were in the active site.

Using the crystal structure of *E. coli* ACC biotin carboxylase (Waldrop *et al.*, 1994), currently the only three-dimensional structure of a biotin dependent carboxylase, it was proposed that the cysteine and lysine residues acting as acid-base catalysts are Cys230 and Lys238 (Jitrapakdee *et al.*, 1996). These residues are located in the active site of biotin carboxylase, and the sulphur atom of Cys230 and ε-amino group of Lys238 are sufficiently close (4.2 angstroms) to allow for cross-linking of these two residues by *o*-phthalaldehyde. Also Cys230 and Lys238 residues are highly conserved within PC and other biotin carboxylases from a number of species, suggesting they may be analogous to the essential cysteine–lysine ion pair implicated in PC catalysis.

A site-directed mutagenesis study of biotin carboxylase subunit of *E. coli* ACC was conducted on the cysteine and lysine residues, proposed by Jitrapakdee *et al.* (1996) to be essential catalytic residues responsible for enolising biotin. It was found that the

cysteine residue played no part in deprotonating biotin and therefore was not involved in the carboxylation of biotin. In contrast, the lysine residue was shown to be critically involved in the carboxylation reaction but the high pK value (greater than 9.4) strongly suggested that lysine did not act as a catalytic base in the deprotonation of biotin (Levert *et al.*, 2000). An alternative hypothesis is required to explain the possibility of there being a concerted deprotonation of biotin and a carboxylation that transfers the carboxyl group from carboxyphosphate to biotin in this reaction. In this case, carboxyphosphate itself may actually function as a catalytic base since the transfer of a carboxyl group to biotin involves the protonation of a carboxyphosphate oxygen atom (Levert *et al.*, 2000).

Acetyl-CoA is an allosteric activator in the carboxylation of biotin in the PC reaction and its effect seems to vary widely between enzymes of different species. For example, PC isolated from chicken PC is absolutely dependent on acetyl-CoA (Utter & Keech, 1963), while PC isolated from rat liver (McClure *et al.*, 1971), sheep (Ashman *et al.*, 1972) and *Bacillus stearothermophilus* (Libor *et al.*, 1978) is also highly dependent on acetyl-CoA with sheep PC having a low level of acetyl-CoA independent activity under special conditions (Ashman *et al.*, 1972). In contrast, yeast PC displays about 50% of its activity in the absence of acetyl-CoA (Cazzulo & Stoppani, 1968). It has been shown that acetyl-CoA is not consumed in the reaction of PC, but instead exerts its effects allosterically (Utter & Keech, 1963). Electron microscope observations suggest that acetyl-CoA may act by stabilising the interaction of the subunits in the enzyme's quaternary structure (Mayer *et al.*, 1980). In addition to stabilising the quaternary structure of PC, there is evidence that the binding of acetyl-CoA also induces conformational changes in the molecules (Attwood & Cleland, 1986; Taylor *et al.*, 1978).

PC from many sources possesses a reactive lysine residue whose integrity is essential for full enzymic activity (Chapman-Smith *et al.*, 1991). Modification of the enzyme with amino group selective reagents generally results in preferential loss of the catalytic activity that is stimulated by acetyl-CoA (Ashman *et al.*, 1973; Scrutton & White, 1973). The modification of one lysine per active site significantly causes the loss of acetyl-CoA dependent activity (Scrutton & White, 1973). Acetyl-CoA has been shown to protect the enzyme against this modification (Ashman *et al.*, 1973; Scrutton & White, 1973). This essential lysine residue has been suggested to form part of the acetyl-CoA binding site, rather than being protected by a conformational change following activator binding (Chapman-Smith *et al.*, 1991). Sequence comparisons of yeast PC with other biotin dependent enzymes and other acyl-CoA binding enzymes have not been able to identify any putative acetyl-CoA binding site on PC (Jitrapakdee & Wallace, 1999). Moreover, the exact role of acetyl-CoA in activating the PC reaction mechanism remains unclear. There is evidence that both partial reactions may be activated (Attwood, 1993; McClure et al., 1971; Phillips *et al.*, 1981). It is probable that acetyl-CoA has several roles.

The active site of PC is thought to consist of two spatially separate subsites with the biotin acting as a mobile carboxyl group carrier, which is carboxylated at one subsite and then transfers the carboxyl group to the second subsite where pyruvate is carboxylated (Keech & Attwood, 1985). The movement of the carboxylated biotin moiety from the first to the second reaction subsite involves in translocation as shown in Figure 1.2. It has been shown that translocation to the second subsite will only occur after dissociation of Mg^{2+} ion (Attwood *et al.*, 1984). Moreover, it has been demonstrated that the binding of pyruvate induced the carboxybiotin to begin translocation to the second subsite (Easterbrook-Smith *et al.*, 1976). The evidence to

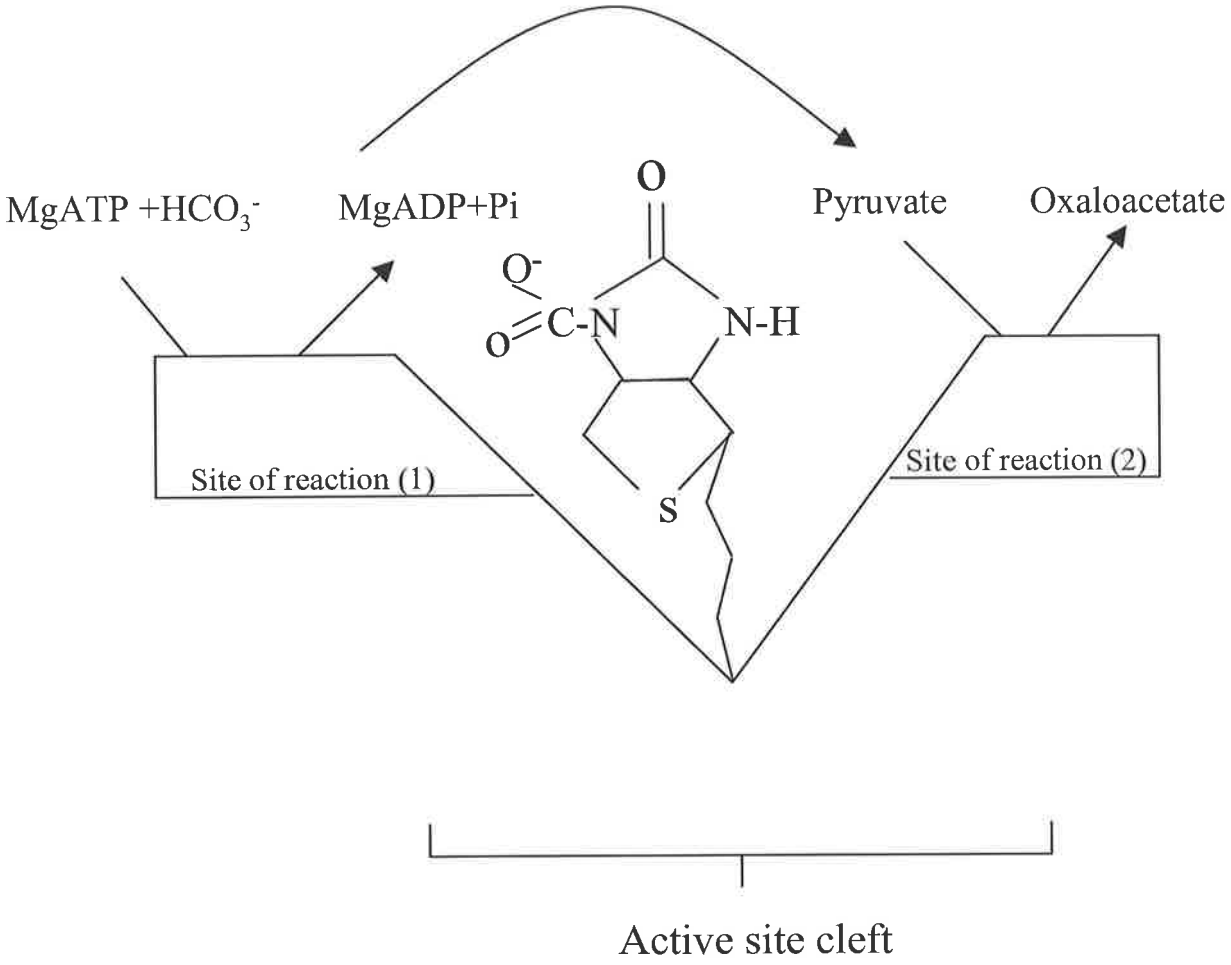

Figure 1.2 A schematic diagram of translocation of the carboxy-biotin moiety from the first to the second partial reaction subsites. The biotin prosthetic group acts as swinging arm to carry the carboxyl group from the first subsite to the second subsite in PC catalytic reaction (Attwood, 1995)

confirm this proposal showed that a number of pyruvate analogues can induce the translocation of carboxybiotin to the second subsite. This binding of pyruvate probably resulted in the dissociation of Mg^{2+} from the first subsite, thus lowering the affinity of carboxybiotin for the first subsite and initiating translocation (Goodall *et al.*, 1981).

The second partial reaction

After translocation of carboxybiotin from the first to the second partial reaction subsite, CO_2 is subsequently transferred from carboxybiotin to pyruvate to form oxaloacetate and a proton is transferred from pyruvate to biotin. Oxamate, an analogue of pyruvate has been shown to induce decarboxylation of the carboxybiotin complex (Goodall *et al.*, 1981). Attwood & Cleland (1986) found that incubation of oxaloacetate in the presence of oxamate resulted in decarboxylation of oxaloacetate, but no ATP generation. The same authors found no evidence for the involvement of ionisable groups in the oxamate-dependent decarboxylation of oxaloacetate (Attwood & Cleland, 1986). This initial study by Attwood & Cleland (1986) indicated that the proton transfer to biotin and CO_2 transfer to pyruvate occurred simultaneously with no detectable ionisable residues involved. Based on the isotope effect and the pH profile data, it was proposed that there is evidence of an involvement of a cysteine-lysine ion pair in the second subsite (Attwood *et al.*, 1986). Recently, Attwood (1995) proposed the detail of the second partial reaction by which the cysteine-lysine pair stabilises the enol form of biotin and participates in the proton transfer between biotin and pyruvate via the –SH group of cysteine.

1.4 STRUCTURE OF PC

1.4.1 Primary structure and domain

The biotin carboxylases all appear to exhibit considerable sequence similarity around the biotin attachment point (Wood & Barden, 1977) and this is consistent with the hypothesis that they share a common evolutionary origin (Lynen, 1975). Several of these enzymes have substrates and regulators in common, and it has been postulated that these multi ligand binding proteins arose by fusion events within a pool of ancestral genes (Lynen, 1975). Early attempts at protein sequencing of these biotin dependent enzymes revealed that there was significant sequence homology between PC from different species and biotinyl subunit of Transcarboxylase (TC) and *E. coli* acetyl-CoA (ACC), particularly at the biotin attachment site (Rylatt *et al.*, 1977; Sutton *et al.*, 1977; Wood & Barden, 1977). With the advent of recombinant DNA technology and genomic libraries, more sequences for PC and other biotin carboxylases were obtained to complete their primary structures. A partial sequence of human PC from cDNA cloning was first determined by Freytag and Collier (1984). The C-terminal 83 amino acid residues of human PC was determined by Lamhonwah *et al.* (1987) and shown that there is a significant homology around the biotin attachment site of human PC with PCC, ACC and TC. Yeast PC (*Saccharomyces cerevisiae)* was the first biotin carboxylase whose complete sequence was determined by Lim *et al.* (1988). It was shown that several regions of yeast PC showed significant homology to sections of other biotin carboxylases as well as to carbamoyl phosphate synthetase and lipoamide transferases.

Most forms of native PC are tetrameric enzymes with identical subunits of molecular mass 120-130 kDa (Wallace & Easterbrook-Smith, 1985). Sequencing of cDNA or genes encoding PC, limited proteolysis and comparison of primary structures

have all shown that PC from different species contains three functional domains. The first of these is the putative biotin carboxylation domain (BC). This is the proposed site of ATP and HCO_3^- binding and therefore the location of the first partial reaction. The second is the putative transcarboxylation domain (TC), which is the proposed site of the second partial reaction and thus would contain the pyruvate-binding site. The third is the biotin carboxyl carrier domain (BCC), which has the biotin prosthetic group covalently attached to a specific lysine residue close to the C-terminal end, in a highly conserved tetrapeptide sequence (AMKM) (Rylatt *et al.*, 1977). These domains may occur as separate subunits depending on the organism. In *Methanobacterium thermotrophicum*, PC has the biotinyl and transcarboxylase domains on one subunit and the biotin carboxylase on another. However, in PC from some bacteria, yeast, insects and vertebrates, all three domains in each subunit are in a single polypeptide chain (Jitrapakdee & Wallace, 1999).

The complete primary structures of PCs from yeast (Lim *et al.*, 1988, Stucka *et al.*, 1991), mouse (Zhang *et al.*, 1993), rat (Jitrapakdee *et al.*, 1996; Lehn *et al.*, 1995), human (MacKay *et al.*, 1994; Walker *et al.*, 1995; Wexler *et al.*, 1994), mosquito (Tu & Hagedorn, 1997), yeast (*Pichia pastoris*) (Menendez *et al.*, 1998), bacteria (Dunn *et al.*, 1996; Koffas *et al.*, 1998; Kondo *et al.*, 1997; Kunst *et al.*, 1997; Mukhopadhyay *et al.*, 1998) and chicken (Jitrapakdee *et al.*, 2002) have been obtained. The deduced amino acids sequences of all PCs have strong similarities to other biotin dependent enzymes and lead to the recognition of the same three functional domains in all examples observed (Figure 1.3).

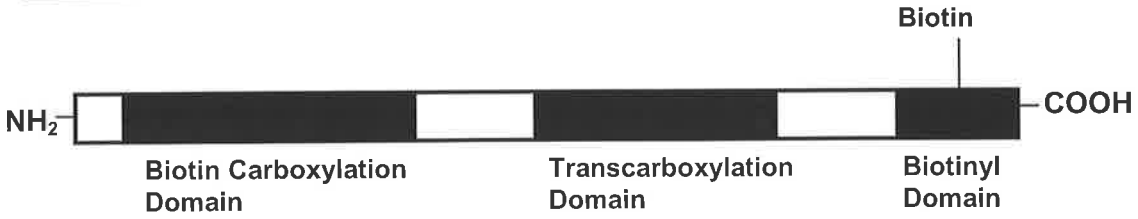

Figure1.3 The putative domain structure of human PC showing the biotin carboxylation domain, transcarboxylation domain and biotinyl domain. The biotin prosthetic group is covalently attached to a specific lysine residue in the biotinyl domain.

1.4.2 Tertiary and quaternary structure

In recent years the primary amino acid structure of PC has been determined for many organisms but a high-resolution three-dimensional structure of the molecule has not so far been obtained. The large size of the intact molecule (≈530 kDa) precludes structural determination by NMR. Moreover, the difficulty of obtaining the large amounts of sufficiently pure PC for producing crystals suitable for structural analysis by X-ray crystallography has not yet yielded results. Therefore, other methods of revealing the structure of PC at lower resolution have been utilised, including chemical modification, immunochemistry and electron microscopy. The most accurate information on the quaternary structure of PC has been obtained from electron microscope studies. Studies of chicken PC, rat PC and sheep PC using electron microscopy revealed that the active form of PC is an tetrahedron-like structure, composed of two pairs of subunits in different planes orthogonal to each other (Figure 1.4). It was found that each of the four identical subunits (α4) has a midline cleft along its longitudinal axis, which is proposed to be the location of the active site since it is less obvious in the presence of Acetyl-CoA (Mayer *et al.*, 1980). Similar results have also been obtained for yeast PC (Rohde *et al.*, 1986).

PC from most species is composed of 4 identical subunits (α4), except for PC from *Pseudomonas citronellolis*, *Azobacter vinelandii* and *Methanobacterium*

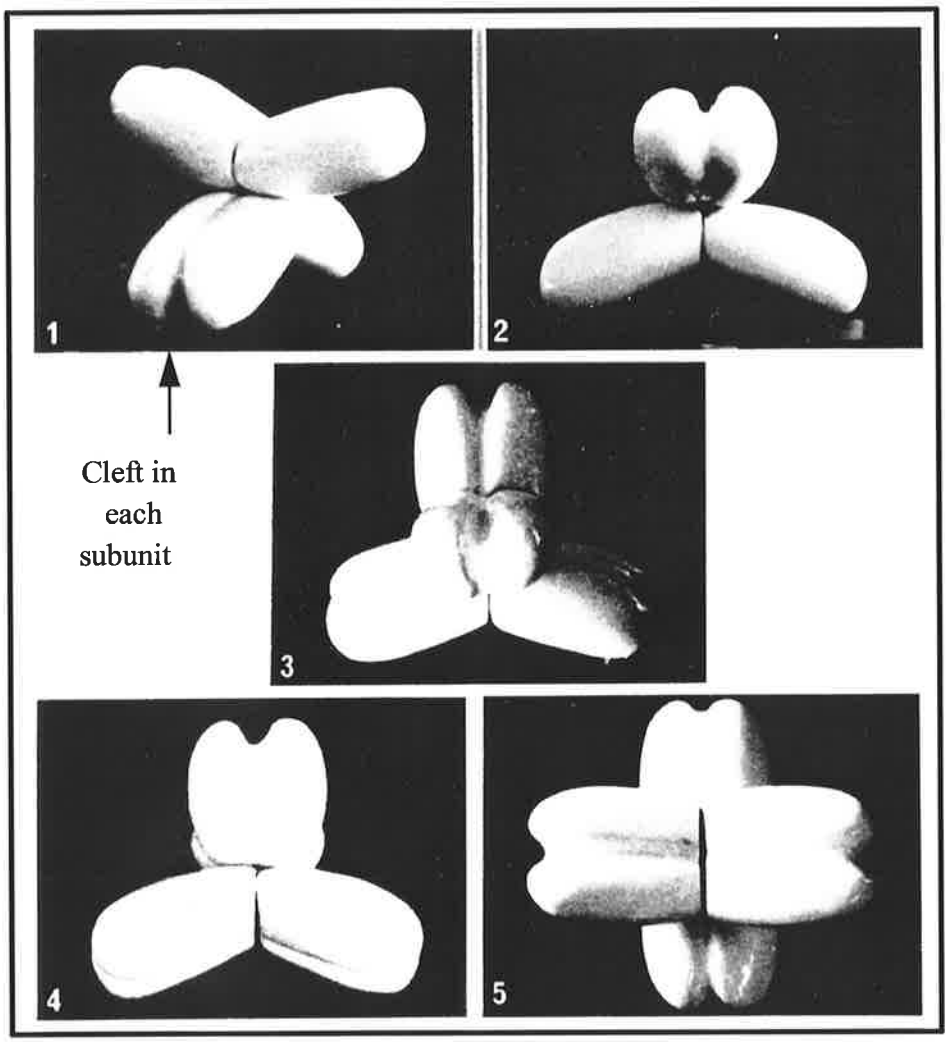

Figure 1.4 A model of the proposed quaternary structure of PC shown from five different angles. The cleft running along the axis of each subunit was shown as indicated by arrow (Mayer, 1980).

thermoautotrophicum which has an $(\alpha\beta)_4$ structure (Goss *et al.*, 1981; Mukhopadhyay *et al.*, 1998; Scrutton & Taylor, 1974). Studies using avidin probes on PC to determine the location of biotin suggest that it is located near the inter-subunit junction where the four component subunits of the tetramer converge (Johannssen *et al.*, 1983).

It has been shown that both sheep PC (Ashman et al., 1972; Khew-Goodall *et al.*, 1991) and chicken PC (Attwood *et al.*, 1993) undergo dilution inactivation concomitant with dissociation of active tetramers of PC into inactive dimers and monomers. Chicken PC is also known to undergo a similar process of cold inactivation during which the active tetramer dissociates into monomeric subunits (Irias *et al.*, 1969). Cold inactivation is dependent on enzyme concentration (Scrutton & Utter, 1965) and can be prevented by the presence of 1.6 M sucrose (Utter *et al.*, 1964) or 0.1 mM acetyl-CoA (Irias *et al.*, 1969).

Dilution of PC in the presence of the allosteric activator, acetyl-CoA prevented the subsequent dissociation of the tetrameric molecule and the associated loss of activity. Addition of acetyl-CoA to partially dilution-inactivated enzyme prevented further loss of enzymatic activity and of tetrameric structure (Attwood *et al.*, 1993; Khew-Goodall *et al.*, 1991). However, Pyc1 isozyme of yeast *Saccharomyces cerevisiae,* expressed from double null PC knockout yeast strain, DM18 (Brewster *et al.*, 1994), does not have an inherently unstable quaternary structure in the way chicken PC has (Branson *et al.*, 2002).

1.5 EPITOPE MAPPING

Epitope mapping is a methodology by which specific determinants (epitopes) can be identified on molecules by reagents derived from the immune system (Saint-Remy, 1997). An epitope has been defined as a unit of immunological significance

carried on an antigenic particle, and a paratope as its combining site, i.e. the area of an antibody in contact with an epitope (Jerne, 1960). The term "epitope mapping" has also been used to describe the attempt to determine all the major sites on a protein surface that can elicit an antibody response, at the end of which one might claim to have produced an epitope map of the protein antigen (Atassi, 1984).

Protein antigenic determinants have been classified as conformational (discontinuous, assembled) or linear (continuous, sequential) epitopes. The conformational epitopes are composed of residues in which distant amino acids in the protein sequence are brought together by protein folding, whereas linear (continuous, sequential) epitopes can often be mimicked by simple peptide sequences (Barlow *et al.*, 1986). Given the nature of protein structures, most epitopes on native proteins are likely to be assembled and consequently, most polyclonal antibodies raised against these proteins do not recognise short peptides (Barlow *et al.*, 1986; Van Regenmortel, 1989 a).

Continuous epitopes can be mapped to small linear peptide sequences of 5-20 amino acids, and conformational epitopes can only be mapped to larger protein domains. These epitopes show interactions with side chains that, although close to each other in the folded protein, are widely separated in the linear sequence. As expected, the epitopes formed by continuous amino acids are resistant to loss through denaturation, whereas those formed from non-contiguous amino acids are lost when the protein unfolds (Zaripov *et al.*, 1999).

1.5.1 Methodology

1.5.1.1 Immune reagent

It might be simpler for the purpose of this work to adopt the operational view that an epitope is defined by an antibody molecule. The potency of the immune system

is extraordinary: it can distinguish between two proteins that differ by only one amino acid, or between two identical molecules exhibiting a different three-dimensional conformation. These properties can be used for identifying epitopes, using antibodies or cells, and form the basis of epitope mapping (Saint-Remy, 1997).

The antibody that defines an epitope is mostly a monoclonal antibody (mAb), although an epitope mapping method can also be applied to polyclonal antisera, which should be regarded as a mixture of mAbs. Since polyclonal antibodies react with a great number of epitopes of the antigen, identifying a difference between two antigens which may differ by just one epitope can therefore be difficult. By definition, monoclonal antibodies have the capacity to recognise single epitopes and are therefore extremely useful for making comparisons between two almost identical molecules (Saint-Remy, 1997).

1.5.1.2 Methods used to localise epitopes in proteins

In general, antibodies induced by a native protein and directed to a complex discontinuous epitope cross-react only weakly with an epitope fragment constituted by a linear peptide. The peptide usually has a conformation different from the corresponding region in the protein leading to this weak cross-reaction (Van Regenmortel, 1989 b). Most studies aimed at unravelling the antigenic structure of proteins have focused not on antigenicity but on the phenomenon of cross-reactive antigenicity between proteins and short peptides (Van Regenmortel, 1989 b).

The different approaches that have been used for mapping protein epitopes are summarised in Table1 (Atassi, 1984; Benjamin *et al.*, 1984). Only method 1 (Table 1) is based on a structural analysis. In contrast, all other methods correspond to a functional analysis taking the form of binding measurements. It has been shown that the structuralist perspective inherent in X-ray crystallography (Table 1) leads to the view

that an epitope consist of approximately 15 residues that are in contact with the paratope (Amit *et al.*, 1986; Colman, 1988; Sheriff *et al.*, 1987). Residues in the interface that actually contribute to the binding energy are identifiable only in binding measurements. It has been demonstrated that methods 2-5 (Table 1) analyse cross-reactivity instead of antigenic reactivity, which leads to the conclusion that a much smaller number of residues (between 1 and 5) are critical to antibody binding. Therefore, the epitope defined in a functional way involves fewer residues than the epitope defined in structural terms (Van Regenmortel, 1989 b).

Method	Type of epitope recognised	Criterion for allocating residues to epitope	Average number of residues identified in epitope
1. X-ray crystallography of antigen-Fab complexes	Discontinuous epitope reacting with homologous antibody (same serotype)	Van der Waal's contact in epitope-paratope interface	15
2. Study of cross-reactive binding of peptide fragments with anti-protein antibodies	Continuous epitope cross-reacting with heterologous antibody (different serotype)	Residual binding of linear fragment above threshold of assay	3-8
3. Study of cross-reactive binding of protein with anti-peptide antibodies	Continuous epitope cross-reacting with heterologous antibody	Induction of cross-reactive antibodies	3-8
4. Determination of critical residues in peptide by systematic replacement with other amino acids	Continuous, cross-reacting epitope containing critical residues interspersed with irrelevant residues	Abrogation of cross-reactivity by substitution of critical and functionally relevant residues	3-5
5. Study of cross-reactivity between homologous proteins or point mutants	Discontinuous epitope	Abrogation of cross-reactivity by substitution of critical residue	1-3

Table 1. Methods used to localise epitopes in proteins (van Regenmortel, 1989 b).

The molecules for which epitope mapping is considered can be used in their native form or as fragments. The protein can be in a soluble form or membrane-bound. Fragments can be generated by recombinant DNA technology or by peptide synthesis. Depending on the antigen, several assay systems can be used.

Chemical modification of the side-chains of residues in protein antigens was one of the first methods developed to investigate epitopes. Together with proteolytic fragmentation, it was first used to assign antigenic determinants on the surfaces of lysozyme and myoglobin (Atassi, 1975; Atassi, 1978). The principle of the method is that alteration of the structure of a key residue in an epitope by a chemical modification reagent will greatly change its reactivity with an antibody to that epitope (Young & Oomen, 1996). This conventional method involves the chemical and enzymatic cleavage of the protein antigen, fractionation of the cleaved protein, and then identification of fragments that react with a given monoclonal antibody by amino acid analysis or sequencing (Rao *et al.*, 1996). The disadvantages are that it is time-consuming and epitopes are also sensitive to indirect disruption by chemical modification that cause even small conformational changes, and hence great care is needed to avoid false positives (Morris, 1996).

Biophysical methods, such as X-ray crystallography or NMR spectroscopy can also be used to map epitopes. Crystallographic approaches are not currently amenable to widespread use in epitope mapping studies owing to the intrinsic complexity and the requirement that the antigen or complex must be isolated in a pure crystalline form. Furthermore, this method identifies residues in close proximity within the antigen-antibody complex (termed structural epitopes) irrespective of whether they are functional in the immune response (Kiselar & Downard, 1999).

X-ray crystallography

Crystallographic investigations of antibody-antigen complexes provide an opportunity to compare predictions from epitope mapping with direct observation of the contacting residues. There have been extensive studies of epitopes by the use of peptides in which an antibody produced in response to a protein antigen can be examined for binding to peptides from that antigen (Davies & Cohen, 1996). The epitope for lysozyme with murine anti-lysozyme antibody (HyHEL-5) was successfully predicted based on the availability of a library of avian lysozymes that were presumed to have approximately the same tertiary structure, but with small differences in the amino acid sequences (Smith-Gill *et al.*, 1982).

Crystallographic studies have shown that some substitutions in escape mutants occur outside the area of the structural epitope; these presumably cause local structural perturbations to nearby epitope residues, thereby disrupting complex formation of the antigen. However, functional studies of antigen variants have in some cases failed to detect epitope residues (often near the periphery of the antibody-antigen interface), presumably owing to local rearrangements of side-chains to allow structural accommodation of the substitutions. These observations emphasize differences between the structural epitope determined by crystallography and functional epitopes determined by amino acid residues that are important for binding and cannot be replaced (Saul & Alzari, 1996). A number of antibody fragments and antigen complexes have been studied by X-ray crystallography, which provides direct observation of the contacting residues (Davies & Cohen, 1996; Wilson & Stanfield, 1994). However, X-ray crystallography ultimately depends on the availability of suitable crystals for analysis.

Nuclear magnetic resonance (NMR)

Despite recent dramatic advances in methodology, the application of nuclear magnetic resonance (NMR) spectroscopy to study antigen-antibody interactions has been limited (Saito & Paterson, 1996; Tsang *et al.*, 1991). This is mainly because the large size of the antigen-antibody complex, particularly in the case where the antigen is a moderately sized protein, excludes standard NMR techniques for complete structure determination (Huang *et al.*, 1998). Moreover, NMR spectroscopy may fail to give a well-resolved structure, especially if the protein has a significant degree of conformational freedom in solution (Saito & Paterson, 1996).

A crucial parameter in NMR studies of large biological complexes is the rate of hydrogen/deuterium exchange of a ligand between its free and bound states (Kustanovich & Zvi, 1996). Epitopes can also be mapped by measuring changes in amide hydrogen exchange rates of the antigen that occur as a result of the formation of an immune complex (Benjamin *et al.*, 1992; Paterson *et al.*, 1990; Williams *et al.*, 1996). These rates can be conveniently measured using NMR techniques. An NMR method based on the protection from hydrogen/deuterium exchange by a mAb was first developed to localise the epitope of an anti-cytochrome C mAb (Paterson *et al.*, 1990). Amide proton exchange in proteins occurs upon transient unfolding of the structure, while solvent accessibility to transiently unfolded areas allows the exchange of the amide protons for other protons, or deuterons, to take place on time scales ranging from minutes to months (Li & Woodward, 1999; Szewczuk *et al.*, 2001). An example for this method is that the epitopes of Der p2 defined by monoclonal antibodies could be identified by comparing amide proton exchange rates in the absence and presence of the antibodies (Mueller *et al.*, 2001).

"Two dimensional nuclear Overhauser effect (2D NOE) spectroscopy, transferred NOE (TRNOE) techniques, including 2D TRNOE difference spectroscopy, and the relaxation time in the rotating frame ($T_{1\rho}$ filtered TRNOE method) are very suitable to study antibody-antigen interactions and intramolecular interactions within the bound peptide" (Anglister *et al.*, 1989; Anglister *et al.*, 1993; Scherf & Anglister, 1993). Alternatively, an isotope filtering method can be applied in the case of tight binding and slow exchange. Tsang *et al.* (1992) used this technique to elucidate amide proton interactions in an antibody bound peptide complex and to characterise the mobility of these protons on binding (Tsang *et al.*, 1992).

Saturation transfer difference (STD) spectroscopy offers an efficient alternative approach to identify the residues or substructures involved in binding to monoclonal antibodies or other receptor proteins. A prerequisite for STD NMR spectroscopy is that the ligand is reversibly bound to the protein (Mayer & Meyer, 1999). This technique was used to identify the *Legionella pneumophila* serogroup 1 lipopolysaccharide (LPS) epitope of a monoclonal antibody. The advantages of this direct approach purpose are a relatively quick and direct epitope determination with a relatively small amount of protein which does not need to be purified to absolute homogeneity (Kooistra *et al.*, 2002). A combination of transferred NOE and STD experiments has been used to probe the conformation of ligands bound to receptors and to define the critical epitope, that is the portions of the ligand in close contact with the protein (Moller *et al.*, 2002; Weimar *et al.*, 2000). Maaheimo and Kosma (2000) have described the use of STD-NMR, in combination with transferred NOESY for the conformational epitope mapping of synthetic disaccharides of Chlamydial lipopolysaccharide to corresponding monoclonal antibodies (Maaheimo *et al.*, 2000).

Most NMR studies of antibody-antigen interactions have relied on selective observation of signals from one part of the complex, typically the antigen. Direct observation of antigen resonances in the complex via isotope-edited techniques has been limited to studies of small antigens (Huang *et al.*, 1998). These include peptide antigens complexed with Fab or Fv fragments (Tsang *et al.*, 1991) and small bacterial antibody-binding proteins complexed with the Fc fragment (Tashiro & Montelione, 1995). The outer surface protein A (OspA) from the Lyme disease spirochete *Borrelia burgdorferi* complexed with Fab appears to be the largest antigen-antibody complex (78 kDa) analysed to date in which an epitope has been mapped by the chemical shift perturbation method using a uniformly isotope-labelled antigen. The chemical shift perturbation method can use essentially all amide protons as structural probes, while the hydrogen exchange method can use only a subset of amide protons with appropriate hydrogen exchange characteristics (Huang *et al.*, 1998).

Competition binding assay

Most epitope mapping by competition assay can be classified into two groups; competition assay with labelled antibody (Figure 1.5a) and with labelled antigen (Figure 1.5b). The determination of epitope specificities of monoclonal antibodies has usually been performed using the competitive assay in which the antigen is immobilised, and a labelled antibody together with competing unlabelled antibodies are mixed in solution (Figure 1.5a). Since the number of antibodies to be screened is usually large, this method is time consuming and tedious, and the instability of radiolabels represents a significant drawback (Kuroki, 1996). Recently, nonisotopic tracers, such as biotin (Bayer & Wilchek, 1990), fluorescein isothiocyanate (Harlow & Lane, 1989) and europium (Nakamura *et al.*, 1992) have been introduced for determination of epitopes, but this method still has the problem of labelling all antibodies to be tested.

An alternative method is a competition assay using labelled antigen. A constant amount of biotinylated antigen is incubated with a given mAb immobilised on solid phase in the presence of increasing amounts of soluble competitor mAbs (Figure 1.5b). The biotinylated antigen bound to the immobilised antibody is then reacted with avidin-peroxidase conjugate, the bound complex is determined by the use of *o*-phenylenediamine and hydrogen peroxidase.

The competition method is used to determine whether two different mAbs can bind to a monovalent antigen at the same time (in which case they must recognize different epitopes) or whether they compete with each other for antigen binding (in which case they must recognize the same epitope, wholly or partially) (Morris, 1996). A traditional approach to competition mapping using a microtiterplate is the ELISA involving labelling either antibody or antigen with enzymes.

Surface Plasmon Resonance in the BIAcore

BIAcore (biomolecular interaction analysis) biosensor is a functional binding assay in which reactants are not labelled, purification is not necessary and small amounts of the reactants are sufficient for epitope mapping (Johne, 1996). The BIAcore biosensor measures biospecific interactions in real time (Jonsson *et al.*, 1991). The principle is to immobilize the antigen on a sensorchip surface (Lofas & Johnsson, 1990) while the antibody is allowed to continuously flow over the surface, or vice versa. The interaction is then detected by surface plasmon resonance (SPR), directly registered and presented as a sensorgram (Liedberg *et al.*, 1983).

Epitope mapping in the BIAcore may be performed to characterise an antigen or a group of specific monoclonal antibodies, or both (Fagerstam *et al.*, 1990). Characterisation of epitope specificity patterns with a panel of mAb gives valuable information for utilizing mAbs in clinical, diagnostic and technical contexts. The

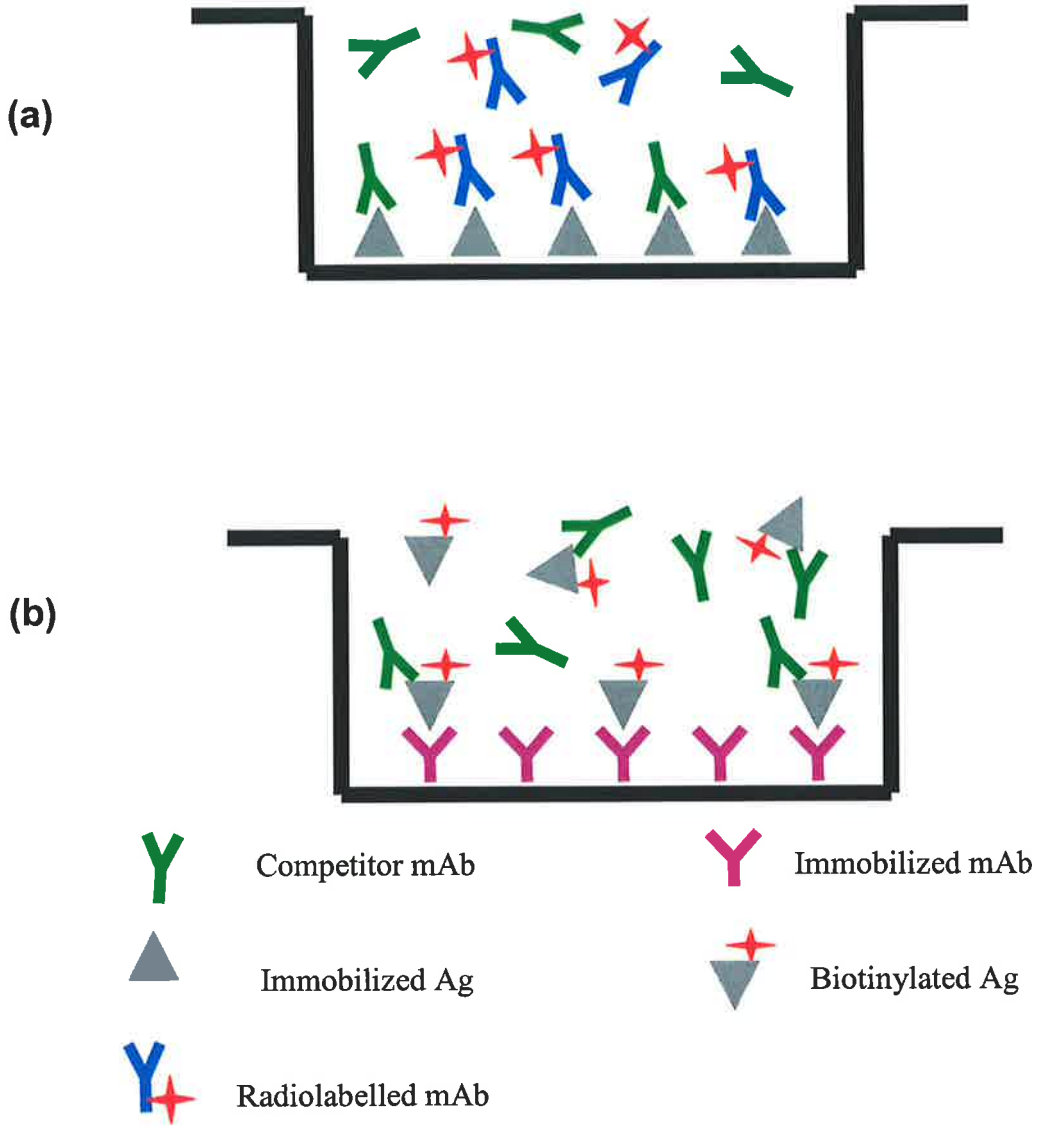

Figure 1.5 A schematic representation of a competition assay with labelled antibody (a) and with labelled antigen (b) used in epitope mapping. In the competition assay with labelled antibody, antigen is immobilised, and a radiolabelled antibody competing with unlabelled antibody are mixed in solution. On the other hand, in the competition assay with labelled antigen, a constant amount of biotinylated antigen is incubated with immobilised antibody coating on the well in the presence of increasing amounts of competitor monoclonal antibodies (Kuroki, 1996).

BIAcore can be used with a capture antibody immobilised to the sensorchip surface. Running multiple combinations of antibodies reveals the competitiveness of the antibodies for different epitopes (Malmborg & Borrebaeck, 1995). This technique was used to characterise the epitopes on recombinant HIV-1 core protein p24 for 29 mouse monoclonal antibodies (Fagerstam *et al.*, 1990). Several studies have defined the epitopes on other proteins also using this technique. For example, the epitopes on human heart myoglobin and human granulocyte colony stimulating factor were described (Johne *et al.*, 1993; Nice *et al.*, 1993).

An alternative approach of epitope mapping is to immobilise the antigen and then analyse the pair-wise binding of different monoclonal antibodies (Figure 1.6). This was carried out for ovine submaxillary mucin (OSM) (Kjeldsen *et al.*, 1988) and with monoclonal antibodies directed against closely related carbohydrate epitopes (Johnson *et al.*, 1986). When using this approach it is important to block all possible sites recognised by the first monoclonal antibody prior to injection of antibody no. 2, as illustrated in the sensorgrams in Figure 1.6 (Malmborg & Borrebaeck, 1995).

Phage display

In recent years bacteriophages have assumed major importance because of their usefulness in cloning and sequencing DNA (Yanisch-Perron *et al.*, 1985) and in phage display, now widely used as a technique for identifying and studying protein-protein interactions (Cortese *et al.*, 1996), in creating novel antibodies (Winter *et al.*, 1994) and in designing model vaccines (Jelinek *et al.*, 1997).

Phage displayed peptide libraries have become powerful tools for identification and characterisation of peptide mimicries that bind to specific antibodies (Cortese *et al.*, 1995; Scott & Craig, 1994). The technology depends on random peptide sequences, displayed on the surface of filamentous bacteriophage, being allowed to interact with

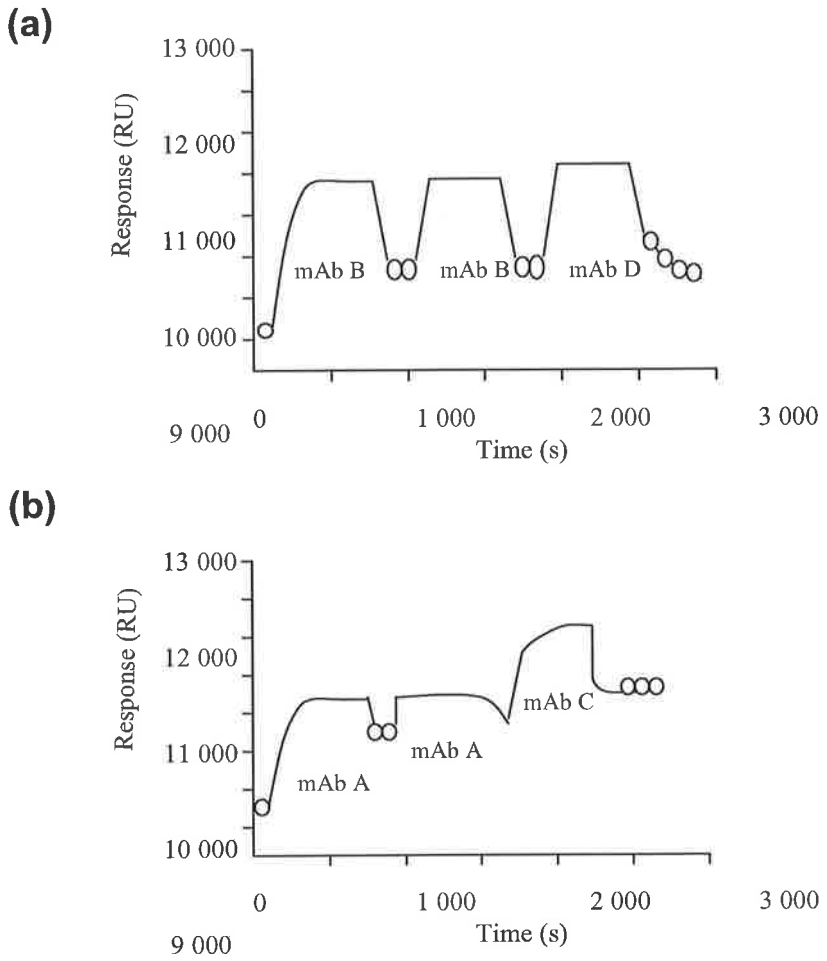

Figure 1.6 A schematic diagram representing sensorgrams determined with the BIAcore technique with antigen immobilised to the sensorchip used in epitope mapping. Two examples of sensorgrams for epitope mapping with the antigen immobilised. The first two pulses represent the saturation of the surface with mAb no. 1, while the third pulse shows the interaction of two different second antibodies that either shared an epitope with antibody no. 1 (a) or did not share an epitope (b) (Malmborg & Borrebaeck, 1995).

antibodies or other ligands. Ligands are usually immobilised on a solid support, such as a petri dish, microplates, or microbeads and binding phage are specifically enriched by several cycles of affinity selection (Parmley & Smith, 1988; Scott & Smith, 1990). The displayed peptides responsible for binding to the antibody can be identified by directly sequencing the encoding insert in the genome of the recombinant phage. This random epitope library strategy has the potential advantage of being able to identify critical residues within an epitope (du Plessis *et al.*, 1994) and of providing mimotopes (Geysen *et al.*, 1986), which can mimic discontinuous epitope structures (Balass *et al.*, 1993; Lane & Stephen, 1993).

Libraries of filamentous phage displaying random peptides have been shown to be highly useful for the identification of epitopes on proteins involved in the binding of mAb or other ligates (Hoess, 1993). Several approaches have been developed to create phage libraries that display discontinuous epitopes within a restricted structural context. By the introduction of a Cys residue at either side of the random peptide a disulphide bond can be generated by oxidation, and this bond constrains the intervening amino acid sequence into a loop (Luzzago *et al.*, 1993). Other methods to obtain highly constrained peptide libraries are based on the integration of random peptides into defined protein scaffolds like immunoglobulin variable domains (Hoogenboom & Winter, 1992; Martin *et al.*, 1994). Moreover, a phage library displaying functional epitopes for human plasminogen-activator inhibitor 1 was constructed by partial digestion of DNA encoding this protein with Dnase I to generate random fragments of 50-200 bp, and this library was successfully used to map the epitope of the monoclonal antibody (van Zonneveld *et al.*, 1995).

Synthetic peptides

The identification of the epitopes with which antibodies react has been done using large libraries of random peptide sequences displayed on the surface of phage particles as described above. Alternatively, vast libraries of random synthetic peptides have been analysed. A relatively simple approach in cases where the overall amino acid sequence of the protein containing the epitopes is known, is to synthesize a defined library of overlapping peptide segments of the protein. These sets of peptide libraries can then easily be tested for binding to the test antibody in simple binding assays and will define the linear epitope to a stretch of 5-15 amino acids (Tribbick *et al.*, 1991).

The multipin method was the first method of multiple peptide synthesis, from its beginnings as a method for testing peptides on the same surface on which they had been synthesized (Geysen *et al.*, 1987). Peptides made using this technology can be applied to the search for and understanding of both linear antibody defined epitopes (B cell epitopes) (Getzoff *et al.*, 1987) and of helper and cytotoxic T cell epitopes (Burrows *et al.*, 1994). The use of peptides permanently attached to the solid phase on which they were synthesized has the advantages of simplicity and sensitivity, but is subject to uncertainty about the quality of the peptides being used, and to artefacts arising from the high density of the peptide and possible interactions with the support matrix (Trifilieff *et al.*, 1991).

An alternative approach to the synthesis of peptides based on the antigen sequence is the use of libraries of completely random peptide sequences. Positional scanning synthetic combinatorial libraries are useful in identifying the amino acid sequences of antigenic determinants recognized by monoclonal antibodies. These libraries are typically composed of tens of millions of non-support-bound peptides, and can be readily screened using ELISA to determine specific sequences that bind to a

target antibody (Pinilla *et al.*, 1996). An advantage shared by all peptide methods is that antigen is not required, which may be important for rare antigens, which are difficult to purify (Morris, 1996).

Recombinant cDNA technology

The advent of systems for the expression of recombinant proteins has allowed an alternative genetic approach to protein fragmentation. In these procedures, the open reading frame encoding the protein is fragmented either randomly or by specific genetic construction, and the reactivity of the expressed fragments of the protein with the test antibody is determined.

The versatility of DNA fragmentation protocols combined with the vast range of available systems for the expression of recombinant protein has created an almost infinite number of variants on this theme. All of these variants are effective, because only small amounts of protein need to be expressed to determine whether an antibody can bind to it (Scott & Smith, 1990). Even if only a small fraction of the expressed protein fragment folds correctly it can be sufficient to give positive antibody binding, making this method useful for mapping the binding sites of antibodies to both conformational and linear epitopes (Mink *et al.*, 1994).

The localization of an epitope follows directly from the location of the gene fragment that on expression yields an antigenic recombinant product (van Vliet *et al.*, 1994). The many prokaryotic expression systems that are available can be combined with several methods to generate fragments from the gene of interest. Restriction enzyme fragments and PCR products yield a rapid localization of the antigenic regions. Expression of oligonucleotides can be useful for an accurate localization as an alternative to synthesizing peptides (Pappu *et al.*, 1993). All of these libraries can be

used in simple immunochemical assays to determine whether they contain the relevant epitope.

Another useful example is a protocol, called expression-PCR (E-PCR), in which defined gene fragments are produced by PCR and then transcribed and translated into protein *in vitro* in the presence of radiolabelled amino acids. This technique is a rapid and simple method for the *in vitro* production of proteins without having to go through the rigors of cloning. The resulting radiochemically pure proteins are useful for a variety of purposes, such as studies on the subunit structure of proteins, epitope mapping and protein mutagenesis (Burch *et al.*, 1993).

The application of mutagenesis techniques has now become a powerful method to identify the amino acids within the epitope that are critical for immune recognition. This is accomplished by testing the role of the critical amino acid residues within the context of short peptides. This enables substitution of specific amino acids within the protein of interest, allowing the production of mutant proteins containing specifically altered amino acid residues (Alexander, 1996). There have been many applications of site-directed mutagenesis in combination with recombinant cDNA technology to distinguish structure and function relationships of proteins using epitope mapping. For example, the functional epitopes within the kinase domain receptor (KDR) of vascular endothelial growth factor (VEGF) for binding to neutralizing anti-KDR antibodies and to the natural ligand, VEGF, were studied by generation of a series of KDR deletion mutants. In combination with alanine mutations, the residues within this region of domain 3 critical for VEGF binding were revealed (Lu *et al.*, 2000). Similarly, the mechanism for interference of serpin plasminogen activator inhibitor-1 (PAI-1) function has been identified using epitope mapping of a monoclonal antibody that inhibits rat

PAI-1 activity and increases the binding of inactive PAI-1 to vitronectin (Ngo *et al.*, 2001).

Mass spectrometry

The methods used for the mapping of linear epitopes in proteins include binding assays of protein components produced by synthetic chemistry, by synthetic and bacteriophage peptide libraries or by recombinant gene expression. Although effective, these methods can be costly and time consuming. Recently, mass spectrometry, a different approach to antigenic site mapping was incorporated into procedures to define epitope mapping. In a mass spectrometric based method, peptide mixtures can be analysed rapidly (<1 min) and accurately at low sample levels (Kiselar & Downard, 1999). The identification of epitopic peptides released from immobilized antibody following limited proteolysis of an immobilized antibody-antigen complex was employed by plasma desorption mass spectrometry (PD-MS) (Suckau *et al.*, 1990). The same strategy was used to localise the epitope of gastrin-releasing peptide with the exception that matrix-assisted laser desorption ionisation mass spectrometry (MALDI-MS) was employed (Papac *et al.*, 1994; Parker *et al.*, 1996).

Recently, affinity directed mass spectrometry has been employed for mapping protein epitopes. The basis of this technique is the use of a direct molecular mass read out from the immune complex to determine the specific component of the protein antigen that interacts with the antibody. Proteolytic digestion and affinity directed mass spectrometry can be used to determine the approximate location of a continuous component of a binding epitope rapidly within a protein ligand (Zhao & Chalt, 1994).

Matrix assisted laser desorption time of flight (MALDI-TOF) mass spectrometry has been used in combination with epitope excision/extraction techniques for the rapid characterisation of linear epitopes. In epitope excision methods, the protein of interest

is complexed with the antibody and then digested enzymatically. Only fragments that are protected by the antibody remain affinity bound and can be identified. In epitope extraction, the antigen of interest is first digested enzymatically and subsequently passed over immobilised antibody beads (Parker *et al.*, 1996). The example demonstrating the use of epitope excision/extraction techniques followed by MALDI-TOF was the elucidation of a discontinuous epitope in the HIV envelope protein HIV-gp120, recognised by the human monoclonal antibody 1331A (Hochleitner *et al.*, 2000). Yi and Skalka (2000) also illustrated this technique in mapping the epitopes of two monoclonal antibodies that bind to the C-terminal domain of HIV type1 integrase (Yi & Skalka, 2000).

1.5.2 Applications for epitope mapping

Epitope mapping has numerous potential applications in many areas as described below:

Physiology

Monoclonal antibodies can play a key role in defining structural, functional and regulatory aspects of complex protein-protein interactions (Lane & Stephen, 1993; Stephen *et al.*, 1995). The interaction of factor VIII with its physiological chaperone i.e. the von Willebrand factor, in the coagulation pathway (Saenko *et al.*, 1994), the interaction of interleukin-2 with its surface receptor (Lorenzo *et al.*, 1991) or the study of the different reacting sites of interleukin 4 (Ramanathan *et al.*, 1993) are examples of this area in defining epitope mapping. This can help analysing the function of a hormone and is physiological regulation (Malthiery *et al.*, 1991; Soos *et al.*, 1992) or of an enzyme (Wasserman *et al.*, 1993).

Pathology

Epitope mapping is useful in analysing the specificity of antibodies spontaneously formed in a number of diseases in which an immune response is an important parameter. These applications are involved in autoimmune diseases, for example myasthenia gravis (Papadouli *et al.*, 1993), type I diabetes (Ujihara *et al.*, 1994) or thyroid diseases (Henry *et al.*, 1992), and immune responses towards exogenous antigens, such as factor VIII in haemophilia A patients (Ware *et al.*, 1992). Understanding the mechanism by which an immune mediated pathology develops requires a precise identification of both B and T cell epitopes on the antigen. This will be essential to unravel the mechanisms by which immune tolerance is established (Saint-Remy, 1997).

Vaccination

The identification of both B and T cell epitopes on a microorganism (Churchill *et al.*, 1994; Moradpour *et al.*, 2002; Oettinger & Andersen, 1994; Wang *et al.*, 1999) or bacterial derived product (such as toxins) (Logan *et al.*, 1991) and Kazemi & Finkelstein, 1991) may have a determining influence on the design of vaccines. This includes not only increasing the efficiency of vaccines, but also potentially the design of vaccines. The modelling of the NMR defined epitope of antigen-antibody complex should not only greatly aid in the design of an effective synthetic peptide vaccine, but should also contribute to the understanding of the molecular factors involved in immunogenicity and pathogenicity (Campbell *et al.*, 1997).

Mechanism of drug action

The use of epitope mapping to study the mechanism of action of drugs is of interest in many applications. For example, using the phage display library method, a biologically active cyclic peptide agonist for erythropoietin receptor was identified

(Dower, 1998). Similarly, Chirinos *et al.* (1997) screened one-bead one-compound (OBOC) peptide libraries with the tumor necrosis factor-alpha, (TNF-α) and anti-TNF-α antibody system, and thus identified peptides able to inhibit TNF-α-mediated cytotoxicity (Chirinos *et al.*, 1997). A phage display library was used to identify peptides that inhibited human complement formation by binding C3 (Sahu *et al.*, 1996).

1.6 PROJECT RATIONALE

PC is typical of many other biotinylated enzymes and metabolically important proteins, and has been widely investigated by many groups since it was first described by Utter and Keech (1960). Studies of the kinetic and physical properties of PC have provided a significant understanding of the chemical mechanism of the catalytic reaction of PC. However, it still remains unknown from these studies how the structure and residue composition of PC enables this critical chemistry to proceed. With the increasing ease with which protein sequences are inferred from cDNA or genomic libraries, more sequence information will become available on PC from a wide diversity of sources. Sequence homologies between these enzymes strongly suggest that all operate via a similar catalytic mechanism. Comparison of these sequences of PC obtained from different organisms would lead to identification of structurally important residues which might play a common role in the catalytic reaction. A comprehensive understanding of PC's catalytic mechanism is therefore important since it could be potentially used as a model system to understand the function of all biotinylated enzymes. In order to fully understand the reaction mechanism of PC, it is necessary to know which amino acid residues are involved in catalysis or substrate binding sites and which residues are important for maintaining the correct conformation.

However, a thorough understanding of the catalytic reaction mechanism of PC will require knowledge of the three-dimensional structure of the molecule, which has not yet been obtained. Due to the absence of high resolution structural determination by NMR or X-crystallography, the elucidation of the catalytic mechanism must be addressed by other means. An immunological approach to the analysis of protein structure, together with identification of epitopes of interest have been used extensively as a method of investigating the functional roles of potential catalytic residues in proteins. Monoclonal antibodies against sheep PC have been developed in our laboratory (Carey, 1988). In addition, a full-length human PC cDNA clone has also been isolated and expressed in 293T cells (Jitrapakdee *et al.*, 1999). This greatly enhances the possibility to obtain more knowledge of the structure-function relationship of human PC by epitope mapping using those monoclonal antibodies. Recent sequencing studies of cDNAs encoding PC have shown that the homology of PC among different mammalian species is very high (≥ 96% between human, rat and mouse) (Jitrapakdee *et al.*, 1996). We expect therefore that monoclonal antibodies against sheep PC will cross-react against human PC.

Antibodies may also be used to study residues important for functional activity of an enzyme. For example, the enzyme activity of luciferase was changed due to polyclonal antibody binding as determined by reaction kinetics (Tsuji *et al.*, 1960). The determination of equilibrium and rate constants of the interaction of an activity-inhibiting monoclonal antibody with alkaline phosphatase of the calf intestine was described by Ehle *et al.* (1989) and Cumme *et al.* (1990). Later, Cumme *et al.* (1995) described the characterisation of the interaction of alkaline phosphatase with an activity inhibiting monoclonal antibody by progress curve analysis. In our laboratory, Carey (1988) has demonstrated that three monoclonal antibodies affected the catalytic

activity of sheep PC and that their effects on enzymatic activity were influenced by various substrates. This finding of inhibitory antibodies may lead to definition of critically functional residues of human PC's epitopes. One could potentially investigate the role of these residues as catalytic residues in PC reaction using site-directed mutagenesis of these residues.

This project will be the first to investigate the hPC's epitope map of inhibitory antibodies, together with site-directed mutagenesis of the critically functional residues and the effect of altering individual residues on the activity of PC.

The specific aims of this thesis were

1. To characterise a number of monoclonal antibodies generated against sheep PC, by assaying cross-reactive binding and their inhibitory effects on the acetyl-CoA dependent activity of human PC using a stable cell line expressing full-length human PC.

2. To define minimal epitopes on human PC for three inhibitory antibodies by expression of fusion protein fragments and mapping by cross-reactive binding assay.

3. To investigate the effect on the activity of PC using site-directed mutagenesis to alter critically functional residues.

4. To establish a high-level expression system for human PC devoid of endogenous PC. This system would be used to express mutants of human PC for further studies of kinetic and physicochemical properties.

CHAPTER 2

Material and General Methods

CHAPTER 2

2.1 CHEMICALS

The following chemicals were obtained from Sigma Chemical Co., St Louis, MO., USA: agarose (type 1), ampicillin, ATP (disodium, grade I), β-mercaptoethanol, bovine serum albumin (BSA), 5-bromo-4-chloro-3-indolyl-β-D-galactopyranoside (BCIG), 5-bromo-4chloro-3-indolyl-phosphate-p-toluidine salt (BCIP), Coomassie Brilliant Blue (G_{250}, R_{250}), cycloheximide, dithiothreitol (DTT), ethidium bromide, ethylenediaminetetraacetic acid (EDTA), nicotinamide adenine dinucleotide (reduced form) [NADH], nitroblue tetrazolium (NBT), phenylmethylsulphonyl fluoride (PMSF), polyoxyethylene-sorbitan monolaurate (Tween-20), puromycin, rubidium chloride, sodium dodecyl sulfate (SDS), sodium pyruvate, glycyl glycine, N,N,N,N-tetramethylethylenediamene (TEMED), Tris (hydroxymethyl)methylamine (Tris) and Triton X-100. Glycogen was purchased from Boehringer Mannheim. Acrylamide and bisacrylamide were purchased from BioRad Laboratories Inc., Herates, CA, USA Sephadex G25, Sepharose CL-6B and Ficoll 400 were purchased from Pharmacia, Uppsala, Sweden. Eu-chelate of N^1-(p-isothiocyanatobenzyl)-diethylenetriamine-N^1 N^2 N^3 N^3-tetraacetic acid (DTTA) was purchased from Delfia, Wallac, Turku, Finland. Other fine chemicals were purchased from Merck Pty. Ltd., Kilsyth, Vic., Australia.

2.2 RADIOCHEMICALS

$NaH^{14}CO_3$ was purchased from Amersham Australia, North Ryde, NSW, Australia.

2.3 OLIGONUCLEOTIDES

All oligonucleotides used in this study were purchased from Geneworks Ltd., Adelaide, South Australia. The oligonucleotides used for PCR and site-directed mutagenesis were described in Chapters 3, 4 and 5. The restriction sites in the oligonucleotides are underlined and mutagenic changes are in bold. The sequences of the oligonucleotides are listed below.

2.3.1 Oligonucleotides using for PCR in Chapter 3

BC for: 5'TTGGTAGAATTCATGCTGAAGTTCCGAACAGTCCATGGG 3'

BC rev: 5'TTAATTCTCGAGTTATCATGGAACAGCTCTGGGTTCTCGTCGATG3'

F1 for: 5'AATTGGTAGAATTCACTGTGGACACCCAGTTCATCG 3'

F1 rev: 5'GAAGTTATGCGGCCGCTTATCAGTACTTGGTGCGGCTGGGGTCGG3'

F2 for: 5'AATTGGTAGAATTCGCCGACCCCAGCCGCACCAAG 3'

F2 rev: 5'GATTAATTCTCGAGTTATCAGACACCGATGTAGCCCTGCAGGA 3'

F3 for: 5'AATTGGTAGAATTCTTCCTGCAGGGCTACATCGGTGTCC 3'

F3 rev: 5'GATTAATTCTCGAGTTATCACTCGATCTCCAGGATGAGGTCG 3'

TB1 for: 5'AATTGGTAGAATTCTTCCTGCAGGGCTACATCGGTGTCC 3'

TB1 rev: 5'GATTAATTCTCGAGTTATCAGAAGACCTGCCTCTGGCCGGCCC 3'

TB2 for: 5'AATTGGTAGAATTCTTTGAGGTGGAGCTGGAGCGGGG 3'

TB2 rev: 5'GATTAATTCTCGAGTTATCACTCGATCTCCAGGATGAGGTCG 3'

NEG for: 5'AATTGGTAGAATTCGCCTTCGACTGCACGGCCACC 3'

NEG rev: 5'GATTAATTCTCGAGTTATCACTCCACCACGGAGCGGGGAAAGG 3'

TB1 80cR: 5'GATTAATTCTCGAGTTATCAAAAGGTGGCAGTGAAGTCCTTG 3'

TB1 40cR: 5'GATTAATTCTCGAGTTATCACAGATCCAGGGGAGGGAGGG 3'

TB1 34cR: 5'GATTAATTCTCGAGTTATCAGGAGGCTCCAGGCCGCCCC 3'

TB1 27cR: 5'GATTAATTCTCGAGTTATCACACCCTTGGCAGGTCCTTCAG 3'

TB1 20cR: 5'GATTAATTCTCGAGTTATCATACCTTAGAGCGAAAGGGTTCGGG3'

TB2 121cR: 5'GATTAATTCTCGAGTTATCACAGTGTCATGTCCTTGGTCAC 3'

TB2 111cR: 5'GATTAATTCTCGAGTTATCAGCGGACAGTACCCTCCATGGGTG 3'

TB2 91cR: 5'GATTAATTCTCGAGTTATCAACACAGGGGCTGGCCCTTGGC 3'

TB2 71cR: 5'GATTAATTCTCGAGTTATCACCCAGGCATGGGCGCCCCG 3'

TB2 44cR: 5'GATTAATTCTCGAGTTATCAGTCCTTGACCAAGATGGACCGC 3'

TB2 37cR: 5'GATTAATTCTCGAGTTATCACAGCTGCCCATTGAGCTCAAAGA 3'

TB2 107nF: 5'AATTGGTAGAATTCGCCGGCCAGAGGCAGGTCTTC 3'

TB2 80nF: 5'AATTGGTAGAATTCATGCACTTCCACCCCAAGGCC 3'

TB2 60nF: 5'AATTGGTAGAATTCAAGGTGATAGACATCAAAGTG 3'

TB2 20nF: 5'AATTCAAGGTTCATGTGACCAAGGACATGACACTGGAAGGTGA
CGACCTCATCCTGGAGATCGAGTGATAAC 3'

TB2 20nR: 5'TCGAGTTATCACTCGATCTCCAGGATGAGGTCGTCACCTT
CCAGTGTCATGTCCTTGGTCACATGAACCTTG 3'

TB2 10nF: 5'AATTCGAAGGTGACGACCTCATCCTGGAGATCGAGTGATAAC3'

TB2 10nR: 5'TCGAGTTATCACTCGATCTCCAGGATGAGGTCGTCACCTTCG 3'

2.3.2 Oligonucleotides using for site-directed mutagenesis in Chapter 4

K969A for: 5'AATTGGTAGAATTCGAACCCTTTCGCTCTAAGGTACTG**GCC**
GACCTGCCAAGGGTGGAGGGG3'

D970A for: 5'AATTGGTAGAATTCGAACCCTTTCGCTCTAAGGTACTGAAG**GCC**
CTGCCAAGGGTGGAGGGGCGG 3'

L971A for: 5'AATTGGTAGAATTCGAACCCTTTCGCTCTAAGGTACTGAAGGAC
GCCCCAAGGGTGGAGGGGCGGCCTG 3'

P972A for: 5'AATTGGTAGAATTCGAACCCTTTCGCTCTAAGGTACTGAAGGAC
CTG***GCC***AGGGTGGAGGGGCGGCCTGGAGCC 3'

V974A for: 5'AATTGGTAGAATTCGAACCCTTTCGCTCTAAGGTACTGAAGGAC
CTGCCAAGG***GCC***GAGGGGCGGCCTGGAGCCTCC 3'

E975A for: 5'AATTGGTAGAATTCGAACCCTTTCGCTCTAAGGTACTGAAGGAC
AAGGACCTGCCAAGGGTG***GCC***GGGCGGCCTGGAGCCTCCCTC 3'

MTC rev: 5'GATTAATTGCGGCCGCTTATCACTCGATCTCCAGGATGAGGTC 3'

MpBlue for: 5'GTTTTCGCCCCGAAGA***G***CGTTTTCCAATGATG 3'

MpBlue rev: 5'CATCATTGGAAAACG***C***TCTTCGGGGCGAAAAC 3'

2.3.3 Oligonucleotides using for site-directed mutagenesis in Chapter 5

M1116AF: 5'GCCAGATCGGGGCGCCC***GCA***CCTGGGAAGGTGATAG 3'

M1116AR: 5'CTATCACCTTCCCAGG***TGC***GGGCGCCCCGATCTGGC 3'

K1119AF: 5'GCGCCCATGCCTGGG***GCA***GTGATAGACATCAAAG 3'

K1119AR: 5'CTTTGATGTCTATCAC***TGC***CCCAGGCATGGGCGC 3'

S1141AF: 5'CCCCTGTGTGTGCTC***GCC***GCCATGAAGATGGAG 3'

S1141AR: 5'CTCCATCTTCATGGC***GGC***GAGCACACACAGGGG 3'

M1143LF: 5'GTGTGTGCTCAGTGCC***CTG***AAGATGGAGACTGTG 3'

M1143LR: 5'CACAGTCTCCATCTT***CAG***GGCACTGAGCACACAC 3'

M1143AF: 5'GTGTGTGCTCAGTGCC***GCC***AAGATGGAGACTGTG 3'

M1143AR: 5'CACAGTCTCCATCTT***GGC***GGCACTGAGCACACAC 3'

D1165AF: 5'GTTCATGTGACCAAG***GCA***ATGACACTGGAAGGTG 3'

D1165AR: 5'CACCTTCCAGTGTCAT***TGC***CTTGGTCACATGAAC 3'

L1168AF: 5'GACCAAGGACATGACA***GCC***GAAGGTGACGACCTC 3'

L1168AR: 5'GAGGTCGTCACCTTC***GGC***TGTCATGTCCTTGGTC 3'

E1169AF: 5'CAAGGACATGACACTG***GCA***GGTGACGACCTCATC 3'

E1169AR: 5'GATGAGGTCGTCACC***TGC***CAGTGTCATGTCCTTG 3'

2.4 MOLECULAR BIOLOGY KITS

The Ultra Clean™ gel spin DNA purification kit and Ultra Clean™ Mini Plasmid Prep kit were purchased from Geneworks, Ltd., Adelaide, South Australia.

2.5 ENZYMES AND PROTEIN MARKERS

All restriction enzymes were purchased from Pharmacia, Uppsala, Sweden and Geneworks Ltd., Adelaide, South Australia. T4 DNA ligase, T4 DNA polymerase, T4

polynucleotide kinase, *Taq* polymerase and Moloney murine leukemia virus reverse transcriptase (MMLV-RT) were purchased from Promega, Madison, WI, USA *Pwo* and avian myeloblastosis virus reverse transcriptase (AMV-RT) were purchased from Boehringer Mannheim. Advantage^{TM}, *Tth* polymerase mix was purchased from CLONTECH, Palo Alto, CA, USA Malic dehydrogenase, RNase A, DNaseI, anti-rabbit IgG-antibodies, and avidin-conjugated with alkaline phosphatase were purchased from Sigma. Biotinylated protein markers was obtained from BioRad. Protein marker (Mark12) was obtained from Novex, Invitrogen (USA). ^{14}C-labelled molecular weight markers were purchased from Amersham.

2.6 BACTERIAL AND YEAST STRAINS

E. coli DH5α: *supE44ΔlacU169(p80lacZΔM15) hsdR17 recA1* endA1 *gyrA96 thi-1 relA1.* The host for recombinant plasmids (New England Biolabs, USA)

E. coli AD494 (λDE3): *Δara-leu7697 ΔlacX74 ΔphoAPvuII phoR ΔmalF3F* [lac^+ *(lacI) pro*] *trxB*::kan (λDE3). The host for recombinant plasmid expression in the pET system (Novagen, Germany)

E. coli BL21 (λDE3): F^- *ompT* $hsdS_B$ ($r_B^- m_B^-$) *gal dcm* (λDE3). The host for expression in the pET system (Novagen, Germany)

E. coli Rosetta (λDE3) pLysS: F^- *ompT* $hsdS_B$ ($r_B^- m_B^-$) *gal dcm lacY1* (λDE3) pLysSRARE (*argU, argW, ileX, glyT, leuW, proL*) (Cm^R). The host for expression in the pET system (Novagen, Germany)

E. coli BL21-codon Plus (λDE3)-RIL: F^- *ompT* $hsdS_B$ ($r_B^- m_B^-$) *gal λ* (DE3) *endA1* (*argU, ileY, leuW,* Cm^R). The host for expression in the pET system (Stratagene, La Jolla, CA, USA.)

E. coli M 15 [pREP4] and SG13009 [pREP4]: *Nal*^{s} *Str*^{s} *rif*^{s} *lac*$^{-}$ *ara*$^{-}$ *gal*$^{-}$ *mtl*$^{-}$ *F*$^{-}$ *recA*$^{+}$ *uvr*$^{+}$. The host for expression in the pQE system (Qiagen, USA)

Yeast strain W303: MATa/*MAT*α*ADE2/ade2 CAN1/can1-100 CYH2/cyh2 his3-11,15/his3-11,15 LEU1/leu1-c LEU2/leu2-3,112 trp1-1:URA3:trp1-3'*Δ */trp1-1 ura3-1/ura3-1.* The host for expression in the pVT-100 system (Vernet *et al.*, 1987)

2.7 BACTERIAL AND YEAST GROWTH MEDIA

2.7.1 Bacterial growth media

LB broth: 1% (w/v) Bacto-tryptone (Difco), 0.5% (w/v) yeast extract (Difco), 1% (w/v) NaCl, adjusted to pH 7.0 with NaOH.

LB agar plates were made by adding 1.5% (w/v) Bacto-agar (Difco) to the LB broth.

LMN agar plate: 0.1% tryptone, 0.5% (w/v) NaCl, 0.4% (w/v) maltose and 0.2% (w/v) $MgSO_4$, 1.5%(w/v) Bacto-agar.

NZCYM agar plate: 1% (w/v) Nzamine, 0.5% (w/v) NaCl, 1% (w/v) casamino acid, 0.5 % (w/v) yeast extract, 0.25% $MgSO_4$ and 0.7% (w/v) Bacto-agar.

Long term storage of plasmids in bacteria was carried out by adding 40% glycerol to an overnight culture of *E. coli* in LB-broth followed by storage at -80°C.

2.7.2 Yeast culture media

YP broth: 1% (w/v) yeast extract (Difco), 2% (w/v) bacteriological peptone.

URA^{-} broth: 0.8% (w/v) yeast nitrogen base, 1.1% (w/v) casein amino acid, 0.02% (w/v) adenine, after autoclaving, glucose, tryptophan and leucine was added to a final concentration of 2%, 0.01% and 0.01% respectively.

URA^{-} agar plates were made by adding 2.2% (w/v) Bacto-agar (Difco) to the URA^{-} broth.

YP broth was used for growth of W 303 yeast strain. URA^- media was used for selection of transformed yeast.

2.8 MAMMALIAN CELL LINES

human embryonic kidney cell line (293T; ATCC: CRL 1573)

2.9 CELL CULTURE MEDIA

Dulbecco's Modified Eagle's Medium (DMEM) (Gibco), 28 mM $NaHCO_3$, 19 mM glucose and 20 mM Hepes, pH 7.3

RPMI 1840 (Gibco) supplemented with 50 mM β-mercaptoethanol, 1 mM sodium pyruvate, 10 mM Hepes, pH 7.35

Fetal calf serum : Gibco, USA

2.10 PLASMIDS

1. pBluescript II (SK); Stratagene, La Jolla, CA, USA

2. pET-32a (+); Novagen, Germany

3. pEFIRES-puro; obtained from Dr. Steven Hobbs, CRC for Cancer Therapeutics, Institute of Cancer Research, London, UK

4. pQE32 ; Qiagen, USA

5. pVT100-U; obtained from Dr. Michelle Walker, University of Adelaide, Australia

6. pMON1503; obtained from Dr. Murray Whitelaw, University of Adelaide, Australia

7. pMON1504; obtained from Dr. Murray Whitelaw, University of Adelaide, Australia

2.11 DNA TECHNIQUES

2.11.1 Small-scale purification of plasmid DNA from E. coli for restriction enzyme digestion and sequencing

A single colony of bacteria was grown in 10ml of LB media in the presence of the appropriate antibiotic at 37°C overnight. Two ml of culture media were centrifuged at 10000 x g for 1 min to pellet the cells. The supernatant was removed, the pellet was recentrifuged for 10 seconds and all remaining supernatant aspirated. The pellet was resuspended in cell suspension buffer (25 mM Tris-HCl pH 8, 10 mM EDTA, RNase A). One hundred microliters of lysis buffer [1% (w/v) SDS in 0.2 M NaOH] were added and mixed by inverting the tube 6 times, followed by 330 µl of neutralisation buffer (3 M potassium acetate, pH 5.2). The cell debris was precipitated by centrifugation at 10,000 x g for 5 min. The supernatant, containing plasmid, was transferred to a spin filter and centrifuged at 10,000 x g for 30 sec, leaving the plasmid DNA bound to the filter membrane. The spin filter membrane was washed with wash buffer (45% Ethanol, 10 mM Tris/NaCl). The plasmid DNA was eluted with 50 µl of sterile water from the spin filter by centrifugation at 10,000 x g for 30 sec.

2.11.2 Restriction endonuclease digestion of DNA

From 5 to 10 µl of DNA (in water) was digested with 5U of restriction enzyme. Restriction digests were performed at the concentration of One-Phor-All Plus buffer (Pharmacia, U.S.A.) recommended by the manufacturer. The reaction was performed in a final volume of 20 µl for 2 hour at 37°C. Five microliters of 5x DNA loading dye (50% glycerol, 1% bromophenol blue, 1% xylene cyanol in TBE) were added to terminate the reaction and 25 µl were loaded onto an agarose gel for electrophoresis.

2.11.3 Agarose gel electrophoresis of DNA

DNA samples were separated by agarose gel electrophoresis. An agarose gel (1% agarose in TBE buffer) was submerged in TBE running buffer (100 mM Tris-borate pH 8.3, 2.5 mM EDTA). The DNA sample in loading buffer (10% glycerol, 0.2% bromophenol blue, 0.2% xylene cyanol in TBE) was loaded into wells nearest the cathode. Electrophoresis was performed at 100-150V for 20-30 min. The gel was then stained in 1.0 μg/ml ethidium bromide for 10 min, followed by destaining in water for 10 min. The DNA sample was then visualised under short or long wavelength UV light.

2.11.4 Purification of DNA fragments from agarose gel using UltraClean GelSpin kit

A slice of agarose containing the DNA fragment of interest was excised under a long wavelength UV-transilluminator and put in a 1.5 ml microtube. Three volumes of GelBind buffer (Geneworks, Australia) [$NaClO_4$ solution] were added to a slice of gel and incubated at 65°C for 5 min. The solution was mixed and transferred onto the spin filter basket followed by centrifugation at 10,000 x g for 10 sec. The bound DNA was washed with 300 μl of Gel wash buffer (Tris/Ethanol solution). The spin filter was centrifuged at 10,000 x g for 10 sec, the flow-through discarded and the filter was centrifuged for another 30 sec. DNA was eluted from the filter with 50 μl of water by centrifugation for 30 sec.

2.11.5 Ligation

Plasmid DNA and insert DNA were digested with restriction enzymes that generated compatible ends. The ligation was routinely carried out in a total volume of 20 μl containing DNA with a ratio of insert : vector of 2:1 (mass ratio). The ligation was performed in 1X ligation buffer (66 mM Tris-HCl, pH 7.5, 5 mM $MgCl_2$, 1.0 mM DTT, 1.0 mM ATP) and 2U of T4 DNA ligase, at 14°C overnight.

2.11.6 Bacterial transformation

A single colony of *E. coli* DH5α was grown in 2 ml of LB broth at 37°C overnight. Overnight culture (330 µl) was then subcultured into 10 ml of LB broth and grown to A_{600} of 0.5-0.6. Five millilitres of the culture wer transferred to a new flask containing 100 ml of LB broth and grown to A_{600} of 0.5-0.6. Cells were pelleted by centrifugation at 5000 x g for 10 min and suspended in 40 ml of transformation buffer-1 (30 mM potassium acetate, 100 mM rubidium chloride, 10 mM $CaCl_2$, 50 mM $MnCl_2$ and 15% glycerol, pH 5.8) and incubated on ice for 10 min. Cells were pelleted by centrifugation at 5000 x g for 10 min and resuspended in 4 ml of transformation buffer-2 (10 mM MOPS acid, 10 mM rubidium chloride, 75 mM $CaCl_2$ and 15% glycerol, pH 6.5) and incubated on ice for 15 min. Competent cells were taken in aliquots (200 µl) and kept at -80°C until required.

Typically, 100 µl of frozen competent cells were thawed out, mixed with 10 µl of ligation reaction and left on ice for 30 min. The DNA and cell mixture was incubated at 42°C for 2 min before being moved back onto ice for 5 min. The transformed cells were allowed to recover by incubation in 2 ml of LB broth at 37°C for 45 min before plating. The recombinant clones were distinguished from non-recombinant clones on the basis of the α-complementation of β-galactosidase (*lac* Z) gene expression, using LB plates containing IPTG as the inducer and X-gal as the substrate of β-galactosidase. Blue colonies indicated the non-recombinant clones while white colonies indicated the recombinant clones as a result of disruption of the β-galactosidase α fragment on the plasmid.

2.11.7 DNA sequencing using Dye Primer sequencing

Plasmid DNA isolated according to the method described in 2.11.1, was further purified by adding 1 µl of 10 mg/ml RNase A to 20 µl of plasmid sample and incubating

at 37°C for 30 min. Twenty-five microlitres of 7.5 M of ammonium acetate and 40 µl of isopropanol were then added, mixed and left at -20°C for 1 h. The tube was then centrifuged at 13,000 rpm for 15 min and the pellet was washed once with 300 µl of 75% ethanol in 50 mM sodium acetate and once with 100% ethanol. The pellet then was dried and dissolved in 20 µl of water. The sequencing reaction was performed in a single 0.5 ml tube containing 1 µg of plasmid template, 8 µl of dye terminator mix and 100 ng of oligonucleotide primer. The reaction was adjusted to a final volume of 20 µl and overlaid with 100 µl of mineral oil before being subjected to PCR. The PCR profile consisted of 25 cycles of denaturation at 96°C for 30 sec, annealing at 50°C for 15 sec and extension at 60°C for 4 min. After the cycles were completed, the mineral oil was removed and the sequencing products were precipitated by adding 0.1 volumes of 3 M of sodium acetate and 2 volumes of absolute ethanol. The DNA was precipitated by centrifugation at 13,000 rpm for 15 min. The pellet was dried under vacuum and submitted to the sequencing service at the Institute of Medical and Veterinary Science, Adelaide.

2.11.8 Polymerase chain reaction (PCR)

PCR reaction mixtures were prepared in a laminar flow cabinet and all apparatus used was UV irradiated before use. The PCR reaction was carried out in 0.5 ml Eppendorf tube in a total volume of 50 µl containing 10-100 ng of template DNA, 100 ng of each oligonucleotide primer, 200 µM of each dNTP and 2.5 U of Pwo DNA polymerase in 1x PCR buffer [10 mM Tris-HCl pH 8.85, 25 mM KCl, 5 mM $[(NH_4)_2SO_4$, 2 mM $MgSO_4]$. After all components were mixed, the reaction was overlaid with 2 drops of light liquid paraffin oil. Thermal cycling was performed in a Perkin Elmer Cetus, DNA Thermal cycle. Cycling profiles varied depending on the length of the template and primer annealing temperature, however a general profile is

presented as follows: The reaction mixture was subjected to 30 rounds of PCR amplification. The PCR profile consisted of an initial denaturation at 95°C for 1 min followed by 30 cycles of denaturation at 95°C for 30 sec, annealing at 60°C for 1 min and extension at 72°C for 1 min. A final extension cycle at 72°C for 5 min was completed before the reaction terminated by lowering the temperature to 4°C. PCR product was analysed by agarose gel electrophoresis as described in Section 2.11.3.

2.11.9 Transformation of plasmid DNA into yeast

Transformation of plasmid DNA into yeast was performed by the Lithium acetate method as follows. A 10 ml overnight culture was set up at 30°C with vigorous shaking. The culture was diluted 1:40 into fresh media and grown under the same condition until the A_{600} = 0.6-0.8. One millilitre of cell culture was taken and centrifuged for 10 sec at 13,000x g in a 1.5ml Eppendorf tube to pellet the cells. The cells were washed once with sterile water and centrifuged as described above followed by the addition of the solution containing 20 µl of 10x TE buffer (0.1 M Tris-HCl and 10 mM EDTA), 20 µl of 1M Lithium acetate in 160 µl of sterile water). A DNA cocktail containing sonicated salmon sperm DNA in water at 10 mg/ml and 20 µg of transforming DNA was denatured at 100°C for 5 min and placed on ice for 5 min before the DNA cocktail was added to the yeast cell. Finally, 1.2 ml of PEG 3350 solution containing 8 volume of 50% PEG 3350, 1 volume of 10x TE buffer and 1 volume of 1 M Lithium acetate was added and the solution gently mixed to evenly suspend the cells. The solution was incubated for 30 min at 30°C and further incubated for 15 min at 42°C to heat shock the cells. The cells were centrifuged at 13,000x g for 10 sec and the supernatant was removed. Then the cells were suspended in 100 µl PBS and 50 µl of the cells were plated on to selection plates with a sterile spreader.

2.11.10 Protein extraction from yeast with lyticase

The protein extraction from yeast was carried out as described by van Burik *et al.* (1998) with some modifications as follows. An overnight 100ml yeast culture was grown to an A_{600} = 0.6-0.8 at 30°C with vigorous shaking. The cells were collected by centrifugation in 50 ml Falcon tubes at 1,500x g for 5 min at 4°C and the pellet was washed twice in 100ml of ice cold water with centrifugation at 1,500x g for 5 min at 4°C between each wash. Pellets were suspended in 5ml of 1M sorbitol containing 50 mM Tris-HCl pH 7.5, and 30 mM DTT, then incubated for 30 min at 30°C. The cell suspension was centrifuged at 1,500x g for 5 min to remove the supernatant and the cell pellet was digested with 1,000U of lyticase (Sigma) in 50 mM Tris-HCl pH 7.5, 1 M sorbitol and 2 mM DTT for 30 min at 30°C. The spheroplasts were pelleted with centrifugation at 1,500x g for 3 min. The pellets were suspended with yeast lysis buffer (100 mM Tris-HCl pH 7.5, 10 mM $MgCl_2$, 5 mM EDTA pH 7, 1 mM PMSF, 1 mM DTT and 8% glycerol). Approximately 0.5 ml of this mixture was added to an equal volume of acid washed 425-600 micron glass beads on ice and placed in a Biospec products Bead Beater at maximum speed three times for 20 sec at 4°C. Samples were placed on ice between bead beat cycles for 1 min to avoid heat build-up. Cell debris was then removed by centrifugation at 20,000x g for 10 min at 4°C. The supernatant was transferred to a new 1.5 ml Eppendorf tube. The supernatant containing PC was further precipitated by adding 100% saturated ammonium sulphate solution pH 7.0 to a final concentration of 40% saturation and stirring at 4°C for 30 min, then centrifuged at 13000× g for 30 min. The precipitate was dissolved in 0.15 ml of 25 mM Hepes (K^+) pH 7.2 containing 1.6 M sucrose, 0.1 mM DTT and 0.1 Mm EDTA. Protein content was determined by the Bradford method as described in Section 2.13.3. The partially purified proteins were stored at –80°C.

2.12 QUANTITATION OF DNA AND IMMUNOGLOBULIN BY SPECTROPHOTOMETRY

DNA, immunoglobulin and fragments of immunoglobulin were quantitated by measuring their absorbances at 260 nm or 280 nm. Samples were routinely measured in a 1 ml volume and concentrations determined using the following extinction coefficients

1.0 A_{260} unit double stranded DNA = 50 µg/ml

1.0 A_{280} unit IgG = 0.699 µg/µl

1.0 A_{280} unit Fab = 0.653 µg/µl

2.13 PROTEIN TECHNIQUES

2.13.1 Polyacrylamide gel electrophoresis (PAGE)

One dimensional gel electrophoresis of protein was performed in a slab gel apparatus utilising the discontinuous system as a modification of the procedure of Laemmli, (1970). For SDS-PAGE, a sample containing 25-50 µg protein was dissolved in an equal volume of 2x loading buffer [0.125 M Tris-HCl pH 6.8, 4% (w/v) SDS, 10% (v/v) glycerol, 0.2% Bromophenol blue] containing 0.1 M dithiothreitol and subjected to reducing SDS-PAGE on a 4% stacking gel and 7.5% polyacrylamide separating gel. For the resolution of high molecular weight proteins, gels were run for 1 hour at 40 mA with glycine running buffer (25 mM Tris-HCl pH 8.3, 0.25 M glycine, 0.1% SDS). For the resolution of small molecular weight proteins, a 10-12% separating gel with tricine running buffer (0.125 M Tris-HCl, 1 M Tricine, 0.1% SDS pH 8.3) was used (Schagger & von Jagow, 1987). The protein band was visualized by fixing the gels [10% (v/v) acetic acid and 50% (v/v) ethanol] and staining with a solution containing 0.3% (w/v) Coomassie Brilliant Blue R250 and 10% (v/v) acetic acid. The

gels were destained in a solution of 10% (v/v) acetic acid and preserved in a solution of 5% (v/v) glycerol, 30% (v/v) ethanol for 1 hour.

For native PAGE, the protocol was followed as described above except that all reagents in the system were prepared without SDS and samples were not denatured before loading on the gel.

2.13.2 Western blot analysis

All immunoblots were performed with a nitrocellulose membrane (Schleicher Schuell, Keene N. H., USA) using a semi-dry electroblotter (Multiphor II Novablot, Pharmacia, Uppsala, Sweden). The proteins were transferred electrophoretically for 1 hour at 50 mA from the gel to a nitrocellulose membrane with a transfer buffer consisting of 25 mM Tris-HCl pH 8.3, 0.25 M glycine, 20% (v/v) ethanol (Towbin *et al.*, 1979). Blots were blocked for overnight at 4°C in 1% BSA in PBS containing 0.05%Tween 20. The membranes were washed with PBS containing 0.05% Tween20 (washing buffer) (three changes within 30 min) at room temperature. Subsequently, the membranes were first incubated with primary antibodies at an appropriate concentration for 1 hour at room temperature in the washing solution on the rotary shaker. The membranes were washed as described above, then incubated with a secondary antibody conjugated to alkaline phosphatase (Sigma Immuno Chemicals) in the washing buffer for 1 hour at room temperature. After washing for 30 min the specific proteins were detected by developing the membranes with 50 mg/ml of BCIP and 70 mg/ml of NBT. Prestained Protein Marker (New England Biolab) was used for the blots.

For identification of biotin containing carboxylase, the blots were probed with avidin alkaline phosphatase (0.05 µg/ml) for 1 hour at room temperature. Bound alkaline phosphatase was detected by developing the blots with BCIP and NBT (Lim *et al.*, 1987).

2.13.3 Protein quantitation

The concentration of a protein solution was determined by Bradford assay (Bradford, 1976). A BSA standard curve was constructed by adding 0, 2, 4, 6, 8 and 10 μg of BSA to 50 μl of water in the wells of a microtiter plate. Two hundred microliters of diluted (1:3) Bio Rad protein assay dye reagent was then added to each well. A_{600} was measured on an Emax Precision microplate reader (Molecular Devices, USA). Samples were prepared by adding 1 μl of sample to 49 μl water plus 200 μl of diluted dye reagent. Using the equation of the line of best fit generated by the BSA standard, the amount of protein in the unknown sample was determined.

2.13.4 Protein A –Sepharose chromatography

Protein A Sepharose affinity chromatography was carried out to purify monoclonal antibody from ascites and cell culture supernatants. Briefly, 2 ml of the culture supernatant was centrifuged for 30 min at 15000 × g, then applied onto a rProtein A Sepharose column (1 ml Hitrap affinity column, Pharmacia Biotech). The column was washed with at least five column volumes of binding buffer (20 mM sodium phosphate pH 7) or until no material appeared in the effluent, and then the antibody was eluted with five column volumes of elution buffer. The elution of mouse IgG_1 subclass was achieved by passage of 10 ml 0.1 M sodium citrate pH 6 through the column. For mouse IgG_{2a} or IgG_{2b} and IgG_3, 0.1M sodium citrate pH 4.5 or pH 3 was passed through the column which was then re-equilibrated with phosphate buffer pH 8. The eluted antibody was neutralized by adding 200 μl of 1 M TrisHCl pH 8 per ml of eluted fraction. Then, after dialyzing the pooled fractions against 10 mM PBS pH 7.2, they were stored frozen at –20°C. The separation of the antibody subclasses from each other and from other serum proteins was monitored by measuring absorbance at a wavelength of 280 nm. The purified IgG fractions were buffer exchanged using PD-10

desalting column. The reuse of Hitrap rProtein A depends on the nature of the sample and was only performed with the identical monoclonal antibody to prevent cross-contamination. Before storage, the column was washed with five column volumes of 20% ethanol to prevent microbial growth and kept at 4°C.

CHAPTER 3

Preliminary Epitope Mapping of Human Pyruvate Carboxylase

CHAPTER 3

3.1 INTRODUCTION

Monoclonal antibodies (mAbs) were generated in our laboratory against purified sheep liver pyruvate carboxylase (sPC) and characterised by ELISA using sPC and the following biotin carboxylases: chicken PC (cPC), yeast PC (yPC), transcarboxylase (TC) from *Propionibacterium shermanii* and sheep liver propionyl-CoA carboxylase (sPCC) (Carey, 1988). Among these, mAb12 and 42 bound to all enzymes except sPCC. Antibodies 80 and 113 bound weakly to cPC and yPC (Carey, 1988). Antibodies 12 and 42 were able to recognise all biotin carboxylases, indicating that there is some structural similarity amongst these enzymes and it is possible that they may have some evolutionary links (Carey, 1988). A set of monoclonal antibodies were characterised for their ability to inhibit enzyme activity. Among these, mAb6, 12, 42 and 113 were able to inhibit the acetylCoA-dependent activity of sPC (Carey, 1988). Antibodies 12 and 42 were also able to inhibit cPC activity. Interestingly, none of these inhibitory antibodies was shown to be directed to the biotin moiety (Carey, 1988). Hence, this approach has the ability to reveal some molecular aspects of the structure-function relationships of PC. This project aims to gain further information about PC using the epitope mapping to define the antibodies' binding sites.

Recent sequencing studies of cDNAs encoding PC have shown that the homology of PC among different mammalian species is very high (≥ 96% between human, rat and mouse) (Jitrapakdee *et al.*, 1996). We expect therefore that our mAbs will be reactive against hPC. Moreover, a stable cell line 293T containing the plasmid pEF-hPC, expressing high levels of hPC, has been generated in our laboratory by Jitrapakdee *et al.* (1999). It will be very useful to analyse the enzyme activity of full-length hPC instead of sPC for which we don't have a cDNA clone. This chapter describes the epitope mapping of these antibodies and their inhibitory effects on acetyl

CoA dependent activity of hPC. So far no research has explored the use of epitope mapping to define the binding sites of monoclonal antibodies on the surface of hPC and to explain the inhibitory effects of these antibodies on enzymatic activity.

3.2 SPECIFIC METHOD

3.2.1 Partial purification of human and rat PC from dried mitochondrial extract

Human PC was prepared from 293T human embryonic kidney cells (ATCC: CRL 1573) stably transfected with the plasmid pEF-PC (Jitrapakdee *et al.*, 1999). This plasmid had been constructed using RT-PCR to introduce the full-length hPC cDNA into the efficient mammalian expression vector pEFIRES (Hobbs *et al.*, 1998). This cell line, expressing high levels of hPC, was routinely maintained for 7 days in Dulbecco's modified Eagle Medium (Life Technologies) supplemented with 10% fetal calf serum, 100 µg/ml streptomycin, 100 units/ml penicillin and 30 µg/ml puromycin. Cells were grown to 80-90% confluence in 175cm^2 flasks at 37°C in a humidified atmosphere of 5% CO_2. The preparation of hPC from mitochondrial extracts was performed as described by Jitrapakdee *et al.* (1999). Briefly, the stably transfected cells were washed twice with phosphate buffer and centrifuged at 1300 rpm for 3 min. The cell pellet was then resuspended in 4 volume of 0.25 M sucrose, 0.1 mM EDTA, 0.5 mM PMSF and 1 mM DTT and homogenised at 4°C for 2-3 min. Unbroken cells were removed by centrifugation at 600 x g at 4°C for 20 min. The supernatant containing mitochondria was further pelleted at 15,000 x g at 4°C for 30 min. The pellet was washed with 4 ml of 0.1 mM EDTA pH 7.0 containing 0.5 mM PMSF and centrifuged as above. The mitochondrial pellet was suspended in 2 ml 0.1 mM EDTA pH 7.0 and freezed-dried overnight. Dried mitochondria were stored at -20°C or used immediately by dissolving in 5 ml of 50 mM Tris-acetate pH 7.0, 5 mM ATP pH 7.0, 5 mM $MgCl_2$ and 0.5 mM EDTA and stirred at 4°C for 30 min. Undissolved materials were removed by centrifugation at 20,000 x g for 10 min. PC was precipitated from the supernatant by adding 100% saturated ammonium sulfate solution pH 7.0 to a final concentration of 40% saturation. The precipitate was then dissolved in 0.5 ml buffer A (25 mM potassium phosphate buffer pH 7.2, 20 mM ammonium sulfate, 1 mM EDTA and 0.1

mM DTT) and excess residual ammonium sulfate removed by passing the solution through a 2 ml Sephadex G-25 column (Pharmacia) equilibrated in buffer A.

For partial purification of rat PC, 120 mg of freeze dried rat PC mitochondria (a gift from Dr. Jitrapakdee) was dissolved in 5 ml of 50 mM Tris-acetate pH 7.0, 5 mM ATP pH 7.0, 5 mM $MgCl_2$ and 0.5 mM EDTA and further purified as described above.

3.2.2 Enzyme linked immunosorbent assay (ELISA) of full-length hPC and chicken PC (cPC)

To test the immunoreactivity of monoclonal antibodies with native PC enzyme, ELISA was performed as follows. The wells of a 96 well microtiter plate (F16 maxisorb, Nunc, U.S.A) were coated with 5 µg of partially purified hPC or purified cPC in 100 µl of coating buffer (0.1 M borate buffer pH 9.5) and incubated at 4°C overnight. The plates were washed with PBS containing 0.05% Tween 20 (PBST). Protein not bound to the plate was removed by inverting and tapping the plate. Non-specific binding sites were blocked by the addition of 1% skim milk in PBS and incubated for 1 hour at 37°C. The plates were then washed three times with PBST. The antibody, diluted in PBS, was added to the wells and incubated for 1 hour at room temperature. The plates were washed as described above to remove unbound antibody. One hundred microliters of a 1:1000 dilution of alkaline phosphatase conjugated to goat anti mouse immunoglobulin (Sigma) in PBS were added to the wells and the plate was incubated for 1 hour at room temperature. Unbound antibody was removed by washing the plate. Alkaline phosphatase activity was developed by the addition of 100 µl of solution containing one tablet of alkaline phosphatase substrate (Sigma, Catalogue 104, lot 108H6122) dissolved in 200 µl water and 800 µl of substrate solution (1 M Tris-HCl pH 8.8, 1.37 M NaCl and 2.5 mM $MgCl_2$). The absorbance was measured at 405 nm with an Emax Precision microtiter plate reader (Molecular Devices) after developing the colour for 20 min.

3.2.3 Spectrophotometric assay of human pyruvate carboxylase activity

The assay for PC activity is a coupled assay based on the procedure whereby the product of the pyruvate carboxylase reaction, oxaloacetate is reduced in the presence of an excess of malate dehydrogenase with the concomitant oxidation of NADH to NAD^+. The NADH reduction was followed by absorbance at 340 nm using a Varian Cary 3Bio UV visible spectrophotometer, at a constant temperature of 37°C. Activity was calculated using an extinction coefficient for NADH at 340 nm of 6.22 mM^{-1} cm^{-1} (Dawson *et al.*, 1969) where one unit of pyruvate carboxylase activity is defined as the amount of enzyme which carboxylates 1 μmole of pyruvate per minute in the assay solution described below. The pyruvate carboxylase activity was carried out as previously described by Scrutton & White (1974) and Jitrapakdee *et al.* (1999) with some modifications. Briefly the assay mixture was equilibrated in a final volume of 0.9 ml at 37°C containing 100 mM Hepes (K^+) pH 7.8, 2 mM Na_2ATP, 6 mM $MgCl_2$, 5 mM sodium pyruvate, 20 mM $KHCO_3$, 0.1 mM acetyl-CoA, 0.15 mM NADH and 2 μg of malate dehydrogenase (10 units/μg). The reaction was initiated by addition of the pyruvate carboxylase and monitored for a period of 10 minutes.

3.2.4 Assay of the inhibition of hPC and sPC activities by monoclonal antibody

For the assay of the inhibition of the acetyl CoA dependent activity of hPC and sPC, 20 mU of recombinant partially purified hPC (19.1 units/mg), (Jitrapakdee *et al.*, 1999) or 20 mU of sPC (19.6 units/mg) diluted in 0.1 M Tris-HCl pH 7.5, were incubated with antibody followed by measurement of the residual activity of the enzyme using the spectrophotometric assay. The reaction mixture was incubated in a total volume of 50 μl containing 1 μg of PC, 500 μM acetyl CoA, 5 μg of IgG of monoclonal antibody or inert IgG in 0.1 M Tris-HCl pH 7.5. The molar ratio of [IgG] / [PC tetramers] was 16:1. The mixture was incubated for 1 hour at room temperature and then was added into the assay solution (Section 3.2.3). The NADH reduction was

followed for 10 min spectrophotometrically at 37°C. The activity of the enzyme incubated with mAb was computed from the decrease in absorbance at 340 nm.

The effect of oxaloacetate on the inhibition of hPC activity by mAb6 was described as follow. The partially purified of hPC (Jitrapakdee *et al.*, 1999) (3.6 mU, 19.1 units/mg) was incubated with IgG of mAb6 (molar ratio of [IgG]/[PC tetramers] = 12:1) in the presence of increasing concentrations of oxaloacetate (0, 1 and 5 mM) for 1 hour at room temperature in 0.1 M Tris pH 7.2 and 250 μM acetyl-CoA. After incubation, the residual activity of enzyme was determined by radiochemical assay (Ballard & Hanson, 1967) as described in Section 6.2.5. The enzymatic activities were expressed as units/mg ± the standard deviation. The percentage inhibition by mAb6 at each concentration of oxaloacetate tested is derived from the value where no antibody was present for that particular oxaloacetate concentration.

3.2.5 Construction of pET plasmid encoding cDNA of human PC biotin carboxylation domain (BC), pET-BC

To generate pET-32a (+) encoding the human PC biotin carboxylation domain fused to thioredoxin (pET-BC), a pair of oligonucleotides was designed to amplify the BC fragment (residues 1-488). The forward primer (BC for) with a unique 5' *Eco*RI site and reverse primer (BC rev) with another unique 3' *Xho*I site were used (Section 2.3.1). The 1464 bp fragment was generated by PCR using pEF-PC encoding hPC as a template (Jitrapakdee *et al.*, 1999) and inserted into the expression vector, pET-32a (+) (Novagen) after this fragment was digested with *Eco*RI and *Xho*I. A recombinant plasmid (designated pET-BC) was obtained. This plasmid, encoding 488 amino acids of the BC fragment, was sequenced (Section 2.11.7) and the protein was expressed in *E. coli* BL21 (Section 3.2.11).

3.2.6 Construction and expression of truncated fragments of the human PC transcarboxylation domain (TC) and the biotin carboxyl carrier domain (BCC)

Five overlapping thioredoxin fusion proteins of truncated fragments of the human PC transcarboxylation domain (TC) and biotin carboxyl carrier domain (BCC), F1 (residues 475-718), F2 (residues 711-954), F3 (residues 947-1178), TB1 (residues 947-1077) and TB2 (residues 1048-1178) covering the complete hPC sequence were generated by PCR using pEF-PC encoding hPC as a template (Jitrapakdee *et al.*, 1999) for a screening of initial antibody binding. The forward primers (F2 for, F3 for, TB1 for and TB2 for) contained a unique 5' *EcoRI* site, whereas the reverse primers (F2 rev, F3 rev, TB1 rev, and TB2 rev) included a unique 3' *XhoI* site (Section 2.3.1). Due to a *XhoI* site at 1661 bp of the hPC sequence, the F1 primer was designed with unique 5' *EcoRI* (F1 for) and 3' *NotI* (F1 rev) sites. The PCR product was generated as previously described in Section 3.2.5, except that the F3 fragment was amplified only when the annealing temperature was decreased from 60°C to 55°C for 1 min. These products were then digested with *EcoRI-XhoI* or *EcoRI-NotI*, and cloned into the corresponding sites of simultaneously digested pET-32a (+) (Novagen) and sequenced (Section 2.11.7). The encoded proteins were expressed in *E. coli* BL21 and assayed for binding by antibody (Section 2.13.2).

3.2.7 Construction of pET vectors encoding cDNAs of overlapping fusion proteins of TB1

To more precisely map the binding site of mAb6, various deletions were constructed of the small fragment of hPC encoding amino acids 947-1048 (fragment TB1) fused to thioredoxin (Figure 3.8). Since the direct purification of PCR products by the QIA quick PCR purification kit (Qiagen) is limited to fragments from 100-10 kb, all deletion fragments also contained the background fragment (residues 847-947), which was used as the negative control fragment and to make the PCR product large

enough to purify with the QIA quick PCR purification kit. The deletion fragments with various lengths deleted from C-terminus of TB1 were constructed as thioredoxin fusion proteins by PCR amplification using the forward primer (NEG for) with an *EcoRI* site and the reverse primers (TB1 80cR, TB1 40cR, TB1 34cR, TB1 27cR and TB1 20cR) with a *XhoI* site (Section 2.3.1). These constructs were generated as TB1 80c (amino acids 847-1027 of hPC), TB1 40c (847-987), TB1 34c (847-981), TB1 27c (847-974), TB1 20c (847-967) and negative fragments (847-947). The PCR reaction was carried out as described in Section 2.11.8. Each resulting fragment was digested and cloned into the pET32a (+) vector (Novagen) digested at the *EcoRI* and *XhoI* sites, and the ligation product was sequenced (Section 2.11.7). The thioredoxin fusion proteins were expressed in *E. coli* BL21. The whole cell lysates were prepared and analysed for mAb6 binding by Western blot (Section 2.13.2) in order to narrow down the epitope of this antibody.

3.2.8 Construction of pET vectors cDNAs with C-terminally truncated fragments of TB2

For the fine epitope mapping of antibodies mAb12 and 42, a series of cDNA fragments encoding C terminal truncations of hPC fragment TB2 (residues 1048-1178) were amplified by PCR (Section 2.11.8). The forward primer (TB2 for) and reverse primers (TB2 121cR, TB2 111cR, TB2 91cR, TB2 71cR, TB2 44cR, TB2 37cR) as shown in Section 2.3.1, were used to amplify the appropriate fragments from plasmid pEF-PC (a pEFIRES derivative containing a DNA fragment encoding full-length hPC) as a template (Jitrapakdee *et al.*, 1999). Restriction endonuclease sites were introduced for *Eco*RI (5' of C terminal fragment) and *Xho*I (3' of C-terminal fragment) to facilitate cloning. PCR reactions were performed as described in Section 3.2.5, the products gel-purified and digested with *Eco*RI and *Xho*I restriction endonucleases. These PCR products were ligated directly into digested pET-32a (+) vector (Novagen) generating an in-frame hPC thioredoxin fusion protein. These constructs encoding a series of

C-terminal deletion fragment were designated as TB2 121c (residues 1048-1168 of hPC), TB2 111c (1048-1158), TB2 91c (1048-1138), TB2 71c (1048-1118), TB2 44c (1048-1091) and TB2 37c (1048-1084) respectively. All constructs were verified by sequence analysis and tested for expression in *E. coli* BL21.

3.2.9 Construction of pET vectors cDNAs with N-terminally truncated fragments of TB2 (107, 80, 60 residues)

The cDNA fragments encoding N-terminally truncated fragments of TB2 were generated by PCR amplification using pEF-PC encoding full-length hPC as a template (Jitrapakdee *et al.*, 1999). The forward primers (TB2 107nF, TB2 80nF and TB2 60nF) with a unique 5' *Eco*RI site, and the reverse primer (TB2 rev) with another unique 3' *Xho*I site shown in Section 2.3.1 were used. The PCR reaction was carried out as previously described in Section 2.11.8. The resulting fragments were further purified, digested and ligated into digested pET-32a (+) (Novagen) vector at the unique *Eco*RI and *Xho*I sites. These constructs were designated as TB2 107n (residues 1071-1178 of hPC), TB2 80n (1098-1178) and TB2 60n (1118-1178), respectively. The DNA encoding the thioredoxin fusion proteins were sequenced to ensure no error was introduced by *Taq* polymerase. These constructs were expressed in *E. coli* BL21 and the immunoreactivity of the antibodies with the expressed proteins was analysed by Western blot (Section 2.13.2).

3.2.10 The annealing of small DNA fragments

To generate the small DNA fragments encoding 10 or 20 amino acids of hPC, the reaction was carried out as previously described by Alexeyev & Winkler (1999) and Anderson *et al.* (1996) with some modifications. Briefly, a pair of complementary oligonucleotides (TB2 10nF and TB2 10nR or TB2 20nF and TB2 20nR) was designed to code for 10 or 20 amino acids of hPC and to also contain a unique 5' *EcoRI* site and unique 3' *XhoI* site, as shown in Section 2.3.1. The reaction was carried out in a total

volume of 20 µl containing 10 µl of distilled water and 500 ng of each oligonucleotide primer. The oligonucleotides in the reaction mixture were denatured at 95°C for 5 min followed by annealing at 37°C for 1 hour. Five microliters of the annealed oligonucleotides were ligated into the *EcoRI* / *XhoI* sites of digested pET 32a (+) vector (Novagen). This resulted in generation of plasmids TB2 10n and TB2 20n encoding hPC fragments of 10 or 20 amino acids fused to thioredoxin. These constructs were sequenced as described in Section 2.11.7 and the proteins expressed as described in Section 3.2.11. The immunoreactivities of the antibodies with the expressed proteins were analysed by Western blot (Section 2.13.2).

3.2.11 Expression of proteins in bacteria

The overexpression of fusion proteins in bacteria was performed as described below. An overnight culture of *E. coli* BL21 containing the expression plasmid was diluted to 1:40 (v/v) into 10 ml of fresh LB (Ampicillin 100 µg/µl) and cultured at 37°C. At an A_{600} of 0.5-0.6, the culture was induced with 0.1 mM IPTG for 3 hours at 37°C. Following the induction, cells were collected by centrifugation (5000 rpm, 5 min, 4°C) and the pellet was washed once with 50 mM Tris-HCl pH 8.0, 0.1 mM EDTA pH 8.0, 0.2 mM DTT, then resuspended with lysis buffer (20 mM Tris-HCl pH 8.0, 0.1% Triton X100, 10 mM EDTA, 0.5 M NaCl, 0.2 mM DTT). The whole cell lysate was diluted 1:1 with 2 x SDS sample buffer (4% SDS) and subjected to SDS-PAGE (Section 2.13.1) and Western blot analysis (Section 2.13.2).

3.3 RESULTS

3.3.1 Characterisation of anti sheep PC monoclonal antibodies against full-length human PC (hPC), rat PC (rPC), chicken PC (cPC) and sheep PC (sPC)

The mAbs 6, 12, 42, 80 and 113 were generated against sPC and with the exception of mAb80 were found to cross-react in ELISA against cPC, and were able to inhibit the acetylCoA-dependent activity of sPC (Carey, 1988). To optimise immunoreactivity of these antibodies, an ELISA assay was performed as described in Section 3.2.2 at the different dilutions of antibodies against cPC. It was shown that the dilution of antibodies, 6, 12, and 42 at which the ELISA absorbance 2.0 at 405 nm were 1:1,000, 1:10,000 and 1:10,000 (Figure 3.1). In contrast, mAb80 and 113 at the dilution 1:100 gave an absorbance 0.5 (Figure 3.1). Based on these data, we tested dilutions of these antibodies in an ELISA assay against native hPC. The dilutions of these antibodies were similar to those results from ELISA used with cPC, except that the dilution of mAb6 against native hPC (dilution 1:100) was lower than that against cPC (dilution 1:1000) [Figure 3.1 and 3.2].

These antibodies cross-reacted with cPC and hPC in an ELISA assay with native enzymes. To confirm the immunoreactivity of these antibodies against PC in a denatured system, immunoblotting against cPC, rPC, hPC and sPC was conducted following SDS-PAGE. As shown in Figure 3.3 antibodies 6, 12 and 42 bound cPC, rPC, hPC and sPC with relatively equal affinity. In contrast mAb113 bound to sPC far more strongly than to cPC, rPC and hPC and mAb80 only bound to sPC. The affinity of mAb12 and 42 was higher than mAb6. Interestingly, antibody 42 cross-reacted with the native hPC in an ELISA assay (Figure 3.2) at the same dilution as that in an immunoblot with denatured enzyme (Figure 3.3). However, mAb6 bound more weakly with hPC in ELISA than in an immunoblot. These data indicate that the folding of this

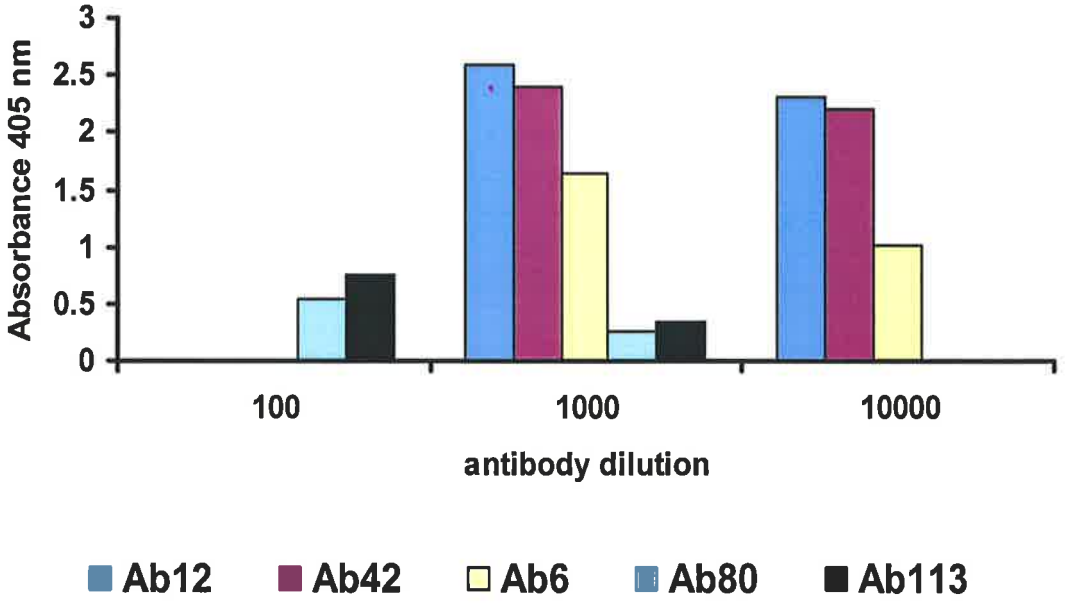

Figure 3.1 ELISA of chicken PC with anti sheep PC monoclonal antibodies. cPC was coated directly onto microtiterplates at a concentration of 50 ng/μl, various dilutions of antibodies were added into the plates, then probed with a second antibody conjugated to alkaline phosphatase. The color was developed and measured at 405 nm. The concentration of undiluted antibody was 1 mg/ml.

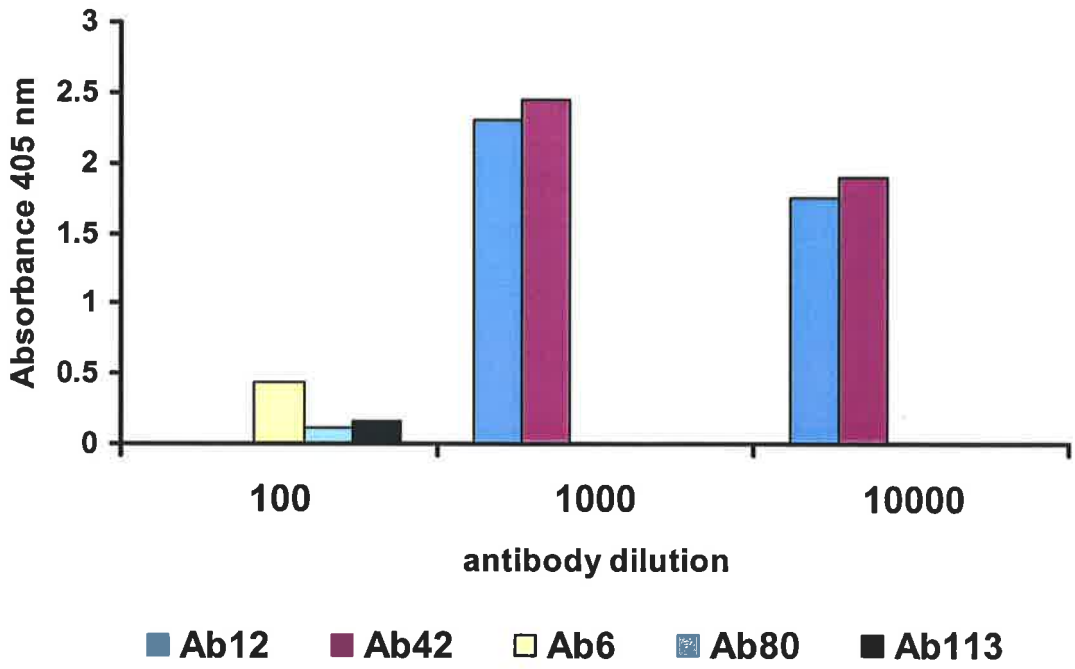

Figure 3.2 ELISA of human PC with anti sheep PC monoclonal antibodies. hPC was coated directly onto microtiterplates at a concentration of 50 ng/µl, reacted with antibodies at different dilutions then probed with a second antibody conjugated to alkaline phosphatase. The color was developed and measured at 405 nm. The concentration of undiluted antibody was 1 mg/ml.

enzyme had no effect on the epitopes' accessibility for mAb42 and 12, but did so for mAb6.

3.3.2 Inhibitory effect of antibodies on AcetylCoA-dependent activity of hPC and sPC

Since a highly specific interaction of mAb6, 12 and 42 with hPC under native conditions was found, we proposed that these mAbs might inhibit hPC activity. To analyse whether monoclonal antibodies 6, 12 and 42 can affect the acetyl-CoA dependent activity of hPC and sPC, constant amounts of purified hPC and sPC were used for the activity assay in the presence of monoclonal antibody purified from ascites fluid by protein A affinity chromatography as described in Section 2.14. Oxaloacetate production by pyruvate carboxylase was coupled to NADH oxidation by malate dehydrogenase and NADH. The NADH oxidation was followed by the loss of absorbance at 340 nm using a spectrophotometer thermostatted at 37°C. Enzymatic activities were then expressed as μmoles of product formed / min/mg of PC.

As shown in Figure 3.4 mAb6 inhibited the acetylCoA-dependent activity of hPC and sPC by 91 % and 96 % respectively when compared to the control reactions in which enzymes were incubated with inert IgG. The inhibitory effects of mAb12 and 42 were 96 and 91 % for sPC and 89 and 90 % for hPC (Figure 3.4). This demonstrates that the acetylCoA-dependent activity of both sPC and hPC were significantly reduced by the addition of mAb6, 12 and 42. Taken together mAb6, 12 and 42 affected the acetylCoA-dependent activity of sPC to the same extent as the activity of hPC.

The effect of oxaloacetate on the inhibition of hPC activity by mAb6 was studied to test the possibility of the catalytic centre being part of the mAb6's epitope. To analyse the effect of oxaloacetate on the inhibition of hPC activity, partially purified hPC was incubated with mAb6 in the presence of increasing concentration of oxaloacetate. As shown in Figure 3.5, in the absence of oxaloacetate mAb6 was able to inhibit 19% of hPC activity. It was observed that in the presence of 1 mM oxaloacetate,

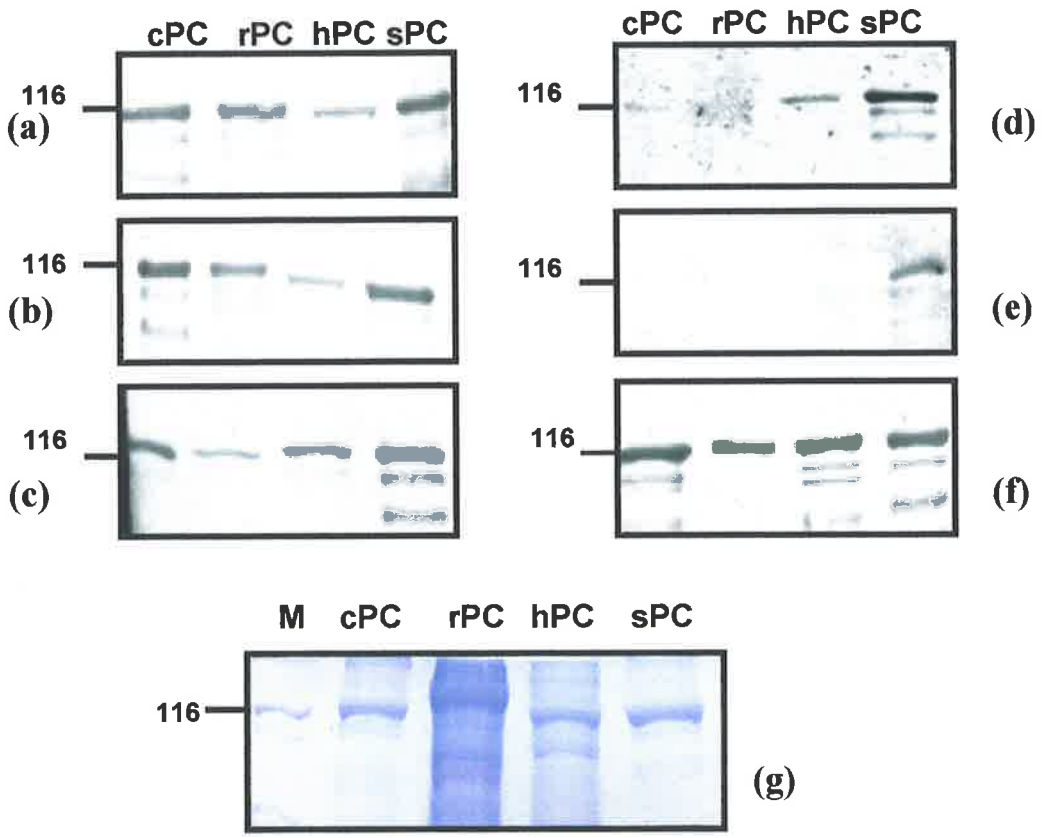

Figure 3.3 **Immunoblot analysis of various pyruvate carboxylases**: cPC, rPC, hPC and sPC reacted with mAb12 dilution 1:2500 (a), mAb42 dilution 1:10000 (b), mAb6 dilution 1:1000 (c), mAb113 dilution 1:100 (d), mAb80 dilution 1:100 (e) and avidin alkaline phosphatase (f). Coomassie staining is shown in panel (g). Biorad broad range markers, M, were used as standards. The concentration of undiluted antibody was 1 mg/ml.

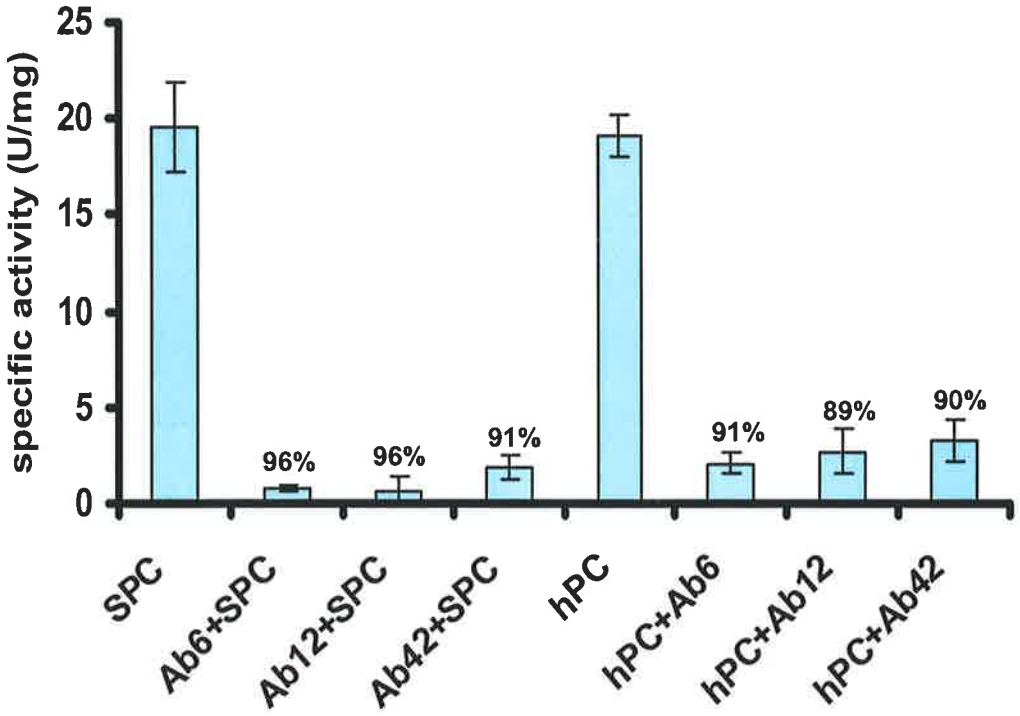

Figure 3.4 Pyruvate carboxylase activity of sPC and hPC in the presence of antibody. Enzyme activity (U/mg of PC) determined in triplicate on partially purified hPC expressed from a mammalian cell line, 293T. Pyruvate carboxylase activity was measured using the spectrophotometric assay either in the presence or absence of mAb6, 12 and 42. Twenty mU of partially purified hPC and purified sPC were incubated with 5μg of IgG of mAb6, 12 and 42 or inert IgG for 1 hr at room temperature (Molar ratio of IgG/PC tetramers = 16:1). After incubation, the residual activity of the enzyme was determined as described in Section 3. Results are the mean of the measurement ± standard deviation (SD). The numbers shown on top of the columns are the mean of the percentage inhibition by the antibodies (mAb6, 12 and 42) compared to the value where inert IgG was present for that assay.

the inhibition of hPC was increased to 36%. Clearly, even 1 mM oxaloacetate had an effect on hPC inhibition by mAb6. A further increase in the molarity of oxaloacetate (5 mM) did not significantly affect any more change in the inhibition of hPC by mAb6 (41%).

3.3.3 Initial screening of BC domain of hPC with monoclonal antibodies

The N-terminal domain of hPC, the biotin carboxylation domain (BC), is thought to be involved in the first partial reaction where the formation of carboxybiotin occurs from HCO_3^- in the presence of MgATP (Jitrapakdee & Wallace, 1999) and (Attwood & Wallace, 2002) via the formation of a carboxyphosphate intermediate (Knowles, 1989). Since all biotin dependent carboxylases share a common reaction mechanism, these enzymes exhibit significant sequence similarities with each other, especially within the biotin carboxylation and biotin carboxyl carrier domains (Jitrapakdee & Wallace, 1999). Sequence analysis of this region in conjunction with the crystal structure of the biotin carboxylase subunit of *E. coli* ACC (Waldrop *et al.*, 1994) has identified 11 highly conserved residues within this domain that are likely to play an important role in catalysis (Jitrapakdee *et al.*, 1996). Domain boundaries, identified by highly significant degrees of similarity with other biotin enzymes, have been established for rat BC domain (residues 1-488) (Jitrapakdee *et al.*, 1996). Since the inferred protein sequence of rat PC is 96.3 % identical with hPC, the biotin carboxylation domain of hPC was chosen as the first domain to be screened for the epitopes of the inhibitory monoclonal antibodies, mAb6, 12 and 42. To test this, whole cell lysates of *E. coli* expressing BC domain of hPC were prepared and assessed for binding with mAb6, 12 and 42 in a Western blot.

As shown in Figure 3.6a, BC domain was overexpressed in *E. coli* BL21 as a thioredoxin fusion protein. SDS-PAGE analysis of whole cell lysates revealed that a protein of 66 kDa was induced compared to cells harbouring the parent vector (Figure

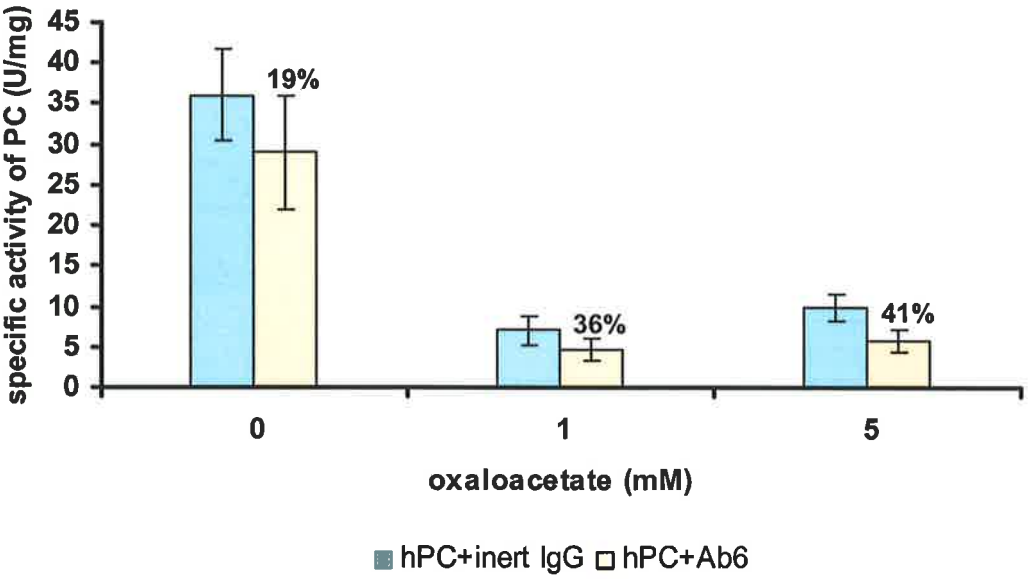

Figure 3.5 The effect of oxaloacetate on the inhibition of hPC activity in the presence of antibody. The partially purified hPC was incubated with 5μg of IgG of mAb6 or inert IgG for 1 hr at room temperature (molar ratio of IgG/PC tetramers = 12:1). After incubation, the residual activity of the enzyme was determined by radiochemical assay. Results are the mean of the measurement ± standard deviation (SD). The numbers shown on top of the columns are the mean of the percentage inhibition by mAb6 in the presence of oxaloacetate compared to the value where inert IgG was present for that assay.

3.6f). Lysates were analysed for antibody recognition by immunoblot and specificity in comparison with the parent vector control. The mAbs, 6,12 and 42 did not recognise the BC domain (Figure 3.6b, c and d). Only partially purified hPC cross-reacted with mAbs, as the positive control for these antibodies (Figure 3.6b, c and d). Very poor reactivity was observed on the blot when probed with rabbit polyclonal anti chicken PC (dilution 1:2500) [Figure 3.6e] but a band around the expected molecular mass (65766 Da) was visualised. Taken together the monoclonal antibodies' epitopes were determined not to reside in the BC domain.

3.3.4 Immunoreactivity against hPC-truncated fragment with monoclonal antibodies: mAb6, 12 and 42

To further identify which regions of hPC (transcarboxylation or biotin carboxyl carrier domain) cross-reacted with mAb6, a series of overlapping truncations of hPC fused with thioredoxin was generated and expressed in *E. coli* BL21. Together these fragments covered the complete hPC sequence except the BC domain and are designated F1, F2, F3, TB1 and TB2 (Figure 3.7a). Total whole cell lysates were prepared from *E. coli* (Section 3.2.11) and fractionated using triplicate polyacrylamide gels. One gel was stained with Coomassie Brilliant Blue to confirm protein expression (Figure 3.7b) and the other two were used for immunoblotting with rabbit polyclonal anti cPC (dilution 1:2500) (Rohde *et al.*, 1991) and mAb6 (dilution 1:1000) as shown in Figure 3.7c and d. The molecular masses of F1, F2, F3, TB1 and TB2 were predicted to be 38832 Da, 37983 Da, 37251 Da, 26258 Da and 26094 Da respectively. All thioredoxin fusion proteins were abundantly expressed as a major band in the cell lysates (Figure 3.7b). As a positive control, the fusion proteins encoding hPC cDNA fragment also cross-reacted with rabbit polyclonal anti chicken-PC (Figure 3.7c). Cells harbouring the parent vector pET 32a (+) did not reacted with either polyclonal antibody or mAb6 (Figure 3.7c and d). Figure 3.7d shows the blot probed with mAb6.

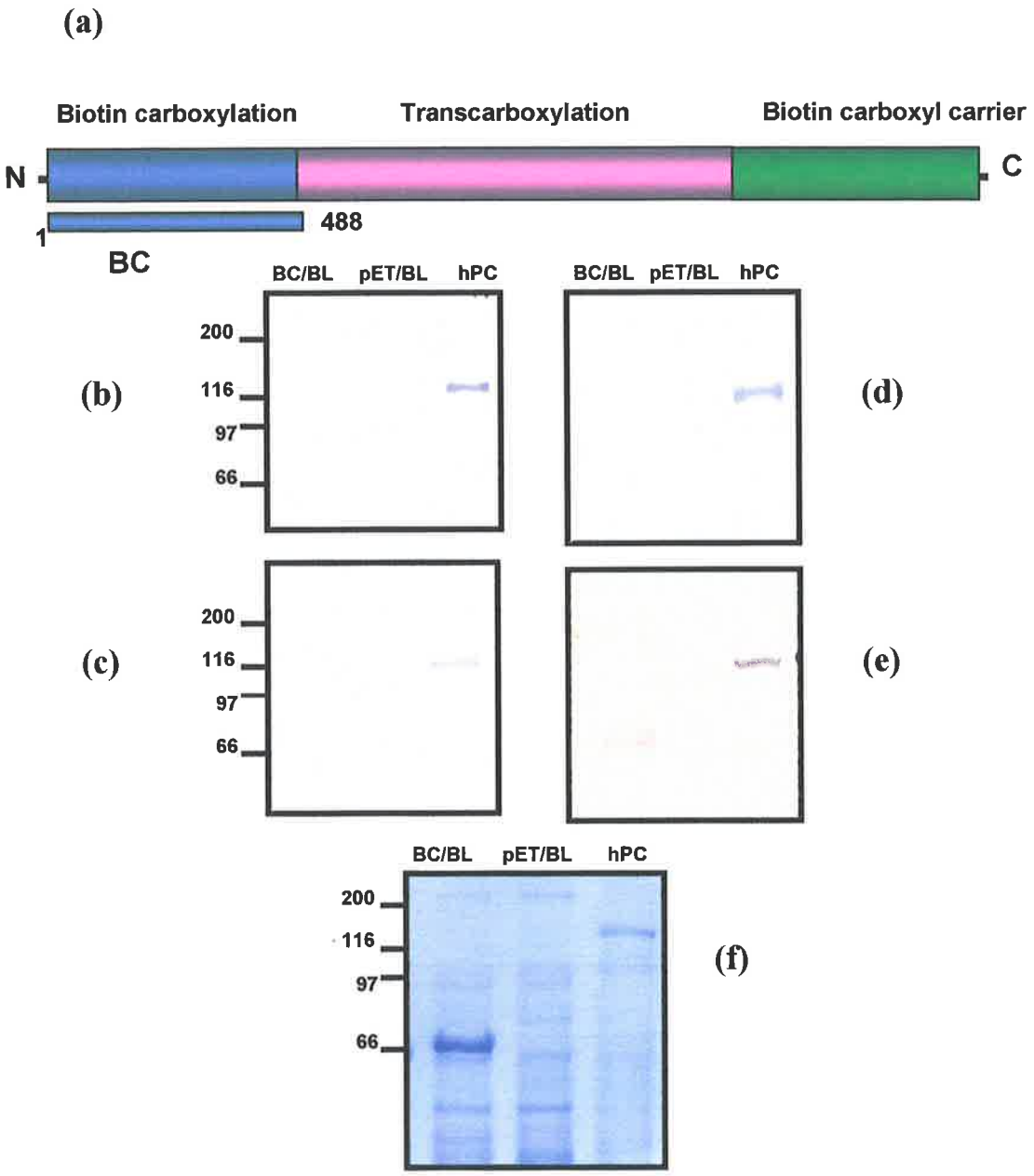

Figure 3.6 Immunoblot analysis of BC domain of human pyruvate carboxylase with monoclonal antibodies. (a) A schematic diagram of three functional domains of PC, ie. Biotin carboxylation domain (BC), transcarboxylation domain (TC) and biotin carboxyl carrier domain (BCC) are shown. BC domain (residues 1-488) of hPC was constructed and expressed in *E. coli* as thioredoxin fusion protein. The blots were reacted with mAb6 dilution 1:1000 (b), mAb42 dilution 1:5000 (c), mAb12 dilution 1:2500 (d), polyclonal anti cPC dilution 1:2500 (e). (f) The expression of proteins were shown on Coomassie staining gel. BL = *E. coli* BL21 (λDE3)

The large fragment F3 cross-reacted with mAb6 but no reactivity was detected against BC, F1 and F2. This indicates that the epitope of mAb6 resides in the C-terminal region of hPC. Further C-terminal deletion of the F3 fragment (residues 947-1178) resulted in a positive reactivity with TB1 (residues 947-1077) but not with the N-terminal deletion, TB2 (residues 1048-1178). This result suggests that the epitope of mAb6 resides in the fragment containing residues 947-1048 at the N-terminal end of biotin carboxyl carrier domain.

For the initial mapping with mAb12, the immunoreactivities of the hPC truncated fragments, F1, F2, F3, TB1 and TB2 were assayed by Western blot against mAb12 at a dilution 1:2500 followed by goat anti mouse IgG conjugated to Alkaline phosphatase (1:10,000). The bands were visualised by developing the colour of BCIP and NBT as previously described in Section 2.13.2.

As shown in Figure 3.7e mAb12 cross-reacted with fragments F3 (residues 947-1178) and TB2 (residues 1048-1178) but not BC (residues1-488), F1 (residues 475-718), F2 (residues 711-954) and TB1 (residues 947-1077). This indicates that the epitope of mAb12 resides in the C-terminal domain (BCC) of hPC (residues 1048-1178).

For mAb42 mapping, the hPC truncated fragments were assayed by Western blot against mAb42 (dilution 1:5000) as described in Section 2.13.2. The result was the same as for mAb12 (Figure 3.6f). The results for the initial screening of hPC fragments recognised by mAb6, 12 and 42 are summarised in Figure 3.8.

3.3.5 Fine mapping of hPC with mAb6

The epitope recognised by mAb6 has been localised broadly to residues 947-1048 at N-terminal of the biotin carboxyl carrier domain. To further define the minimal residues for the epitope mapping recognised by mAb6, various overlapping fragments covering residues 947-1048 representing regions of hPC were generated as

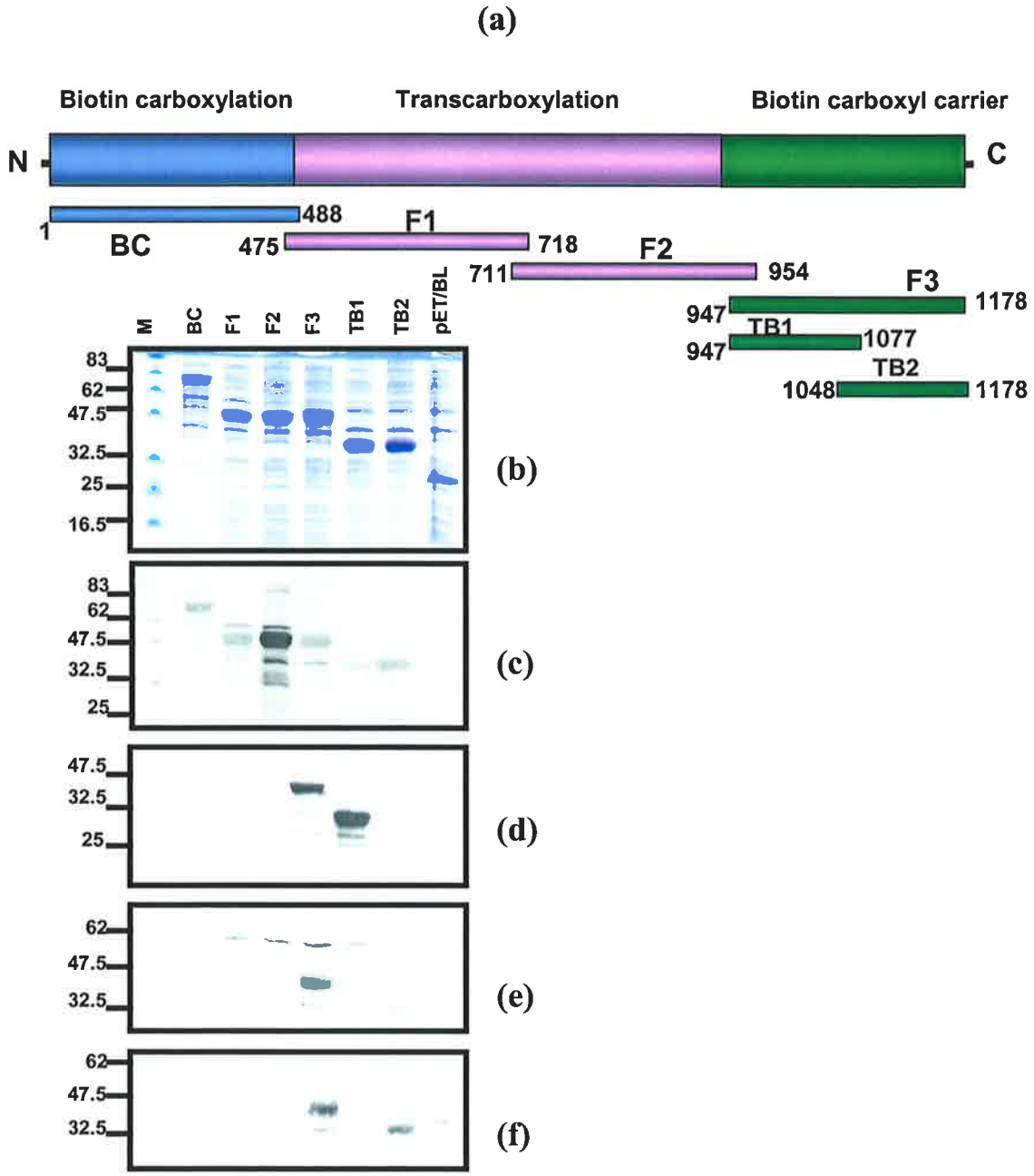

Figure 3.7 Immunoblot analysis of various deletion fragments with polyclonal and monoclonal antibody to PC. (a) All truncated proteins expressed in *E. coli* BL21 as fusion proteins with the 109aa thioredoxin proteins are shown as colour bars. Numbers are position of residues at the putative boundaries of different regions. The cell lysates were subjected to SDS-PAGE and analysed by both Coomassie brilliant blue staining (b) or Western blot (c, d, e, f). The antibody binding was assayed by immunoblotting with polyclonal anti cPC (1:2500)[c], mAb6 (1:1000)[d], mAb12 (1:2500)[e] and mAb42 (1:5000)[f]. M= Prestained Protein Marker (New England Biolab).

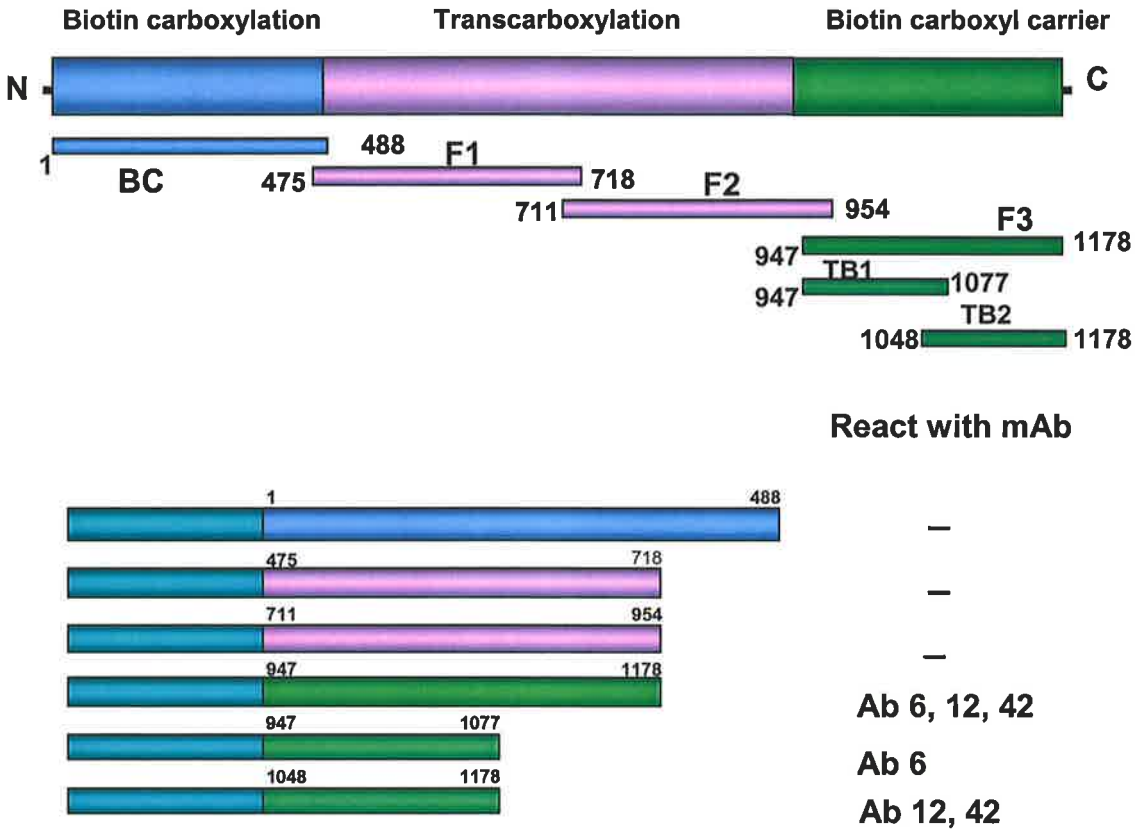

Figure 3.8 Three functional domains of PC and immunoreactivity of truncated fusion proteins of hPC with mAbs. A schematic diagram of three functional domains of PC, ie. biotin carboxylation (BC), transcarboxylation (TC) and biotin carboxyl carrier domain (BCC) and various deletion fragments are shown. Numbers are position of residues at the putative boundaries of different regions. The overlapping fragments are shown as color bars with the 109aa thioredoxin proteins indicated as blue bars. These constructs containing cDNA of hPC were amplified and designated BC (residues 1-488; 65766 Da), F1 (residues 475-718; 38832 Da), F2 (residues 711-954; 37983 Da), F3 (residues 947-1178; 37251 Da), TB1 (residues 947-1077; 26258 Da) and TB2 (residues 1048-1178; 26094 Da). Immunoreactivity of all these fragments against mAb6, 12 and 42 are summarised.

described in Section 3.2.7. A panel of five overlapping fragments were constructed representing 80, 40, 34, 27 and 20 residues at the C-terminus of the sequence between residues 847-1048 of hPC along with the fragment 847-947 as the negative control (Figure 3.9a). These hPC thioredoxin fusion proteins were abundantly expressed as major bands at 31-45 kDa when analysed by SDS-PAGE (Figure 3.9b). The antibody binding was assayed by immunoblot with mAb6 (Figure 3.9c). All deletion fragments representing residues 847-1027 (TB1 80c), residues 847-987 (TB1 40c), residues 847-981 (TB1 34c) and residues 847-974 (TB1 27c) cross-reacted with mAb6 but no binding was seen when the fragment was deleted between residues 974 and 967. Appropriately, no binding of mAb6 to the control fragment (residues 847-947) was detected. The molecular masses of all deletion fragments; negative control, TB1 80c, TB1 40c, TB1 34c, TB1 27c and TB1 20c were predicted to be 22710 Da, 31540 Da, 27003 Da, 26354 Da, 25699 Da and 24878 Da respectively. These results indicate that this linear epitope is located within the region containing 7 residues between residues 974 and 967. This region contains the amino acid sequence LKDLPRV (residues 968-974) which occurs at the N-terminal of the biotin carboxyl carrier domain.

3.3.6 Fine mapping of mAb12 and 42

The initial screening result revealed that mAb12 and 42 were not bound to the BC domain but only bound to the F3 fragment (residues 947-1178) and the TB2 fragment (residues 1048-1178). To further define the minimal epitopes, which these antibodies recognised, various deletions of the TB2 fragments were constructed, resulting in truncated proteins that lacked amino acids at the C terminus. These proteins were expressed very well at a similar level (Figure 3.10b). All these C-terminally truncated proteins failed to cross-react with both antibodies (Figure 3.10c and d). They also failed to react with avidin alkaline phosphatase, indicating that they were not biotinylated (Figure 3.10e). As TB2 121c and TB2 111c contain Lys^{1144}, which is

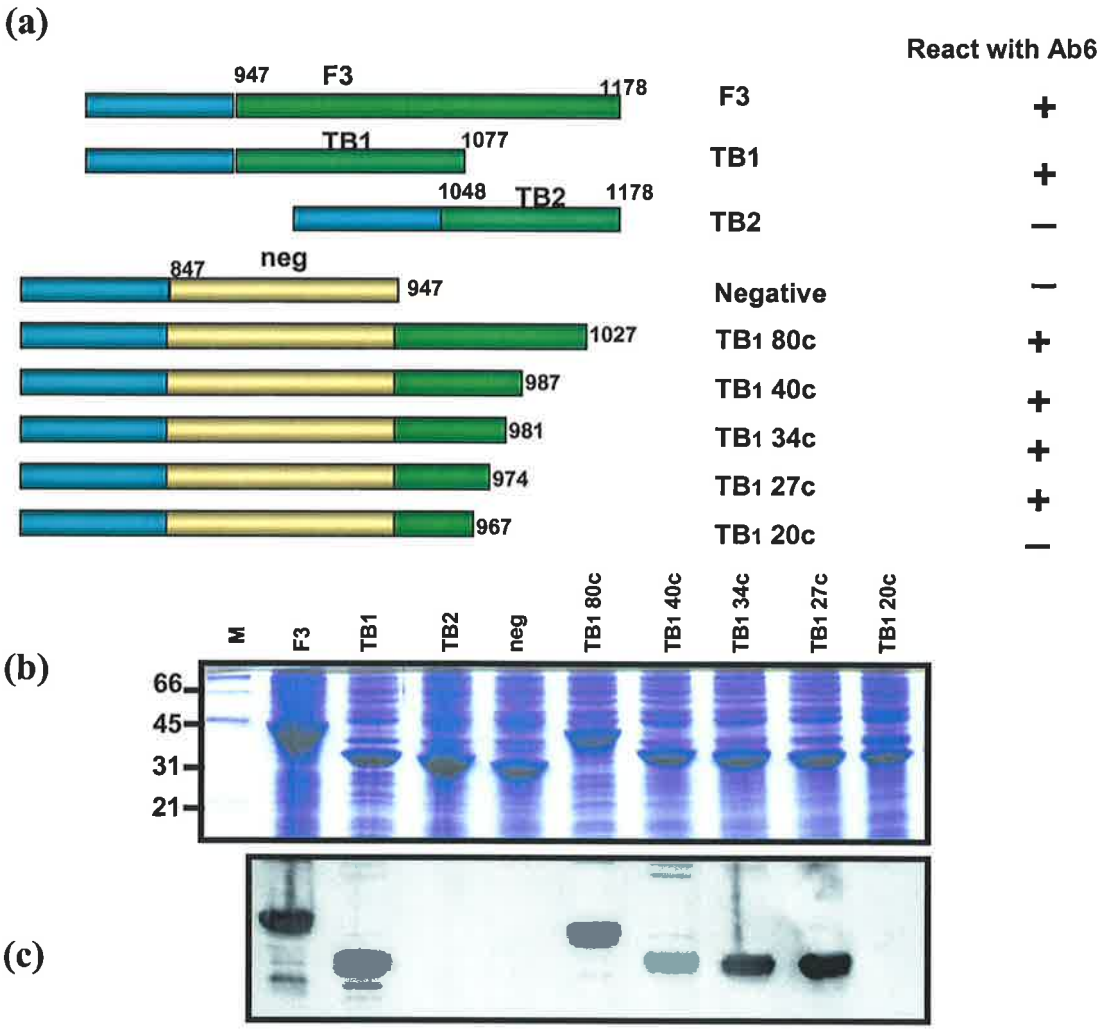

Figure 3.9 Epitope mapping of hPC with mAb6. (a) A schematic diagram of the different truncated hPC fusion proteins encoding amino acids 847-1027. Truncated proteins were designated neg (847-947; 22710 Da), TB1 80c (847-1027; 31540 Da), TB1 40c (847-987; 27003 Da), TB1 34c (847-981; 26354 Da), TB1 27c (847-974; 25699 Da) and TB1 20c (847-967; 24878 Da). (b) These regions of hPC were expressed as proteins fused to thioredoxin and analysed by SDS/PAGE. (c) The proteins were assayed for the binding of mAb6 by Western blot. The numbers at the top of the panel denote the residues present in the different truncated hPC proteins. The blue bars represent the 109aa thioredoxin proteins. (a) Results of antibody immunoblots are summarised beside. M=Broad range standard Protein Marker (Biorad).

biotinylated in TB2, it appears that these truncated fragments are not folded correctly to interact with biotin protein ligase. These results suggest the epitopes of mAb12 and 42 are conformational in nature.

Consequently, to test this hypothesis, we further mapped these epitopes with N-terminal truncations of the hPC biotin carboxyl carrier domain fused to the C-terminus of thioredoxin. The expression of these proteins are shown in Figure 3.11b to be at a similar level on SDS-PAGE analysis. As shown in Figure 3.11c and d, the fragments encoding residues 1071-1178 (TB2 107n) and 1098-1178 (TB2 80n) cross-reacted with both antibodies but fragments encoding residues 1168-1178 (TB2 10n), 1158-1178 (TB2 20n) and 1118-1178 (TB2 60n) did not react with either antibody. The molecular masses of TB2 107n, TB2 80n, TB2 60n, TB2 20n and TB2 10n were predicted to be 23473 Da, 20383 Da, 18141 Da, 14129 Da and 12933 Da respectively. The same pattern of reactivity was seen with the avidin blot (Figure 3.11e). These results clearly demonstrate that the conformation of the BCC domain is critical for these epitopes. Taken together, these results allowed us to map the mAb12 and 42 epitopes to a fragment comprised of residues 1098-1178. Truncation of this by 20 residues from the N or 10 residues from the C-terminal results in loss of reactivity with both antibodies and loss of biotinylation. Accordingly these residues which constitute the core of the hPC biotin carboxyl carrier domain, form conformation-dependent or discontinuous epitopes for mAb12 and 42.

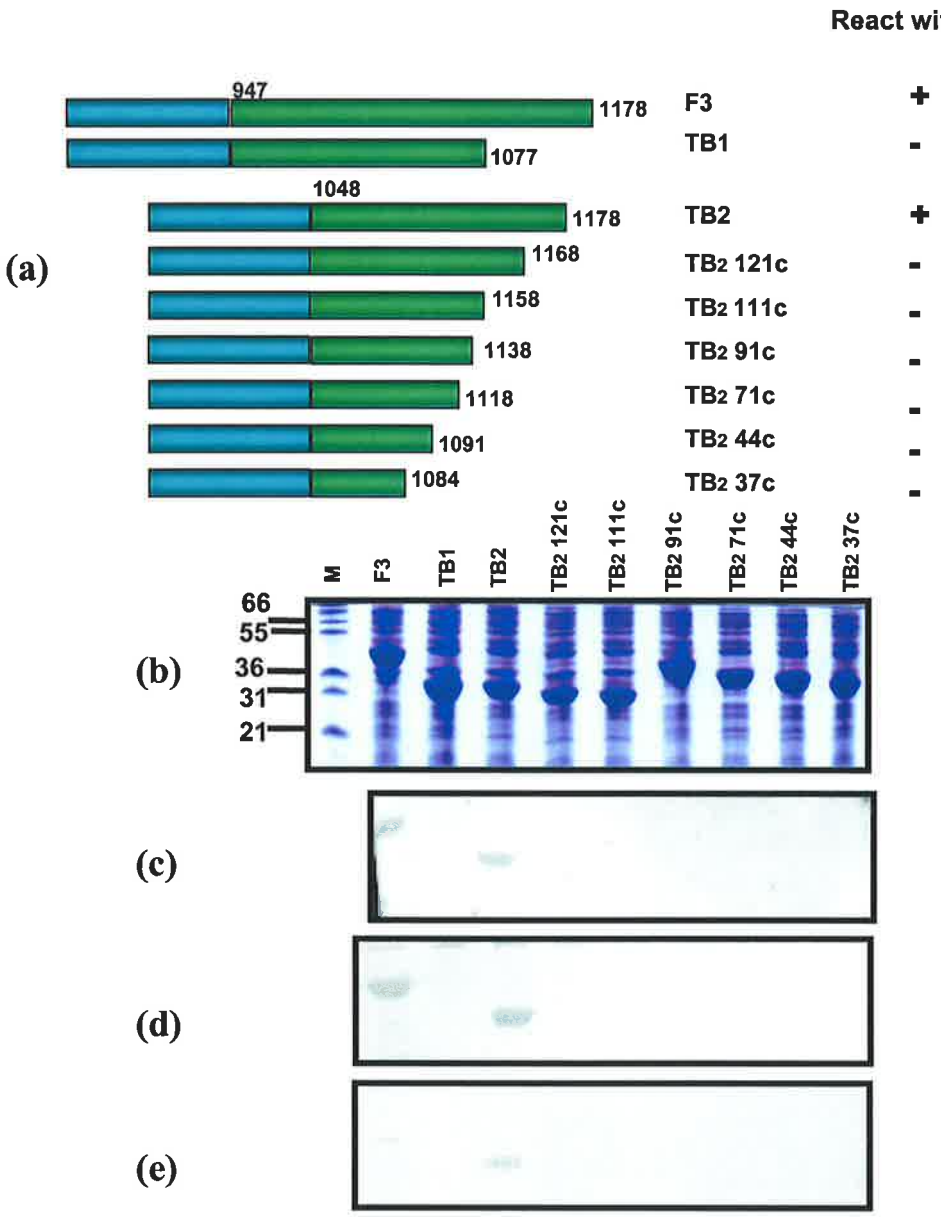

Figure 3.10 Immunoblot of C terminally truncated fragments of human biotin carboxyl carrier domain with mAb12 and 42. (a) A schematic diagram representing C terminally truncated fragments of human biotin domain: TB2 121c (24967 Da), TB2 111c (23813 Da), TB2 91c (21664 Da), TB2 71c (19645 Da), TB2 44c (16714 Da) and TB2 37c (15903 Da) respectively. The cell lysates were prepared and analysed by SDS-PAGE. The over-expressed protein band was stained with Coomassie brilliant blue (b) and probed with mAb12 (c) and mAb42 (d) and streptavidin alkaline phosphatase (e). The 109aa thioredoxin proteins tagged with these proteins are shown as blue bars. (a) Results of antibody immunoblots are summarised beside. M= Protein marker (Mark12, Novex)

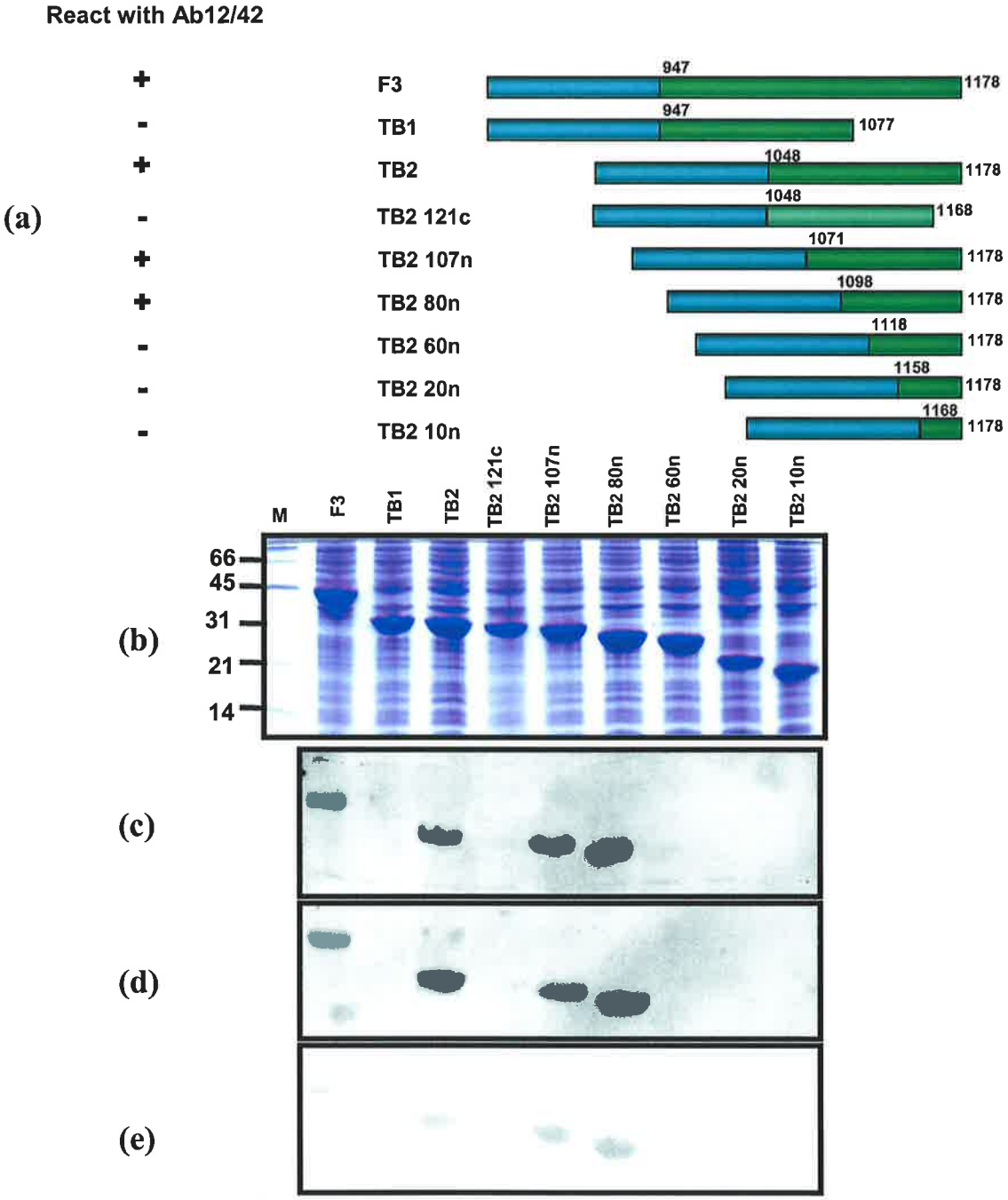

Figure 3.11 Immunoblot of N-terminally truncated fragments of human biotin carboxyl carrier domain with mAb12 and 42. (a) A schematic diagram representing N-terminally truncated fragments of human biotin domain: TB2 107n (23473 Da), TB2 80n (20383 Da), TB2 60n (18141 Da), TB2 20n (14129 Da), TB2 10n (12933 Da) and F3 (37251 Da), TB1 (26258 Da), TB2 (26094 Da), TB2 121c (24967 Da). The over-expressed protein band of cell lysate was stained with Coomassie brilliant blue (b) and probed with mAb12 (c) and mAb42 (d) and streptavidin alkaline phosphatase (e). Blue bar represents the 109aa thioredoxin protein. Results are summarised in part (a) for antibody immunoblot. M=Broad range Protein Marker (Biorad).

3.3 DISCUSSION

Pyruvate carboxylase is a member of the biotin-dependent family of enzymes found widely distributed throughout nature. Because of its importance in the intermediary metabolism of prokaryotes and eukaryotes, PC has been investigated in detail with respect to its reaction mechanism, its subunit structure, the relation between structure and activity, and the regulation of its catalytic activity (Attwood, 1995; Attwood & Geeves, 2002; Attwood & Graneri, 1992; Branson *et al.*, 2002; Jitrapakdee *et al.*, 2002; Jitrapakdee *et al.*, 2001; Rohde *et al.*, 1991; Val *et al.*, 1995; Wallace, 1985; Wexler *et al.*, 1994). However, a thorough understanding of the catalytic reaction mechanism of PC will require knowledge of the three-dimensional structure of the molecule which has not been obtained yet. Where no structure is available, monoclonal antibody binding is often taken as evidence for structural similarities between proteins and can even be interpreted to mean that the proteins have similar functions (Gershoni *et al.*, 1997). This is due to the fact that antibodies can exhibit exquisite specificity for their corresponding epitopes. With this advantage of monoclonal antibodies (mAbs), the epitope mapping of hPC using monoclonal antibodies will be useful to elucidate more information for structure-function studies of hPC.

In this chapter, three mAbs against sPC, designated mAb6, 12 and 42 were investigated to define their epitopes. It was shown that mAb6, 12 and 42 strongly recognised cPC and hPC in ELISA, and that they efficiently inhibited the acetylCoA-dependent activity of hPC by 91, 89 and 90% when compared to the control activity of hPC. This may indicate that the blocking antibody exerts its activity by partially shielding the substrate recognition domains of the enzyme or that they may induce some change to a conformation unfavourable to the catalytic activity of hPC. The inhibition of acetylCoA-dependent activity of sheep PC by mAb6, 12 and 42 was investigated in the presence of various concentrations of substrates for the two partial

catalytic reactions of PC. The inhibition of sheep PC by mAb12 and 42 was shown to be reversed in the presence of oxaloacetate, but to be increased for mAb6 (Carey, 1988) [Section 1.1 in Appendix I]. These results are consistent with our hypothesis that the epitopes of these three blocking antibodies are likely to be functional epitopes involved in some part of the catalytic reaction of PC. These data also indicate that the mAb6 epitope is distinct from the epitopes of mAb12 and 42.

To localize the epitope of mAb6 on hPC, we screened the binding of this antibody to a series of fragments of hPC using thioredoxin fusion protein technology. The results from immunoblots probed with mAb6 showed that this antibody bound to the fragments F3 (residues 947-1178) and TB1 (residues 947-1048). Using a panel of five overlapping fragments, this epitope was further determined and found to reside within the amino acid sequence LKDLPRV (residues 968-974). Although this epitope of mAb6 is highly conserved in vertebrates such as human (Walker *et al.*, 1995), rat (Jitrapakdee *et al.*, 1996), mouse (Zhang *et al.*, 1993) and chicken (Jitrapakdee *et al.*, 2002), these residues are not conserved in yeast and prokaryotes, *Rhizobium etli* and *Mycobacterium tuberculosis* (Dunn *et al.*, 1996) as shown in Figure 3.12. Of the residues in the mAb6's epitope only Leu^{968} (in the hPC sequence) is conserved between species. In contrast, other residues in the region 950-961 of hPC for example, Gly^{950}, Gly^{953}, Pro^{955}, Gly^{958}, Pro^{960} and Glu^{961}, are all highly conserved among vertebrate PCs, yeast PC, *R. etli* (Re) PC and *M. tuberculosis* (Mt) PC (Figure 3.12).

In addition to the mapping studies, mAb6 was tested with partially purified hPC and cPC under native conditions for binding in an ELISA. Although it also cross-reacts with native hPC enzyme in an ELISA assay (Figure 3.2) the affinity was lower (dilution 1:100) than the result from immunoblotting (dilution 1:1000) with denatured hPC (Figure 3.3) or fusion protein fragment (Figure 3.7). This suggests that the structure of this epitope in the fusion protein fragment or denatured enzyme is more accessible for

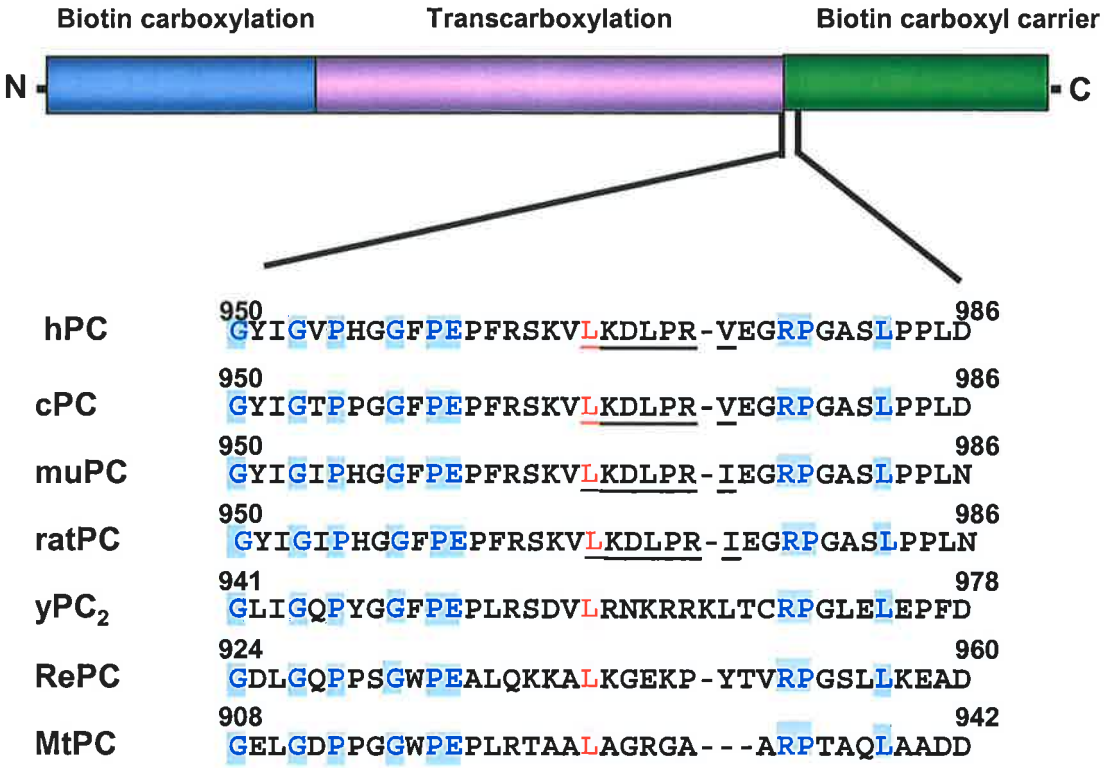

Figure 3.12 **Sequence alignment between hPC, yPC2, cPC, mouse PC, rat PC, *R. etli* (Re) PC and *M. tuberculosis* (Mt) PC.** Sequence alignment of amino acid 950-986 in hPC sequence is indicated. The region to which mAb6 epitope localised is shown underlined. Leucine^{968} in hPC sequence, the only totally conserved amino acid in this epitope region, is indicated as red colour. Amino acids conserved in these PC sequences are indicated as blue colour.

the antibody to bind than that of native PC containing 4 subunits to form a homo tetramer. Thus the ability of antibody to bind the active site in terms of assembled enzyme is lower than that in the fusion protein or denatured enzyme. Until now the quaternary structure of PC has only been obtained by electron microscopic studies, which have shown that PCs from different species are tetrahedron-like structures, composed of two pairs of subunits in different planes orthogonal to each other (Mayer *et al.*, 1980). This observation suggests that the three-dimensional structure of hPC, a tetrahedron-like structure, constitutes a steric hindrance for the mAb6 antibody's access to its epitope. Since antibodies must have access to an antigenic site in order to bind, this has led to the view that antibody accessibility is the primary intrinsic determinant of antigenicity (Novotny *et al.*, 1987).

Studies of competition of avidin or anti-biotin with mAb6 to bind with sheep PC showed that the binding of mAb6 to sheep PC was not affected by avidin or anti-biotin (Table 1.4 in Appendix I). This suggests that the mAb6's epitope might not be within the avidin or anti-biotin exclusion areas (Carey, 1988). Studies using avidin probes on PC to determine the location of biotin suggest that it is located on the external face of each subunit within 3 nm of the inter-subunit junction (Johannssen *et al.*, 1983). Thus, the mAb6's epitope may be located at the side or underneath the PC subunit and nearby the inter-subunit junction but not in the area excluded by avidin (Figure 1.6 in Appendix I).

In all PCs with an α_4 subunit composition, the transcarboxylation domain is located centrally in the polypeptide connected N-terminally to the biotin carboxylation domain and C-terminally to the biotin carboxyl carrier domain by proline rich sequences. These sequences have been suggested to form hinge-structures that allow the three domains of PC to fold together to form a single active site (Jitrapakdee *et al.*, 1996). Analysis of the distribution of proline residues in the hPC sequence (Table 3.1)

showed that two segments containing residues 501-550 and 951-1000 have 24 and 14 % of their residues as proline, higher than the average of proline in the whole hPC sequence (5.68%). Thus mAb6's epitope, LKDLPRV (residues 968-974) is in a segment containing residues 951-1000, which is rich in proline.

Table 3.1 The distribution of proline residues in human PC sequence. The percentage of proline distribution in sections of human PC sequence is shown by calculation of proline residues in each section of 50 residues of human PC sequence.

Human PC residues	Proline distribution	% of proline distribution
1-50	3	6
51-100	2	4
101-150	2	4
151-200	4	8
201-250	2	4
251-300	2	4
301-350	0	0
351-400	3	6
401-450	2	4
451-500	2	4
501-550	12	24
551-600	2	4
601-650	3	6
651-700	2	4
701-750	2	4
751-800	2	4
801-850	3	6
851-900	1	2
901-950	2	4
951-1000	7	14
1001-1150	4	8
1051-1100	0	0
1101-1150	4	8
1151-1178	1	3.7
Total	67	5.68

The sequence alignment among various PCs in Figure 3.13 showed that this epitope is localised between the transcarboxylation and the biotin carboxyl carrier domains. Consistent with the structural domain map of yeast PC determined using limited proteolysis of PC with several different proteases (Figure 3.14), the localisation of epitope of mAb6 is in the linker (amino acids 900-1080) between the transcarboxylation and biotinyl domains (Lim *et al.*, 1988). This indicates that the

mAb6's epitope might be associated with mobility of the biotin carboxyl carrier domain operating as a swinging arm that conveys a covalently-bound intermediate (CO_2) between the different subsites in the catalytic reaction of PC.

This proposal is consistent with effects of substrates on the inhibition of acetylCoA-dependent activity of sheep PC by mAb6. The results showed that only the presence of 1 mM oxaloacetate (but not pyruvate, Mg^{2+} or $MgATP^{2-}$) increased the % inhibition by mAb6 (Table 1.1.1 in Appendix I) (Carey, 1988). A similar result was obtained for the presence of 1 mM oxaloacetate to increase the % inhibition of hPC activity by mAb6 (Figure 3.5). In contrast, the % inhibition of sheep PC was not increased by Mg^{2+} and $MgATP^{2-}$ in the presence of mAb6 (Table 1.3.1 in Appendix I) (Carey, 1988) suggesting that the increasing amount of Mg^{2+} might inhibit the activity of sheep PC. The binding of mAb6 to human or sheep PC might affect the mobility of the biotin carboxyl carrier domain in its translocation between the first and the second subsite in the partial second reaction of PC, resulting in increasing the % inhibition by mAb6. It has been shown that increasing the amount of Mg^{2+} was inhibitory with regard to the induction of the decarboxylation of the isolated enzyme-carboxybiotin complex of sheep PC by analogues of pyruvate (Goodall *et al.*, 1981). A similar result was shown by Attwood *et al.* (1984) and these authors proposed that the inhibitory action of Mg^{2+} arises because it enhances the binding of the carboxybiotin to the site of the biotin carboxylation reaction (Attwood *et al.*, 1984; Goodall *et al.*, 1981).

Consistent with our proposal that mAb6's epitope being in a proline rich region involves the mobility of the biotin carboxyl carrier domain is the evidence that the linker regions of *E. coli* pyruvate dehydrogenase (PDH) complex have been studied and found to be highly mobile and exposed to solvent (Cronan, 2002). The mobility of these linker regions was first detected by NMR studies of the intact complex (Perham *et al.*, 1981; Radford *et al.*, 1987). Studies were made of synthetic peptides identical to or

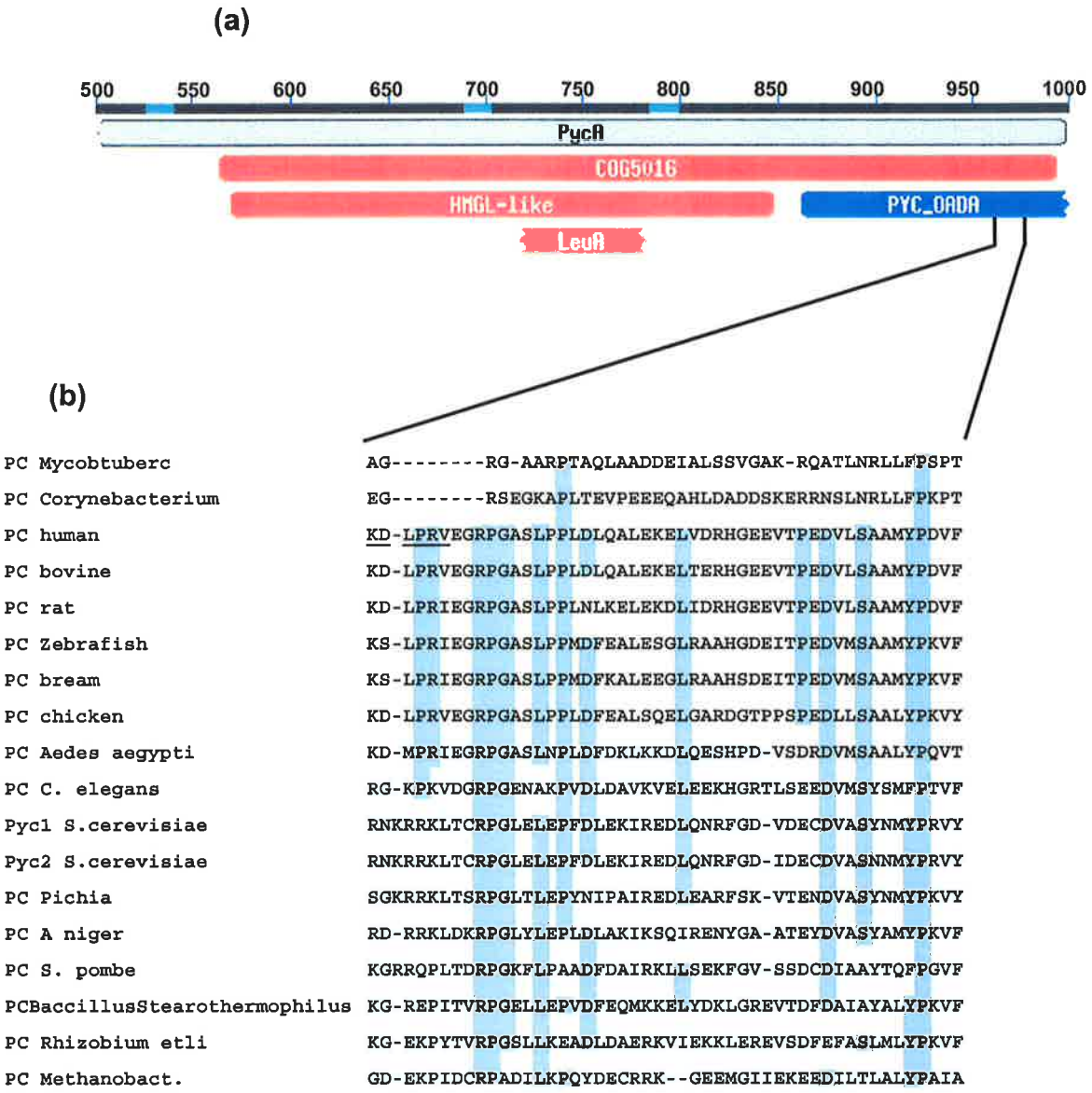

Figure 3.13 Diagram showing the putative transcarboxylation domain aligment among various PCs. (a) The alignment of biotin enzyme family, Pyruvate carboxylase (PycA), Pyruvate/oxaloacetate carboxyltransferase(PYC-OADA), HMGL-like domain, Pyruvate /oxaloacetate carboxyltransferase (COG5016) and Isopropylmalate/homocitrate/citramalate synthases (LeuA) is shown by NCBI Conserved Domain Search (www.ncbi.nlm.nih.gov/Structure/cdd/wrpsb.cgi). (b) The alignment among various PCs showing the location of mAb6's epitope (underlined in hPC sequence) in a proline-rich region, with substantial sequence conservation (indicated as blue box).

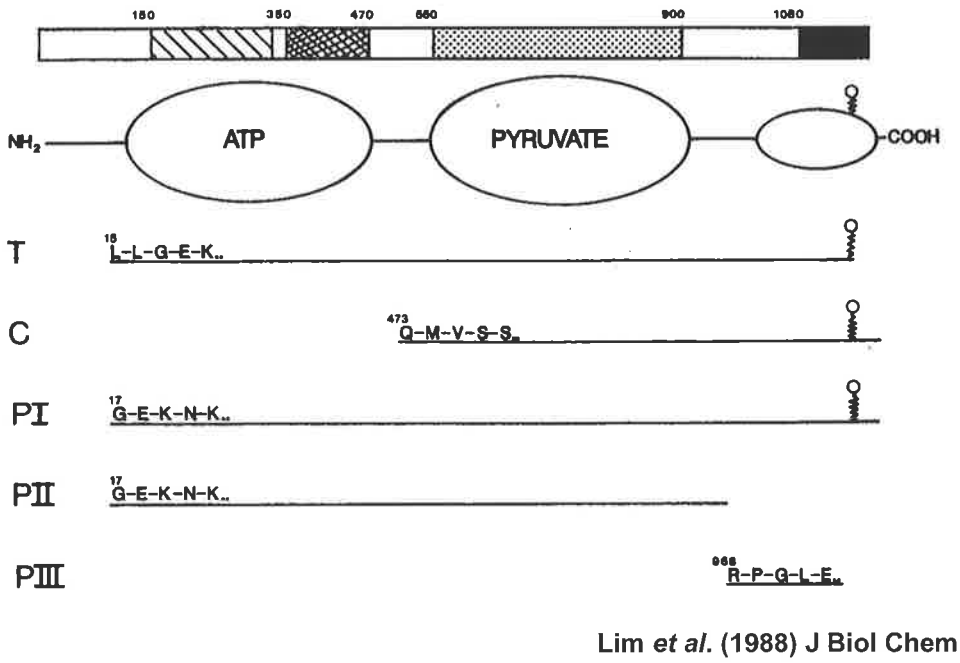

Figure 3.14 Diagram showing the structural domain map of yeast pyruvate carboxylase. The amino-terminal sequences of the major polypeptides derived from limited proteolysis by thermolysin (T), chymotrypsin (C) and proteinase K (PI, PII, PIII) are aligned within the total protein sequence. The numbers given are relative to the amino terminus and the block diagram is shown for comparison. The putative binding sites for ATP and pyruvate are indicated. [reproduced from Lim *et al.* (1988)]

related to the long (alanine + proline)-rich region of the polypeptide chain that links the innermost lipoyl domain to the dihydrolipoamide dehydrogenase-binding domain in the dihydrolipoyl acetyltransferase component of PDH of *E. coli* using NMR spectra. It was found that these three long (alanine + proline)-rich regions are exposed to solvent, and are involved in substantial conformational flexibility in the enzyme complex. This may reflect structural tuning of these segments to optimise lipoyl domain movement in the catalytic reaction mechanism of the enzyme (Radford *et al.*, 1989a).

The epitopes for mAb12 and 42 can only be mapped to a region of approximately 80 residues within the biotin carboxyl carrier domain of hPC on fragments TB2 80n. It was shown that if this fragment TB2 80n was truncated to TB2 60n, it no longer bound these antibodies. Although, TB2 (131 residues) was positive with these antibodies, the C-terminally truncated fragments, TB2 121c (121 residues) and TB2 111c (111 residues) were not. Thus these epitopes appear to be discontinuous or conformationally-dependent epitopes.

The deletion of 10 and 20 residues from the C-terminal of TB2 or 20 residues from the N-terminal of human PC biotin carboxyl carrier domain (TB2 80n) also abolished *in vivo* biotinylation. This result is in agreement with the evidence showing amino acid residues located 30-40 residues either side of the biotin-attachment site have been shown to be essential for biotinylation (Cronan, 1990; Murtif & Samols, 1987; Reed & Cronan, 1991). It has been demonstrated that in yeast PC, the C-terminal 104 residues of the biotinyl domain can act as an independent domain in the biotinylation reaction *in vitro* (Val *et al.*, 1995). In the α-subunit of human PCC, it has been shown that the Pro-Met-Pro motif (26 residues N terminal of the target lysine) is critical for biotinylation. Deletion of this motif abolished biotinylation (Leon-Del-Rio & Gravel, 1994). A protein fragment consisting of the C-terminal 87 residues of the biotin carboxy carrier protein from *E. coli* acetyl-CoA carboxylase was overexpressed in *E.*

coli. The peptide is recognised by biotin ligase *in vivo* and *in vitro* and can be fully biotinylated by coexpression with *E. coli* biotin ligase (Chapman-Smith *et al.*, 1994). The *in vivo* biotinylation of human PC biotin carboxyl carrier domain (TB2 107n or TB2 80n) will be investigated in more detail in Chapter 5.

In summary the epitopes of mAb6, 12 and 42 on hPC were determined using recombinant DNA technology to express various truncated fragments as thioredoxin fusion proteins. The minimal epitope of mAb6 was shown to be residues 968-974 (LKDLPRV) that are localised between the transcarboxylation and the biotin carboxyl carrier domains. The mAb6's epitope, in a proline rich region of hPC, might be associated with the mobility of the biotin carboxyl carrier domain in catalysis by PC. Site-directed mutagenesis of specific residues representing this epitope of mAb6 will be further investigated in Chapter 4. For mAb12 and 42, their epitopes were localised on hPC within the biotin carboxyl carrier domain on fragment TB2 80n, and more detail of these epitopes will be presented in Chapter 5.

CHAPTER 4

Mutation of the Epitope of Monoclonal Antibody 6

CHAPTER 4

4.1 INTRODUCTION

A full-length clone of human pyruvate carboxylase (hPC) has been obtained (Jitrapakdee *et al.*, 1999). To map the epitopes on this enzyme, the expressed hPC has been characterized using monoclonal antibodies: 6, 12 and 42, that were raised against sheep PC, but which cross-reacted with PC of other vertebrate species. In Chapter 3 it was shown that antibody mAb6 recognized a distinct linear epitope located between the transcarboxylation and the biotin carboxyl carrier domains at residues 968-974 of human PC, which is in a proline-rich region. Moreover, the acetylCoA-dependent activity of hPC was inhibited in the presence of mAb6 and this may reflect the restricted movement of the biotin carboxyl carrier domain in enzyme catalysis. To investigate the structural and functional significance of particular residues within this epitope, site-directed mutagenesis was carried out to generate single alanine substitution mutants by replacing individual amino acids in the epitope.

Mutagenesis is an important tool in probing the structural and functional significance of particular amino acids within a protein sequence (Knowles, 1987; Shaw, 1987). Amino acid residues might be altered to test for their participation in catalysis, cofactor or substrate binding, molecular and receptor recognition, domain interfaces and oligomeric interactions (Bordo & Argos, 1991). "In protein engineering as well as molecular modelling, where new structures are built from those with known tertiary and homologous primary structures, it is essential to know which residues can be substituted safely" (Sali *et al.*, 1990). Safe substitutions are a pre-requisite for the success of the mutant probe as an indicator of critical residues in structure and function. "The general idea is that the substitution of an amino acid with another amino acid with similar physicochemical properties should not influence the stability of the protein" (Jonson & Petersen, 2001). It has been shown that the Gly-Ala substitution is one of the most

frequently mentioned in specific point mutations for several molecular species (Shaw, 1987). However, alanine has a high negative correlation with all but the non polar residues. A serine residue has been proposed to be used as a substitute for the residues that are negatively correlated with alanine (Jonson & Petersen, 2001).

In this chapter, site-directed mutagenesis was performed upon the ^{968}LKDLPRV^{974} epitope of hPC to generate six single substitution mutants by replacing amino acids in this epitope with alanine. Alanine screening involves the substitution of residues to alanine, based on the assumption that alanine is a neutral residue. These mutants were expressed as thioredoxin fusion proteins in *E. coli* and analysed for these bindings by mAb6. Finally, histidine-tagged full-length hPC mutants were generated to investigate the function of critical residues representing this epitope, by comparing the enzymatic activity of these mutants to wild type hPC expressed in 293T cells.

4.2 SPECIFIC METHOD

4.2.1 Site-directed mutagenesis

Mutagenesis was performed with the Quickchange site-directed mutagenesis kit. Two complementary oligonucleotides were designed containing the desired mutation and a silent mutation to facilitate the cloning step. The reaction was carried out in a total volume 50 µl containing of 70 ng of double stranded pBluescript II ks(+), 125 ng of each primer and 200 µM dNTPs mix in 1X buffer [20 mM Tris-HCl pH 8, 10 mM KCl, 6 mM $(NH_4)_2SO_4$, 2 mM $MgCl_2$, 0.1% Triton X100, 100 µg/ml nuclease-free bovine serum albumin (BSA)]. *Pfu* DNA polymerase (2.5 U) was then added and each reaction was overlaid with 30 µl of light liquid paraffin oil. The reaction mixture was subjected to 16 rounds of temperature cycling. The profile consisted of an initial denaturation at 95°C for 30 sec followed by 16 cycles of denaturation at 95°C for 30 sec, annealing at 55°C for 1 min and extension at 68°C for 7 min. After thermal cycling, *Dpn* I (10 U) was added and the solution was incubated at 37°C overnight to digest the methylated parental (non mutated) DNA. Ten microliters of this solution were then introduced into 50 µl of competent DH5α cells (Section 2.11.6). Transformation was performed as described in Section 2.11.6.

4.2.2 Construction of six mutants of pET-hPC encoding residues 961-1178 (pET-hPC 217)

Site-directed mutagenesis of the LKDLPRV residues within the 961-1178 region of hPC was performed by PCR using pEF-PC as a template (Jitrapakdee *et al.*, 1999). The primers: K969A for, D970A for, L971A for, P972A for, V974A for and E975A for with a unique 5' *Eco*RI site and another unique 3' *Not*I site for MTC rev in Section 2.3.2 were used. These primers were designed to mutate each residue of the LKDLPRV region individually and systematically to alanine (Figure 4.1). These constructs were designated as K969A, D970A, L971A, P972A, V974A and E975A. The PCR profile

was as described in Section 2.11.8. The 651bp product for mutant L971A was amplified only when the primer annealing temperature was decreased from 55°C to 45°C. These fragments were then digested (Section 2.11.2) and ligated (Section 2.11.5) into the *Eco*RI and *Not*I sites of pET-32a (+) vector (Novagen). The six mutant constructs were isolated from transformants (Section 2.11.1) and sequenced (Section 2.11.7) to confirm the generated mutations (Figure 4.3).

4.2.3 Transient and stable transfection of 293T cells

The human embryonic kidney cell line, 293T, was routinely maintained in Dulbecco's modified Eagle Medium (Life Technologies) supplemented with 10% fetal calf serum, 100 µg/ml streptomycin and 100 U/ml penicillin. Cells were grown to 80-90% confluence in 175 cm^2 flasks at 37°C in a humidified atmosphere of 5% CO_2. Cells were washed twice with PBS, trypsinised and counted. Cells (1x 10^6) were resuspended in 5 ml of DMEM supplemented with 10% fetal calf serum, plated in 6-well plates and incubated at 37°C in a humidified atmosphere of 5% CO_2 overnight. Each well of cells was transfected with 4 µg of plasmid (eg. 6His mutant pEF-hPC) using Lipofectamine 2000 reagent (Invitrogen, life technologies). Briefly, 10 µl of Lipofectamine 2000 reagent was diluted in 250 µl of Opti-MEM Medium and the mixture was incubated for 5 min at room temperature. Once the Lipofectamine 2000 reagent was diluted, DNA was added and incubated at room temperature for 20 min to allow DNA-Lipofectamine 2000 reagent complexes to form. This solution was directly added to each well of the plates containing cells, mixed gently and incubated at 37°C for 4-6 hours. Five milliliters of DMEM supplemented with 10% fetal calf serum were added to each well and mixed gently. Transfected cells were allowed to recover in DMEM supplemented with 10% fetal calf serum at 37°C for 48 h before the lysates were prepared (as described in Section 4.2.5) and analysed by SDS-PAGE and Western blot.

For the generation of stable clones, transfected cells were plated on 10 cm^2 petri dishes and initially selected by adding 2 μg/ml puromycin to the culture medium for 1-2 weeks until resistant colonies were formed. Higher expressing clones were selected by gradually increasing the concentrations of puromycin to 2, 5, 10, 20 and 30 μg/ml and maintaining for 2-3 weeks. Pooled clones that resisted high concentrations of puromycin were expanded and analysed. Cell lysates were prepared as described in Section 4.2.4 and analysed by SDS-PAGE and Western blot analysis to monitor the expression level.

4.2.4 Protein extraction from 293T cells for measurement of PC activity

Stable cell lines were grown in DMEM plus 10% fetal calf serum supplemented with 100 μg/ml of streptomycin, 100 unit/ml of penicillin and 10 μg/ml of puromycin for 7 days. The cells were washed twice with phosphate buffer and centrifuged at 1300 rpm for 3 min. The cell pellet was suspended in 2 volumes of 0.25 M sucrose, 0.1 mM EDTA, 0.5 mM PMSF and 1 mM DTT at 4°C, and vortexed with an equal volume of cold glass beads for 3 × 10 sec with 10 sec cooling intervals in ice. Cell debris was removed by centrifugation at 13000 × g for 10 min. The supernatant containing PC was further fractionated by adding 100% saturated ammonium sulphate solution pH 7.0 to a final concentration of 40% saturation and stirring at 4°C for 30 min, then centrifuged at 13000 × g for 30 min. The precipitate of PC was dissolved in 0.15 ml of 25 mM Hepes (K^+) pH 7.2 containing 1.6 M sucrose, 0.1 mM DTT and 0.1 mM EDTA. Protein content was determined by the Bradford method as described in Section 2.13.3.

The enzymatic activity of pyruvate carboxylase was measured by following the production of NAD^+ using the coupling enzyme, malic dehydrogenase, as previously described in Section 3.2.3 with some modifications. Unrelated oxidation of NADH activity needed to be accounted for in order to accurately measure the activity of PC. As streptavidin has a very high affinity for biotin, it is a potent and highly specific

inhibitor of biotin dependent carboxylases. It has been shown that the enzyme-avidin complex was relatively unstable and undergoes an irreversible loss of activity at a rate which was 5 times the rate of avidin dissociation (Duggleby *et al.*, 1982).

In order to correct for the NADH oxidation of the partially purified enzyme preparation, PC in the assay solution (Section 3.2.3) was incubated with 4 μg of streptavidin at 37°C for 5 min before the addition of 0.1 mM acetyl-CoA for the background control. Thus biotin dependent carboxylases in the lysates were bound to streptavidin and inactivated and residual NADH oxidation measured directly. The reaction assays were performed under the same conditions in the absence of the streptavidin and the reaction was performed for 10 min. To calculate the net activity of the expressed hPC, the background activity of untransfected 293T cells was subtracted from the observed activity.

4.3 RESULTS

4.3.1 Immunoblot of yPC_2 against mAb6

As the results from Chapter 3 showed, mAb6 bound to PC from sheep, chicken and rat. This epitope on hPC was defined by deletion mapping as the sequence ^{968}LKDLPRV^{97}. Based on sequence alignment among PCs from human, yeast, chicken, mouse and rat, this epitope is highly conserved among higher eukaryotes but not yeast (Figure 4.1). This suggests that mAb6 should not react with yPC_2. To test this possibility, the binding of mAb6 to yPC_2 was assayed by Western blot. The cell lysate of yPC_2 expressed from yeast (strain W303) bearing plasmid pVT100-PYC_2 with myc tag (constructed by S. Jitrapakdee) was prepared (Section 2.14.2) followed by SDS-PAGE. The blot was probed with mAb6 (dilution 1:1000) and avidin-alkaline phosphatase (dilution 1: 20,000). The expression of yPC_2 was seen on SDS-PAGE gel at the similar molecular weight of partially purified hPC (≅116 Kda) [Figure 4.2a]. The heavily overexpressed yPC_2 myc did not cross-react with mAb6 as evidenced by the similar result to the negative control, untransfected yeast strain W303, with the only positive band being seen with hPC (Figure 4.2b). The expression of yPC_2 was confirmed on the avidin blot (Figure 4.2c) and also an endogenous PC band was found in yeast W303.

4.3.2 A choice of amino acids substitution of six mutants of pET-hPC encoding residues 961-1178

As we have shown that mAb6 reacted positively with PC from human, sheep, rat and chicken but not from yeast, the amino acid sequences of these proteins for the region corresponding to and flanking residues 968-974 of hPC were compared in Figure 4.1. Whereas there was a complete conservation of the sequence LKDLPRV for the epitope of mAb6 (underlined in Figure 4.1) among PC of vertebrate species, only two of these residues are present in yPC_2 indicated as blue colour in Figure 4.1 (Leu^{968} and

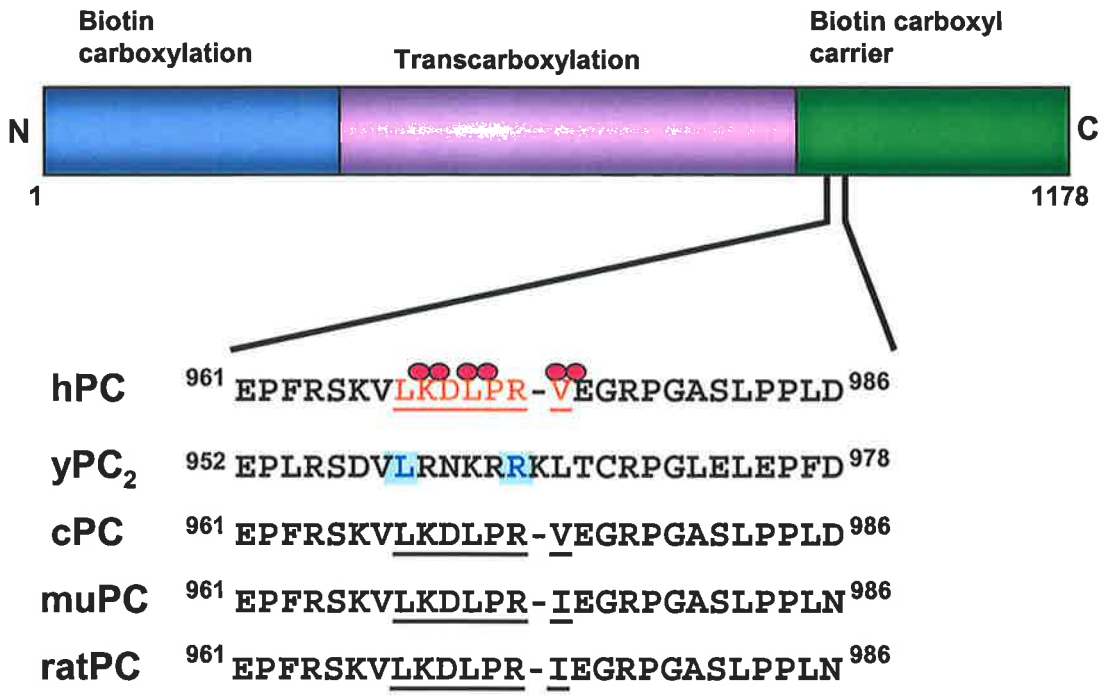

Figure 4.1 Sequence alignment between hPC, yPC_2, cPC, muPC, and rat PC in the region of the mAb6 epitope. Sequence alignment of amino acids 961-986 of hPC in the N-terminal of biotin carboxyl carrier domain of hPC is indicated. The region to which the mAb6 epitope localised is shown in red and underlined. The individual residues within the hPC epitope LKDLPRV were systematically replaced with alanine by site directed mutagenesis (circled). The residues, Leu^{959} and Arg^{964} of yPC_2 are conserved in this region, and are indicated in blue.

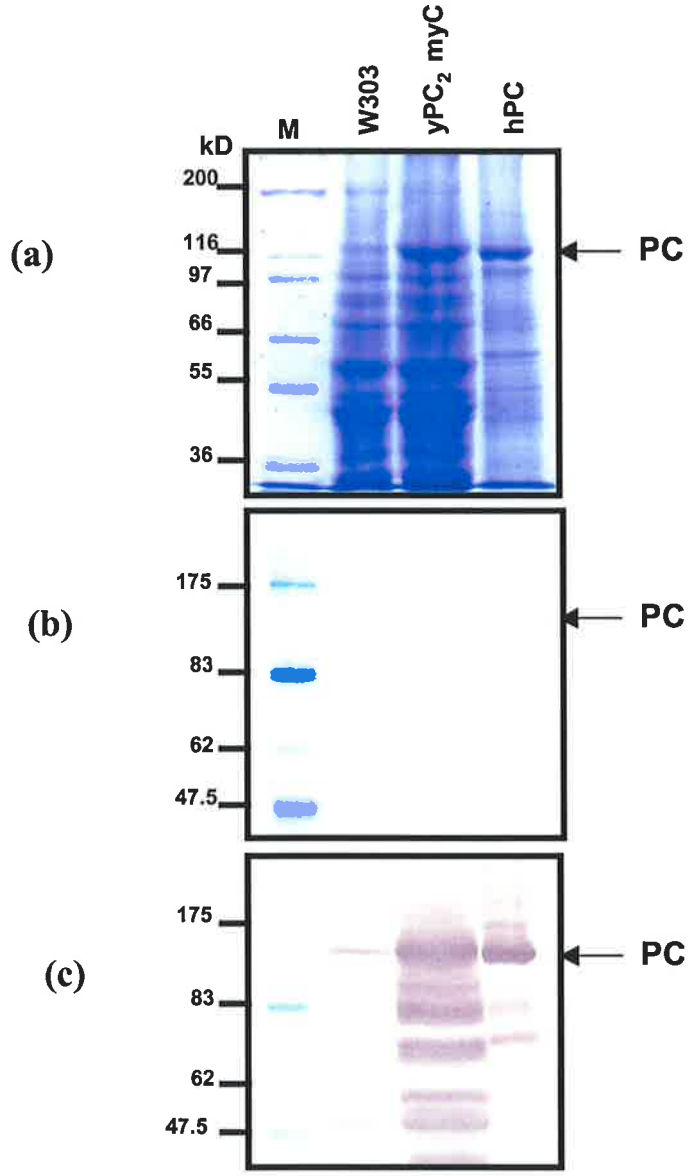

Figure 4.2 Immunoblot analysis of yeast strain W303, $yPC_2$with myC tag and hPC with mAb6. The lysate of yeast (W303) and yPC_2 with myc tag was performed as described in Section 2.14.2. The cell lysate was prepared and analysed on SDS-PAGE. The expression of proteins was stained with Coomassie brilliant blue (a) and probed with mAb6, dilution 1:1000 (b) and avidin alkaline phosphatase (c).

Arg^{973} of hPC corresponding to Leu^{959} and Arg^{964} of yPC_2). Therefore, the five residues that differed within this epitope (residues 968-974) were selected for mutagenesis (circled in Figure 4.1). These five residues, Lys^{969}, Asp^{970}, Leu^{971}, Pro^{972} and Val^{974}, but not Leu^{968} or Arg^{973} in the LKDLPRV epitope, were replaced by alanine. This resulted in five mutants, K969A, D970A, L971A, P972A and V974A. However, Glu^{975} positioned next to this epitope and thus likely to have an effect on the structural and functional relations was also replaced with alanine. To test the effect of this neighbouring amino acid on this epitope, E975A was also generated. Thus six mutants were generated as thioredoxin fusion proteins encoding amino acids 961-1178 of hPC and were characterised as described below.

4.3.3 Characterisation of six mutants of pET- hPC encoding residues 961-1178

The six mutations encoding K969A, D970A, L971A, P972A, V974A and E975A were constructed by site directed mutagenesis and confirmed by DNA sequencing (Figure 4.3). All mutants were expressed as fusion proteins with thioredoxin in *E. coli* BL21 as described in Section 3.2.7 except the temperature for incubation of overnight culture and induction was 30°C to avoid aggregation or incorrect folding of the proteins. The cell lysates from bacteria bearing the expression plasmids were harvested, subjected to SDS-PAGE (Section 2.13.1) and assayed by Western blot with mAb6 (dilution 1:1000).

As shown in Figure 4.4, all mutants were expressed at a similar level (Figure 4.4a). Five mutants, K969A, L971A, P972A, V974A and E975A were bound by mAb6 to a similar extent (Figure 4.4b). In contrast, the binding of mAb6 to mutant D970A was completely abolished, suggesting that Asp^{970} is critical to the binding of mAb6 in terms of the fusion protein fragment.

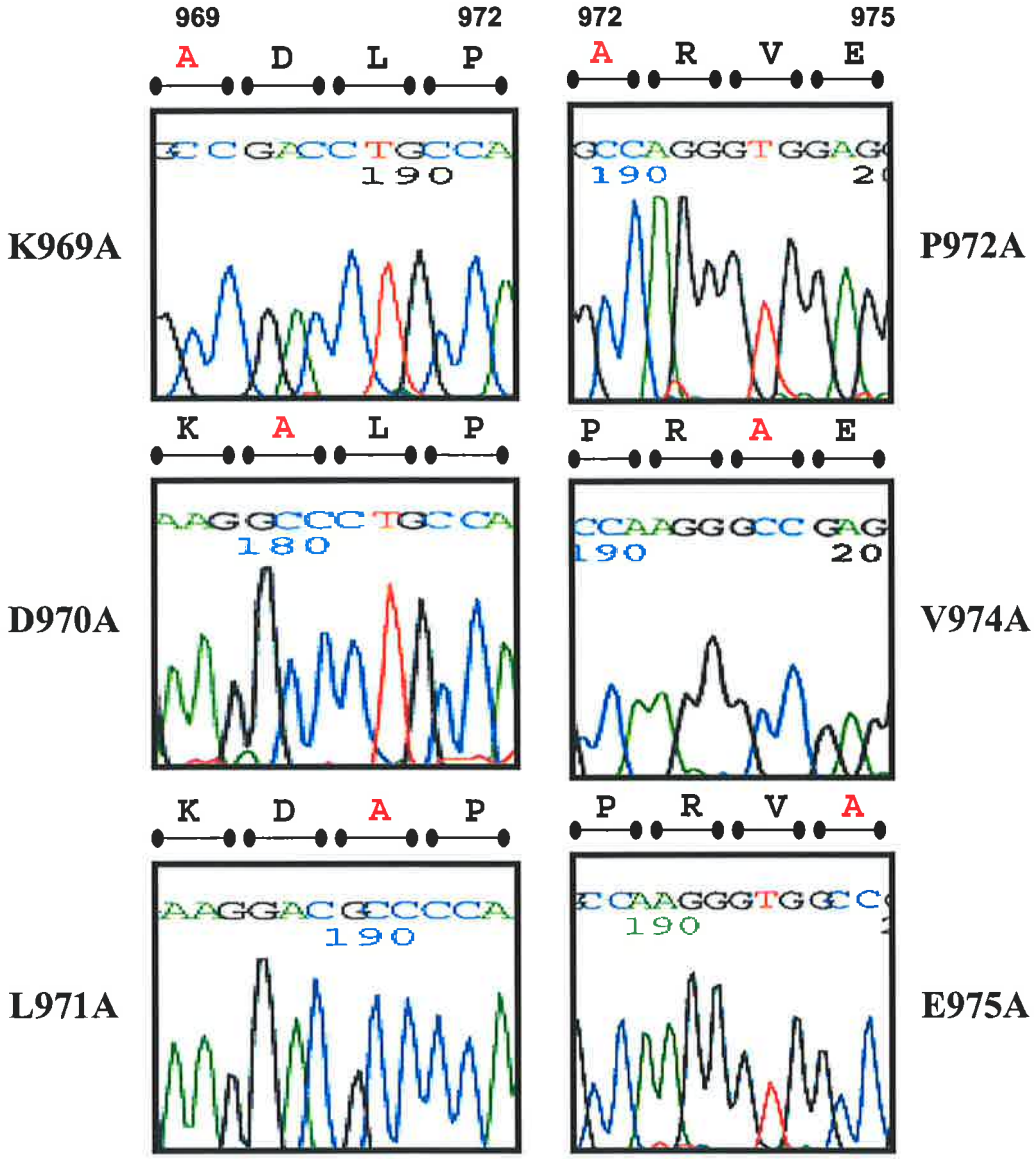

Figure 4.3 **Mutant sequencing results.** Residues, K969, D970, L971, P972, V974 and E975 were changed to alanine within the hPC sequence LKDLPRVE by site directed mutagenesis as described in Section 4.2.1. Sequencing was performed as described in Section 2.11.7.

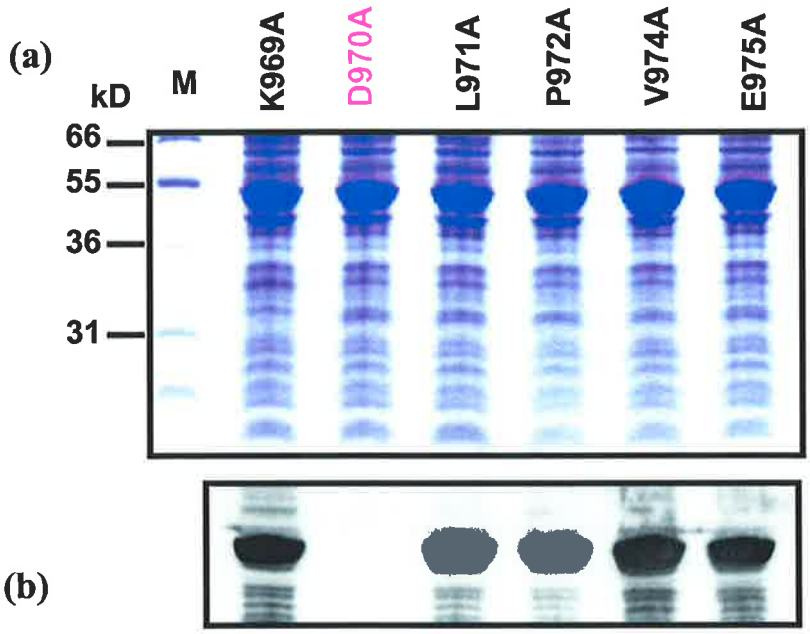

Figure 4.4 Immunoblot analysis of six mutants expressing 217 residues fragments of hPC. Six mutants containing pET-hPC encoding cDNA of 217 residues of hPC were expressed as fusion proteins with thioredoxin in *E. coli* BL21. The whole cell lysates were separated by SDS-PAGE and stained with Coomassie brilliant blue (a) and assayed with mAb6 (1:1000) by Western blot analysis (b). M = Wide Range Protein Standard Marker (Mark12, Novex).

4.3.4 Construction of mutated pBlue scriptII ks(+) (mpBlue)

Since mAb6 binding to hPC inhibited enzymatic activity the residues representing this epitope (LKDLPRV) in particular Asp^{970} might be important for the activity of the enzyme. To investigate the importance of the amino acids chosen for mutation for enzymatic activity, the six alanine substitution mutants were reconstructed as full-length hPC and expressed in a mammalian system. However, due to the presence of a *Xmn*I restriction site in the cloning vector pBluescript II ks(+), it was not possible to excise a single insert containing the designed mutation by digesting with *Xmn*I (at 5'-end) and *Not*I (at 3'-end). Therefore, the *Xmn*I site was abolished using site-directed mutagenesis to silently alter the codon for glutamic acid 62 in the ampicillin resistance gene to generate mpBlue (Section 4.2.1). This allowed the *Xmn*I site in the hPC gene to be used in subsequent cloning steps (Figure 4.5). This silent mutation was made by the Quickchange method (Stratagene) using complementary primers (forward and reverse MpBlue) given in Section 2.3.2. The mutagenesis reaction was carried out as previously described in Section 4.2.1. This new plasmid, containing one base substitution (A186→G position in the ampicillin resistance gene) was confirmed by restriction digestion with *Xmn*I and *Bam*HI. Only one fragment was digested from the *Bam*HI site to make the linearised plasmid for the positive clone. For the negative clone, the two fragments were produced from the *Xmn*I and *Bam*HI sites.

4.3.5 Construction of 6His-wt and mutant pEF- hPC (6His pEF-hPC)

The mutant plasmid (mpBlue) was generated to abolish an *Xmn*I site, which is unique in hPC sequence (Section 4.3.4). This plasmid is useful for the next step of cloning of full-length hPC. In order to construct the plasmid containing the cDNA of mutant full-length hPC with a histidine tag, the protocol was carried out as follows. Briefly, the full-length hPC fragment from pEF-PC (Jitrapakdee et al., 1999) was cloned into mpBlue vector at the *BamH*I and *Not*I sites. This resulting construct was

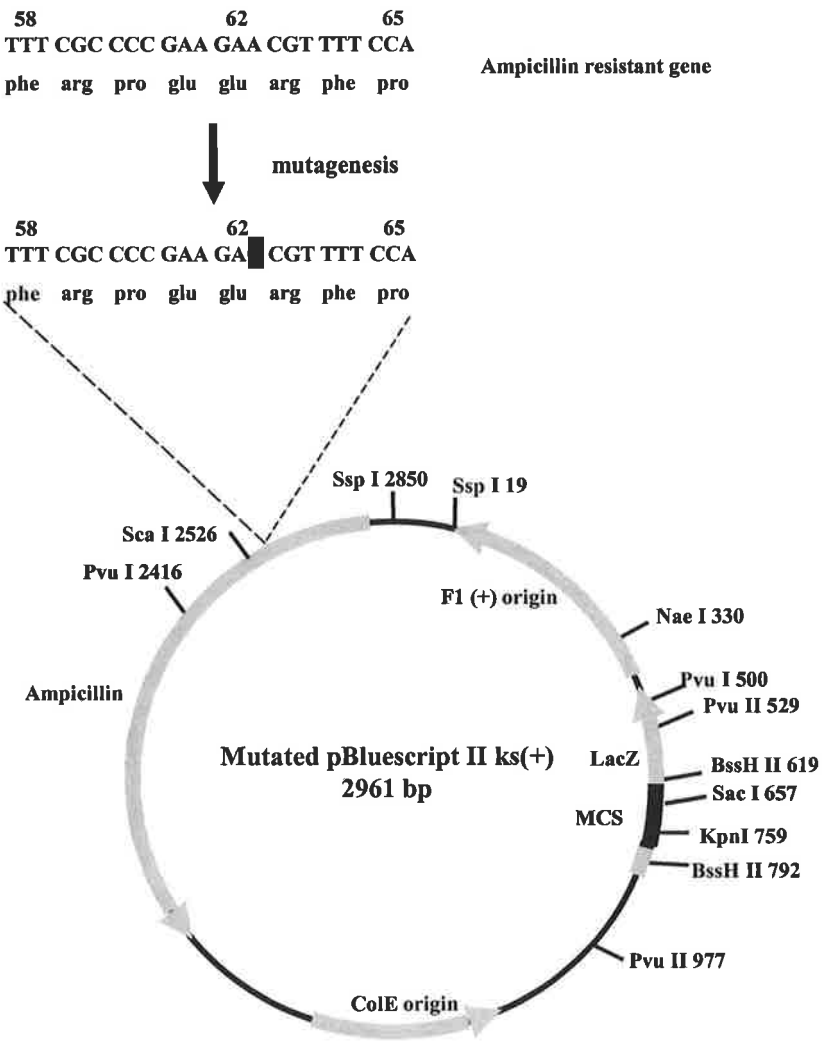

Figure 4.5 The mutated pBluescript II ks(+), mpBlue plasmid. The XmnI site was abolished using site-directed mutagenesis to silently alter the codon for glutamic acid 62 as shown in green shade in the ampicillin resistance gene resulting in mpBlue plasmid (Section 4.3.3). This plasmid is used in subsequent cloning step for construction of full length hPC.

designated mpBlue-hPC and then digested with *Xmn*I and *Not*I. The *Xmn*I-*Not*I fragment containing one point mutation (K969A, D970A, L971A, P972A, V974A or E975A) from mutant pET-hPC encoding amino acids 961-1178 of hPC fragment (pET-hPC 217) was ligated into pBluescript-hPC at the *Xmn*I and *Not*I sites. This yielded mpBlue-mutant hPC plasmid, which contained full-length mutant hPC. This full-length mutant hPC was excised by digestion with *BamH*I and *Not*I and then cloned into digested pET-32a (+) at the *BamH*I and *Not*I sites to create mutant pET-hPC plasmids containing full-length mutant hPC (pET-hPC MF). Due to two *BamH*I sites in 6His-wt pEF-PC (constructed by Jitrapakdee) three fragments ligation were used to clone full-length mutant hPC into mammalian expression vector. The next step, adding a 6histidine tag was carried out by digestion of pET-hPC MF with *Bst*EII and *Xho*I and 6His-wt pEF-PC with *Bst*EII and *Eco*RI. These two fragments were then ligated into *Xho*I and *Eco*RI site of 6His-wt pEF-PC yielding full-length 6His-tagged pEF-hPC mutant, 6His-mutant pEF-hPC (Figure 4.6). These plasmids (Figure 4.7) were subsequently transfected into mammalian cells, 293T for transient and stable transfection, as described in Section 4.2.2.

4.3.6 Characterisation of mutant full-length hPC expressed in mammalian cells

The six single point mutations representing the mAb6 epitope were transferred into 6His-tagged full-length hPC and transfected into the 293T cell line (Section 4.2.3). Stable clones producing the full-length hPC mutants, K969A, D970A, L971A, P972A, V974A and E975A were obtained. Protein extracts from the six stable cell lines were prepared and analysed for activities (Section 4.2.4).

The level of hPC expression at different concentrations of puromycin was determined by Western blot in order to obtain stable clones producing the highest level of protein. Since hPC and puromycin resistance proteins are co-transcribed on the same mRNA, clones that are able to grow in high concentrations of puromycin should also

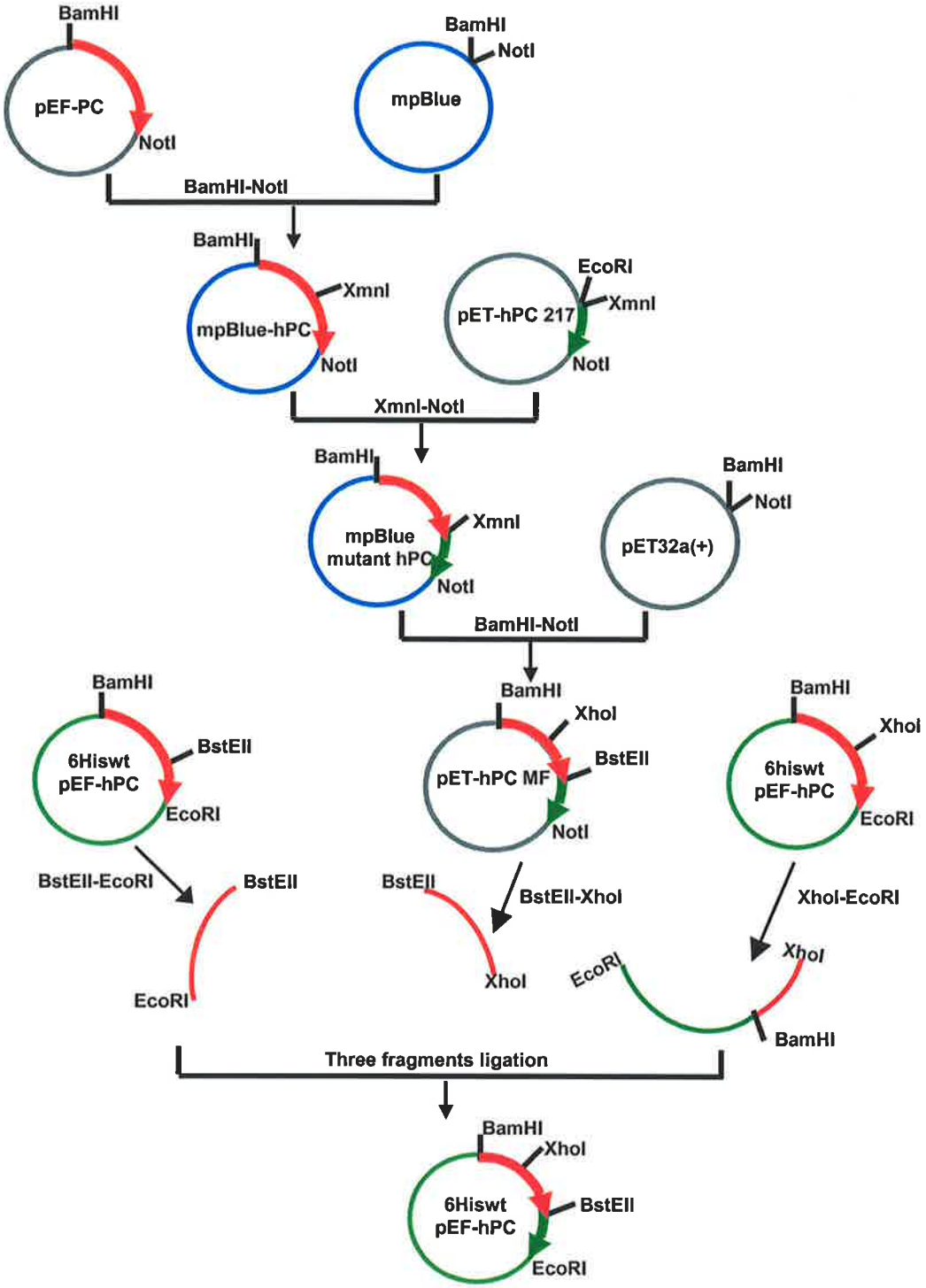

Figure 4.6 Construction of a plasmid for expression of 6 histidine tagged full-length mutant hPC (6His mutant pEF-hPC). The strategy for constructing a plasmid for expression of 6His mutant pEF-hPC was described in Section 4.3.5. These 6His wild type and mutant pEF-hPC plasmids were transfected into mammalian cells and the expressed proteins were analysed.

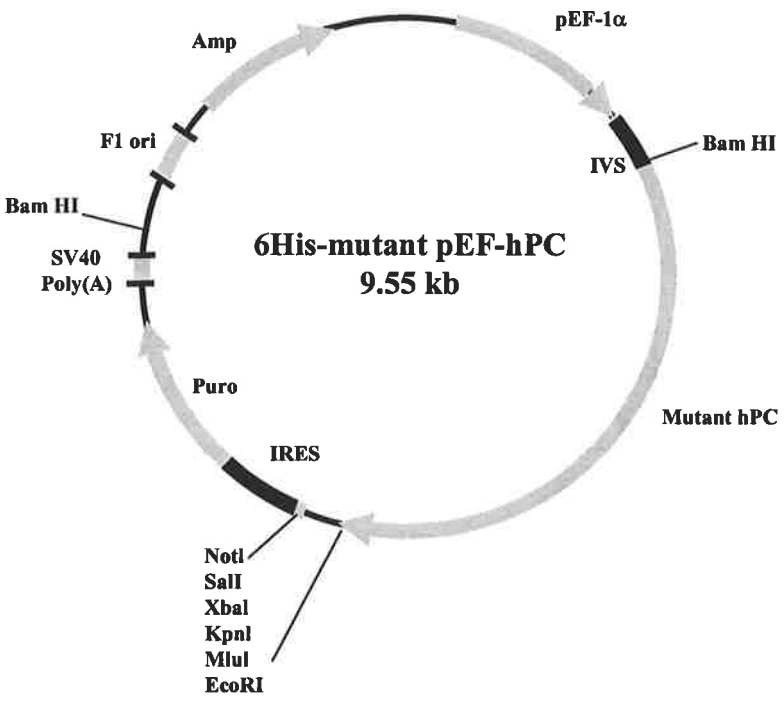

Figure 4.7 The 6His-mutant pEF-hPC plasmid containing mutant full-length hPC with 6histidine. This plasmid was constructed (Section 4.3.4) and subsequently transfected into mammalian cell, 293T for transient and stable transfection (Section 4.2.2). IRES, internal ribosome entry site; Puro, puromycin acetyl transferase gene; SV40 poly(A), SV40 polyadenylation signal; Amp, ampicillin resistance gene; pEF-1α, human polypeptide elongation factor 1α promoter; IVS, synthetic intron that enhances stability of the mRNA.

express high levels of hPC. Cells selected are those that become resistant to increasingly higher concentrations of puromycin because the heterologous DNA has integrated into chromosomal positions that are efficiently expressed and amplified. After several rounds of increasing puromycin selection, the final cell line obtained is usually composed of cells derived from one or a few transformants. Therefore pools of stable clones expressing each mutant were obtained from the resistant clones, which allowed any colonies that express a higher level of PAC to be expanded while any colonies that poorly expressed the puromycin resistance gene will die off.

Six constructs of mutant pEF-hPC were transfected as described in Section 4.2.3. After transfection they were transferred into Petri dishes and transfectants were initially selected by adding 1 μg/ml of puromycin in the culture media. After being cultured in this media for 3 weeks, more than 50% of cells had died off, and resistant colonies had started to form. A polyclonal pool of cells was used to select highly expressing clones by increasing the concentration of puromycin to10 μg/ml for 1 week, then subsequently to 20 and 30 μg/ml at weekly intervals. To test the expression of hPC from each stable pooled clone, the partially purified enzyme was prepared and analysed by Western blot, and the enzymatic activity was assayed as described in Section 4.2.4.

As shown in Figure 4.8, the expression levels of K969A and E975A were not higher enough to be seen clearly on a Coomassie stained gel (Figure 4.8a) but was detected on an avidin blot (Figure 4.8b). However, from this blot, the expression level of hPC of E975A mutant was similar at 10, 20 and 30 μg/ml of puromycin. Interestingly, the expression of enzyme from K969A at 30 μg/ml of puromycin was markedly decreased when compared to clones grown in 10 and 20 μg/ml of puromycin (Figure 4.8b). The activity of the K969A enzymes from both clones, at 20 and 30 μg/ml of puromycin was negligible (Figure 4.9). In contrast, the specific activities of enzymes from E975A were found to be not significantly different (Figure 4.9). Therefore, the

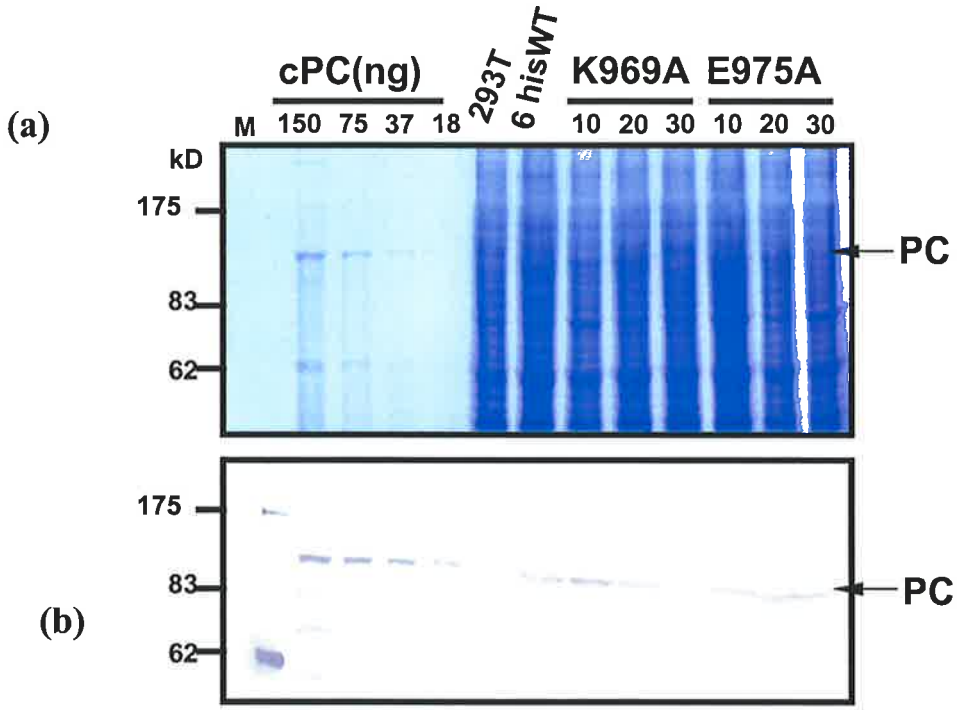

Figure 4.8 Expression of two mutants, K969A and E975A in 293T at different concentrations of puromycin. The stable clones were grown in media containing either 10, 20 or 30 µg/ml of puromycin and the cell lysates were prepared and analysed by Western blot. PC was stained on Coomassie brilliant blue gel (a) and detected on an avidin alkaline phosphatase blot (b). The amount of PC band was quantitated on an avidin blot compared to the known amounts of purified cPC. M= Prestained Protein Marker, broad range (New England Biolab).

stable clones of all of six mutants and the wild type control were cultured and prepared for the activity assay at a puromycin concentration of 10 μg/ml.

As observed in the stably transfected 293T cell lines, the expression level of wild type full-length hPC 6His-tagged and the other mutants was not sufficient to see clearly on a Coomassie stained gel (Figure 4.10a). However, as judged by Western blot analysis using avidin alkaline phosphatase detection, expression levels were similar for all PCs (Figure 4.10b). As shown in Figure 4.10c and quantitated in Figure 4.11, no significant differences in binding of mAb6 to four of the mutants, K969A, L971A, V974A and E975A, were seen as compared to histidine-tagged wild type. This demonstrates that antibody binding to these mutants in terms of full-length enzyme was unchanged, indicating that any structural effects of the mutations did not alter the ability of mAb6 to bind. Only the binding of mutant D970A by mAb6 was completely abolished, whereas the binding of mutant P972A mutant was reduced to 34% of histidine-tagged wild type hPC (Figure 4.11). This indicates that the binding of antibody mAb6 to mutant D970A was significantly reduced in terms of both the full-length enzyme and the thioredoxin fusion protein fragment. For mutant P972A the binding of antibody to full-length enzyme was partially reduced, but binding to the fusion protein fragment (amino acids 961-1178) containing the P972A single point mutation was only slightly affected (Figure 4.4).

PC activity assays were performed with partially purified protein (Section 4.2.5) from these seven cell lines grown at 10 μg/ml of puromycin. A histidine tag on the enzyme was found not to affect the activity of enzyme (Figure 4.12), as it has been shown that the specific activity of recombinant hPC with no histidine tag expressed from 293T cell line was 20 U/mg protein (Jitrapakdee *et al.*, 1999). Interestingly, the mutations did not significantly affect the specific activities of PCs for any mutants except D970A, where the specific activity was decreased to 11.5 U/mg (Figure 4.12).

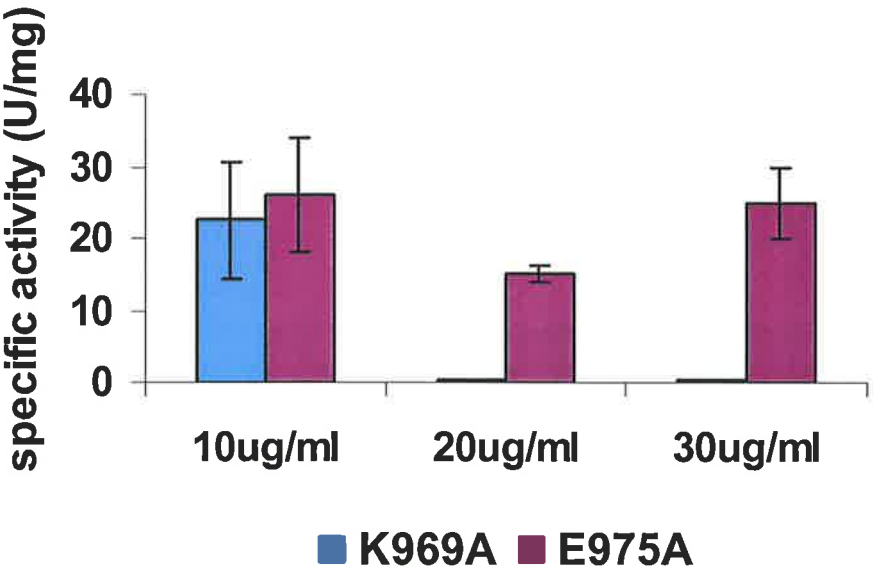

Figure 4.9 Specific activity of full-length 6His mutants of pEF hPC expressed in 293T cells. Two mutants containing 6His pEF-hPC encoding full-length hPC cDNA were expressed and lysates prepared for determination of the enzymatic activity. The given values are the mean of the measurement ± standard deviation (SD). Enzyme units (U/mg of PC) were determined in triplicate on partially purified enzyme preparations made from mutants grown in 293T at puromycin concentrations of 10, 20 and 30 µg/ml. PC activity was measured by spectrophotometry and the background of endogenous PC, determined by adding streptavidin under the same conditions, was subtracted.

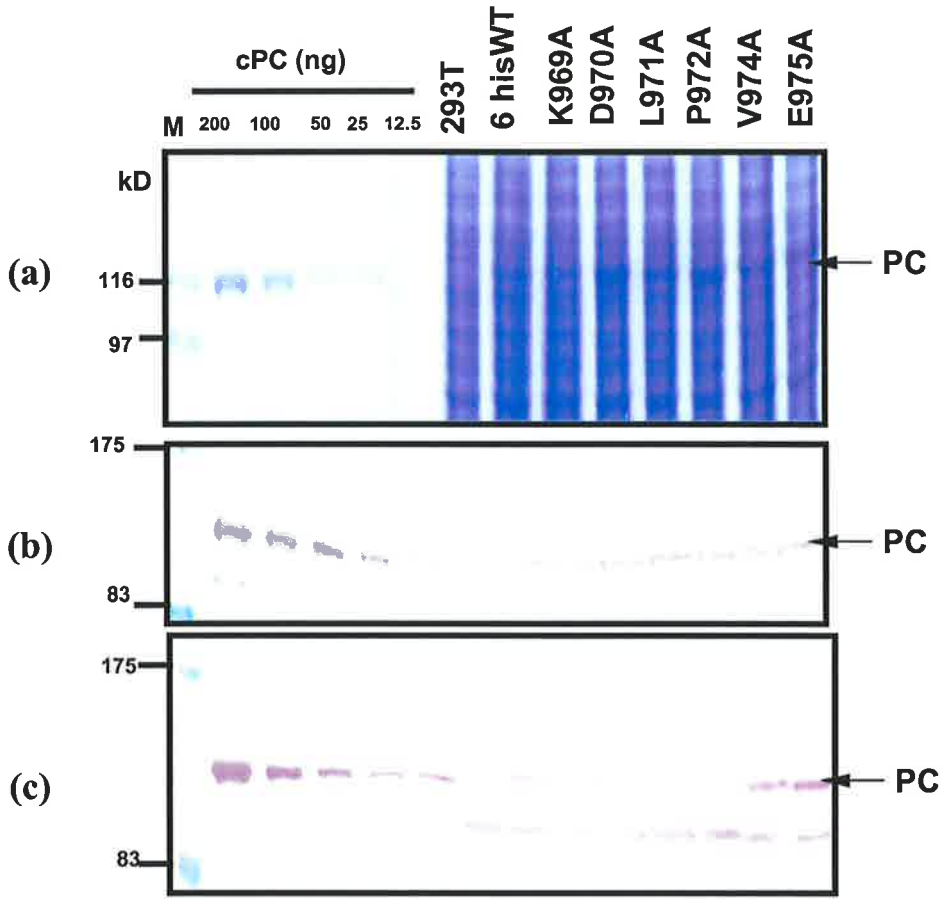

Figure 4.10 Expression of wild type and six full-length epitope mutants of hPC in 293T cells. The stable clones were grown in media containing 10 μg/ml of puromycin and the cell lysates were prepared and analysed by Western blot. SDS-PAGE was performed and stained with Coomassie brilliant blue gel (a). The blots were reacted with avidin alkaline phosphatase (b) and mAb6 dilution 1:1000, conc.1 μg/ml (c). The PC band was quantitated on an avidin blot compared to the known amounts of purified cPC. M = Wide Range Protein Standard Marker (Mark12, Novex) for Coomassie stained gel and Prestained Protein Marker (New England Biolab)for the blots.

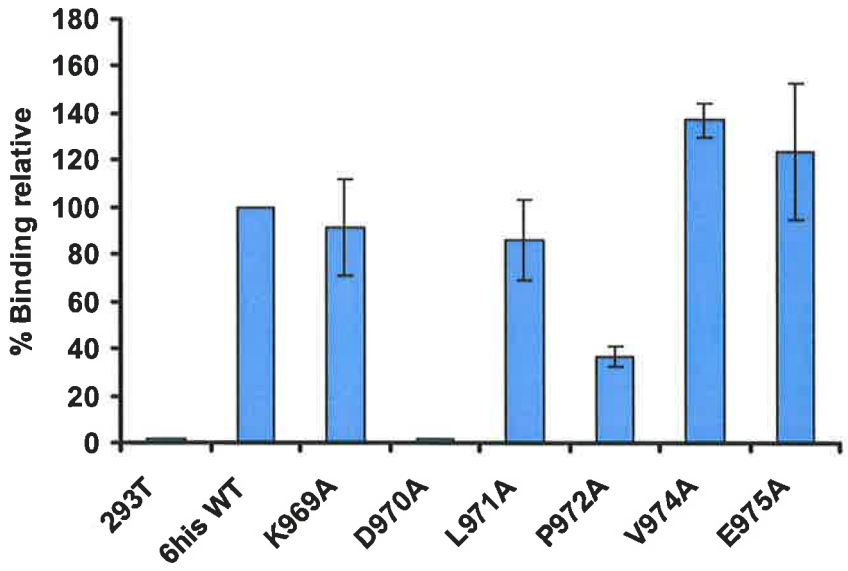

Figure 4.11 Binding of mAb6 to the six epitope mutants compared to wild type and 293Tcells. Six mutants and full-length hPC cDNA were expressed as 6histidine tagged proteins and lysates prepared for the binding with mAb6 at a concentration of 1μg/ml (dilution 1:1000). The results are quantitated data of the antibody blots from Figure 4.10 and shown as the mean of the measurement ± standard deviation (SD). The percent relative bindings compared with wild type were determined in triplicate of the lysates prepared from mutants, wild type or 293T.

This result suggests that the enzymatic activities of five mutants (K969A, L971A, P972A, V974A and E975A) were unchanged and the structural integrity of the enzymes was maintained in these mutants.

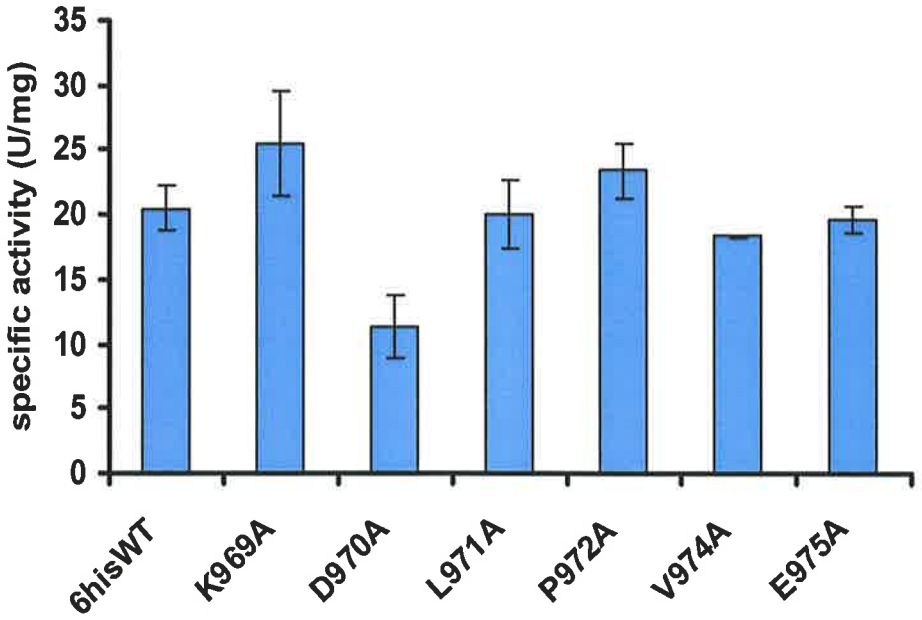

Figure 4.12 **Specific activity of 6His wt and epitope mutant full length hPC in 293T**. Wild type and six mutant full-length hPC cDNA were expressed as 6histidine tagged proteins and lysates prepared for determination of enzymatic activity. The given values are the mean of the measurement $\pm$ standard deviation (SD). Enzyme units (U/mg of PC) were determined in triplicate on partially purified enzyme made from either wild type or mutant grown in 293T. PC activity was measured by spectrophotometry and the background of endogenous PC, determined by adding streptavidin under the same conditions was subtracted (4.2.4). Protein quantitation was determined from an avidin-alkaline phosphatase blot (4.2.5).

4.4 DISCUSSION

The minimal epitope of mAb6 was defined in Chapter 3 as a linear epitope of seven amino acids, LKDLPRV (residues 968-974). In the presence of mAb6, the activity of hPC was inhibited by 91% when compared to that of hPC in the absence of mAb6. To test whether the residues critical for antibody binding would also influence acetyl-CoA dependent activity of hPC, we introduced the alanine mutations into a fragment of hPC encoding residues 961-1178 and expressed these as both thioredoxin fusion proteins in *E. coli* and full-length hPC in a mammalian cell line. The use of 293T cells to produce human PC might have some advantages over heterologous expression system such as *E. coli*, since the 293T cells were derived from human kidney, a cell type in which PC is expressed naturally. Thus 293T cells can provide the folding machinery required to process recombinant PC into its native form.

For the expression of full-length mutant hPC, K969A at 10, 20 and 30 μg/ml puromycin, expression at 20 and 30 μg/ml yielded a lower detectable level of hPC protein and no activity for hPC. The frequent loss of protein expression may be a consequence of the unlinked expression of the selection marker and the gene of interest since the selective pressure is only exerted on the drug resistance marker (Mielke *et al.*, 2000). In addition, high but mostly unphysiological concentrations of the desired protein can often-even lead to a counter selection against stable cell clones (Mielke *et al.*, 2000). A number of reports describe the development of bicistronic expression vectors containing drug-selectable genes under the control of an IRES element that allow the efficient creation of stably expressing cell lines (Aran *et al.*, 1994; Gurtu *et al.*, 1996; Hobbs *et al.*, 1998; Rees *et al.*, 1996). In addition, expression of the protein of interest can be maintained over a period of time by maintaining transfected cells in media containing an antibiotic as both proteins are simultaneously produced from the same mRNA (Hobbs *et al.*, 1998). However, in this experiment one cell line (K969A)

grown in 30 μg/ml puromycin, did not yield any detectable amounts of hPC. The loss of enzyme production might be caused by altered methylation or chromosomal instability of the transfected DNA. It has been previously reported that a high copy number of a transgene in one clone can be heavily methylated, whereas the low copy clones did not show any methylation of the tested promoter site (Mielke *et al.*, 2000).

As the identical epitope is not present in the yeast PC sequence and mAb6 does not bind to yeast PC, we used site-directed mutagenesis to change to alanine six residues within the binding site of mAb6 that are different from the sequence of yPC_2. Alanine was used as a substitute because it is uncharged and has the smallest side chain, except glycine, which is not preferred because it can alter the main chain conformation of the protein (Kim *et al.*, 2000). Only one of six mutants, D970A, expressed both as a fusion protein fragment in *E. coli* and as full-length hPC in mammalian cell line showed a similar effect of complete loss of binding to mAb6. This suggests that the negatively charged side chain of Asp^{970} plays an important role in binding with the antibody. Since the binding sites of antibody molecules recognize patches at the surface of antigens that are complementary to them in shape and chemical properties, disruption of the epitope site can lead to loss of antibody binding (Novotny *et al.*, 1987). It could be proposed that the charged residue modified in D970A mutant must be required for maintaining the structural integrity for this epitope. Curiously, replacement of the other residues within this epitope, Lys^{969}, Leu^{971}, Val^{974} and Glu^{975} does not seem to impair functionality of the hPC epitope in binding with mAb6 nor did it affect the catalytic activity, indicating that the proper three dimensional conformation of this epitope is of little importance for correct folding. Only the P972A mutant when expressed as the full-length protein in mammalian cells, caused a reduction of binding with mAb6 to 34%, when compared to that of wild type hPC (Figure 4.11). However, the catalytic activity of this mutant is similar to 6histidine tagged wild type PC (20 U/mg). This

suggests that the epitope in the P972A mutant was less accessible on assembled enzyme and the change from proline to alanine in the assembled enzyme was not disruptive to a protein structure but caused minor disruption to the immunoreactivity of mAb6 with the full-length protein but not with the fusion protein fragment. However, this does not affect enzymatic activity. A mechanism known to regulate epitope immunoreactivity is an interaction between proteins that prevent exposure of the epitope (Eto *et al.*, 2000).

The structural integrity of the alanine mutants used to delineate the functional epitope was subsequently assessed by measuring the specific activity in terms of acetylCoA-dependent activity of hPC per amount of expressed PC. The specific activities of five alanine mutants, K969A, L971A, P972A, V974A and E975A were essentially unchanged indicating the structural integrity of PC is maintained in these mutants or that the mutations do not result in gross structural perturbations within hPC. These five mutants displayed the catalytic activities that were nearly identical with the wild type enzyme and thus it appears that residues, Lys^{969}, Leu^{971}, Pro^{972}, Val^{974} and $Glu^{975}$are not important either for protein structure or catalytic activity of hPC. In contrast the replacement of the aspartic acid at position 970 with alanine resulted in a mutant that had completely lost its ability to bind mAb6. In addition, the acetylCoA-dependent activity was significantly reduced to 50% indicating Asp^{970}, which is likely to exposed on the surface of the enzyme, may be involved in significant side-chain interactions of the enzyme and possibly minor movement of the backbone conformation (Getzoff *et al.*, 1988). Thus, the substitution of Asp^{970} to alanine might have caused a local conformational disruption in the structure of the enzyme and the activity was reduced. Further characterisation of purified D970A mutant with more kinetic analyses may yield more information on the effect of Asp^{970} on the catalytic reaction mechanism of PC.

The presence of oxaloacetate increased the % inhibition of acetylCoA-dependent activity of sheep PC (Carey, 1988) and human PC (Chapter 3) by mAb6. Together with the location of this epitope between the transcarboxylation and biotin carboxyl carrier domains (Chapter 3) suggests that this epitope might be involved in mobility of the biotin carboxyl carrier domain of PC as the biotinoyl and lipoyl domains of *E. coli* ACC and PDH. Both domains are thought to act as swinging arms that convey covalently bound intermediates between active sites of a multienzyme complex (Perham, 2000). It was shown that BCCP function is not dependent on the length of the linker region. Although a defined overall length was not important, deletions of some linker segments resulted in acute losses of function (Cronan, 2002). This supports our proposal that the mAb6's epitope is likely to be some part of the proline rich segment close to the biotin carboxyl carrier domain of PC and involved in movement of this domain in PC catalysis. Further work will be required to test this hypothesis. The seven amino acids (LKDLPRV) of this epitope (residues 968-974) upstream sequences of the biotin carboxyl carrier domain might be deleted and then expressed as full-length hPC. The acetylCoA-dependent activity of hPC might be affected by deleting this segment as did the mAb6 have an inhibitory effect on hPC (Chapter 3).

Finally, with the results from chapter 3 and 4, it was concluded that the linear epitope, LKDLPRV (residues 968-974) is recognized by mAb6. This inhibitory antibody has an effect on the acetylCoA-dependent activity of hPC. The mAb6's epitope is localized in the proline rich region (residues 951-1000) between the transcarboxylation domain and the biotin carboxyl carrier domain, and might be near the inter-subunit junction of assembled hPC (Carey, 1988). Together with data obtained through mutational analysis for these mutants representing this epitope, Asp^{970} changed to alanine reduced the activity to 50% compared to wild type. This proposal will need more data from kinetic analysis of this mutant and the three-dimensional structure of the

molecule to understand the mechanism of the specific residue involved in catalytic reaction. Alternative study of this epitope associated with mobility of the biotin carboxyl carrier domain might be further investigated by construction of hPC mutant by deletion of this epitope and tested for the activity of hPC. Since pyruvate carboxylase shares many catalytic and structural features with other biotin dependent enzymes, elucidation of the mechanism of this enzyme will also be of great help in understanding how these other enzymes function (Attwood, 1995).

CHAPTER 5

Biotin Domain of Human PC

CHAPTER 5

5.1 INTRODUCTION

A number of monoclonal antibodies raised against sheep PC have been partially characterised in this laboratory (Carey, 1988) providing powerful probes for studying the structure-function relationships of PC. For example, the effect of mAb12 on the acetyl-CoA activity of sheep PC (sPC) demonstrated that mAb12 was able to completely inhibit the activity of sPC, whether it be acetylCoA-dependent or independent. This indicates that the epitope of mAb12 would not be at or close to the acetyl-CoA binding site and that the binding of acetyl-CoA to sPC does not alter or induce a conformational change in PC which affects the binding of mAb12 in its inhibition of the activity of PC (Carey, 1988). In Chapter 3 it was shown that mAb12 and 42 were also able to inhibit the acetylCoA-dependent activity of hPC. The epitopes of mAb12 and 42 were revealed as discontinuous epitopes contained within the minimal C-terminal 80 residues of the biotin carboxyl carrier domain (BCC) of hPC (Chapter 3).

Several methods for mapping epitopes have been developed. For a linear epitope, a series of short synthetic peptides that encompass the protein sequence can be tested for mAb binding. However, the identification of a conformational epitope may require additional mutagenesis experiments to identify critical residues (Frillingos *et al.*, 1997; Jin *et al.*, 1992). Biophysical methods such as X-ray crystallography or NMR spectroscopy can also be used to map a mAb epitope. X-ray crystallography has provided detailed models for a number of mAb-protein complexes (Davies & Cohen, 1996). However, the success of this method is limited by the availability of suitable crystals for structural analysis. NMR has also been used to identify antibody binding surface but the technique is restricted to proteins of a modest molecular mass.

For the structure of biotin carboxyl carrier domain, the recent NMR determination of the three-dimensional structure of the entire 1.3 S subunit of

Propionibacterium shermanii transcarboxylase, showed that the C-terminal half of this subunit is folded into a compact domain (Reddy *et al.*, 1998). This fold is homologous to that determined by X ray analysis of the carboxyl carrier protein of *E. coli* ACC (Athappilly & Hendrickson, 1995; Roberts *et al.*, 1999), and to the lipoyl domains, to which this domain exhibits 26-30 % sequence similarity (Reddy *et al.*, 1998). As yet the three-dimensional structures of the biotin carboxyl carrier (BCC) domains of yeast PC and human PC have not been determined. Only the predicted structure of the BCC domain of yeast PC (yPC_1104) has been described based on the structures of holo- and apo-BCCP of *E. coli* ACC and of the lipoyl domain of pyruvate dehydrogenase (Polyak *et al.*, 2001).

Mutational analysis is a powerful method to focus on specific residues that might be critical for mAb binding (Moore *et al.*, 1994). Mutations in either antibody or antigen can be used to analyse the contributions of individual residues to the formation of the complex. There have been several such studies where the binding effects have been correlated with the known three-dimensional structure (Davies & Cohen, 1996). The power of mutational analysis has been revealed in a comparison of the structural and functional epitopes of the human growth hormone (hGH) receptor system by a systematic analysis of the residues interacting with hGH by replacing each residue in turn with alanine. Only one quarter of the buried side chains could account for most of the binding energy (Cunningham & Wells, 1993; Wells, 1996).

In this chapter a competition binding assay was carried out with europium labelled antibody to determine the inhibitory effect of one antibody to inhibit the binding capability of another antibody, and thus to determine whether both antibodies bind to distinct sites on a protein antigen. If there is a competitive effect, it is possible that these two antibodies recognise identical or sterically overlapping epitopes. In contrast, if the two antibodies do not interfere with each other's binding and can both

bind simultaneously to the antigen, then the antibodies must recognise discrete epitopes. The epitopes for mAb12 and 42 on the C-terminal 107 residues of biotin carboxyl carrier domain (BCC) of hPC was also investigated using site-directed mutagenesis to demonstrate the effect of critical residues on the binding of mAb12 and 42, and to analyse their effects on biotinylation.

5.2 SPECIFIC METHODS

5.2.1 The fragmentation of IgG to Fab using papain

Papain digestion of IgG produces Fab fragments. Pilot experiments were performed where both the concentration of papain and the time of digestion were varied to determine the optimal conditions. Purified monoclonal antibody was digested with papain in the presence of the reducing agent cysteine. The method was performed according to Raychaudhuri *et al.* (1985) and Lutomski *et al.* (1995), with some modifications. The reaction was carried out in a total volume of 2 ml containing 1 ml of 4 mg/ml of purified IgG in PBS and 1 ml of 0.2 mg/ml papain (Boehringer Mannheim GmbH) in digestion buffer [PBS pH 7.5, 0.02 M cysteine and 0.02 M EDTA (disodium salt)]. The ratio of papain : antibody was 1:20 (w/w) and the antibody was digested for 7 hours at 37°C. The reaction was stopped by adding iodoacetamide to a final concentration of 30 mM. The digested antibody was then dialysed into PBS at 4°C overnight, and the Fab and Fc fragments were separated by protein A-Sepharose chromatography column (1 ml Hitrap affinity column, Pharmacia Biotech) as described in Section 2.13.4. The Fab fragment in the flow-through fraction was collected, while the Fc fragment remained bound to the column. Protein A binds specifically to the Fc region of immunoglobulin molecules, especially IgG for which it has four high affinity binding sites.

Purity of the fragments was assessed by 10% native gel as described in Section 2.13.1. The native PAGE gel was carried out and followed by both Coomassie staining and Western blot. The blot was reacted with goat anti mouse IgG (Fab specific) alkaline phosphatase at a dilution of 1: 10000 and developed with NBT and BCIP as described in Section 2.13.2.

5.2.2 Europium labelling of Fab

For europium labelling, antibody was labelled according to the protocol of Delfia, Wallac (Turku, Finland). The labelling reagent is the Eu-chelate of N^1-(p-isothiocyanatobenzyl)-diethylenetriamine-N^1 N^2 N^3 N^3-tetraacetic acid (DTTA). The DTTA group forms a stable complex with Eu^{3+} and the isothiocyanate group reacts with primary aliphatic amino group on the protein at alkaline pH to form a stable, covalent thiourea bond (Figure 5.1). Briefly, 0.4 mg of Fab42 in 0.1 M sodium carbonate pH 9.3 was mixed with 50 µg of europium labelling reagent (Delfia, Wallac) at a europium : antibody ratio of 1:8 (w/w) in a final volume of 250 µl. The reaction was incubated overnight at 4°C. Separation of the labelled antibody from free Eu^{3+} chelate was performed by gel filtration on a PD-10 column (Pharmacia). The mixture was applied directly to the equilibrated column (0.1 M sodium carbonate pH 9.3) and 0.5 ml fractions were collected with elution buffer (50 mM Tris-HCl pH 7.8 containing 0.9% NaCl and 0.05% sodium azide). The fractions from the first peak with the highest Eu^{3+} counts were pooled and characterised. Protein concentrations in the pooled fractions were calculated from the absorbance at 280 nm.

5.2.3 Competition Europium labeled antibody-binding assay

To determine whether two monoclonal antibodies bind to distinct sites on the biotin carrier protein domain of hPC, a competition assay was carried out to determine the capacity of one antibody to inhibit the binding of another antibody. In brief, 0.1 µg of streptavidin (Sigma, U.S.A.) in 100 µl of 0.1 M borate buffer pH 9.5 was added to the wells of microtiter plates (Lumitrac 600 white 96 well plate, Griener, Germany) and incubated for two days at 4°C. The plate was washed three times with TBS-Tween20 (25 mM Tris-HCl pH 7.5, 150 mM NaCl, 0.05% Tween20). A blocking solution consisting of 1% bovine serum albumin in TBS was added to each well, and the plate was incubated for 2 hours at 37°C. One microgram of the whole cell lysate of *E. coli*

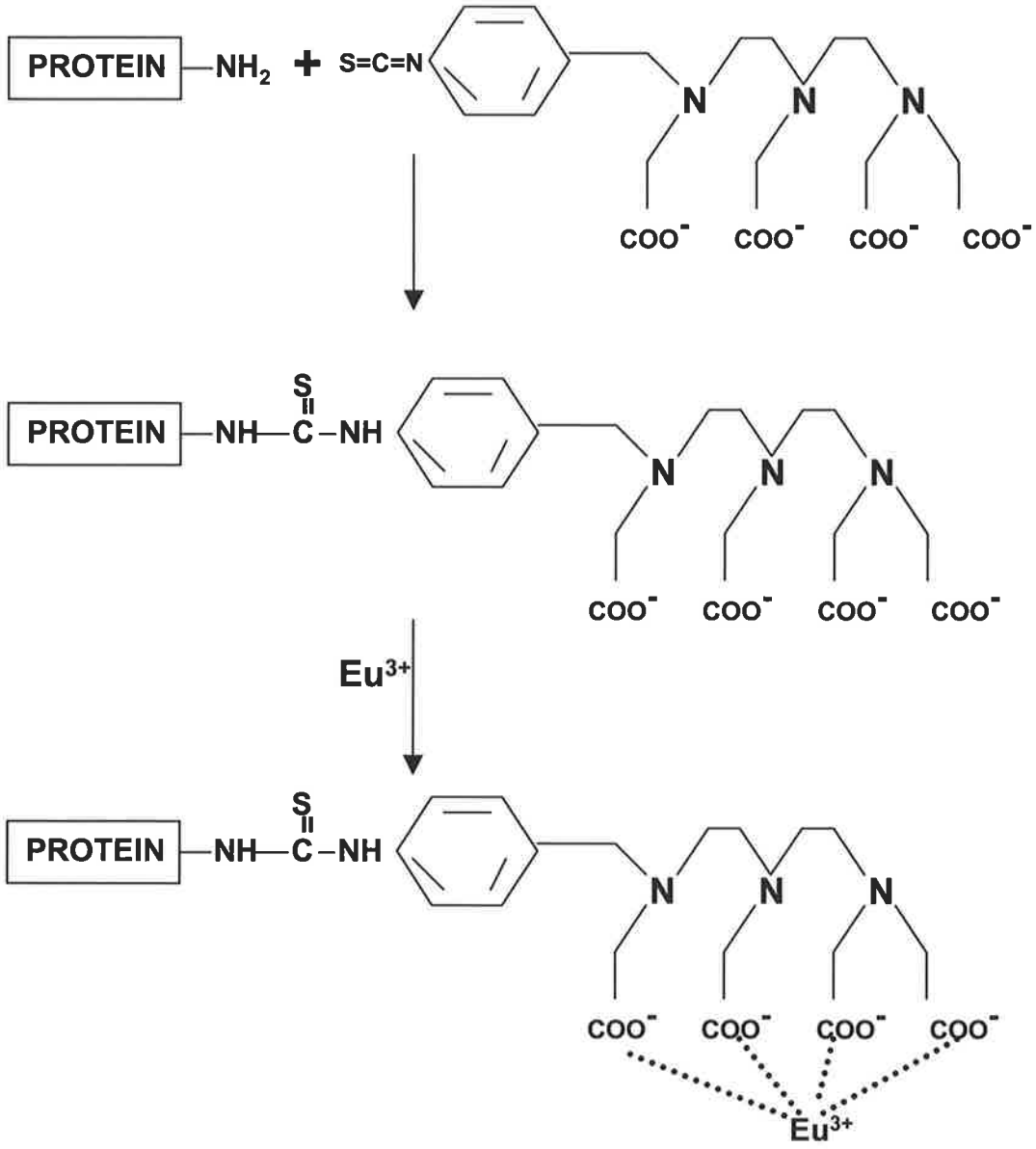

Figure 5.1 **Protein labelling with N-(p-isothiocyanatobenzyl)-diethylene-triamine N^1, N^2, N^3, N^3 tetraacetic acid.** Fab42 was mixed with 50 µg of europium labelling reagent in 0.1 M sodium carbonate pH 9.3 at a europium : antibody ratio of 1:8 (w/w). The reaction was incubated overnight at 4°C. Separation of the labelled antibody from free europium chelate was performed by gel filtration on a PD10 column.

containing the biotin carboxyl carrier protein domain of hPC (TB2 107n) [Figure 3.10] was bound to the streptavidin coated plates for 2 hours at 37°C. After washing with TBS-0.05% Tween-DTPA (Tris-HCl pH 7.5, 0.05% Tween20, 0.8 µg/ml diethylene triamine pentaacetic acid) three times, antibody competition was performed in a 100 µl volume consisting of 50 µl of europium labelled Fab42 (8448 cps/125 ng of Fab42) and various concentrations of unlabelled Fab42 or 12. Addition of the different concentrations of unlabelled Fab42 or 12 was made as indicated in the text (Figure 5.3). The reaction was incubated overnight at 4°C. After washing five times in TBS-0.05% Tween-DTPA and three times in water, the enhancement solution (Delfia, Wallac) was applied. A time resolved fluorimeter (Fluostar, BMG Labtechnologies, Victoria, Australia) was used for the measurement of europium (Eu^{3+}).

Concentrations of streptavidin, biotin domain and europium labelled antibody were chosen by checkerboard titrations to give a maximum europium count of approximately 30000 after 2 minutes enhancement. Under these conditions, blank values obtained with the cell lysate of *E. coli* containing the fragment encoding amino acids 1118-1178, TB2 60n (as described in Section 3.2.9) were negligible. Since mAb12 and 42 were not bound to this fragment, as shown in Chapter 3 (Figure 3.10), it was used as a background control for this assay.

5.2.4 Construction of mutants of the biotin carboxyl carrier domain of hPC

Site-directed mutagenesis was performed with the Quick-change site-directed mutagenesis kit as described in Section 4.2.1. Since the mutagenesis efficiency may be considerably reduced with plasmids greater than 6 kb in length when using the Quick-change site directed mutagenesis kit, mutagenesis was performed directly on a 2.9 kb pBluescript [pBluescriptII ks(+)] based plasmid. The procedure was as follows. The plasmid pET-107 encoding 107 residues of the human PC biotin carboxyl carrier domain (as described in Section 3.2.9) was digested with *Xho*I and *Bam*HI restriction

enzymes and the 321 bp fragment of human biotin domain was isolated by agarose gel electrophoresis and excised. DNA was purified and subcloned into pBlue scriptII ks(+) digested with the same restriction enzymes. The resulting plasmid (pBlue-107) was used as a template for all subsequent mutagenesis.

The Quick-change mutagenesis kit method requires two complementary oligonucleotide primers. Primers were designed with 10-15 perfectly matching bases on either side of regions with altered nucleotides so they would anneal correctly to the template. Codon usage was taken into account when designing the mutated codons. These codons were compared to *E. coli* codon usage (Sharp *et al.*, 1988) to ensure that they were not very rare. The forward primers (M1116AF, K1119AF, S1141AF, M1143LF, M1143AF, D1165AF, L1168AF and E1169AF) and reverse primers (M1116AR, K1119AR, S1141AR, M1143LR, M1143AR, D1165AR, L1168AR and E1169AR) used to introduce these mutations are listed in Section 2.3.3. The reaction was carried out as described in Section 4.2.1. These constructs were designated as M1116A, K1119A, S1141A, M1143L, M1143A, D1165A, L1168A and E1169A. The 321 bp products for mutants, M11116A and M1143A were amplified successfully only when the primer annealing temperature was decreased from 55°C to 45°C. The PCR products of the human biotin domain coding region containing all residues to be mutated were then digested with *Bam*HI / *Xho*I and ligated into *Bam*HI / *Xho*I digested pET32a (+) vector (Novagen). The eight mutants were verified by sequence analysis as described in Section 2.11.7. A correct, sequenced clone was transformed into *E. coli* BL21 for expression and the lysate was assayed for binding by mAb12 and 42.

5.2.5 The effect of the mutations on the in vivo biotinylation of the biotin carboxyl carrier domain of hPC

Comparative *in vivo* biotinylation of mutants of biotin carboxyl carrier domain of hPC was performed essentially as described previously by Val *et al.* (1995). Briefly, the expression of the mutant biotin carboxyl carrier domains (Section 5.2.4) of hPC was followed as described in Section 3.2.11 except that the cells were grown at 37°C or 30°C and induced with 0.1 mM IPTG. The time course for induction was carried out for 0.5, 1, 2 and 3 hours at 37°C and 30°C. After harvesting and lysing cells, the cell lysate was denatured (as described in Section 3.2) and loaded on a 12% tricine gel. Proteins were transferred onto a nitrocellulose membrane by semi-dry transfer and probed with avidin alkaline phosphatase as described previously by Chapman-Smith *et al.* (1994). Protein expression was visualized by staining with Coomassie brilliant blue. After scanning the membrane and protein gel, a plot of spot intensities was obtained with the NIH Image software (Molina *et al.*, 1996). The extent of *in vivo* biotinylation was expressed as biotinylated protein divided by the total biotin domain protein, in arbitary units, for each mutant.

5.3 RESULTS

In Chapter 3 it was shown that mAb12 and 42 recognised conformational epitopes represented by the minimal C-terminal 80 residues of BCC domain of hPC (TB2 80n). The aim of this chapter is to determine whether these epitopes for two antibodies are apart or close to each other. Although the minimal fragment was 80 amino acids we chose to use the fragment 107 amino acids. In yeast PC comparison of the extent of biotinylation of the C-terminal 85 and 104 amino acids of biotin carboxyl carrier domain suggests that the 19 amino acid N-terminal extension present in yPC_1104 produced a 6-fold increase in biotinylation (Val *et al.*, 1995). Therefore, other parts of the domain may contribute to its stability or efficiency of biotinylation.

5.3.1 Competition assay

A europium competition assay was used to determine whether the two antibodies that recognize conformational epitopes on BCC of hPC (TB2 107n) bind to sterically discrete or overlapping sites on this domain. Due to their bivalency, mAb12 and 42 were digested with papain to produce Fab for use in the competition assay. The removal of Fc part of IgG molecule can be of great importance for reducing steric hindrance in blocking of the epitopes. The higher affinity mAb42 was labelled with europium since the sensitivity of the assay depends on the affinity of the labelled antibody (Nakamura *et al.*, 1992).

The principle of time-resolved fluorescence measurement is as follows. If a mixture of short-lived and long–lived (lanthanide chelates) fluorescent compounds is excited with a short pulse of light lasting less than 1 μs, the excited molecules will emit fluorescence which is either short-lived or long-lived. In both cases, the fluorescence decay follows an exponential curve, but short-lived fluorescence will dissipate to nearly zero very quickly. Thus, the long-lived fluorescence signals arising from the lanthanide chelate can be measured with very high sensitivity under conditions of nearly zero

background. Eu^{3+} is one of the 4 rare earth metal ions (Sm^{3+}, Eu^{3+}, Tb^{3+} and Dy^{3+}) for which the fluorescence of simple inorganic salts of these ions is relatively weak. The fluorescence is dramatically enchanced when the metal ion forms a chelate with appropriate organic ligands. The antibody labelled with a lanthanide metal by the procedure in Section 5.2.2 is nonfluorescent. Therefore, fluorescence enhancement is needed, which means that the ligands around the lanthanide must be changed for others that are able to transmit excitation energy to the chelated cations. Thus, in assays in which a Eu^{3+} labelled antibody is used, after the immunoreaction is completed, an enhancement solution is added which (i) has a pH of 3.2 and causes dissociation of Eu^{3+} from the antibody-chelate complex and (ii) contains organic reagent (2-naphthoyl-trifluoroacetone) which form a highly fluorescent complex with the lanthanide ion. This complex emits strong fluorescence at 615 nm.

In this assay (Figure 5.2), the biotin carboxyl carrier domain of hPC (TB2 107n) is bound to the streptavidin coating plate, and then labelled Fab42 was added at a fixed amount in free solution along with increasing amounts of a challenge Fab. The europium labelled Fab42 competes with the unlabelled Fab42 or 12 for the epitopes on the bound of TB2 107n.

Figure 5.3 shows a typical competition assay in which labelled Fab42 was challenged with either increasing amounts of unlabelled Fab42 or unlabelled Fab12. Unlabelled Fab42 competed efficiently with labelled Fab42 to bind BCC domain. When unlabelled Fab12 was used as the challenge protein, it also competed with labelled Fab42, showing a competition of around 70% at the highest level. It can be seen that 75 and 230 ng of unlabelled Fab42 and Fab12 were required to give 50% competition with labelled Fab42. Thus, the difference in competition observed indicates that the mAbs' epitopes are distinct but close enough to each other to observe some competition for binding. mAb42 recognised a conformational epitope on the

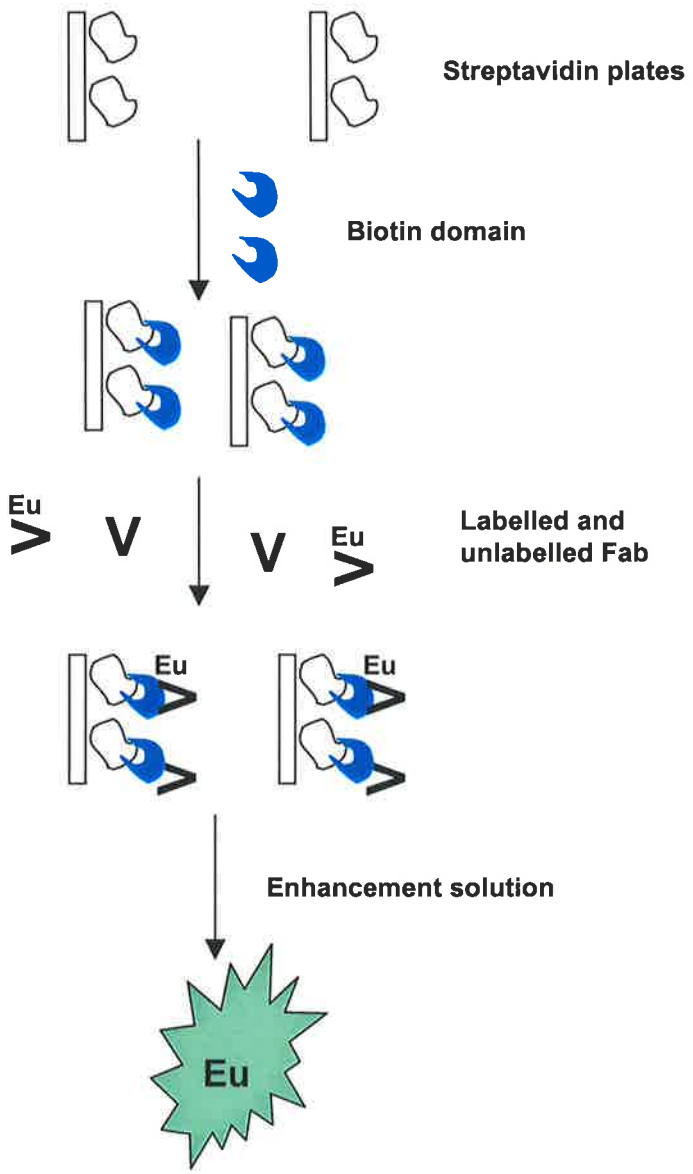

Figure 5.2 Europium competition assay of biotin carboxyl carrier domain of hPC. The assay is performed in polystyrene microtiter plates coated with streptavidin in borate buffer pH9.5. The biotin domain of hPC (TB2 107n) was bound to the streptavidin coated plates for 2 hours at 37°C. Addition of the different concentrations of unlabelled Fab42 or 12 was made as indicated in Figure 5.3. After competition of the unlabelled Fab with the fixed amount of labelled Fab42, the excess reagents were washed out and enhancement solution was added. A time resolved fluorimeter was used for the measurement of europium released from the bound Fab tracer.

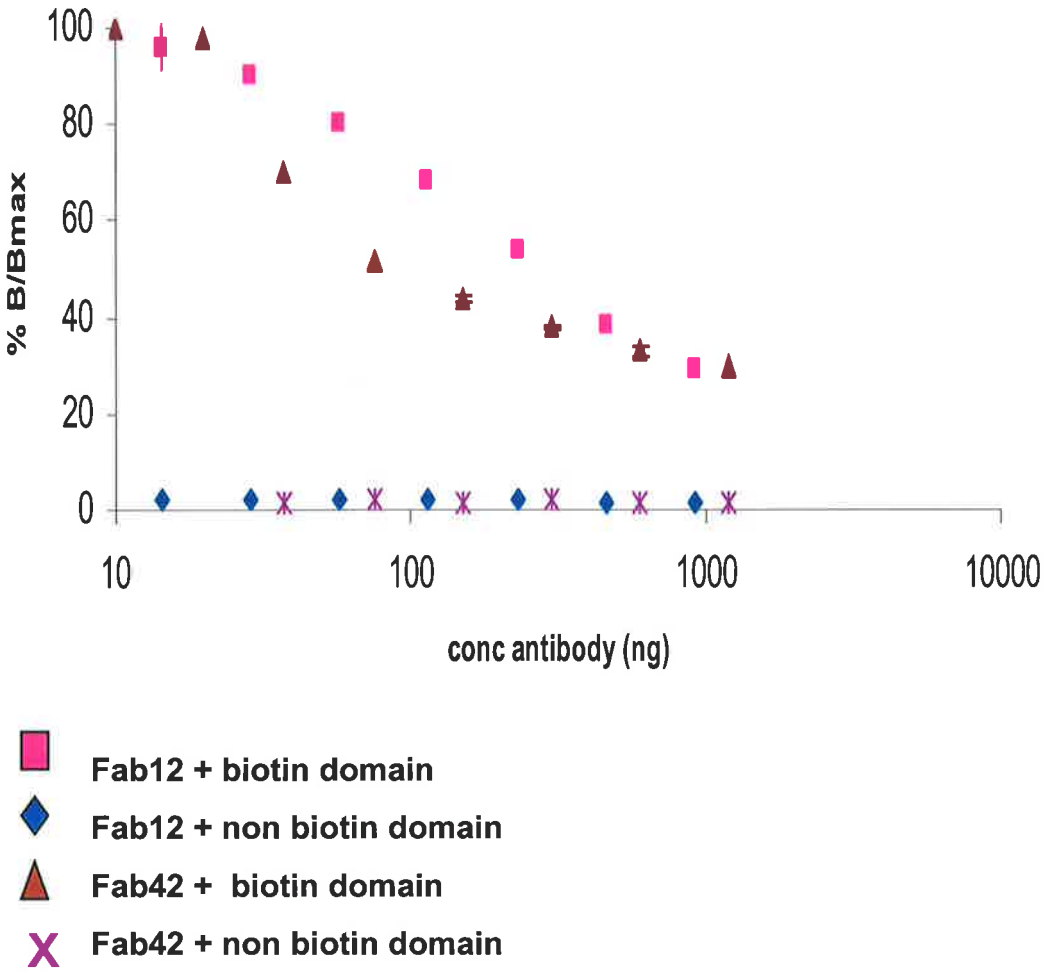

Figure 5.3 Europium competition assay of Fab12 and 42. Streptavidin was coated directly onto microtiter plates at a concentration of 1 ng/µl to tether the BCC of hPC expressed in 1µg of whole cell lysate of *E. coli* transfected with the plasmid pET-107 (Section 3.2.9). Various concentrations of unlabelled Fab12 or 42 (14-1195ng) were added to compete with the fixed amount (125 ng) of labelled Fab42. The reaction was incubated overnight at 4°C. The enhancement solution (Delfia, Wallac) was applied and a time-resolved fluorimeter (Fluostar, BMG Labtechnologies, Victoria, Australia) was used for the measurement of europium (Eu^{3+}).

same hPC biotin carboxyl carrier domain with higher affinity than did mAb12. Their binding sites on this domain may overlap sterically in such a way that both are not able to bind to the domain at the same time. Further definition of these mAbs' epitopes was investigated by mutagenesis studies.

5.3.2 Characterisation of the binding of mAb12 and 42 with biotin carboxyl carrier domain (BCC) of yeast PC (yPC$_1$ 104) and E. coli acetyl-CoA carboxylase (E. coli ACC)

5.3.2.1 Characterisation of the binding of mAb12 and 42 with yPC$_1$ 104, mutant yPC$_1$ 104 and BCCP of E. coli ACC (E. coli BCCP)

The epitopes of mAb12 and 42 were revealed as discontinuous epitopes which were confined to the minimal C-terminal 80 amino acids of the human biotin carboxyl carrier domain. A number of residues within the biotin carboxyl carrier domain of all known PCs show significant identity with other biotin containing enzymes, ODCα (oxaloacetate decarboxylase α subunit), PCCα (propionyl-CoA), ACC (acetyl-CoA carboxylase) and TC (transcarboxylase) suggesting that they fold to a similar structure (Figure 5.4) (Chapman-Smith & Cronan, 1999b). This indicates that these epitopes might be present in some of the other biotin containing enzymes. To investigate this, the biotin carboxyl carrier domains of yeast PC_1 (yPC_1104) and yeast PC_2 (yPC_287) [constructed by Val *et al*, 1995] were expressed and analysed by SDS-PAGE and Western blot. The SDS-PAGE analysis indicated successful production of the C-terminal 104 residues of yPC_1 and C-terminal 87 residues of yPC_2 as shown by protein bands of around 11 kDa, after induction with IPTG (Chapman-Smith *et al.*, 1994)[Figure 5.5a]. The antibody blots demonstrated that both antibodies (mAb12 and 42) cross-reacted with yPC_1104 and yPC_287 (Figure 5.5b and c). Since TB2 was recognised by mAb12 and 42, but TB1 was not (Chapter 3), these fragments were used as positive and negative controls respectively in this assay.

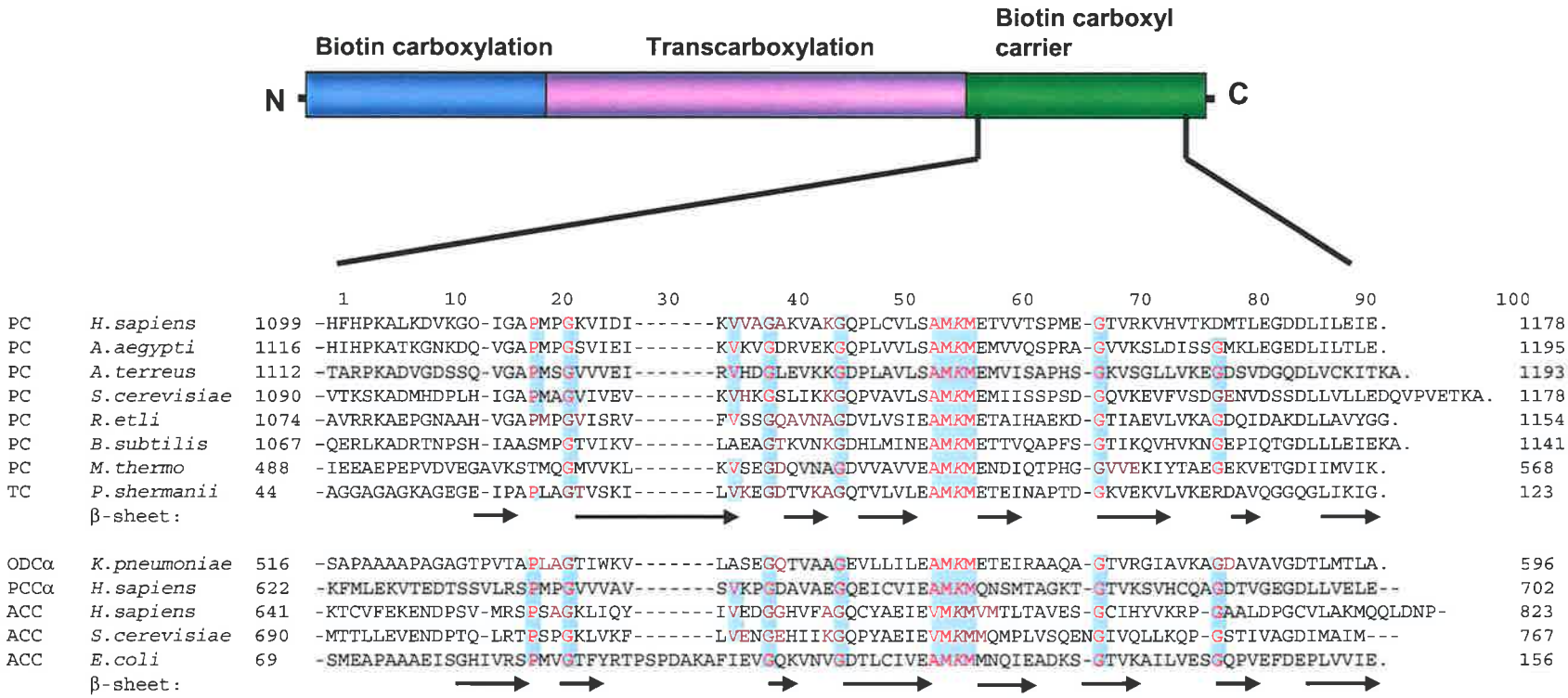

Figure 5.4 Multiple sequence alignment of biotin carboxyl carrier domain (BCC) of PC with other biotin dependent enzymes. Sequence alignment showing the amino acid sequence from biotin carboxyl carrier domain for the following enzymes: PC *Homo sapiens* (Human), PC *Aedes aegypti*, PC *Aspergillus terreus*, PC1 *Saccharomyces cerevisiae* (yeast), PC *Rhizobium etli*, PC *Bacillus subtilis*, PC *Methanobacterium thermoautotrophicum*, Transcarboxylase (TC) of *Propionibacterium shermanii*, oxaloacetate decarboxylase α subunit (ODC) of *Klebsiella pneumoniae*, Propionyl-CoA (α PCC) of human, Acetyl-CoA carboxylase (ACC) of human, yeast and *E. coli*. The highly conserved residues are indicated by violet shading. The biotinylated lysine residue is red colour and italic. The ß strands (arrows) observed in the crystal structure of BCC domain of *E. coli* ACC and in the NMR structure of 1.3S subunit of TC *P. shermanii* are shown. Adapted from Jitrapakdee & Wallace (1999).

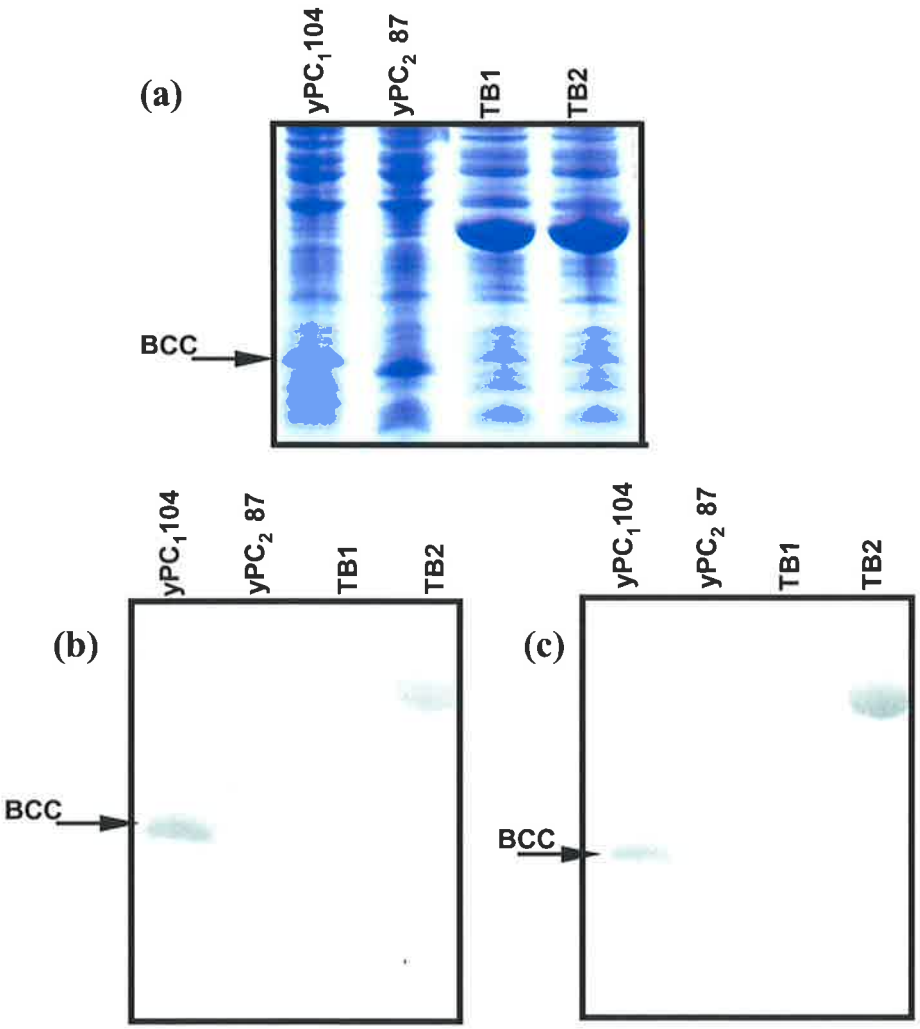

Figure 5.5 Immunoblot analysis of the BCC of yeast PC with mAb12 and 42. Yeast PC (yPC_1104 and yPC_287) was constructed and expressed in *E. coli* BL21 (Section 5.3.2). The cell lysates were prepared and analysed by SDS PAGE followed by Western blot. (a) The expression of proteins were shown on Coomassie staining gel. The blots were reacted with mAb12 dilution 1:2500 (b) and mAb42 dilution 1:5000 (c).

The biotin carboxyl carrier domain of yeast (yPC_1104) cross-reacted with both mAb12 and 42 indicating that this domain contains similar part of epitopes as human BCC domain. In order to define the discontinuous epitopes of these antibodies, several mutants of yPC_1104 as well as purified holo (biotinylated) and apo (unbiotinylated) BCCP-87 of *E. coli* ACC (Chapman-Smith *et al.*, 1994) were analysed for the binding of antibody 12 and 42. Polyak *et al.* (2001) generated fifteen mutants of yPC_1104 (A1081P, S1162P, H1102R, S1141P, H1117R, M1107T, V1166A, D1099V, V1116A, R1083G, V1148A, M1134V, M1134T, K1135L and F1152I) for their interaction with biotin protein ligase by screening a library of randomly mutated polypeptides using phage display coupled with an *in vivo* selection in *E. coli*. Two classes of mutations to the BCC domain of yeast PC were isolated. The first class contained two distinct, conservative substitutions of the Met residue immediately at the N-terminal of the target Lys (M1134V, M1134T and K1135L). The second class, which were temperature sensitive mapped to residues some distance from the target lysine (Polyak *et al.*, 2001). Therefore these 15 mutants of yPC_1104 were expressed in *E. coli* and the cell lysates were prepared (Section 3.2.11) for screening their binding to mAb12 and 42. These proteins were analysed by SDS-PAGE followed by Western blot (Section 2.13.2).

Figure 5.6 shows the binding of 11 mutants of the biotin carrier domain of yPC_1104 (A1081P, S1162P, H1102R, S1141P, H1117R, M1107T, V1166A, D1099V, V1116A, R1083G and V1148A) to antibody 12. The protein pattern of all mutants and Western blot analysis using mAb12 are shown in Figure 5.6. These mutants were all detected by Coomassie staining gel (Figure 5.6a, c) and were recognised by antibody 12 (Figure 5.6b, d). Only the holo form of *E. coli* BCCP-87 showed a positive result with this antibody. This result was similar to the results for yPC_1104. The purified apo form of yPC_1104 did not react with mAb12 while the holo form in the lysate of wild type yPC_1104 was positive (Figure 5.6b, d). Nevertheless, the addition of free biotin (77 or

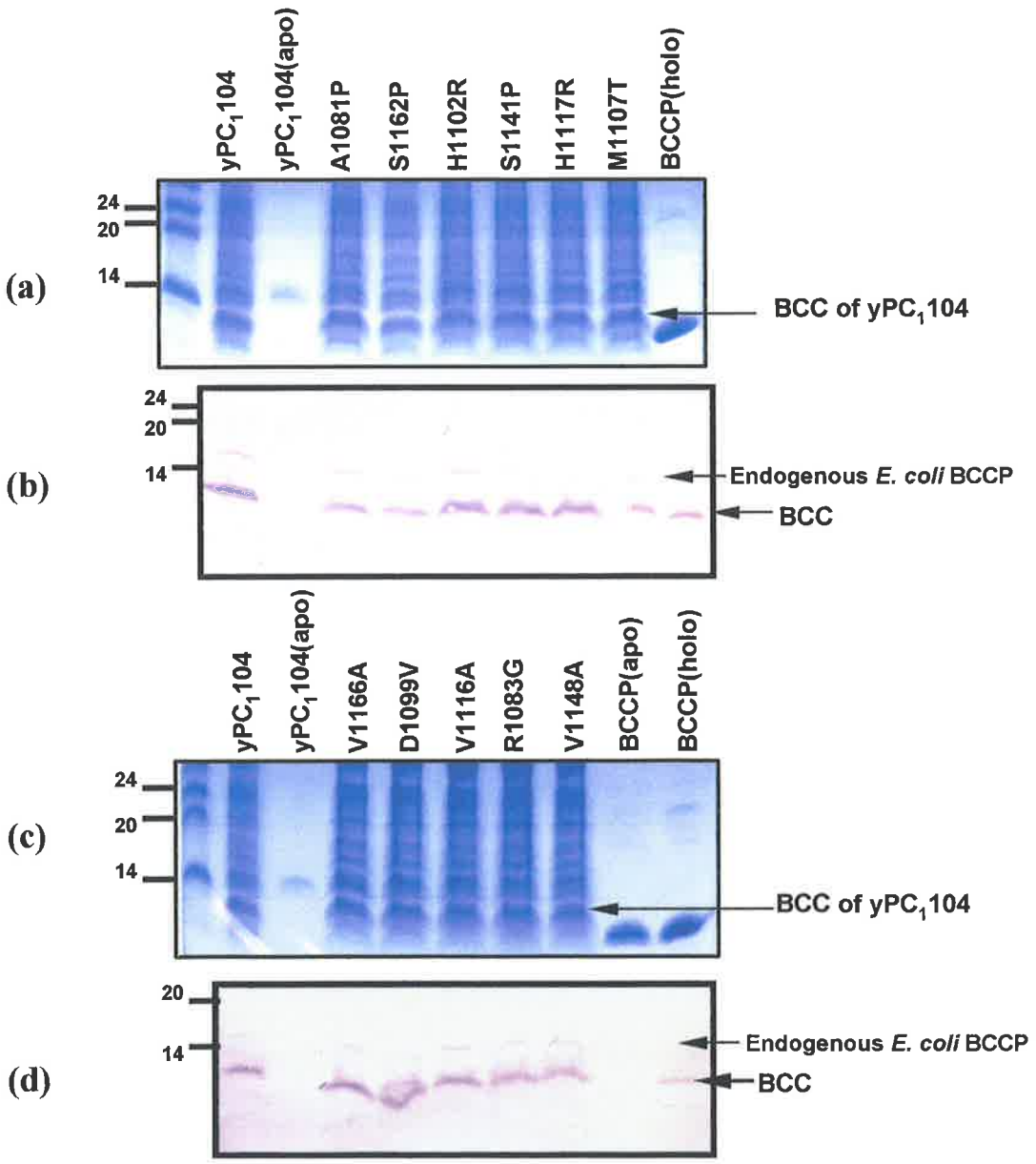

Figure 5.6 Immunoblot analysis of mutants of yPC$_1$104 and wt BCCP of *E. coli* ACC with mAb12. The mutants of yPC$_1$104 and wt BCCP of *E. coli* ACC (as described in Section 5.3.2) were prepared and analysed by SDS-PAGE followed by Western blot. (a, c) The expressed proteins were shown on Coomassie staining gel. The blots were reacted with mAb12 dilution 1:2500 and probed with goat anti-mouse conjugated to alkaline phosphatase (b, d). M= protein marker

385 μM) did not inhibit the binding of any of the mAbs to PC (Carey, 1988) (Table 1.5 in Appendix). This indicates that the conformational epitope of mAb12 is composed of discontinuous residues which are conserved among biotin carboxyl carrier domain of human PC, yeast PC and *E. coli* ACC.

The result of the binding of these mutants and yPC_1104 against mAb42 was similar to those obtained from mAb12 except that neither the holo form nor the apo form of *E. coli* BCCP-87 reacted with mAb42 (Figure 5.7c and d). This therefore indicates that the epitope of mAb42 is different from the epitope of mAb12. For mAb42, the residues are conserved only between human PC and yeast PC but not *E. coli* ACC. All eleven mutants of yPC_1104 do not affect the binding of mAb12 or 42, indicating these residues are not likely to be involved to any significant extent in the epitopes of BCC domain of yeast PC.

Positive results for binding assays with mAb12 and 42 were also obtained for the mutant F1152I indicating that this mutant does not affect these epitopes (data not shown). All twelve mutations of yPC_1104 that do not affect the binding of mAb12 or 42 are shown in Figure 5.12 and the results are summarised in Table 5.1.

It has been shown that the binding of avidin, which binds tightly to the biotin moiety of sheep PC, reduced the binding of mAb 12 and 42 to the enzyme, indicating these antibodies bind within the area excluded by avidin (see Figure 1.6 in Appendix I) (Carey, 1988). Moreover, the binding of anti-biotin antibodies was also shown to decrease the binding of mAb12 and 42 (Carey, 1988) [Table 1.4 in Appendix]. The biotinyl-lysine is found in the motif M-K-M, which is highly conserved in all biotin domains (Chapman-Smith & Cronan, 1999a). These data suggest that the motif M-K-M might be involved in part of these epitopes. To prove this hypothesis, mutants of this motif (constructed by Polyak *et al.* 2001) M1134V, M1134T, K1135L were

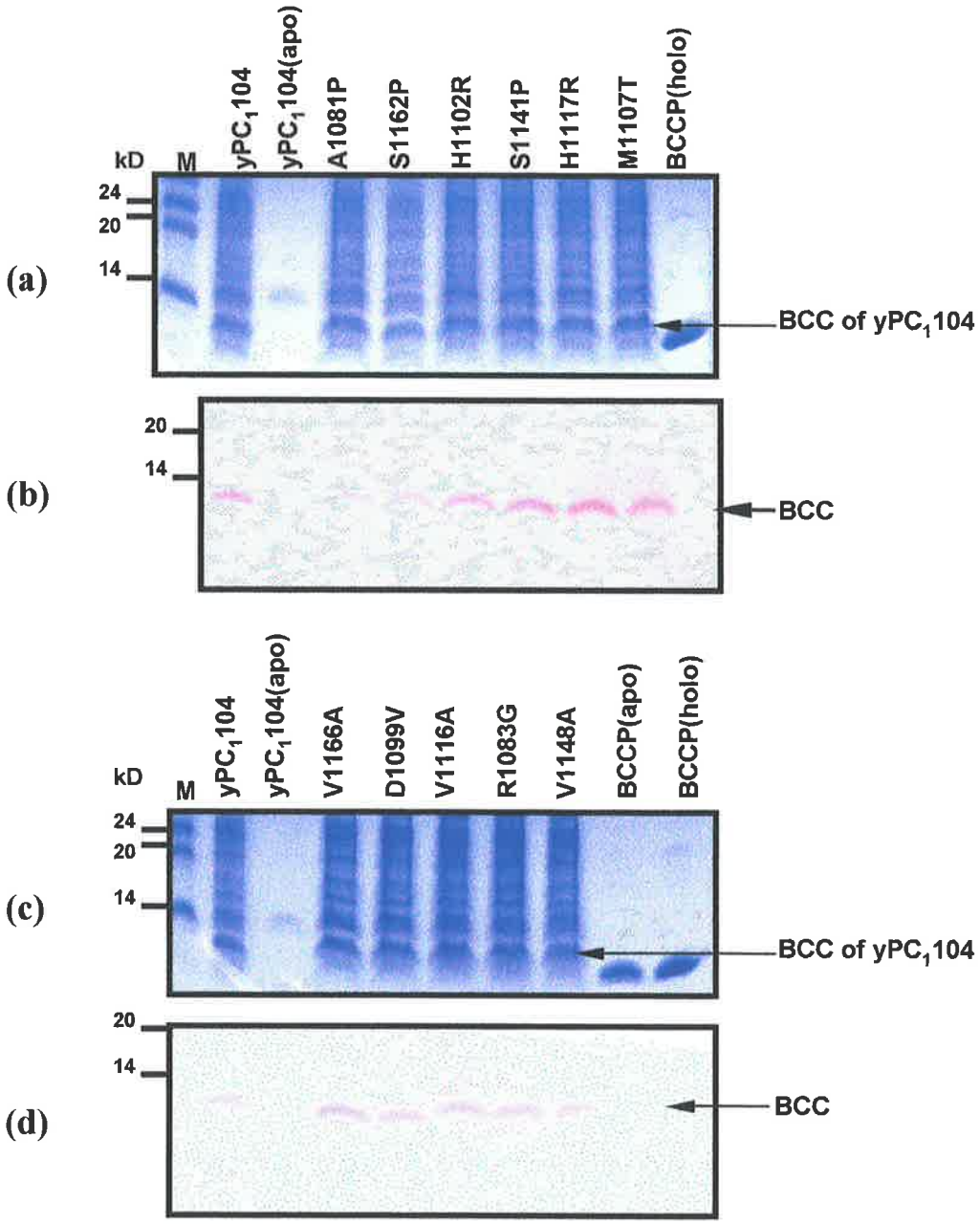

Figure 5.7 Immunoblot analysis of mutants of yPC_1104 and wt BCCP of *E. coli* ACC with mAb42. The mutants of yPC_1104 and wt BCCP of *E. coli* ACC (as described in Section 5.3.2) were prepared and analysed by SDS-PAGE followed by Western blot. (a, c) The expressed proteins were shown on Coomassie staining gel. (b, d) The blots were reacted with mAb42 dilution 1:5000 and probed with goat anti-mouse conjugated to alkaline phosphatase. M= protein marker

expressed and analysed by SDS-PAGE followed by Western blot as described above. The blots were probed with either mAb12, 42 or avidin-alkaline phosphatase.

The expressed biotin carboxyl carrier domains of wild type yPC_1104 and three mutants (M1134V, M1134T, K1135L) were shown as a band between 6 and 14 kDa on Coomassie stained gel (Figure 5.8a). The binding of M1134V and M1134T against mAb12 was slightly positive compared to wild type yPC_1104 (Figure 5.8b). In contrast, K1135L was not bound by mAb12 (Figure 5.8b). Two mutants (M1134V and M1134T) were positive albeit somewhat less so than wild type on the avidin blot indicating the substitution of M1134V and M1134T did not grossly alter the conformation of the enzyme for the biotinylation (Figure 5.8c). As expected K1135L abolished biotinylation shown by the negative result on the avidin blot (Figure 5.8c). This suggests that the exposed hairpin loop containing residues Met^{1134} and Lys^{1135} of the biotin carboxyl carrier domains of yPC_1104 significantly reduced the binding of mAb12 and may contribute to the epitopes recognised by mAb12. Therefore, Met^{1143} and Lys^{1144} of hPC (corresponding to Met^{1134} and Lys^{1135} of yPC_1104) might similarly be involved in the epitope of BCC of hPC, and this was tested as described below.

For the binding against mAb42, the results of the expressed proteins and avidin blot were similar to those with mAb12 (Figure 5.9a and c) except that (cf. Figure 5.8) there was no interaction with the endogenous BCCP of the *E. coli* host of yPC_1104 and the three mutants M1134V, M1134T and K1135L. The substitutions M1134V, M1134T and K1135L completely abolished the binding of mAb42, again indicating a difference between the epitopes of mAb12 and 42 (Figure 5.9b). This suggests that the M1134V, M1134T and K1135L substitutions in the biotin carboxyl carrier domains of yPC_1104 significantly affect the binding and the conformation of the epitope of mAb42 on yPC_1104. The homology of the BCC domain between yPC_1104 and hPC exhibits 41% sequence similarities (Figure 5.10). Therefore, it is predictable that the BCC of

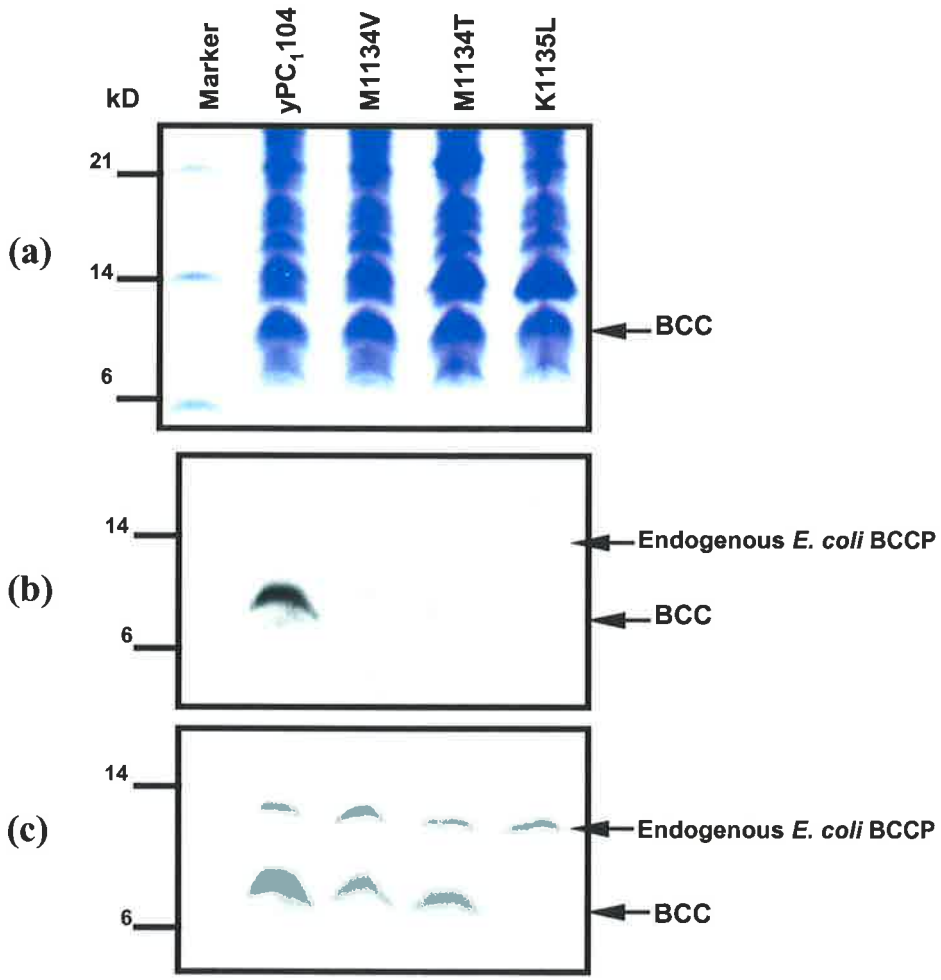

Figure 5.8 Immunoblot analysis of three mutants of yPC_1104 with mAb12. The mutants of yPC_1104; M1134V, M1134T and K1135L (as described in Section 5.3.2) were prepared and analysed by SDS-PAGE followed by Western blot. (a) The expressed proteins were shown on Coomassie staining gel. The blots were reacted with mAb12 dilution 1:2500 and probed with goat anti-mouse conjugated to alkaline phosphatase (b), and avidin-alkaline phosphatase (c).

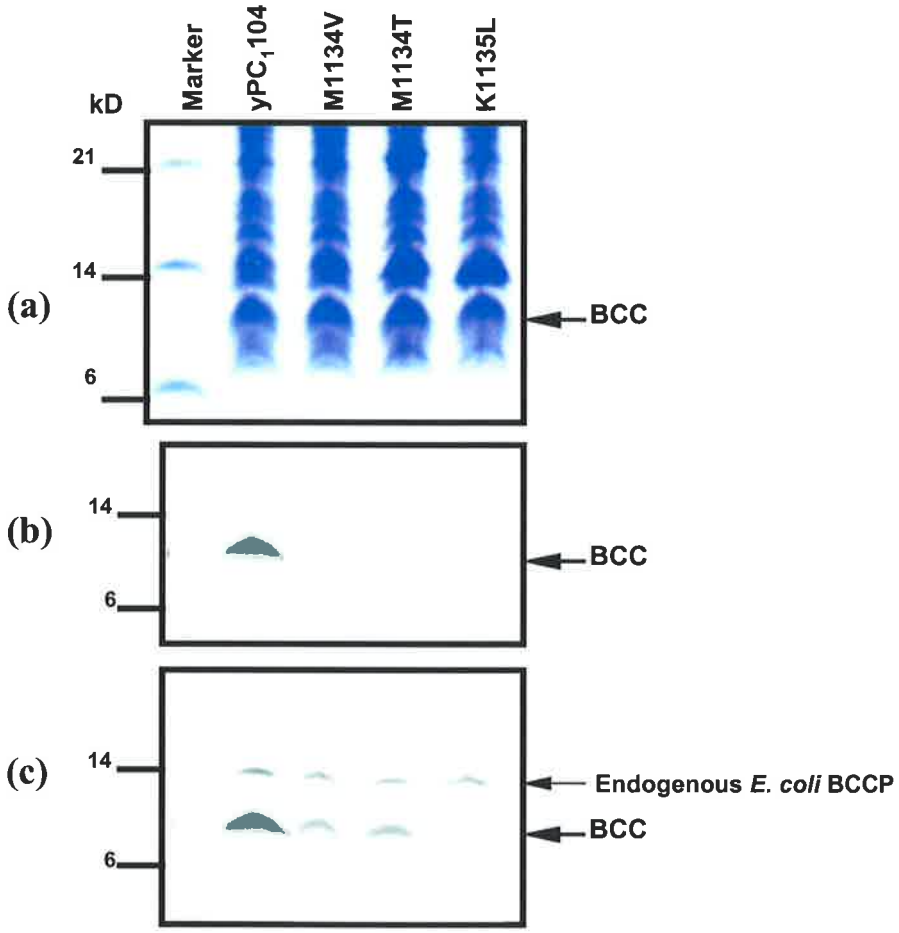

Figure 5.9 Immunoblot analysis of three mutants of yPC_1104 with mAb42. The mutants of yPC_1104; M1134V, M1134T and K1135L (as described in Section 5.3.2) were prepared and analysed by SDS-PAGE followed by Western blot. (a) The expressed proteins were shown on Coomassie staining gel. The blots were reacted with mAb42 dilution 1:5000 and probed with goat anti-mouse conjugated to alkaline phosphatase (b), and avidin-alkaline phosphatase (c).

hPC would fold to a similar structure as yPC_1104. Thus, these residues Met^{1143} and Lys^{1144} of hPC (corresponding to Met^{1134} and Lys^{1135} of yPC_1104) might also be one part of this epitope of mAb42 on BCC of hPC.

5.3.2.2 Characterisation of the binding of mAb12 with mutants of BCCP of E. coli acetyl-CoA carboxylase

It was shown that only the holo (biotinylated) form of the 87 C-terminal residues of the biotinyl carboxyl carrier domain of *E. coli* acetyl-CoA carboxylase (BCCP) bound to mAb12, but did not bind to mAb42. Therefore, to further define this epitope of mAb12 the binding of mAb12 to five mutants of BCCP was investigated. These mutants (G143E, V146I, E147K, E119K and G133S) were constructed using ACP-BCCP fusion strategy incorporating labelled ^{3}[H]-β-alanine and ^{3}[H]-biotin and purified by gel filtration chromatography using Superdex 75 (Chapman-Smith *et al.*, 1999). Five micrograms of each purified mutant protein (Chapman-Smith *et al.*, 1999) were loaded and analysed on a 12% tricine gel followed by Western blot with mAb12 (Section 2.13.2).

As shown in Figure 5.11a, all mutants of BCCP and wt BCCP (holo and apo form) exhibited a major band at about 10 kDa (predicted size). Figure 5.11b shows strong binding of mAb12 to two mutants, E147K and G133S and the positive control TB2 107n with thioredoxin fusion protein (refer Figure 3.10). The abilities of these individual mutant proteins of BCCP to act as substrates for *E. coli* biotin ligase *in vitro* were described by Chapman-Smith *et al.* (1999). The G143E protein had a similar affinity for the enzyme as wild type BCCP87, whereas the V146I protein was a slightly poorer substrate (Chapman-Smith *et al.*, 1999). This suggests that the mutation of G143E and V146I did not cause significant conformational change to the apo BCCP. The G143E and V146I were not bound by this antibody, indicating that these residues were critical for the binding of mAb12 on BCCP (Figure 5.11b). In contrast, the E119K

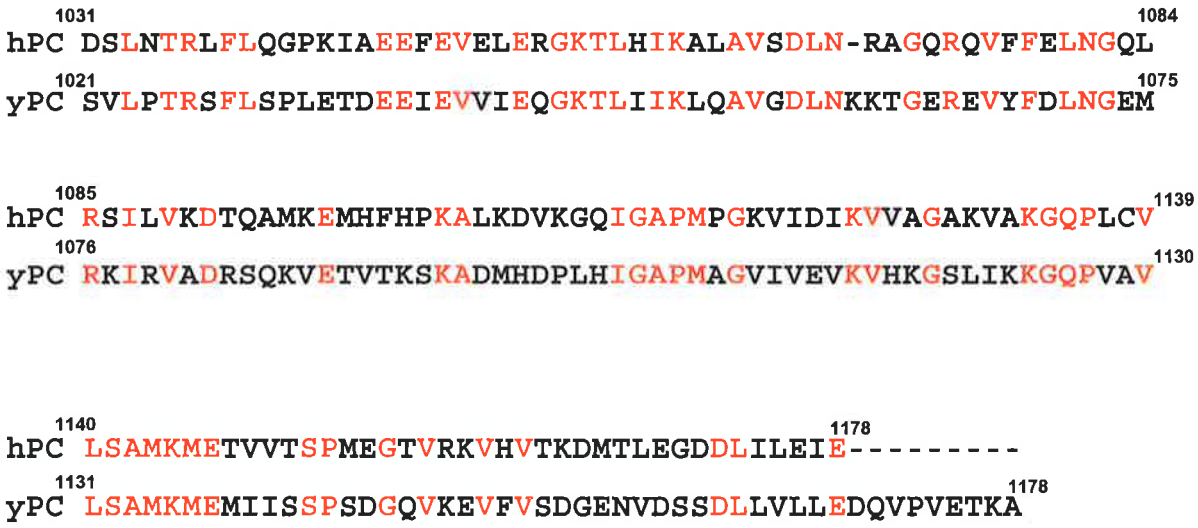

Figure 5.10 Sequence alignment of biotin carboxyl carrier domains for hPC and yPC$_1$. The amino acid sequences of biotin carboxyl carrier domains of human PC (hPC) and yeast PC$_1$ (yPC$_1$) are compared using Clustal W. The highly conserved residues are indicated in red color.

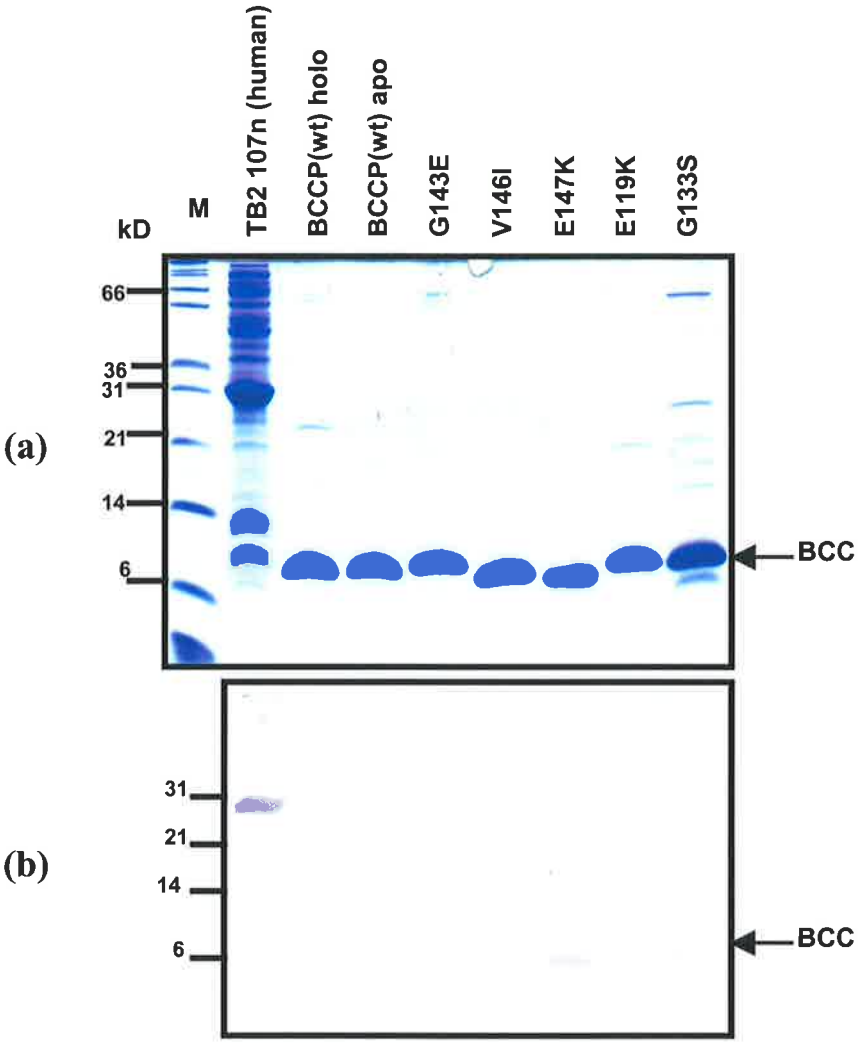

Figure 5.11 Immunoblot analysis of the mutants of BCCP of *E. coli* ACC with mAb12. The mutants of BCCP of *E. coli* ACC (as described in Section 5.3.2) were prepared and analysed by SDS-PAGE followed by Western blot. (a) The expressed proteins were shown on Coomassie staining gel. (b) The blots were reacted with mAb12 dilution 1:2500 and probed with goat anti-mouse conjugated to alkaline phosphatase. M= Wide Range Protein Standard Marker (Mark 12, Novex).

apparently has a significant conformational change to its structure (Chapman-Smith *et al.*, 1999) and the binding by mAb12 was affected (Figure 5.11b). Therefore, Glu^{119}, Gly^{143} and Val^{146} of *E. coli* ACC might contribute to the epitope of mAb12 on the BCCP of *E. coli* ACC.

5.3.3 Construction of eight mutants of the human biotin carboxyl carrier domains

A number of mutants of the BCC domain of hPC (TB2 107n) were constructed to test the contribution to binding of different residues in the predicted epitopes for binding to mAb12 and 42. Seven mutants within the BCC domain of hPC (TB2 107n) were analysed and systematically changed to alanine and one to leucine. The position of Met^{1143} of hPC was changed to either alanine or leucine, since leucine is neutral and similar in size to methionine. It was shown previously (Section 5.3.2) that the M1134L and M1134T substitutions of yPC_1104 dramatically decreased the binding of mAb12 and completely abolished binding of mAb42, as did K1135L for both antibodies (Figure 5.8b and 5.9b). This indicates that Met^{1134} in yPC_1104 might be involved in some part of these epitopes. Therefore, the analogous mutants were constructed in BCC of hPC (TB2 107n), i.e. M1143L and M1143A (Met^{1134} of yPC_1104 corresponding to Met^{1143} of hPC).

The sequences of the biotin carboxyl carrier domains of hPC, yPC_1104 and *E. coli* ACC are compared in Figure 5.12. The E119K of *E. coli* ACC, an extremely poor biotinylation substrate (Chapman-Smith *et al.*, 1999) was also not bound by mAb12 (Figure 5.11b). In both situations this may have resulted from the reversal of side chain charge from negative to positive or to a change in conformation of the BCCP. Therefore, the Ser^{1141} of hPC (corresponding to Glu^{119} of *E. coli* ACC) was mutated to alanine to investigate its role in the epitope map of these antibodies. The Asp^{1165} and Leu^{1168} of hPC (corresponding to Gly^{143} and Val^{146} of *E. coli* ACC) were selected for mutagenesis to alanine since with the mutants G143E and V146I were also negative

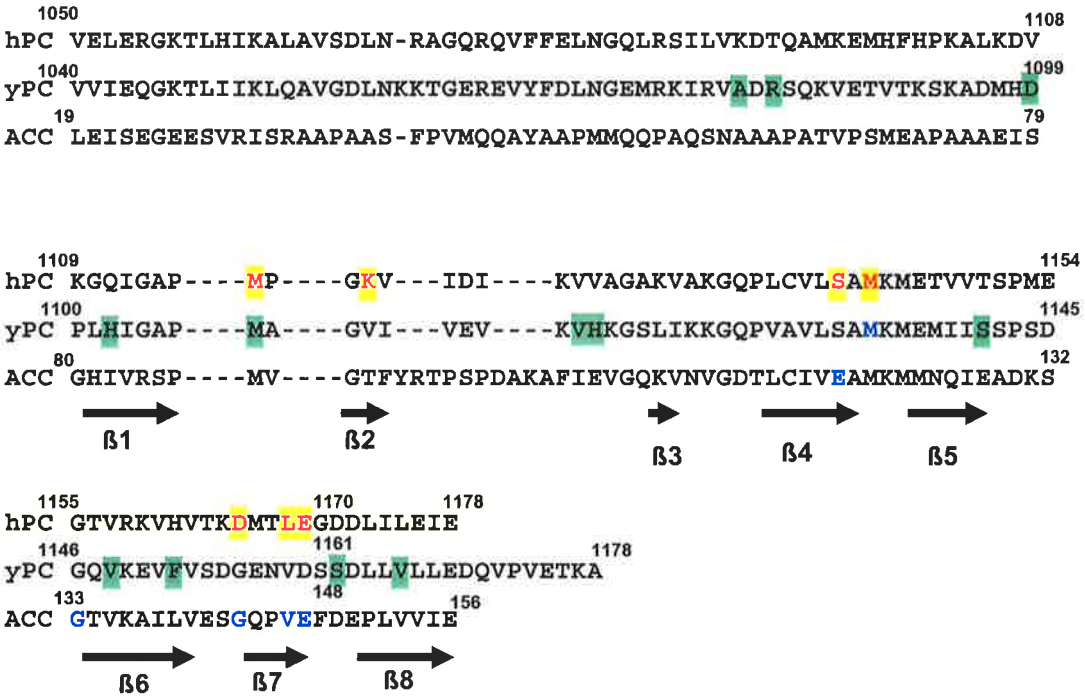

Figure 5.12 Comparison of the amino acid sequences of biotin enzymes in the region of the biotin carboxyl carrier domain. The sequence of human PC (hPC) and yeast PC (yPC1) were aligned with *E. coli* acetyl CoA carboxylase (ACC). The residues forming ß strands in the BCCP of *E. coli* ACC are shown as arrows. The seven residues mutated in BCC of hPC were constructed and indicated as red on yellow shade, based on the predicted structure of hPC BCC and the binding effect of yeast and *E. coli* ACC mutants. The mutants of BCCP of *E. coli* ACC (Chapman-Smith *et al.*, 1999) that affect binding of mAb12 are shown in blue and pink shade. Twelve individual mutations of yPC_1104 that do not affect the binding of both mAb12 and 42 are shown as green shade and the mutation that did affect binding in blue with pink shade.

with mAb12 (Figure 5.11b), though both had been shown to be biotinylated (Chapman-Smith *et al.*, 1999).

Protein structures in the protein databank predicted to have homology with the biotin domain of human pyruvate carboxylase (hPC, residues 1108-1178) were identified by Mr. C. Stojkoski using the gapped BLAST method as implemented in the WU-BLAST2 server (version 2.0; Altschul & Gish, 1996). Acetyl-CoA carboxylase from *Escherichia coli* (1BDO; Athappilly & Hendrickson, 1995) had a statistically significant probability of 6.4×10^{-5} and was used to derive the spatial restraints for the homology modelling process. The model structure of hPC was further refined by restrained molecular mechanics employing a CHARMM (Brooks *et al.*, 1983) force field. The program MODELLER (Sali & Blundell, 1993) was used to construct the homology model. Mutant pyruvate carboxylase structures were modelled using the wild type MODELLER model as a template.

The crystal structure of a BCCP of *E. coli* ACC domain together with mutational studies gave a good indication of which amino acids were most likely involved in the antibody binding site. This information and alignment of several BCC domains facilitated prediction of the amino acids in these epitopes. Based on the predicted structure of BCC domain of hPC (as generated by Mr. C. Stojkoski) three additional mutants of hPC M1116A, K1119A and E1169A were created since the Met^{1116} and Lys^{1119} in BCC of hPC are in close proximity to each other on the surface of the hPC BCC domain (β_2 sheet) (Figure 5.12 and 5.13). The Glu^{1169} in BCC of hPC is therefore close to Leu^{1168} on the surface of BCC of hPC (Figure 5.13). These residues might also affect the binding of mAb12 and 42. Therefore, eight mutants of the biotin carboxyl carrier domain of hPC; M1116A, K1119A, S1141A, M1143L, M1143A, D1165A, L1168A and E1169A were constructed for investigation of the residues that are

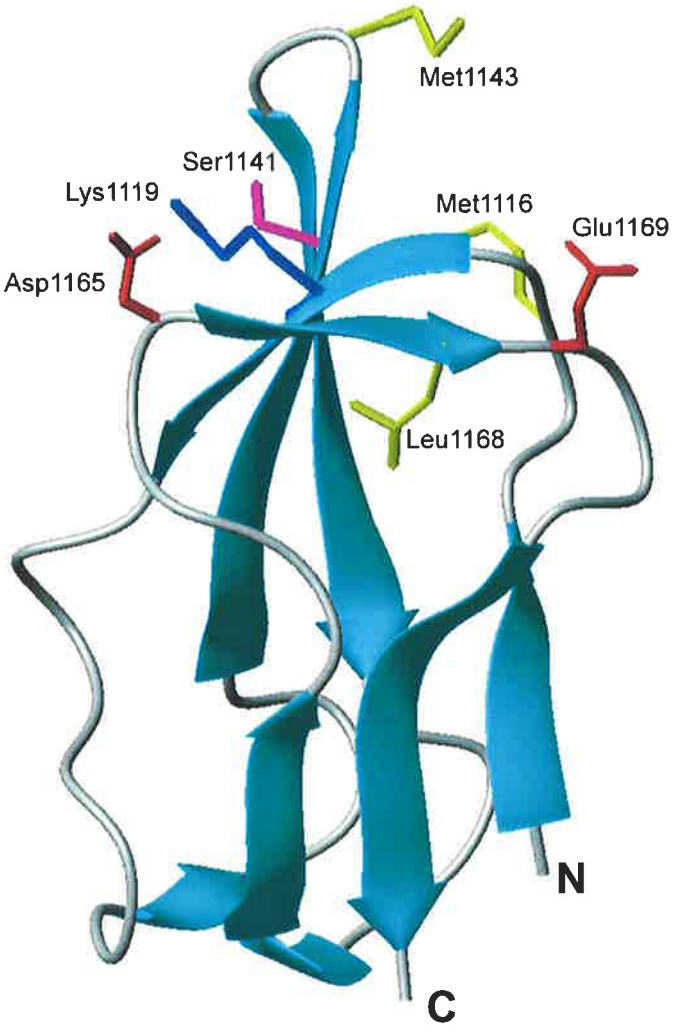

Figure 5.13 Predicted structure of biotin carboxyl carrier domain (BCC) of human PC.* The predicted three-dimension structure of human PC BCC domain, with the position of single amino acid substitution in this domain is shown. The alanine substitutions were introduced to Met^{1143}, Met^{1116}, Lys^{1119}, Ser^{1141}, Asp^{1165} Leu^{1168}, Glu^{1169} and leucine substitution was also introduced to Met^{1143}. *Kindly provided by Mr. C. Stojkoski (School of Molecular and Biomedical Sciences, University of Adelaide).

potentially involved in these conformational epitopes (Figure 5.13). The characterisation of these mutants is described below.

5.3.4 Structural integrity of eight mutants of biotin carboxyl carrier domains (BCC) of hPC

The eight mutants of the biotin carboxyl carrier domain of hPC were constructed using Quick-change mutagenesis (Section 4.1). The clones were sequenced (Figure 5.14) and expressed as thioredoxin fusion proteins in *E. coli* BL21 (Section 5.2.5). The structural integrity of these mutants was tested by checking its ability to be biotinylated by BirA (biotin protein ligase) in *E. coli*, as described in Section 5.2.5.

Induced *E. coli* lysates were prepared from cells containing each of the constructs (as described in Section 5.2.5) and endogenous *E. coli* biotin ligase. Samples of each lysate were subjected to SDS-PAGE in duplicate, one gel was Coomassie Blue stained and the other was used for Western blotting and detection of biotinylated proteins with an avidin-alkaline phosphatase probe. The extent of biotinylation of each protein *in vivo* was estimated by determination of the intensity of the biotinylated band detected on an avidin-alkaline phosphatase blot. This value was then divided by the intensity of the Coomassie Blue-stained band of expressed protein, quantified by NIH software as described in Section 5.2.5. This experiment was done in triplicate and the constructs being compared were all analysed on the same gels and Western blots. The BCCP subunit of ACC is the only endogenous biotinylated protein in *E. coli*, and has a molecular mass of 16.7 kDa (Li & Cronan, 1992). Therefore, it is clearly distinguishable from the ≈ 31 kDa of biotin carboxyl carrier domain of hPC (TB2 107n) expressed as a thioredoxin fusion protein, which was abundantly expressed as a major band in the Tris/tricine gel system (Figure 5.15a).

The comparative extent of *in vivo* biotinylation for the various mutants of biotin carboxyl carrier domain of hPC was calculated from a number of such gels and Western

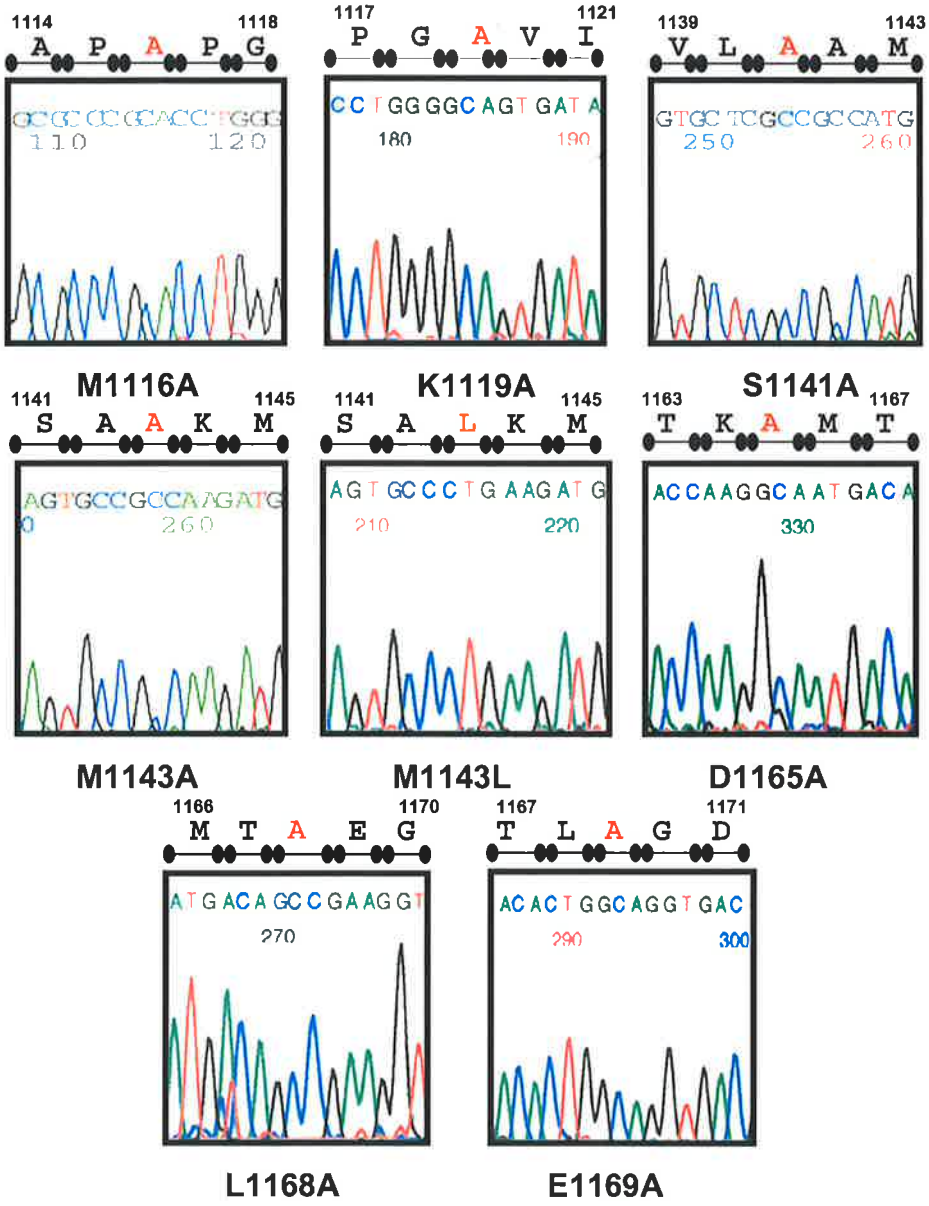

Figure 5.14 **Sequence analysis of eight mutants of biotin carboxyl carrier domain of hPC.** The alanine substitutions were introduced to M1116, K1119, S1141, M1143, D1165, L1168 and E1169 using site directed mutagenesis. The residue M1143 was changed to alanine and leucine as M1143A and M1143L. Sequencing was performed as described in Section 2.11.7.

blots, compared to wild type (Figure 5.15). As shown in Figure 5.15a the eight mutants of BCCP of hPC were over-expressed as a major band at around 31 kDa at a similar level to wild type (TB2 107n), suggesting that the mutations did not cause unstable synthesis of BCCP domain of hPC due to misfolding of the proteins. The extent of *in vivo* biotinylation of the mutants is shown in Figure 5.15b and indicates that two mutants (D1165A and L1168A) were biotinylated less efficiently than wild type.

The extent of *in vivo* biotinylation of eight mutants was assayed at 30°C and 37°C with induction by IPTG for 0.5, 1, 2, or 3 hours (Figure 5.16 and 5.17). Five of the mutants, M1116A, K1119A, M1143A, M1143L and E1169A showed a high level of protein expression and the biotinylation by biotin ligase was not affected either at 30°C or 37°C. All these mutants were maximally biotinylated at 2 hours after induction by IPTG at 30°C (Figure 5.16). Moreover, there was little difference in the extent of the biotinylation between 30°C and 37°C. This indicates that the structural integrity of these mutants was maintained and they were favourable substrates for biotin ligase at both 30°C and 37°C. The binding assays with the two antibodies mAb12 and 42 for these five mutants were therefore performed using lysates from cells grown at 30°C and induced for 3 hours with IPTG (Section 5.3.4).

For mutants S1141A, D1165A and L1168A, the relative biotinylation of these three mutants was shown in Figure 5.17. The maximum biotinylation was found to be at 2 hours whether the cells were cultured at 30°C or 37°C. However, the biotinylation was significantly reduced at 3 hours after induction for both 30°C and 37°C incubation presumably due to proteolytic degradation. Thus, the binding of these antibodies was analysed with these three mutants using the cell lysates grown at 30°C, induced for 3 hours and confirmed with the lysates of the cells incubated at 30°C and 2 hours induction.

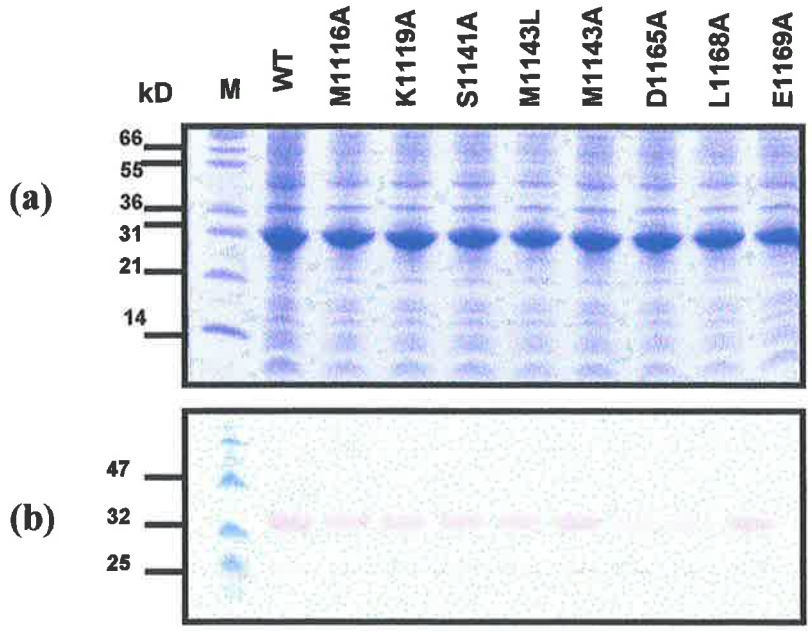

Figure 5.15 **Immunoblot analysis of eight mutants of biotin carboxyl carrier domain of hPC with avidin .** These mutants were constructed (as described in Section 5.2.4) and expressed in *E. coli* BL21. The cell lysates were prepared and analysed by SDS-PAGE followed by Western blot. (a)The over-expressed proteins were shown at 31 kDa band on Coomassie staining gel. (b) The blots were reacted with avidin-alkaline phosphatase. M=Wide Range Protein Standard Marker (Mark 12, Novex) for the Coomassie gel and Prestained Protein Marker, broad range (New England Biolab) for the avidin blot.

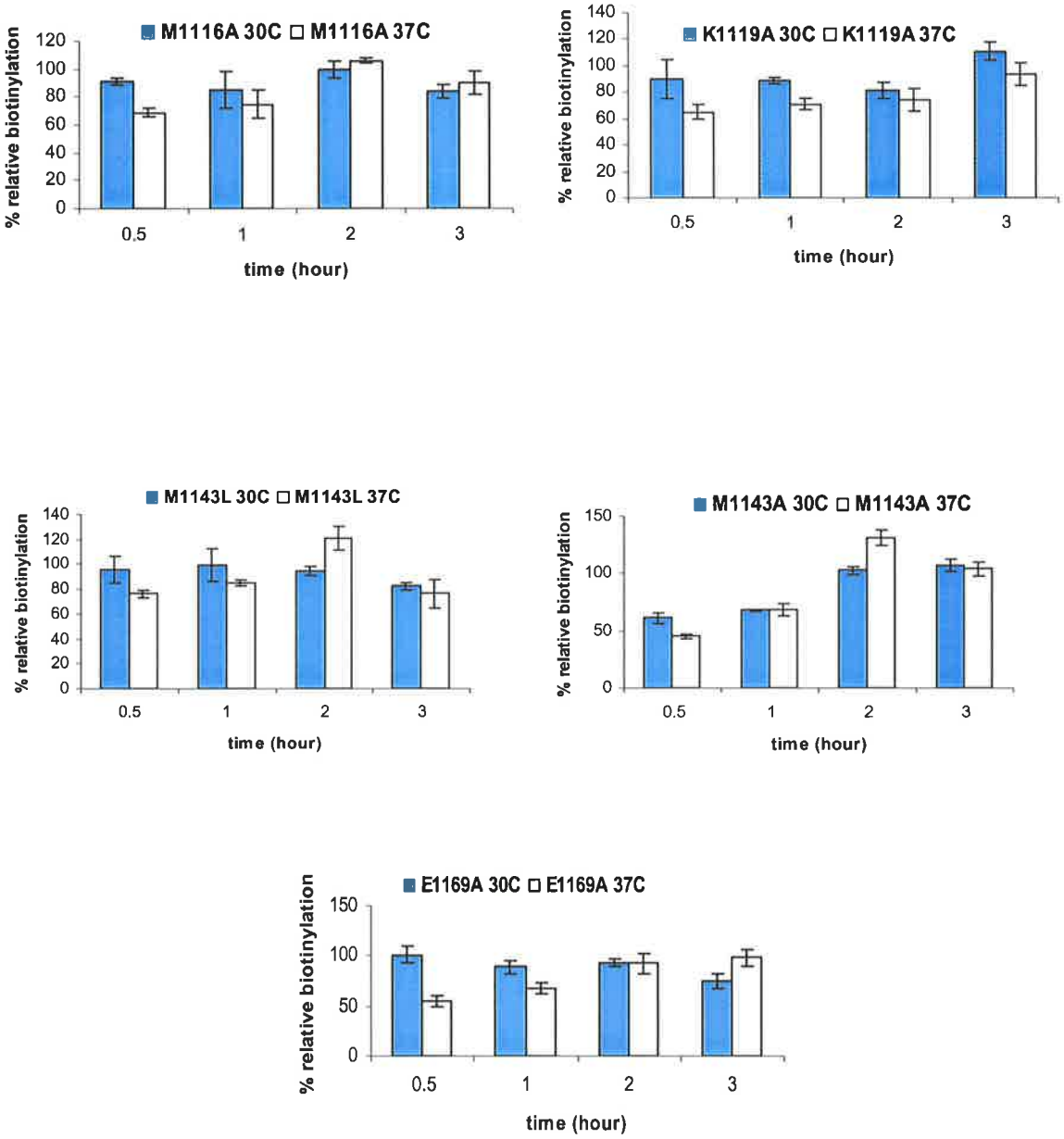

Figure 5.16 Comparative *in vivo* biotinylation of five mutants of biotin carboxyl carrier domain (BCC) of hPC at different times. The *in vivo* biotinylation of five mutants of BCC of hPC was performed (Section 5.2.5) following 0.5, 1, 2 and 3 hours of induction with 0.1 mM IPTG. The cells were grown at both 30°C or 37°C then induced with IPTG and the lysates were prepared for SDS-PAGE analysis followed by Western blot. The extent of *in vivo* biotinylation is expressed as biotinylated protein divided by the total biotin domain protein, in arbitary units, for each mutant relative to wild type (Section 5.2.5).

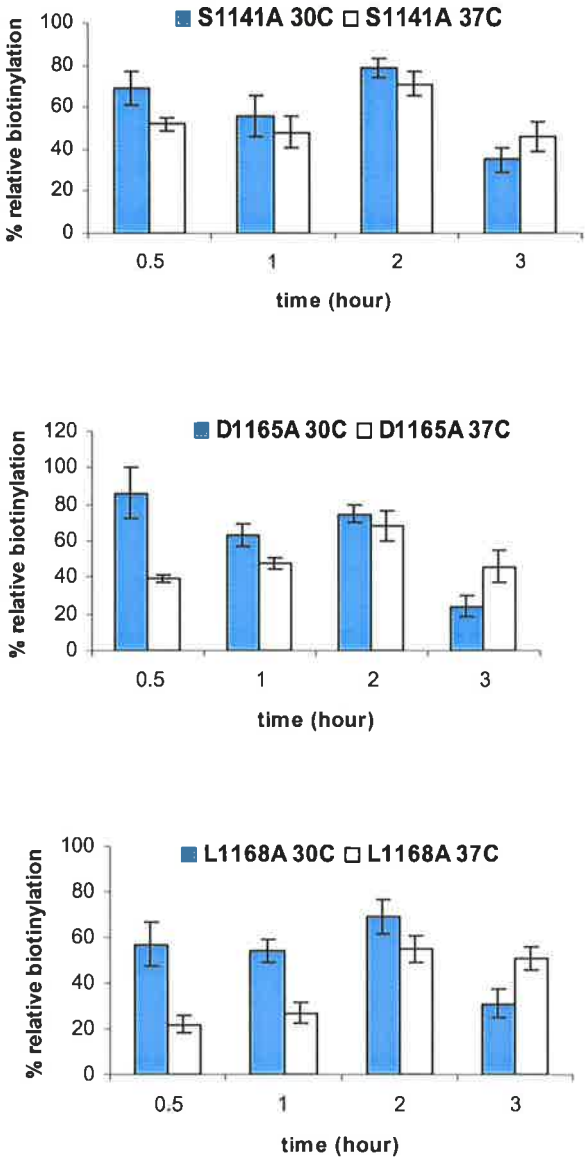

Figure 5.17 The effect of temperature on comparative *in vivo* biotinylation of three mutants of biotin carboxyl carrier domain (BCC) of hPC at different times. The *in vivo* biotinylation of these mutants of BCC of hPC was performed (Section 5.2.5) following 0.5, 1, 2 and 3 hours of induction with 0.1 mM IPTG. The cells were grown then induced with IPTG at either 30°C or 37°C. Lysates were prepared for SDS-PAGE analysis followed by Western blot. The extent of *in vivo* biotinylation is expressed as biotinylated protein divided by the total biotin domain protein, in arbitary units, for each mutant relative to wild type (Section 5.2.5).

The summarised results of the relative biotinylation of the 2 hours induction are shown in Figure 5.18. The extent of biotinylation of M1116A, M1143L, M1143A and E1169A was essentially similar to wild type (TB2 107n) at 30°C and 37°C, while K1119A and S1141A were slightly reduced to 80%, indicating that these substitutions did not result in substantial structural alteration for *in vivo* biotinylation. However, the extent of biotinylation of D11165A and L1168A was reduced to 70% at 30°C and 50-60% at 37°C compared to wild type, indicating the substitutions of these mutants may have had some effect on the overall structure of the domain for *in vivo* biotinylation. None of these mutants of the BCC of hPC was found to be grossly temperature sensitive.

5.3.5 Characterisation of eight mutants of the human biotin carboxyl carrier domains with mAb12 and 42

To further define the critical residues within the biotin carboxyl carrier protein domain (BCC) of hPC for the binding of mAb12 and 42, the eight mutants were expressed as described above. The whole cell lysates were prepared, separated by SDS-PAGE and immunoblotted with mAbs. The blots were probed with mAb12 (dilution 1:2500) and mAb42 (dilution 1:5000) followed by goat anti mouse IgG conjugated to alkaline phosphatase.

All proteins were over-expressed on Coomassie stained gel at similar levels compared to wild type as shown in Figure 5.19a. Figure 5.19b shows the binding of mAb12 to the eight mutants of the BCC domain of hPC. The results of the relative bindings of mAb12 and 42 were quantitated and summarised in Figure 5.20 and 5.21. For mAb12 (Figure 5.20), binding to M1143A was completely abolished, whereas when Met^{1143} was mutated to leucine, the binding was reduced to 40%. This indicates that the alanine substitution at the position 1143 caused a major loss of affinity for this antibody. Single substitutions within this domain, M1116A, M1143L, D1165A and E1169A

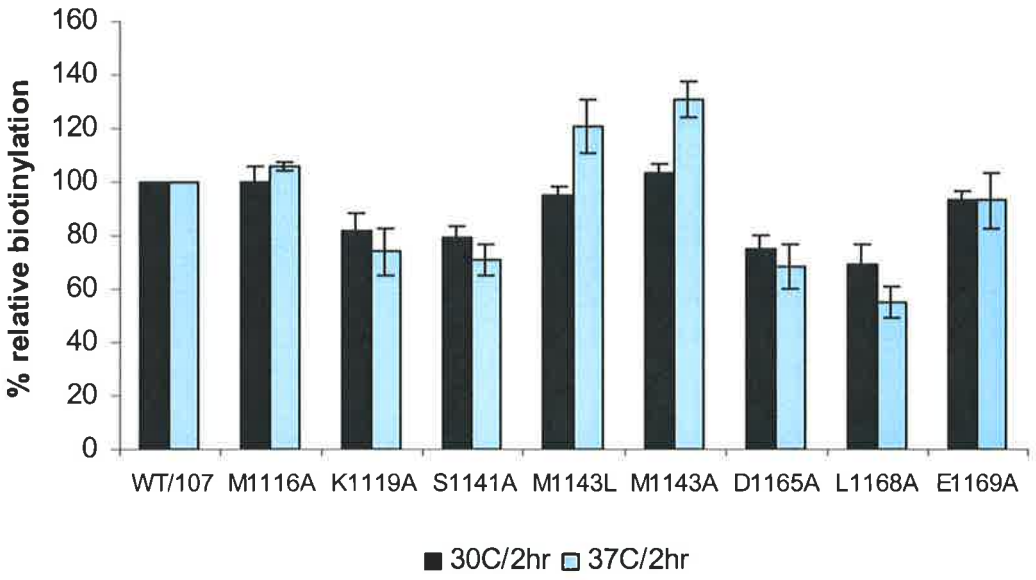

Figure 5.18 **The percent relative *in vivo* biotinylation of eight mutants of biotin carboxyl carrier domains (BCC) of hPC compared to wild type.** Expression of eight mutants of BCC of hPC was induced with IPTG and lysates prepared 2 hours after induction at 30°C or 37°C. The results were quantitated from the avidin blots from Figure 5.15b and are shown as the mean of the measurement ± standard deviation (SD). The assays were performed in triplicate.

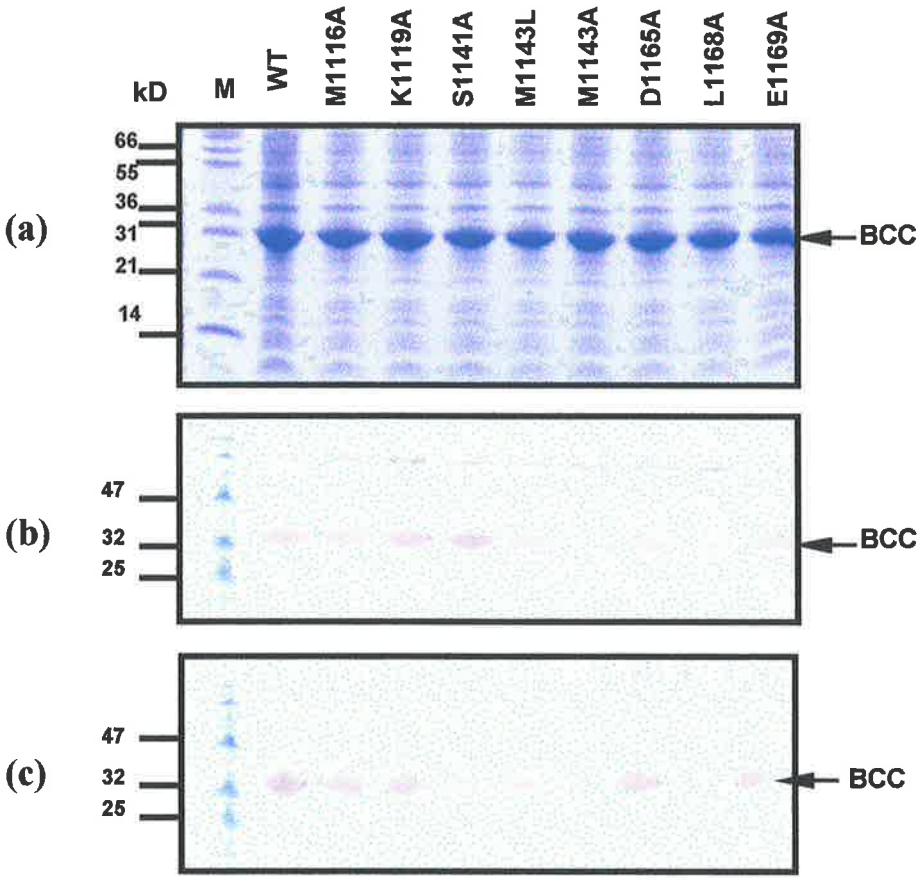

Figure 5.19 Immunoblot analysis of eight mutants of biotin carboxyl carrier domain of hPC with mAb12 and 42. These mutants were constructed (as described in Section 5.2.4) and expressed in *E. coli* BL21. The cell lysates were prepared and analysed by SDS-PAGE followed by Western blot. (a) The over-expressed proteins are shown as the 31 kDa band on Coomassie stained gel. The blots were reacted with mAb12, dilution 1:2500 (b) and mAb42, dilution 1:5000 (c) then probed with goat anti mouse conjugated to alkaline phosphatase. M = Wide Range Protein Standard Marker (Mark 12, Novex) for the Coomassie gel and Prestained Protein Marker, broad range (New England Biolab) for the avidin blot.

caused the reduction of binding by mAb12 to 64, 40, 44 and 58% of wild type, respectively (Figure 5.20). For K1119A and S1141A binding was increased to 104 and 114% respectively indicating both mutants did not affect the structural integrity and binding for this epitope of mAb12. Mutant L1168A and M1143A caused significantly reduced binding to 27% and 2% of wild type (TB2 107n) (Figure 5.20). These data suggest that Met^{1116}, Asp^{1165} and Glu^{1169} contribute the binding of mAb12 on BCC domain of hPC, but Leu^{1168} and Met^{1143} are the most significant contributors for the binding to mAb12.

For mAb42, four mutants, M1116A, K1119A, D1165A and E1169A moderately reduced the binding to 46-54% (Figure 5.21). Another three mutants, S1141A, M1143A and L1168A severely reduced the binding to 13, 6 and 8% respectively. In contrast, the mutation of Met^{1143} to Leu^{1143} had a significant but lesser effect than M1143A in reducing the binding to mAb42. These data suggest that Ser^{1141}, Met^{1143} and Leu^{1168} are critical to the binding of mAb42 and they might form part of the epitope. However, mutating Met^{1116}, Lys^{1119}, Asp^{1165} and Glu^{1169} individually caused approximately 50% reduction of the binding against mAb42 and thus the epitope might also contain these residues.

The result of the binding assay against mAb12 and 42 with the lysates of four mutants cultured at 30°C and 2 hours induction was shown in Figure 5.22. Consistent with the result in Figure 5.20 and 5.21, the alanine substitution of Ser^{1141}, Met^{1143} and Leu^{1168} are critical for mAb42 binding but not important to mAb12, which bound to the mutant S1141A almost as well as it did to wild type

(a)

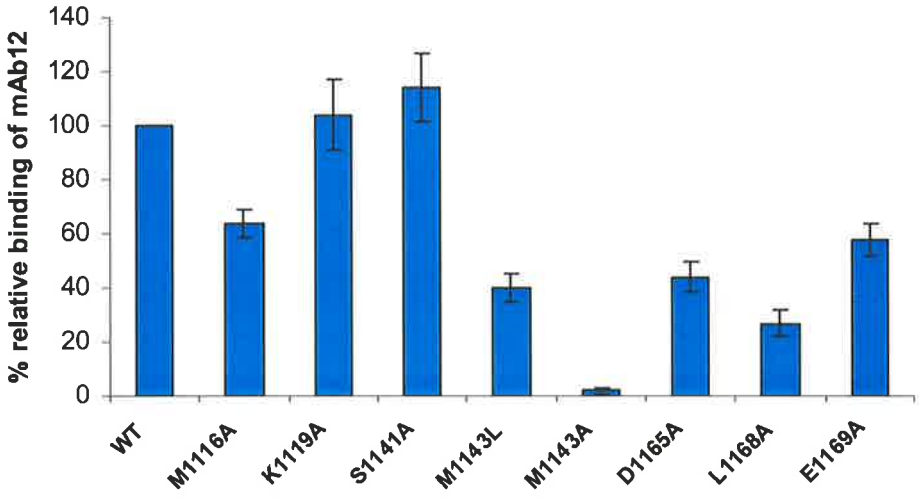

(b)

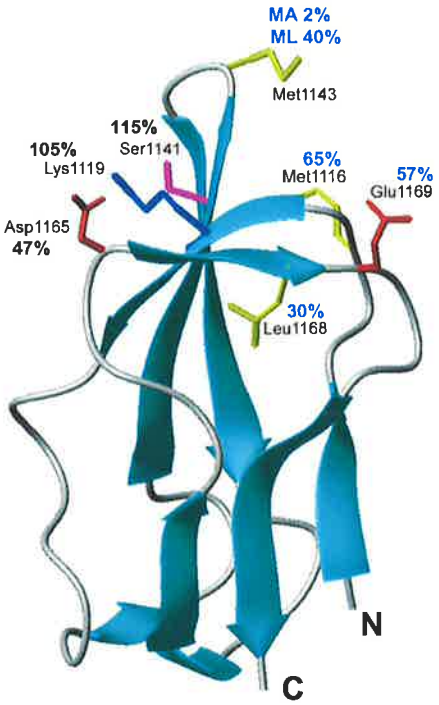

Figure 5.20 The percent relative binding of mAb12 with eight mutants of biotin carboxyl carrier domains (BCC) of hPC compared to wild type at 3 hours induction. (a) Eight mutants of BCC of hPC were expressed and lysates prepared for the binding with mAb12 after IPTG induction. The results were quantitated from the antibody blots from Figure 5.19b, c and are shown as the mean of the measurement ± standard deviation (SD). The percent relative bindings compared with wild type (TB2 107n) were determined in triplicate. (b) The predicted three-dimensional structure of hPC BCC, with summarised results of percent bindings of mAb12 to eight mutants was shown in black colour. The reduction of binding by critical residues which may be the part of mAb12's epitope was shown in blue colour.

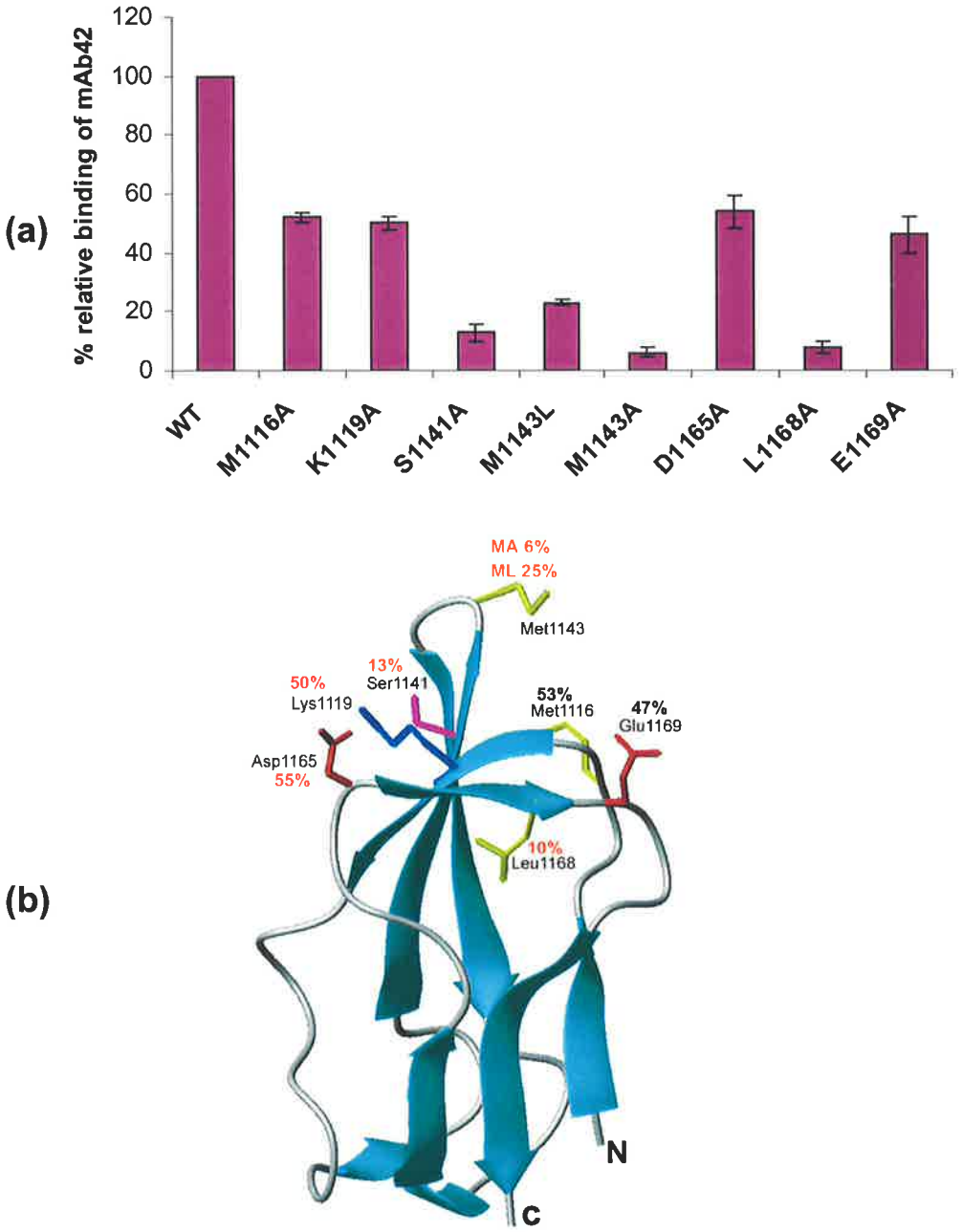

Figure 5.21 The percent relative binding of mAb42 with eight mutants of biotin carboxyl carrier domains (BCC) of hPC compared to wild type at 3 hours induction. (a) Eight mutants of BCC of hPC were expressed and lysates prepared for the binding with mAb42 after 3 hours induction. The results were quantitated from the antibody blots from Figure 5.19b, c and are shown as the mean of the measurement ± standard deviation (SD). The percent relative bindings compared with wild type (TB2 107n) were determined in triplicate. (b) The predicted three-dimensional structure of hPC BCC, with summarised results of the percent bindings of mAb42 to eight mutants was shown in black colour. The reduction of binding by critical residues which may be the part of mAb42's epitope was shown in red colour

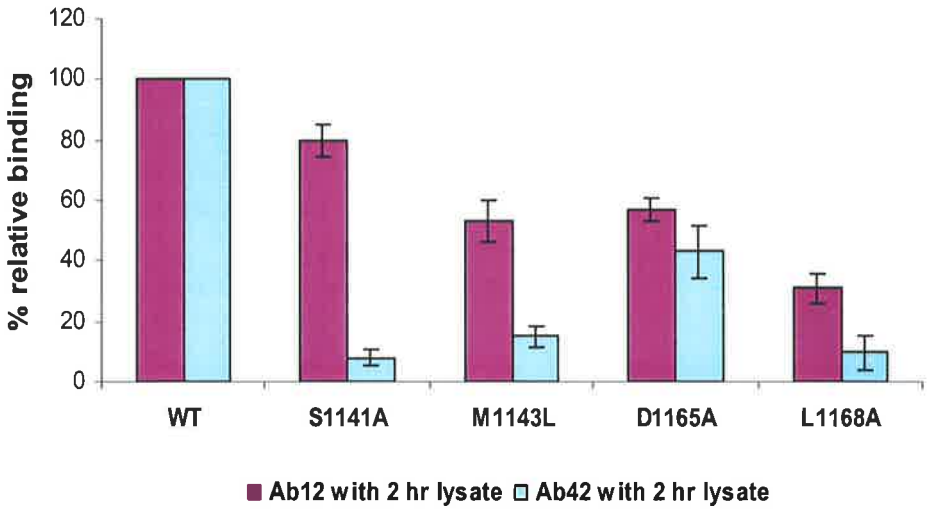

Figure 5.22 The percent relative binding of four mutants of biotin carboxyl carrier domains (BCC) of hPC compared to wild type at 2 hours induction. These mutants of BCC of hPC were expressed and lysates prepared for the binding with mAb12 and 42 after 2 hours induction at 30°C. The results were quantitated from the data of the antibody blots and are shown as the mean of the measurement ± standard deviation (SD). The percent relative bindings compared with wild type (TB2 107n) were determined in triplicate.

5.4 DISCUSSION

The results in Chapter 3 demonstrated that mAb12 and 42 are inhibitory antibodies against sheep PC, human PC, rat PC and chicken PC. These antibodies were mapped to the minimal C-terminal 80 residues of the human PC biotin carboxyl carrier domain. It is likely that when bound to the BCC of these enzymes, mAb12 and 42 would interfere sterically with the function of the biotinyl domain as a mobile carboxyl group carrier between the sites of the first and second partial reactions.

To localize these epitopes on the hPC biotin carboxyl carrier domain, the previous study (Chapter 3) showed that these epitopes are discontinuous or dependent on the conformation of the minimal C-terminal 80 residues of this domain. This result parallels the *in vivo* biotinylation study of the deletion fragments of this domain showing the fragment consisting of C-terminal 60 residues is not biotinylated, similar to the negative result of the binding of this fragment to mAb12 and 42 (Chapter 3). The results are consistent with a study that showed the C-terminal 55 or 67 residues of BCCP of *E. coli* ACC were not biotinylated *in vivo* (Morris, 1994). It has also been shown that amino acids located 30-40 residues either side of the biotin attachment site are essential for biotinylation (Cronan, 1990; Murtif & Samols, 1987; Reed & Cronan, 1991). These data suggest that this hPC biotinyl carboxyl carrier domain could be deleted to the C-terminal 70 residues fragment to define the minimal residues of the epitopes. However, the initial screening of a D1099V mutant of yPC_1104 showed no effect on the binding of mAb12 and 42 (Figure 5.6d and 5.7d), indicating that Asp^{1099} in the yPC_1 sequence (corresponding to Val^{1108} in hPC sequence, see Figure 5.10) of the C-terminal 70 residues fragment is not critical for these epitopes.

In yeast PC and *E. coli* ACC, the binding of the holo (biotinylated) form of the BCC domain of yPC_1104 and *E. coli* ACC was positive to mAb12 but the apo (unbiotinylated) form was not. The structure of the apo (unbiotinylated) form of the

BCCP domain of *E. coli* ACC was determined by NMR and compared with the high solution structure of the holo (biotinylated) form that had been solved by X-ray crystallography. The overall folding of the two proteins is highly similar with small local conformational changes observed in the β-turn that contains the lysine residue modified in the biotin ligation reaction (Yao *et al.*, 1997). This indicates that the conformation of the β-turn containing the lysine residue is critical for the epitopes of mAb12 on yPC and *E. coli* ACC and it could be significant for hPC as well. However, the competition europium assay of labelled mAb42 and unlabelled mAb12 revealed that the mAbs' epitopes were not directed only to the lysine prosthetic group because in this assay both mAbs still can bind to the BCC domain of hPC (TB107n) that is bound to a streptavidin-coated microtiterplate.

No structural information for this region is yet available from X-ray-crystallographic and NMR experiments with the BCC domain of hPC. To define the specific residues for these conformational epitopes, eight mutants of the BCC of hPC were constructed based on not only the sequence alignment of hPC, yPC_1104 and BCCP of *E. coli* ACC but also on the predicted structure of the BCC of hPC (Figure 5.13). The structural integrity of the eight mutants was demonstrated by their abilities to be biotinylated by BirA (biotin protein ligase) in *E. coli* (Figure 5.18). The single substitution of alanine for each of seven amino acids in the biotin domain of hPC and leucine for the eight did not alter the overall structural integrity of the domains for *in vivo* biotinylation at 30°C during a 2 hour induction. In addition, the extent of *in vivo* biotinylation at 30°C of two mutants M1143A and M1143L behaved similarly to wild type. This result is consistent with the study on transcarboxylase (TC, EC 2.1.3.1) showing the residues adjacent to the biotinylated lysine are important for carboxy transfer, but can be altered without affecting biotinylation (Shenoy *et al.*, 1992). Mutants made by substitution of Met^{1134} (corresponding to Met^{1143} of hPC) by Thr or

Val in yPC_I104 were biotinylated to the same extent at both 30°C and 37°C, indicating these substitutions did not result in a structural alteration (Polyak *et al.*, 2001). However, the substitution of methionine flanking the targeted lysine of the biotin carboxyl carrier protein of *E. coli* ACC did affect the biotinylation reaction (Reche *et al.*, 1998).

By using mAbs as probes, the binding measurements of mutants were used for mapping hPC's epitopes. The hPC mutant M1143A exhibited dramatically reduced binding of mAb12 and 42, whereas the mutant M1143L had a significant but less effect on reducing the binding of mAb12 (Figure 5.20 and 5.21). This result indicates that Met^{1143} is likely to be one of the critical residues of the epitope of mAb42 on hPC. Consistent with the previous result in Figure 5.9b, two mutants of yPC_I104, M1134V and M1134T completely abolished the binding of mAb42. However, the binding of M1143L against mAb12 was reduced only to 40% indicating that Leu^{1143} can substitute for part of M1143's component of the epitope of mAb12. This result is in agreement with the result of two mutants of yPC_I104, M1134V and M1134T, which are slightly positive with mAb12 (Figure 5.8b). Again this result suggests that Met^{1143} mostly affects mAb42's epitope and has less effect on mAb12's epitope.

Comparison of the epitope mapping results of Carey (1988) provides further evidence consistent with the proposed residues being involved in structural and functional roles in PC. The binding of anti-biotin antibodies to sheep PC reduced the binding of mAb12 and 42 (Carey, 1988) [Table 1.4 in Appendix I]. The binding sites of mAb12 and 42 can also be excluded by preincubation of PC with avidin, confirming that mAb12 and 42 bind to an epitope within the biotin moiety in the native molecule (Carey, 1988). This supports the possibility that these epitopes are likely to be the parts of the motif MKM.

As shown in Figure 5.23, based on the predicted model of M1143A showed the effect of this mutation on the reduction binding of these two predicted epitopes on upstream of the domain indicated in red box. Again, this suggests Met^{1143} may be one of the overlapping residues of these epitopes. From the europium competition assay, unlabelled Fab12 can compete with europium-labeled Fab42 to give 50% inhibition at 230 ng of Fab12 whereas only 75 ng of Fab42 gave 50 % inhibition. Thus, it is possible that the binding sites of these two antibodies are close to each other or overlap. This result is consistent with these epitopes probably overlapping at one amino acid residue, Met^{1143}.

As shown in Figure 5.20 and 5.21, the mutant S1141A significantly reduced the binding of mAb42 to 13%, whereas it increased the binding of mAb12 to 114%. This result indicates that the Ser^{1141} is critical for the binding of mAb42 but not mAb12. The Ser^{1141} is conserved in human and yeast PC and is also close to the lysine prosthetic group in the motif MKM. Studies of the antigen binding residues of antigen antibody complexes concluded that tryptophan, tyrosine, serine and asparagine residues were most abundant in six crystallographically determined antibody antigen complexes (Mian *et al.*, 1991). The Ser^{1141} is likely to be a surface residue on the biotin domain of the epitope of mAb42, whereas it does not contribute to the epitope of mAb12. An alignment of BCC domain with human PC, yeast PC and *E. coli* ACC in Figure 5.12 showed that Ser^{1141} in human PC corresponds to Glu^{119} in the wild type BCCP of *E. coli* ACC to which mAb42 does not bind (Figure 5.7). Therefore, the mutation of Ser^{1141} to Glu, for a negatively charged residue, or to Cys, for a non polar side chain residue, should be further investigated to confirm the effect on the binding of mAb42.

In *E. coli* ACC, mAb12 was bound to wild type BCCP (holo) but mAb42 was not (Figure 5.7). Comparing the three-dimensional structure of the holo BCCP domain of *E. coli* ACC to the predicted structure of hPC (Figure 5.24), there is a "thumb"

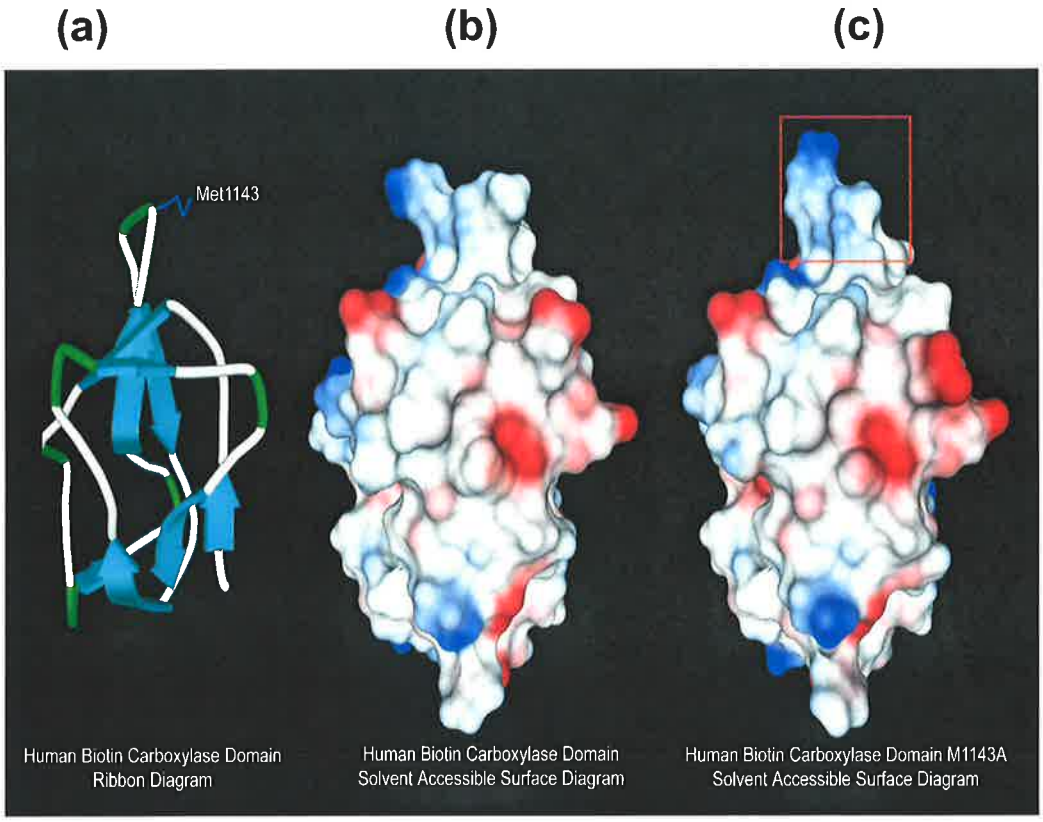

Figure 5.23 Predicted structure of mutant biotin carboxyl carrier domain (BCC) of human PC, M1143A*. (a) A ribbon diagram of the predicted structure of wild type of hPC BCC domain, with the position of Met1143 shown and the ß sheets indicated as blue arrows. (b) The computational model of wild type hPC BCC domain was compared to alanine substitution mutant, M1143A (c). The conformation change of mutant M1143A (c) compared to wild type (b) was indicated as red blocks. *Kindly prepared by Mr. C. Stojkoski (School of Molecular and Biomedical Sciences, University of Adelaide).

structure found in the BCCP sequence (Figure 5.4). This thumb is composed (largely) of the seven additional residues (^{95}PSPDAKA^{101}) found in *E. coli* BCCP but not in the predicted structure of hPC. The mutation K1119A significantly reduced the binding of mAb42 to the BCCP of hPC by 50% but the binding of mAb12 was not reduced (105%). Similarly, the mutation S1141A reduced mAb42 binding by 87% but increased mAb12 by 15%. Ser^{1141} is close to Lys^{1119}. Therefore, mAb42 might bind to hPC BCC domain at a surface containing Lys^{1119}, Ser^{1141} and Met^{1143} which are close to the biotin moiety. Again, this suggests that the mAb12's epitope might be more towards the opposite site of the domain.

Based on the computational model of hPC BCC domain (Figure 5.13) the side chain of Leu^{1168} is predicted to be buried yet, the mutant L1168A significantly reduced the binding of mAb12 to 27% and of mAb42 to 8% (Figure 5.20 and 5.21). These results suggest that as Leu^{1168} is a large hydrophobic residue its replacement by alanine may significantly affect the conformation of the domain resulting in reduction of the binding of these antibodies. This is consistent with the extent of biotinylation of L1168A was reduced to 70% at 30°C and 55% at 37°C compared to wild type, indicating the substitutions of mutant L1168A may have had some effect on the overall structure of the domain for *in vivo* biotinylation and these antibody binding sites.

Functional studies on other protein-protein complexes also indicate that a small number of residues can confer tight binding affinity (Clackson & Wells, 1995). Mutational analysis of antibodies (Hawkins *et al.*, 1993) or protein antigen (Jin *et al.*, 1992) has shown that only 3 to 10 side chains can account for most of the binding energy, although the structures of complexes between antibodies and protein antigens (Davies *et al.*, 1990) show that typically between 14 and 21 residues are in contact. The predominant role of these side chains is to slow the dissociation of the complex (Davies & Cohen, 1996). Our result is consistent with these studies showing the alanine

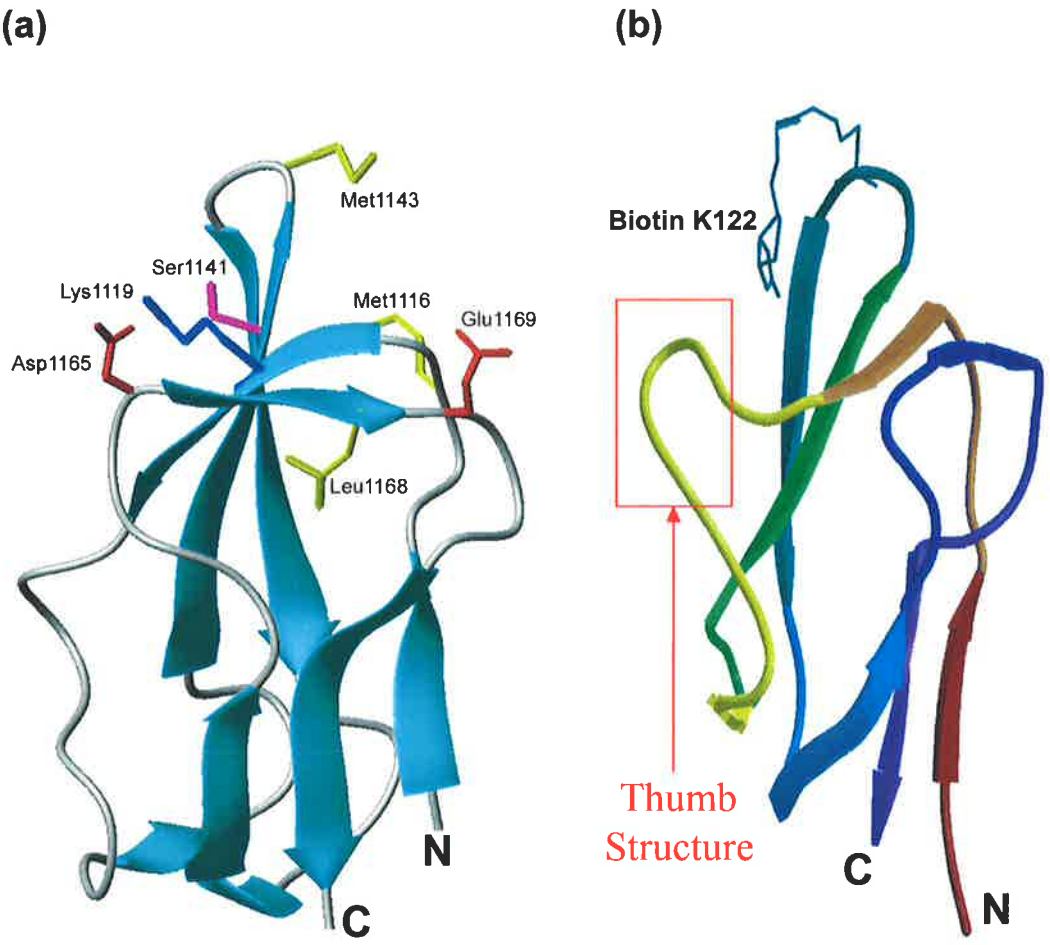

Figure 5.24 Predicted structure of biotin carboxyl carrier domain (BCC) of human PC compared to three dimensional structure of *E. coli* ACC. (a) The predicted three dimensional structure of hPC BCC domain shown, compared to the three dimensional structure of the BCCP of *E. coli* ACC (b) with its "thumb" structure indicated.

substitution of Met^{1116}, Met^{1143} and Glu^{1169} can account for the reduction of the binding of mAb12. Leu^{1168} also contributes most significantly to the binding of mAb12. For mAb42, the alanine substitution of Ser^{1141}, Met^{1143} and Leu^{1168} most significantly accounts for reduction of binding to hPC, and Met^{1116}, Lys^{1119}, Asp^{1165} and Glu^{1169} are also modest contributors to mAb42's binding.

The reduction in binding affinities, which occurred as a result of the various mutations, was likely to be caused by changes in the direct interaction of the mAb with the altered residue. Alternatively, the mutation may have affected the secondary or tertiary structure of the biotin carboxyl carrier domain of hPC (TB2 107n) resulting in the secondary consequence of conformational changes of the epitopes and hence an indirect reduction of the binding affinity. Therefore, it would be valuable to obtain the enzymatic activity of the eight mutant full-length hPC expressed in 293T cell lines to specify the critical residues of these epitopes on the catalytic activity of hPC. Furthermore, purification and kinetic analysis of these mutants compared to wild type for the interaction of the substrates in the two partial reactions would further investigate the critical role of these residues in the catalytic reaction. For example, the analysis of the effects of substrates on the inhibition of sheep PC by these antibodies, revealed that oxaloacetate at a concentration between 1-10 mM was able to significantly reduce the level of inhibition caused by mAb12 (Carey, 1988) [Table 1.1.1 in Appendix I]. This observation is further evidence to contribute to a structure and function relationship model, in that the binding of oxaloacetate (at the pyruvate/oxaloacetate binding site) is able to influence the binding of mAb12 site on the biotin carboxyl carrier domain. This indicates either that the epitope of mAb12 on the BCC domain might at times be close to the pyruvate/oxaloacetate binding site or that the formation of carboxybiotin from oxaloacetate may in some way reduce mAb12 binding to its epitope.

Moreover, the presence of $MgATP^{2-}$ (Table 1.3.2 in Appendix I) was able to significantly reduce the level of inhibition by mAb42 to 10% (Carey, 1988) indicating either that the binding site of mAb42 may be close to the other subsite of the PC active site ($MgATP^{2-}/HCO^{3-}$) or that formation of carboxybiotin renders the mAb42 epitope largely inaccessible. It is known from the work of Goodall *et al.* (1981) and Attwood & Wallace (1986) that the presence of Mg^{2+} was favour the retention of the carboxybiotin in the first subsite whereas oxo-acids induce the carboxybiotin to move to the second subsite. Confirmation of these findings would be expected from experiments measuring the ability of substrates to alter the effect of these antibodies on the activity of hPC. These antibodies were produced by the original cell lines but were a different batch to those that were characterized against sheep PC.

The mutants M1143L, S1141A, K1119A and D1165A are most critical for the binding site of mAb42; changing these to positively charged residues, except Lys^{1119} changing to a negatively charged residue would be useful to obtain more information about the notion of a matching charged surface. It has been shown (Wilson *et al.*, 1992) that several positively charged residues on the surface of the biotin-binding pocket of the BirA protein may be involved in the correct positioning of the biotin acceptor protein at the catalytic site. Thus, alteration of the surface charge on the biotin domain surface that interacts with the ligase may affect the recognition between the two proteins (Chapman-Smith *et al.*, 1999). Moreover, the mutation studies of the biotin domain of human propionyl-CoA carboxylase showed that changing the conserved PMP motif to PKP had a more pronounced effect on the efficiency of biotinylation than replacing all three residues with alanine (Leon-Del-Rio & Gravel, 1994). Interestingly, the functionally analogous interaction between lipoate ligase and the lipoyl domains appears to require charge conservation at position Glu^{119} in BCCP of *E. coli* ACC sequence, corresponding to Ser^{1141} in BCC of human PC. The substitution of lysine for

the Glu found two residues upstream of the lipoylated Lys in many lipoyl domains dramatically reduces lipoylation of both human glycine cleavage enzyme and *E. coli* pyruvate dehydrogenase (Fujiwara *et al.*, 1991; Wallis & Perham, 1994).

From the work of Johannssen *et al.* (1983) it is known that the biotinyl prosthetic group is close to the intersubunit junction as indicated in Figure 1.7 of the Appendix I. Any proposed mutations in the BCC domain would therefore need to be interpreted with the recognition that mutation could significantly affect the assembly of the PC tetramer. Mutations in one of PC's subunits could affect the function in a variety of ways, including PC assembly, substrate binding, catalytic efficiency of the overall reaction, or catalytic efficiency in either of the partial reactions. Mutations in the subunits of PC could lead to loss of structure and hence the ability to assemble PC and to act as carboxyl carrier. In order to test the ability of the mutant BCC of hPC to promote assembly, the full-length mutant PC would be purified using HPLC to exhibit the different forms of PC as monomer, dimer or tetramer. If the introduction of residues affects the overall catalytic activity of PC, another approach is to test the chemical cross-linking of the mutant which would promote the assembly of PC and increase the activity of the mutant compared that to wild type. This will imply that the introduced residues change the ability of mutant PC to assemble and affect the overall catalytic activity.

In summary, the epitopes of the two monoclonal antibodies, mAb12 and 42 that are inhibitory to hPC were mapped to the C-terminal 107 residues of the biotin carboxyl carrier domain of hPC and shown to be two overlapping epitopes in which the antibodies are able to block each other's binding to the domain. The mutants designed on the basis of the predicted structure of hPC BCC domain viz M1143A, M1143L, S1141A, K1119A, D1165A and L1168A significantly reduced the binding of mAb42 indicating that the Met^{1143}, Ser^{1141}, Lys^{1119}, Asp^{1165} and Leu^{1168} are likely to be part of

the epitope, and this epitope may be involved in or be part of the second subsite of the catalytic reaction. For the epitope of mAb12, the substitution of Met^{1143} by alanine and leucine has a most significant effect on the binding, suggesting this residue may be part of this epitope or be part of the overlapping of these epitopes. Therefore, mAb42 might bind to hPC BCC domain to the surface of the BCC structure containing Met^{1143}, Asp^{1165}, Leu^{1168}, Lys^{1119} and Ser^{1141} which are close to the biotin moiety. However, mAb12's epitope appears to be on the opposite site of the biotin moiety, and includes Met^{1116}, Met^{1143}, Leu^{1168} and Glu^{1169}. The Met^{1143} and Leu^{1168} may be part of the overlap of these epitopes.

CHAPTER 6

Expression of Human PC in Bacteria and Yeast

CHAPTER 6

6.1 INTRODUCTION

In Chapters 3 and 4, the minimal epitope of mAb6 was shown to be LKDLPRV (residues 968-974) and to be localised between the transcarboxylation and biotin carboxyl carrier domains of hPC. This epitope is not present in the yeast PC sequence and mAb6 does not bind to yeast PC. We used site-directed mutagenesis to change to alanine six residues in hPC within the binding site of mAb6 that are different from the sequences of yPC_1 and yPC_2. Only one of six mutants, D970A, expressed both as a fusion protein fragment in *E. coli* and as full-length hPC in a mammalian cell line, showed a complete loss of binding to mAb6. In addition, the acetylCoA-dependent activity of the D970A mutant was significantly reduced to 50% of wild type activity. Asp^{970} as one part of the functional epitope site, is likely be exposed to the surface of the enzyme and may be involved in significant side-chain movements of the enzyme and possibly minor movement of the backbone conformation (Getzoff *et al.*, 1988). An inhibition study of mAb6 on acetylCoA-dependent activity of human (Chapter 3.3.2) and sheep PC (Carey, 1988) showed that as little as 1 mM oxaloacetate had significantly augmented enzymatic inhibition. To test whether Asp^{970} residue is involved in the reaction mechanism or whether it only changes the conformation of the epitope, a kinetic and physical study of the D970A mutant of hPC should be undertaken. This might reveal how whether the blocking activity of mAb6 or the D097A mutation is involved in the reduction of enzymatic activity. For this study and the ultimate description of the structure of hPC by X-ray diffraction of hPC crystals significant quantities of the highly purified enzyme will be required.

Purification of the hPC mutants from dried mitochondrial extracts was limited by the low expression level and the cost of producing large amounts of the permanently transfected cultured human cells. Loss of proteins from the purification during lysis of

cells and mitochondria, made it difficult to purify sufficient protein for a kinetic and physicochemical study. Moreover, a major disadvantage of mammalian cells is a contamination of the recombinant PC with the endogenous wild type PC. To eliminate this problem, *E. coli* is an alternative expression system that does not have any endogenous PC. In this Chapter, I describe attempts to improve the expression of hPC in *E. coli* and *S. cerevisiae* expression systems.

Escherichia coli expression system

"Among the many systems available for heterologous protein production, the gram-negative bacterium *Escherichia coli* remains one of the most attractive because of its ability to grow rapidly and at high density on inexpensive substrates, its well-characterised genetics and the availability of an increasingly large number of cloning vectors and mutants host strains (Baneyx, 1999). Although for most applications it is desirable to achieve maximal production within the cytoplasm, targeting the protein to extracellular compartments may offer an alternative, especially when cytoplasmic production results in toxicity or improper folding (Baneyx, 1999; Cornelis, 2000)". Recent work has shown that mutants with modulated activities of the disulfide oxidoreductases DsbA and DsbC can be used to enhance disulfide isomerization and protein folding in the periplasm (Bessette *et al.*, 2001). In an alternative approach, Fab antibody fragments were expressed in the cytoplasm of *trx*B thioredoxin reductase mutants in which a variety of chaperones were co-expressed and seen to have effects on folding (Levy *et al.*, 2001).

Although the various promoter systems commonly used for *E. coli* have been well described, several recent reports have demonstrated new options (Andersen & Krummen, 2002). In one particularly notable result, secondary structure was engineered into mRNA transcripts to manipulate message stability and correspondingly, the expression level (Smolke *et al.*, 2000). This provides another technique, along with

manipulation of translation initiation strength via the ribosome binding site, for controlling the relative strength of expression of genes independently (Simmons & Yansura, 1996).

Another problem encountered in the control of heterologous gene expression occurs at the level of codon usage, which is again based on discrepancies in the G+C content among different organisms (Connell, 2001). GC content is a major determinant of codon usage, and codon adaptation indices (CAI values) have provided a reliable, empirically determined estimate of gene expression level for specific groups of organisms (Saier, 1995). Translation errors during protein synthesis are a well-documented phenomenon. They can have several different effects including frame shifts (Spanjaard *et al.*, 1990), premature truncation leading to low expression (Rosenberg *et al.*, 1993) and misincorporation (Seetharam *et al.*, 1988). However, site-directed mutagenesis of codons in the open reading frame (ORF) can be used to alter the GC content and adjust the requirement for specific tRNAs (Connell, 2001) or a host containing a plasmid with the appropriate tRNAs can be used.

Two main approaches have been used to correct codon bias effects in *E. coli*. The first is to resynthesize the heterologous gene, replacing potentially problematic codons with those preferred by the host (McNulty *et al.*, 2003). An experiment of replacing three AGA codons with CGC was successful in eliminating high level lysine substitution for arginine in an HIV-1 gp 160 fragment (Calderone *et al.*, 1996). A more preferable strategy may be the co-expression of rare tRNAs on a separate compatible plasmid. This approach has been equally successful in alleviating translational errors (McNulty *et al.*, 2003). Co-expression of the *ileX* gene recognising the rare isoleucine codon AUA improved expression of a Staphylococcal leucyl-tRNA synthetase from below detectable levels to levels approaching 30% of total cellular protein (Del Tito *et al.*, 1995). The value of this approach is substantiated by the appearance of

commercially available plasmid vectors encoding combinations of several of the rarest tRNAs including *arg*U (AGA/AGG), *ile*X (AUA), *leu*W (CUA), *pro*L (CCC) and *gly*T (GGA) (Novy *et al.*, 2001).

Yeast expression system

The yeast system has emerged as a popular model organism for the production of eukaryotic proteins because it is highly amenable to genetic and biochemical manipulation. Yeast is a single cell eukaryotic organism with properties similar to higher eukaryotic organisms. The expression of native as well as foreign genes in yeast has generally relied on creating transcriptional fusions with well-characterised yeast promoters (Cheng *et al.*, 2000). Non-inducible promoters, such as those found at *CYC1, ADH1, TEF2* and *GPD* are used for constitutive expression of heterologous genes. Inducible promoters, such as those found at *GAL1*, *MET25* and *CUP1* are used when conditional expression is required. The use of inducible promoters, however, is subject to limitations. They can yield undesirable levels of over-expression, and are not entirely 'off ' in the absence of inducer (Mumberg *et al.*, 1995).

Our purpose was to develop a bacterial expression system which can efficiently overcome common limitations in terms of yield, folding and functionality when expressing wild type full-length hPC. Another approach to the expression of hPC was investigated in a yeast system (*Saccharomyces cerevisiae)* with a view to improve the production and specific activity of hPC.

6.2 SPECIFIC METHODS

6.2.1 Construction of pQE-hPC wild type and expression in E. coli

To generate the vector pQE-hPC wild type encoding full-length hPC, pEF-PC (Jitrapakdee *et al.*, 1999) was digested with *Bam*HI, *Kpn*I and *Hind*III. Digestion of pEF-PC with *Bam*HI alone results in two fragments, hPC (4 kb) and vector (5.3 kb), which were not easily separated in agarose gel purification. The addition of *Hind*III resulted in digestion of the vector (5.3 kb) into two smaller fragments. Then the 4 kb fragment of hPC was ligated into the vector pQE-32 (Qiagen) at the *Bam*HI and *Kpn*I sites. The proteins were expressed in *E. coli* M15 and SG13009. This construct was verified by sequence analysis and the expression of protein was investigated by SDS-PAGE and Western blot.

6.2.2 Construction of E. coli M15/pLysS/ Rare codon and SG13009/pLysS/ Rare codon

To investigate the effect of rare codon usage on protein expression in *E. coli* M15 and SG13009, M15/pLysS/ Rare codon and SG13009/pLysS/ Rare codon were generated as follows. The plasmid pLysS/Rare codon was purified from *E.coli* Rosetta BL21 (λDE3) pLysS/Rare codon (Novagen) in LB media containing chloramphenicol 30 μg/ml as described in Section 2.11.1. One microliter of plasmid pLysS/Rare codon was transformed into competent cells of M15 and SG13009 (Section 2.11.6). The transformed cells containing plasmid pLysS/Rare codon were obtained and made competent. The plasmid pQE-hPC was transformed into these cells and proteins were expressed in *E. coli* M15/pLysS/Rare codon and SG13009/pLysS/Rare codon. The expression of protein was followed as in Section 3.2.11 with a concentration of IPTG of 2 mM, at 30°C for 3 hours or overnight. The cell lysates were prepared and analysed by SDS-PAGE. The activity of hPC was measured using the radiochemical assay described in Section 6.2.5.

6.2.3 Construction of vector pVT-hPC without mitochondrial targeting sequence (pVT-hPC-21)

The cDNA encoding the first 930 N-terminal residues of hPC was generated by PCR amplification using pEF-PC, encoding full-length hPC, as a template (Jitrapakdee et al., 1999). The forward primer (5'ATACAAGCTTATGGCCCCCGCTGCCTCCCCAAATG3') with a unique *Hind*III site at the 5' end (underlined) was designed without the first 21 N-terminal residues of hPC, as this region contains a mitochondrial targeting sequence found using a computer software program (http:www.mips.biochem.mpg.de/cgi-bin/proj/medgen/mitofilter). The reverse primer, hPC/930R (5'CTCGTAGCCCACCTGTTTAGCGAG 3') was used in the PCR reaction (Section 2.11.8). The 930 bp PCR product was purified and ligated into pGEM-T easy vector (Promega, USA). The reaction mixture was carried out in total volume of 10 µl containing of 5 µl of 2X rapid ligation buffer, 1 µl of pGEM-T easy vector, 3 µl of PCR product, and 10 U of T4 DNA ligase. The reaction was incubated at 4°C for overnight and transformed into competent DH5α cells (Section 2.11.6). A clone confirmed by sequencing, was designated pGEM-hPC (no mitochondria) and digested with *Hind*III and *Sac*II. The resulting fragment was ligated into the same sites in digested vector pET-hPC HD encoding a 1091 amino acid fragment of hPC, yielding the vector pET-hPC (-21). The vector pET-hPC HD was constructed by religation of full-length hPC from mpBlue-hPC (Section4.3.5) into vector pET-32a (+) at the *Hind*III and *Not*I sites. To incorporate the full-length hPC with no mitochondrial targeting sequence into a yeast expression vector (pVT-100U), a *Xho*I-*Xba*I fragment from pEF-PC and a *Xho*I-*Hin*DIII fragment from the vector pET-hPC (-21) were ligated into the *Hind*III-*Xba*I digested pVT-100U. This construct was designated pVT-hPC-21 (Figure 6.1) and transformed into yeast strain W303 (Section 2.11.9). The recombinant protein was expressed in yeast strain W303 and the cell lysate was prepared as described in

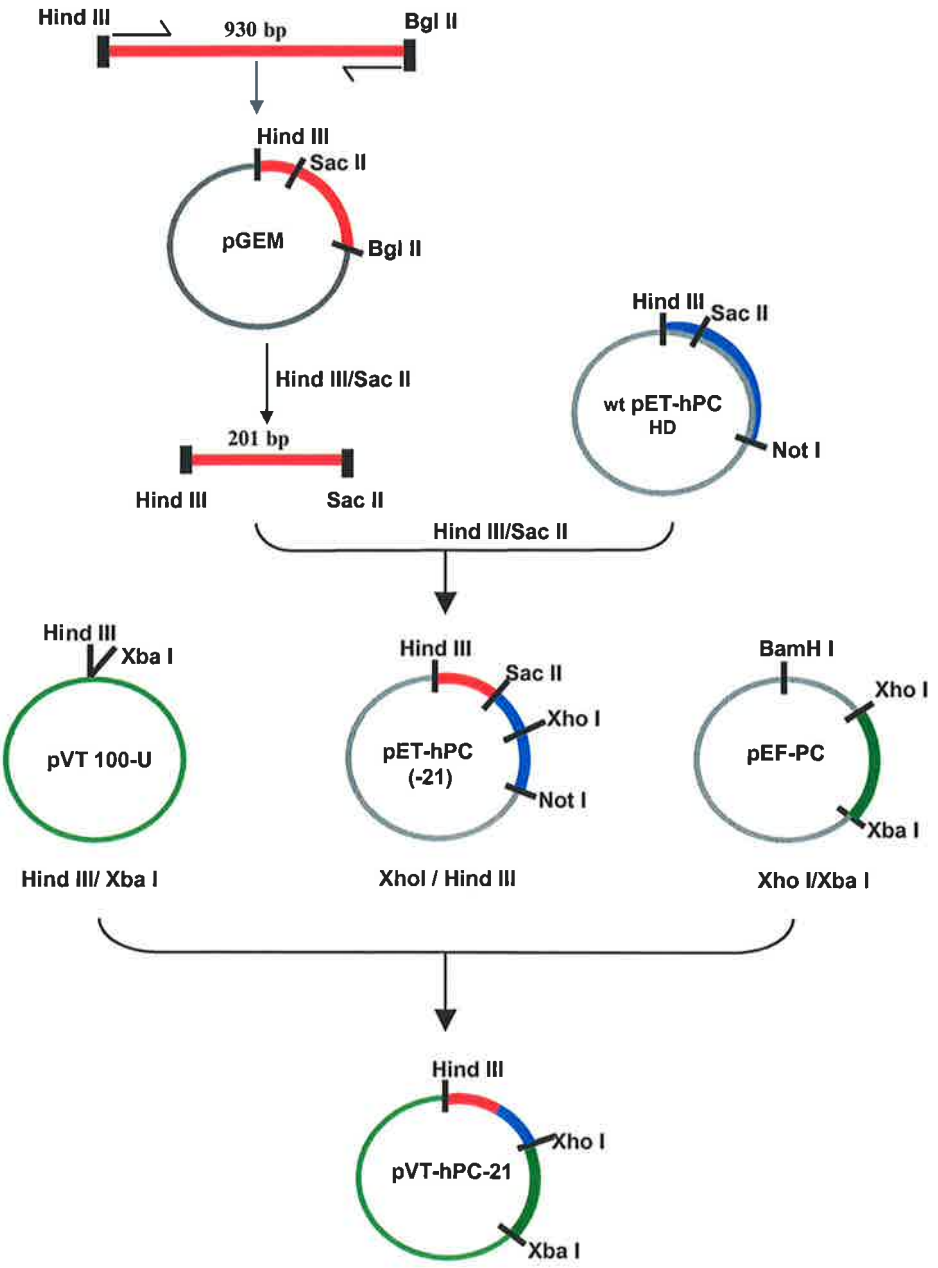

Figure 6.1 Construction of a plasmid pVT-hPC-21 for expression of full-length hPC without mitochondrial targeting sequence in *Saccharomyces cerevisiae*. The strategy for constructing plasmid pVT-hPC-21 for expression of hPC in yeast was described in Section 6.2.3. This plasmid was transformed into yeast strain W303 and proteins were analysed by SDS-PAGE analysis and Western blot.

Section 2.11.10. The protein expression was analysed by SDS-PAGE followed by a Western blot probed with avidin alkaline phosphatase (Section 2.13).

6.2.4 Construction of vector myc tagged pVT-hPC without a mitochondrial targeting sequence (myc pVT-hPC-21)

To generate myc tagged pVT-hPC without a mitochondrial targeting sequence, the cDNA encoding the first 930 residues of hPC with a myc tag at the N-terminus was generated by PCR amplification using pEF-PC encoding full-length hPC as a template (Jitrapakdee *et al.* 1999). The forward primer (5'ATACAAGCTTATG**GAGCAGAAGCTGATCAGCGAGGAGGACCTG**GCCCCCGCTGCCTCC CCAAATGTCCGG3') with a unique *Hind*III site at the 5' end, (underlined) and myc tag (bold) was used in the PCR reaction with the reverse primer, hPC/930R. The PCR product was purified and ligated into pGEM-T easy vector as described above. A positive clone was sequenced and digested with *Hind*III and *Sac*II. This fragment was ligated into the vector pVT-hPC-21 digested with *Hind*III and *Sac*II, yielding vector myc pVT-hPC-21 (Figure 6.2). The protein was expressed in yeast strain W303 (Section 2.11.9) and the cell lysate was prepared (Section 2.11.10) followed by SDS-PAGE. The Western blot was probed with avidin alkaline phosphatase.

6.2.5 Enzymatic activity by a radiochemical assay

The PC activity in crude extracts was assayed by a $^{14}CO_2$ fixation assay described by (Ballard & Hanson, 1967) except that the reaction was coupled to the conversion of oxaloacetate to malate by malic dehydrogenase. A master mix was made containing 145 mM Tris-HCl pH 7.5, 58 mM sodium pyruvate, 15 mM Na_2ATP pH 7, 440 µM acetyl-CoA, 30 mM $NaH^{14}CO_3$ (370 µCi/ml), 30 mM $MgCl_2$, 82 µg/ml malic dehydrogenase and 0.88 µg/ml NADH. Then 190 µl of the master mix was added in a 1.5 ml Eppendorf and pre-incubated at 37°C for 2 min, followed by the addition of 50 µg of whole cell lysate. The tube was vortexed and incubated at 37°C for exactly 2 min.

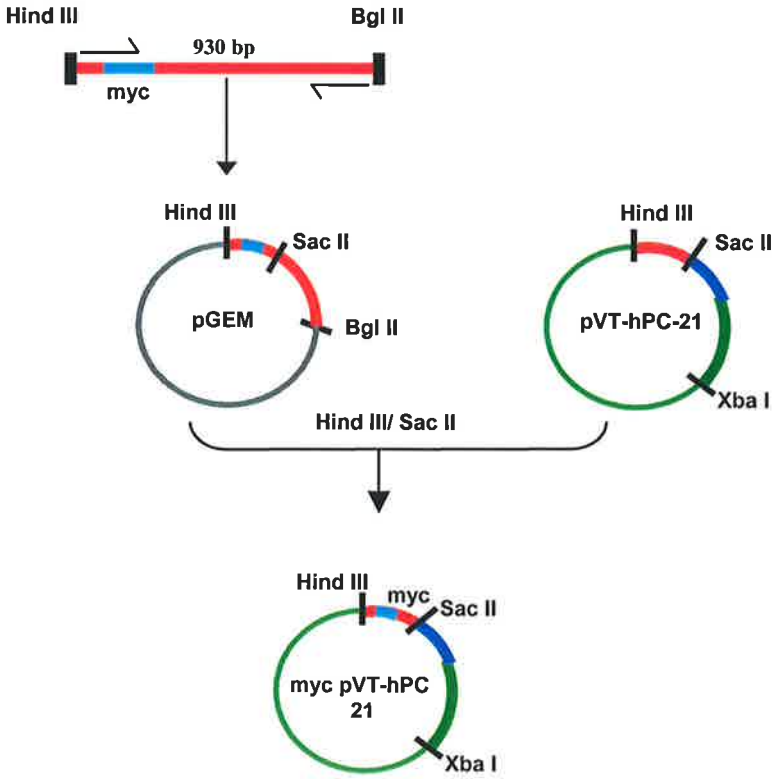

Figure 6.2 Construction of a plasmid myc pVT-hPC-21 for expression of myc tagged full-length hPC without mitochondrial targeting sequence in *Saccharomyces cerevisiae*. The strategy for constructing plasmid myc pVT-hPC-21 for expression of hPC in yeast was described in Section 6.2.4. This plasmid was transformed into yeast strain W303 and proteins were analysed by SDS-PAGE analysis and Western blot.

The reaction was terminated by adding 100 µl of 2 M HCl and the tube was left open in the fume hood for 1 hour to allow unfixed $^{14}CO_2$ to evaporate. Fifty microlitres of reaction mix were spotted onto $2cm^2$ Whatman 3MM paper filters which were then dried at 100°C for 5 min. The amount of $^{14}CO_2$ fixed as malate was determined by counting the filters in LKB Optiscint 'HiSafe' scintillation fluid for 10 min in a Pharmacia 1214 Rackbeta liquid scintillation counter.

The counts that were specific to PC activity were determined by subtracting the counts from a blank (assay solution only, no cell lysate) from the sample count. The specific activity of $NaH^{14}CO_3$ was determined by spotting 50 µl of a 1 mM solution of $NaH^{14}CO_3$ onto Whatman 3MM paper treated with 1% $BaCl_2$ and scintillation counting as previously described. One unit of PC activity was defined as the conversion of 1 µmol of $NaH^{14}CO_3$ to oxaloacetate in one minute.

6.3 RESULTS

6.3.1 Characterisation of vector pET-hPC expressed in E. coli

6.3.1.1 Expression of mutant pET-hPC in BL21

The hPC mutants (mutant pEF-hPC) were expressed in the mammalian cell line, 293T but the level of expression of functional hPC was not sufficient for further purification from dried mitochondria (Chapter 4). Moreover, the background of endogenous PC expression and activity in 293T can affect the activity assay of the mutant. The expression of hPC in *E. coli* is an alternative way to attempt to improve the expression of hPC, due to the absence of endogenous PC in *E. coli*. Although there is no guarantee that a recombinant gene product will accumulate in *E. coli* at high levels in a full-length and biologically active form, a considerable amount of effort has been directed at improving the expression in this system.

In Chapter 4, the vectors bearing mutant pET-hPC were generated and the initial expression of hPC as a thioredoxin fusion protein in the pET32a (+) system was carried out as follows. These constructs of mutant pET-hPC (pET-hPC MF) (Section 4.3.5) were transformed into *E. coli* BL21 (Section 2.11.6). The expression of these constructs in *E. coli* BL21 was performed (Section 3.2.11) and the optimisation of protein expression was investigated using different concentrations of IPTG at 0.1, 0.5 and 1 mM to induce for 3 hours at 37°C. The expression of protein was analysed by SDS-PAGE (Section 2.13.1).

As shown in Figure 6.3, the six mutants of hPC were expressed as a protein band around 116 kDa, as identified by the positive control, partially purified hPC. The hPC band was not seen in lane of pET/BL bearing the parent vector pET 32a (+) as a negative control. The level of expression of the six mutants was different at IPTG concentrations 0.5 and 1 mM (Figure 6.3b and c). The Coomassie stained gel of 0.1 mM of IPTG (Figure 6.3a) showed a lower level of hPC than those of IPTG at 0.5 and 1

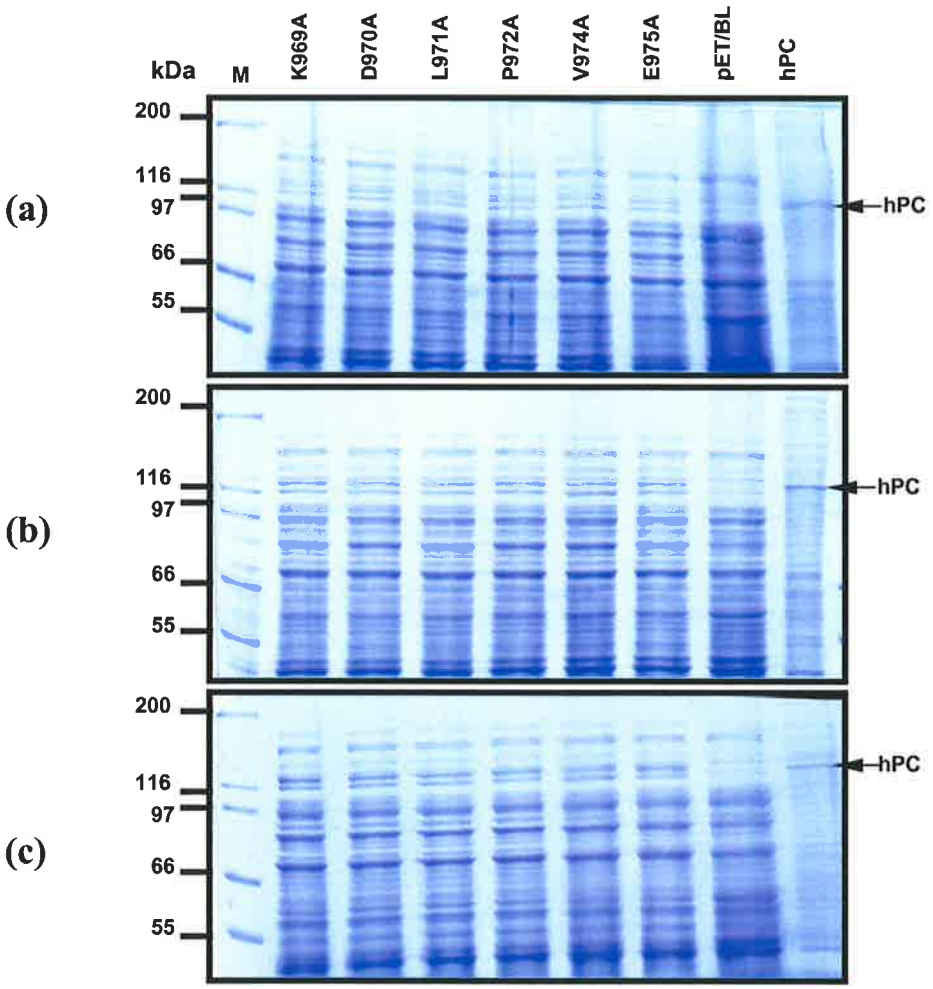

Figure 6.3 Expression of hPC mutants (mutant pET-hPC) in *E. coli* BL21. Six hPC mutants (mutant pET-hPC) were expressed in E. coli BL21 after induction with IPTG at various concentrations 0.1 (a), 0.5 (b) and 1 (c) mM. The cell lysates were prepared and analysed by SDS-PAGE. Partially purified hPC, expressed in 293T (around 116 kDa) was used as a positive control, a bacterial extract from a strain bearing the parent vector (pET/BL) as a negative control. M = Wide Range Protein Standard Marker (Mark12, Novex).

mM. Thus a concentration of IPTG of 1 mM was used to induce the expression of hPC in bacteria.

6.3.1.2 Expression of vector wt pET-hPC in BL21 and enzymatic activity of hPC

Ideally, the protein of interest will be produced in an active form and in sufficient amounts to allow its isolation. However, the protein may be made either in very small amounts or in an insoluble form, or both.

In Section 6.3.1.1, we have shown that the bacteria bearing mutant pET-hPC (pET-hPC MF) slightly expressed the hPC at 1 mM of IPTG induction (Figure 6.3). We do not know whether wt hPC expressed in *E. coli* is active or inactive. Thus, wild type hPC was expressed in *E. coli* and tested for the activity. To test this possibility, wt pET-hPC was constructed by digestion of mpBlue-hPC (Section 4.3.5) at the *Bam*HI and *Not*I sites, the full-length hPC was ligated into pET-32a (+) at the same sites. This construct was transformed (Section 2.11.6) and expressed in *E. coli* BL21 (Section 3.2.11). The protein expression was analysed by SDS-PAGE followed by Western blot. The activity of cell lysate was investigated using radiochemical assay (Section 6.2.4).

Figure 6.4 revealed the expression of wt hPC as thioredoxin fusion protein in *E. coli* BL21 and the enzymatic activity. The level of wt hPC at 1 mM of IPTG was not seen clearly on the Coomassie stained gel compared to the positive band of partially purified hPC (Figure 6.4a). The avidin blot showed the hPC band of partially purified hPC but only a faint band of wt hPC was seen on this blot (Figure 6.4b). The enzymatic activity of wt hPC was negligible compared to the positive control of 1 μg of hPC expressed in 293T in 50 μg of whole cell lysate (Figure 6.4c). This suggests that the expression of wt hPC in the whole cell lysate was too low to be detected by enzymatic activity or it is inactive.

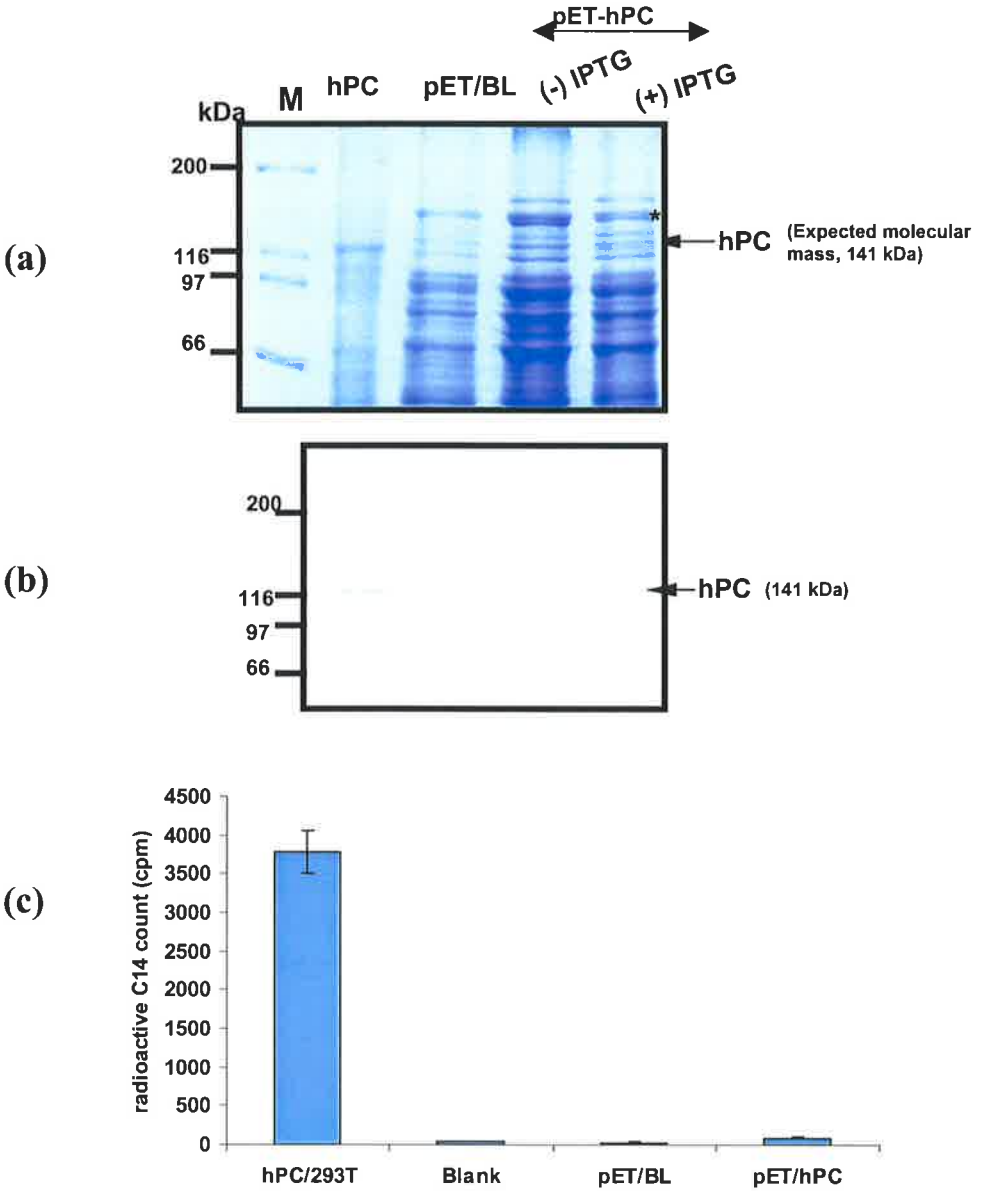

Figure 6.4 Expression of vector wt pET-hPC in BL21 and enzymatic activity of hPC. The vector wild type pET-hPC was constructed and transformed into *E. coli* BL21 (Section 6.3.1.2). After induction with 1 mM IPTG, cells were harvested and prepared for SDS-PAGE analysis and enzymatic activity. The expression of hPC was shown on Coomassie gel (a) and avidin blot (b). The enzymatic activity (Section 6.2.5) of expressed hPC in 50 µg of whole cell lysate was analysed using a radiochemical assay, and compared to 1 µg of hPC expressed in 293T (c). M = Wide Range Protein Standard Marker (Mark12, Novex).

Note. The prominent asterisked band, although apparently partially inducible by IPTG, is not hPC with thioredoxin fusion protein.

6.3.1.3 Effect of rare codon usage on high-level expression of heterologous protein in E. coli

The initial expression of wt hPC in *E. coli* BL21 revealed that the level of expression was very low (Figure 6.4) and that the activity of the enzyme is low. It is important to monitor translation errors in studies using overexpressed recombinant eukaryotic genes. "The misincorporation of amino acids can drastically affect protein function and lead to a discrepancy between apparent and actual specific activity" (Calderone *et al.*, 1996). If the sequence of the cloned gene contains codons used infrequently in *E. coli* (rare codons) this is usually not a rate-limiting problem, but if four or more happen to occur contiguously, they can reduce expression significantly (Robinson *et al.*, 1984). Differences in codon usage between prokaryotes and eukaryotes can have a significant impact on heterologous protein production. The arginine codons AGA and AGG are rarely found in *E. coli* genes, whereas they are common in *Saccharomyces cerevisiae* and higher eukaryotes. The presence of such codons in cloned genes affects protein accumulation levels, mRNA and plasmid stability, inhibits protein synthesis and cell growth (Zahn, 1996). These problems can usually be addressed by co-overexpressing the *argU, argW, ileX, glyT, leuW, proL* genes which encode tRNAs for the codons AGG, AGA, AUA, GGA, CUA and CCC. To address this approach, the wt pET-hPC was transformed into *E. coli* Rosetta (λDE3) pLysS/RARE (*argU, argW, ileX, glyT, leuW, proL*) [Novagen] and BL21 codon plus (λDE3) RIL (*argU, ileY, leuW*) [Stratagene]. The effect of temperature and concentration of IPTG on induction of expression of hPC was also investigated as described below.

6.3.1.3.1 Optimisation of temperature on growth of Rosetta (λDE3) pLysS/RARE and BL21 codon plus (λDE3) RIL

Proper protein folding is often favoured under low temperature cultivation conditions (Baneyx, 1999). Many proteins are more soluble at lower than at higher temperatures. *E. coli* can synthesize proteins at temperatures ranging from 10°C to 43°C (Ausubel *et al.*, 1998). Thus, the expression of wt pET-hPC in *E. coli* Rosetta (λDE3) pLysS/RARE (*argU*, *argW*, *ileX*, *glyT*, *leuW*, *proL*) [Novagen] and BL21 codon plus (λDE3) RIL (*argU*, *ileY*, *leuW*) [Stratagene] was investigated at different temperatures of incubation (25°C, 30°C and 37°C) with induction by 1 mM of IPTG for 3 hours (Figure 6.5a). The expression of protein was analysed by SDS-PAGE.

As shown in Figure 6.5a the expression of hPC from the Rosetta strain was not clearly seen at 25°C, 30°C or 37°C on a Coomassie stained gel. The level of the expressed hPC band around 141 kDa from BL21 codon plus (λDE3) RIL at 30°C was more clearly seen than that at 25°C and 37°C, compared to partially purified hPC (130 kDa) but the expression was still low. This indicates that the level of expressed hPC was slightly increased in bacteria BL21 codon plus (λDE3) RIL at 30°C.

6.3.1.3.2 Optimisation of concentration of IPTG for BL21 codon plus (λDE3) RIL

The expression of hPC from BL21 codon plus (λDE3) RIL bearing wt pET-hPC was best at 30°C with 1 mM IPTG induction for 3 hours (Figure 6.5a). To further improve the expression of hPC, different concentrations of IPTG to induce *E. coli* BL21 codon plus (λDE3) RIL were investigated as follows. The effect of concentrations of IPTG at 1 and 5 mM was demonstrated by induction of E. coli BL21 codon plus (λDE3) RIL (argU, ileY, leuW) [Stratagene] bearing wt pET-hPC at 30°C for 3, 4 hours and overnight. The expression of protein was analysed by SDS-PAGE. The levels of

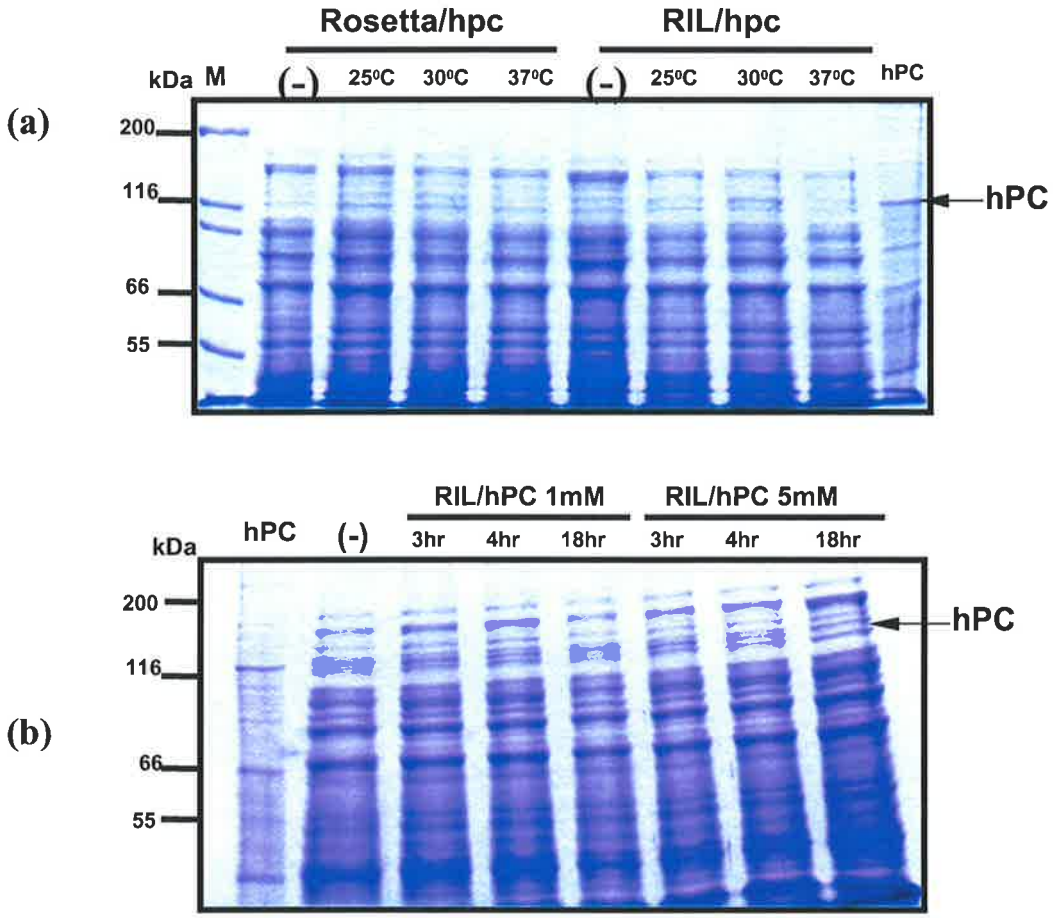

Figure 6.5 The effect of complementing for rare codons on hPC expression. The wild type hPC (wt pET-hPC) was expressed in bacteria containing tRNAs for rare codons (Rosetta and BL21 RIL strains). (a) Bacteria were grown at 25°C, 30°C and 37°C after induction with 1 mM IPTG for 3 hours. (b) The BL21 RIL bearing plasmid pET-hPC and rare codons was incubated at 30°C after induction with 1 and 5 mM IPTG. Then cells were harvested at various times, 3 hours, 4 hours and overnight. The cell lysates were analysed by SDS-PAGE. M = Wide Range Protein Standard Marker (Mark12, Novex). (-) indicates no induction with IPTG.

expression of hPC at 1 and 5 mM of IPTG after induction for 3 hours, 4 hours or overnight were not different and not clearly seen on the Coomassie stain gel (Figure 6.5b). The hPC was not significantly expressed from *E. coli* Rosetta (λDE3) pLysS/RARE (argU, argW, ileX, glyT, leuW, proL) and BL21 codon plus (λDE3) RIL (argU, ileY, leuW). Therefore, the enzymatic activity and avidin blot were not done for this expressed hPC due to very low levels of hPC. This suggests that either rare codons in the wild type gene are not the limiting factor for its expression in *E. coli* or that the synthetic hPC gene has some other feature (e.g. unfavourable mRNA secondary structure) that outweighs the optimisation of the hPC codon usage.

6.3.1.4 Effect of overexpression of folding modulators on the in vivo folding of heterologous protein in E. coli

The level of expression of hPC was not significantly improved by using bacteria expressing rare tRNAs (Figure 6.5). An alternative explanation for low expression may be that the protein folding is incorrect and may be affecting the expression level. Overproduction of heterologous proteins in the cytoplasm of *E. coli* is often accompanied by their misfolding and segregation into insoluble aggregates known as inclusion bodies. The recognition that *in vivo* protein folding is assisted by molecular chaperones, which promote the proper isomerisation and cellular targeting of other polypeptides by transiently interacting with folding intermediates, and by foldases which accelerate rate-limiting steps along the folding pathway, has provided powerful tools against the problem of inclusion body formation (Thomas *et al.*, 1997). The best characterised molecular chaperones in the cytoplasm of *E. coli* are the ATP-dependent DnaK-DnaJ-GrpE and GroEL-GroES system (Bukau & Horwich, 1998). DnaK binds to hydrophobic regions exposed to the solvent by nascent or stress-unfolded polypeptides, thereby preventing off-pathway reactions leading to aggregation. The GroEL and GroES are the prokaryotic homologues of eukaryotic Hsp60/Hsp10, which

harbor an ATPase domain and are thought to assist polypeptide folding by partially unfolding non-functional conformations that thus escape degradation, and can reinitiate the folding process (Feldman & Frydman, 2000). Increasing the pool of chaperones may therefore increase the fraction of protein that acquires a functional conformation.

6.3.1.4.1 Effect of GroEL-GroES (Hsp60) and DnaK-DnaJ-GrpE (Hsp70) system co-expressed in Rosetta (λDE3) pLysS/RARE and BL21 codon plus (λDE3) RIL

There is extensive evidence that co-overproduction of the DnaK-DnaJ or GroEL-GroES chaperones can greatly increase the soluble yields of aggregation-prone proteins. The plasmid pMON 15903 encoding cDNA of GroEL-GroES (Lee & Olins, 1992) and pMON 15904 encoding cDNA of DnaK-DnaJ-GrpE (Lee & Olins, 1992) compatible with plasmid pET-hPC were generated for this purpose. The expression of hPC was carried out using bacteria co-transformed with plasmids pET-hPC and pMON 15903. Rosetta (λDE3) pLysS/RARE and BL21 codon plus (λDE3) RIL strains were tested. To do this, transformation of *E. coli* Rosetta (λDE3) pLysS/RARE and BL21 codon plus (λDE3) RIL bearing plasmid pET-hPC (Section 6.3.1.2) were carried out as described (Section 2.11.6). The plasmid pMON 15903 was transformed into these competent cells yielding the expressed bacteria, Rosetta/hPC/GroEL-GroES and RIL/hPC/GroEL-GroES. The plasmid pMON 15903, containing the origin of replication pACYC together with compatible kanamycin-resistance was co-transformed and maintained in bacteria with plasmid pLysS/RARE containing the origin of replication pACYC, with compatible chloramphenicol-resistance. For the effect of DnaK-DnaJ-GrpE, plasmid pMON 15904 was transformed into *E. coli* BL21, yielding the bacteria BL21/dnaK. The plasmid pET-hPC was re-transformed into the competent BL21/dnaK cells resulting in *E. coli* BL21 containing plasmid pMON 15904 and pET-hPC (BL/hPC/dnaK). The cultivation temperatures for these bacteria

Rosetta/hPC/GroEL-GroES, RIL/hPC/GroEL-GroES and BL/hPC/dnaK were 30°C and 25°C with 1 mM IPTG for induction of protein. The expression of protein was analysed by SDS-PAGE.

As shown in Figure 6.6a and b, the level of expression of hPC from BL/hPC/dnaK, BL/hPC, RIL/hPC/GroEL and Rosetta/hPC/GroEL was extremely low on Coomassie stained gel at both 30°C and 25°C. The level of co-expression of hPC from both chaperones was as low as that of BL/hPC. This indicates that co-expression of hPC with molecular chaperones, GroEL-GroES and DnaK-DnaJ-GrpE in bacteria BL21, Rosetta and RIL was not suitable for the hPC expression.

6.3.1.4.2 Effect of DnaK-DnaJ-GrpE (Hsp70) co-expressed in AD494 (λDE3)

The co-expression of hPC from a plasmid containing pET-hPC and molecular chaperones (pMON 15903 and pMON 15904) did not improve the expression of hPC which is similar to complementing the effect of rare codons by use of *E. coli* Rosetta and RIL strains. The *trxB* mutant strain, AD494 (Novagen) has potential general utility for the production of properly folded, active proteins in the *E. coli* cytoplasm.

This was tested by co-expressing plasmids pMON 15904 (Hsp70) and pET-hPC in bacteria strain AD494 (Novagen) for the effect of molecular chaperone and *trxB* mutant *E. coli*. However, plasmid pMON 15903 (Hsp60) containing kanamycin-resistance gene cannot be transformed into AD494 strain containing kanamycin resistance gene. Also we cannot construct bacteria strain AD494 containing three plasmids of GroEL-GroES, DnaK-DnaJ-GrpE or tRNA rare codons. The bacteria AD494 bearing plasmid pMON15904 and pET-hPC was constructed by transformation of plasmid pMON15904 into competent cells of AD494 followed by transformation of plasmid pET-hPC into competent cell of AD494/dnaK. The expression of hPC was

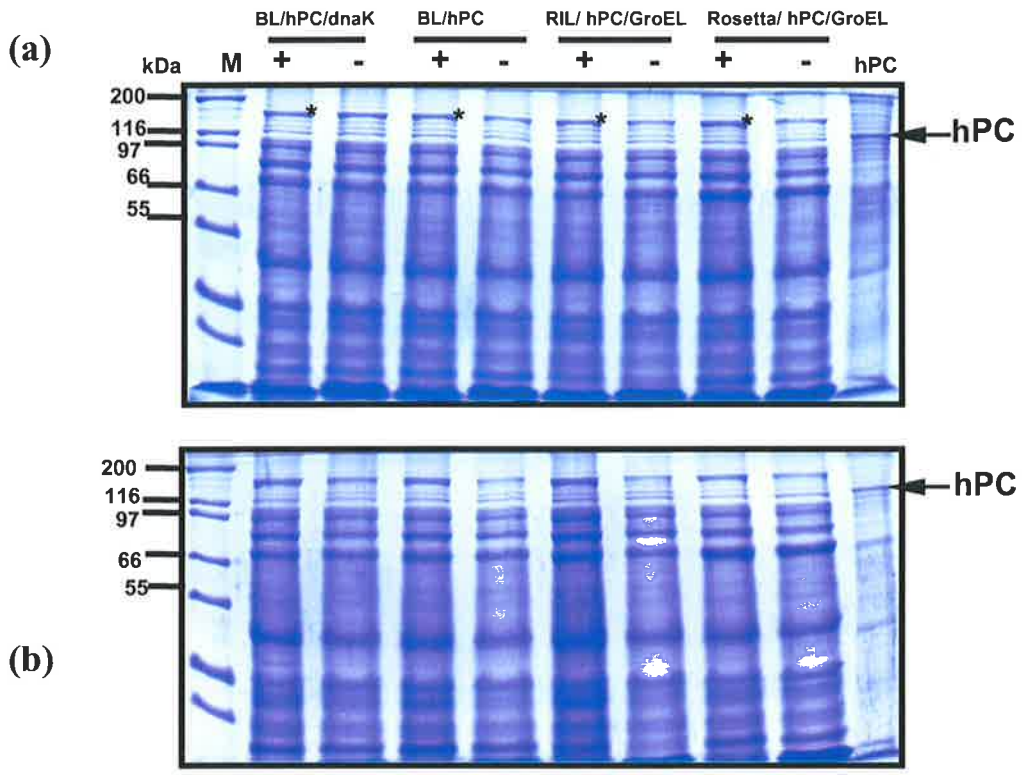

Figure 6.6 The effect of GroEL-GroES (Hsp60) and DnaK DnaJ-GrpE (Hsp70) system co-expressed in Rosetta (λDE3) pLysS/RARE and BL21 codon plus (λDE3) RIL. The plasmid wt pET hPC was co-expressed with chaperones, GroEL-GroES and DnaK-DnaJ GrpE in bacteria resulting in BL/hPC/dnaK, RIL/hPC/GroEL and Rosetta/hPC/GroEL. The hPC expression from three different bacteria was compared to *E. coli* BL21 containing plasmid pET-hPC (BL/hPC) and partially purified hPC. The bacteria was incubated at 30°C (a) or 25°C (b) after induction of 1 mM IPTG. The cell lysates were prepared for SDS PAGE analysis. M = Wide Range Protein Standard Marker (Mark12, Novex). (+) = after induction, (-) = before induction

Note. The prominent asterisked band, although apparently partially inducible by IPTG, is not hPC with thioredoxin fusion protein, as is evident in Figure 6.4b and also many other Westerns not presented here.

carried out in *E. coli* AD494/hPC and AD494/hPC/dnaK at 30°C with 1 mM of IPTG induction. The SDS-PAGE was analysed for the expression of hPC.

Figure 6.7 showed the level of expression of hPC from AD494 and AD494 bearing plasmid pMON 15904 encoding cDNA of DnaK-DnaJ was not seen any PC band (expected molecular mass, 141 kDa) as partially purified hPC (130 kDa). The expressed hPC was not significant enough to test on an avidin blot. This result indicates that the co-expression of pET-hPC and DnaK-DnaJ chaperones (plasmid pMON 15904) in AD494 strain was not achieved in this system.

6.3.2 Expression vector pQE-hPC

6.3.2.1 Optimisation of temperature and concentration of IPTG on growing K12 derived E. coli strain M15 and SG 13009

The expression of hPC with thioredoxin fusion protein in pET 32a (+) system using *E. coli* Rosetta (λDE3) pLysS/RARE, BL21 codon plus (λDE3) and AD494 were shown not to be successful. Even with the co-expression of GroEL-GroES and DnaK-DnaJ chaperones, the level of expression was hardly seen on the protein gel. An additional limitation of the T7 and other strong promoter systems is that the target protein is often unable to reach a native conformation and either partially or completely segregates within inclusion bodies. Although this problem was addressed by co-expressing folding modulators or through fusion protein technology, an alternative approach is to use pQE plasmid consisting the *E. coli* phage T5 promoter, two *lac* operator sequences and 6 His tag coding sequence.

The *E. coli* host cells in this system contain multiple copies of the plasmid pREP4, which carries the *lacI* gene encoding the *lac* repressor (K12 derived *E. coli* strains M15 [pREP4] and SG13009 [pREP4]). The multiple copies of pREP4 present in the host cells ensure high levels of *lac* repressor and tight regulation of protein expression. The expression from pQE vector is rapidly induced by the addition of

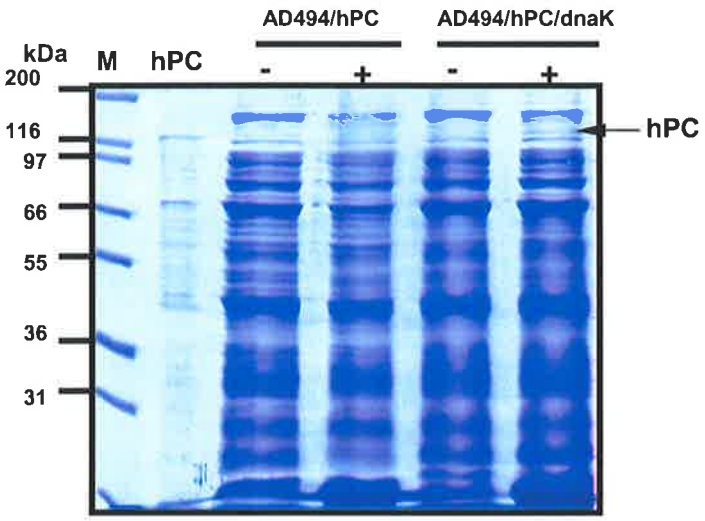

Figure 6.7 The effect of DnaK-DnaJ-GrpE (Hsp70) co-expressed in AD494 (λDE3). The bacteria AD494 containing plasmid wt pET-hPC and AD494 containing plasmid wt pET-hPC and DnaK-DnaJ-GrpE were induced for hPC expression. The bacteria were incubated at 30°C after induction of 1 mM IPTG. The cell lysates were prepared for SDS-PAGE analysis. M = Wide Range Protein Standard Marker (Mark12, Novex). (+) = after induction, (-) = before induction

IPTG, which inactivates the repressor and clears the promoter. The special double operator system in this system, in combination with the high levels of *lac* repressor provided by pREP4, permits some control over the level of expression.

Since the optimisation of the pET32a (+) system did not result in an elevated level of hPC synthesis, we were interested to see if changing the pET vector which expressed protein as thioredoxin fusion protein to pQE vector would improve expression. To do this, plasmid wt pQE-hPC encoding full-length hPC was constructed (Section 6.2.1) and transformed into K12 derived *E. coli* strains M15 and SG 13009. Maximum accumulation of soluble products is best achieved by testing expression in several strains and at several temperatures, and picking the combination that works best. Thus, the expression of hPC using pQE system was optimised as described below.

For the optimisation of expression of protein in *E. coli* M15 and SG13009 cell bearing pQE-hPC, bacteria were induced with different concentrations of IPTG, 2 and 5 mM at 30°C and 37°C for 3 hours. As the optimisation of IPTG to induce the expression of hPC in bacteria using pET system was 1 mM (Section 6.3.1.1), the concentrations of IPTG induced in this pQE system were 2 and 5 mM. The cell lysates were prepared (Section 3.2.11) and analysed by SDS-PAGE followed by Western blot probed with avidin alkaline phosphatase.

As shown in Figure 6.8a the level of expression of hPC (expected molecular mass, 130 kDa) was clearly seen on a Coomassie stained gel for both bacteria M15 and SG13009 incubated at 30°C and slightly seen on that incubated at 37°C. The concentrations of 2 and 5 mM IPTG to induce hPC gave similar expression. A similar result was seen on an avidin blot (Figure 6.8b). This suggests that hPC was expressed from bacteria M15 and SG13009 bearing plasmid pQE-hPC which was incubated at 30°C and induced with 2 mM IPTG.

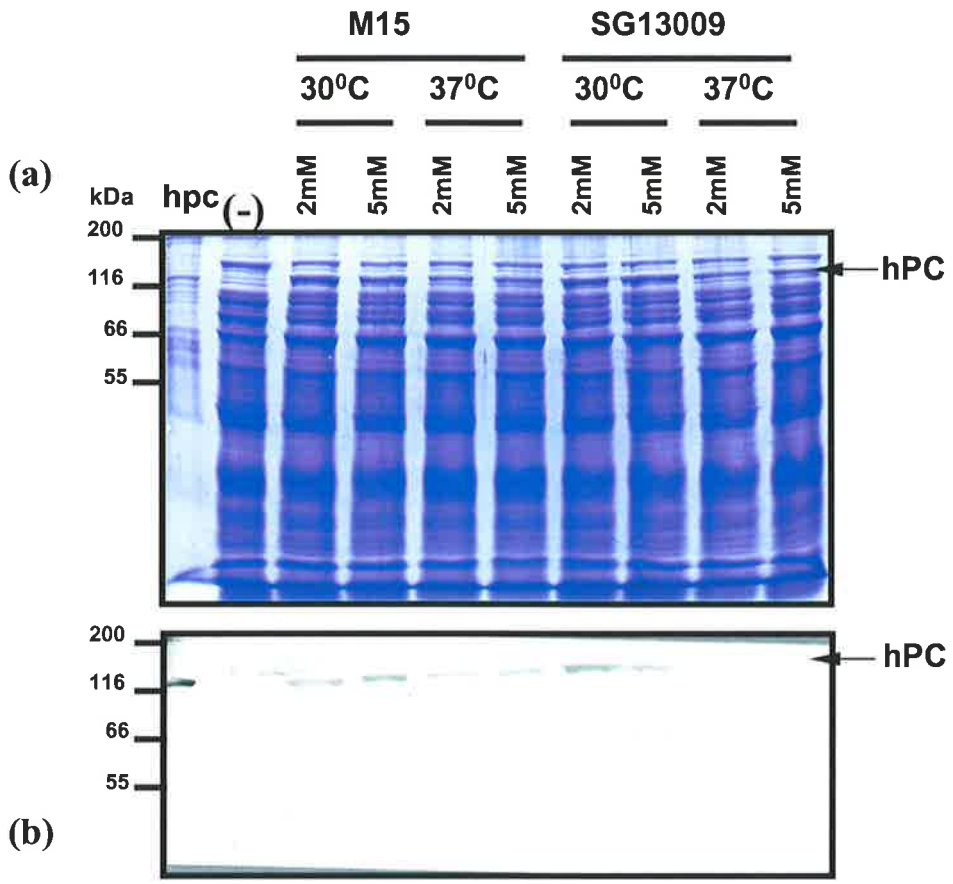

Figure 6.8 The expression of hPC (wt pQE-hPC) in *E. coli* M15 and SG13009 cell. The bacteria M15 and SG13009 bearing plasmid pQE-hPC (Section 6.2.1) were incubated at different concentrations of IPTG, 2 or 5 mM for induction at 30°C and 37°C for 3 hours . The cell lysates were prepared for SDS-PAGE analysis. The expression of hPC is shown on Coomassie gel (a) and avidin blot (b).

To test the effect of temperature of incubation on expression of hPC, bacteria M15 and SG13009 bearing plasmid pQE-hPC were incubated at 4°C, 25°C, 30°C and 37°C with 2 mM of IPTG. The cultures were induced with 2 mM IPTG at 25°C, 30°C and 37°C for 3 hours except the culture at 4°C which was induced overnight. The cell lysates were prepared (Section 3.2.11) and analysed for SDS-PAGE followed by Western blot probed with avidin alkaline phosphatase. The hPC expression was clearly seen on Coomassie stained gel at 4°C, 25°C and 30°C but not 37°C (Figure 6.9a). A similar result was seen on an avidin blot (Figure 6.9b). The presence of expressed hPC at lower molecular weight than 116 kDa as shown on the avidin blot, indicates that degradation of hPC during expression might be contributing to the problem of inactive enzyme or misfolding. Nevertheless, these data show that bacteria M15 and SG13009 bearing plasmid pQE-hPC expressed hPC at significant levels at 30°C following the induction with 2 mM IPTG for 3 hours.

6.3.2.2 Enzymatic assay of hPC from bacteria M15 and SG13009 bearing pQE-hPC

To test the activity of hPC expressed by bacteria M15 and SG13009 bearing plasmid pQE-hPC incubated at 25°C and 30°C, cell lysates were prepared and analysed using the radiochemical assay (Section 6.2.4). The specific activities of hPC from both bacteria M15 and SG13009 incubated at 25°C and 30°C were negligible compared to the cell lysate of hPC expressed in 293T as a positive control (Figure 6.9c).

6.3.2.3 Optimisation of temperature on growing M15 pLysS/Rare codon and SG13009 pLysS/Rare codon

It was clearly demonstrated that hPC was expressed from bacteria M15 and SG13009 bearing plasmid pQE-hPC at 30°C with the induction of 2 mM IPTG for 3 hours. However, this hPC was inactive. Inactive hPC expressed in *E. coli* system using pQE vector might result from poor mRNA translation fidelity due to the effect of rare

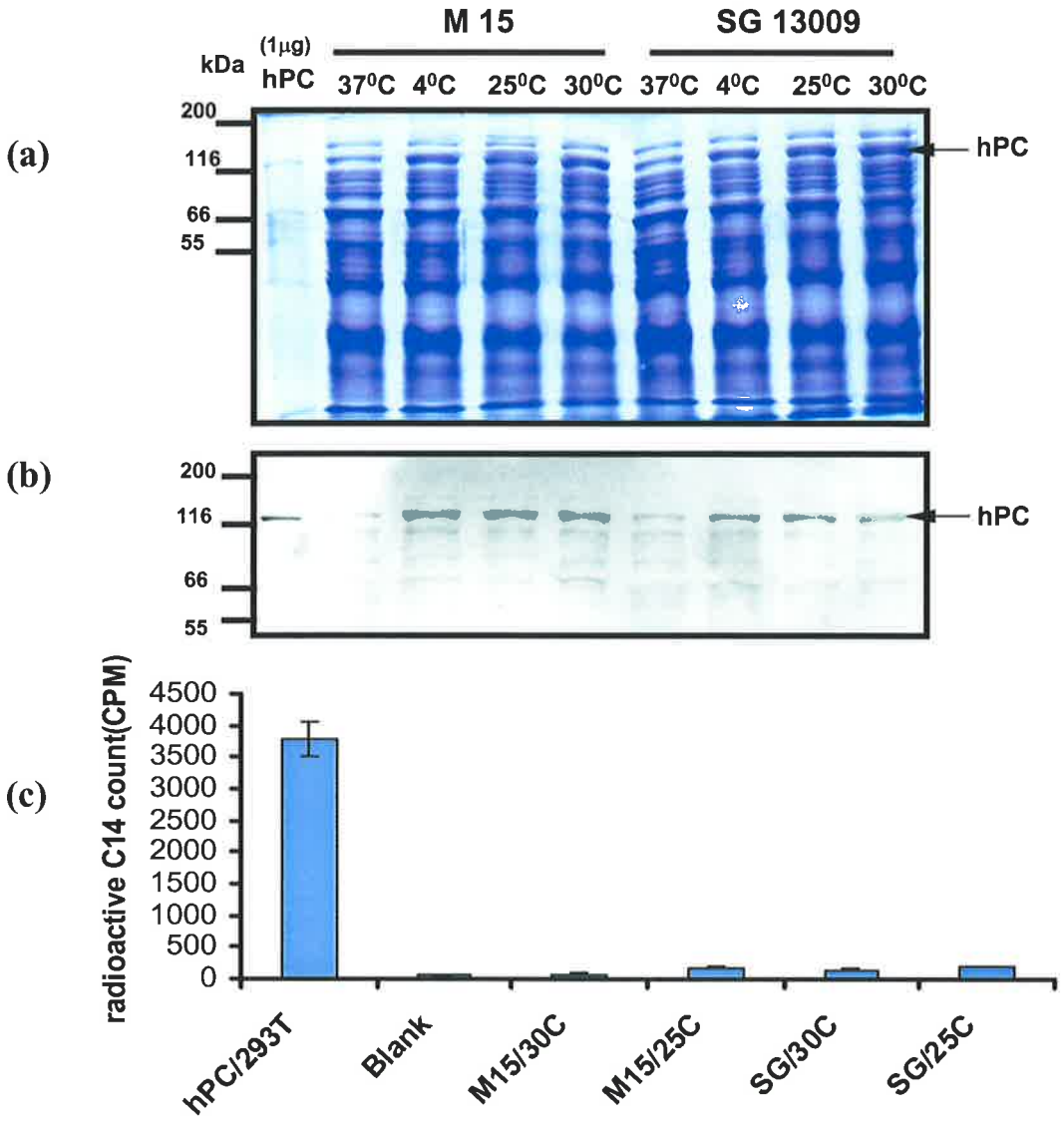

Figure 6.9 The effect of temperature on expression of hPC (wild type pQE-hPC) in *E. coli* M15 and SG13009. The bacteria M15 and SG13009 bearing plasmid pQE-hPC (Section 6.2.1) were incubated at various temperatures, 4°C, 25°C, 30°C and 37°C with 2 mM of IPTG for induction for 3 hours. The cell lysates were prepared for SDS-PAGE analysis. The expression of hPC was shown on Coomassie gel (a) and avidin blot (b). The enzymatic activity (Section 6.2.5) of expressed hPC in 50 µg of whole cell lysate was analysed using a radiochemical assay, compared to 1 µg of hPC expressed in 293T (c).

codons. To test this possibility, the bacteria M15 and SG13009 containing pLysS/Rare codon were constructed (Section 6.2.2) and plasmid pQE-hPC was transformed into these competent cells. All three plasmids are compatible and stable in the host cell with three different antibiotic resistance genes. The M15/pLysS/Rare codon and SG13009/pLysS/Rare codon cells bearing plasmid pQE-hPC were incubated at 30°C with induction by 2 mM IPTG for 3 hours and overnight. The expression of hPC was analysed by SDS-PAGE and the lysates were prepared for the analysis of enzymatic activity using radiochemical assay (Section 6.2.2).

As shown in Figure 6.10a, hPC expression in M15/ pLysS/Rare codon was not present without IPTG, but it was expressed following induction with 2 mM IPTG for 3 hours and slightly increased by induction overnight. A similar result was seen in SG13009/pLysS/Rare codon. The level of hPC expression from M15/ pLysS/Rare codon was slightly better than from M15 (Figure 6.9a) at different incubation temperatures (4°C, 25°C, 30°C and 37°C). However, the specific activity of hPC from M15/pLysS/Rare codon and SG13009/pLysS/Rare codon incubated at 30°C following induction with IPTG for 3hours or overnight was negligible compared to the cell lysate of hPC expressed in 293T as a positive control (Figure 6.10b). This result shows that the hPC was expressed significantly in *E. coli* M15 and SG13009 using plasmid pQE-hPC but was not functional.

6.3.3 Expression of vector pVT-hPC in yeast Saccharomyces cerevisiae

The expression from the pET system was very low compared to the expression of hPC in M15/pLysS/Rare codon and SG13009/pLysS/Rare codon bearing the plasmid pQE-hPC. Although, an increased level of hPC expression was achieved by using the pQE system, the enzymatic activity of hPC was still negligible. Unfortunately, the failure of hPC to form its correct tertiary structure may preclude the use of bacterial expression to detect even the most rudimentary level of activity. hPC expression in

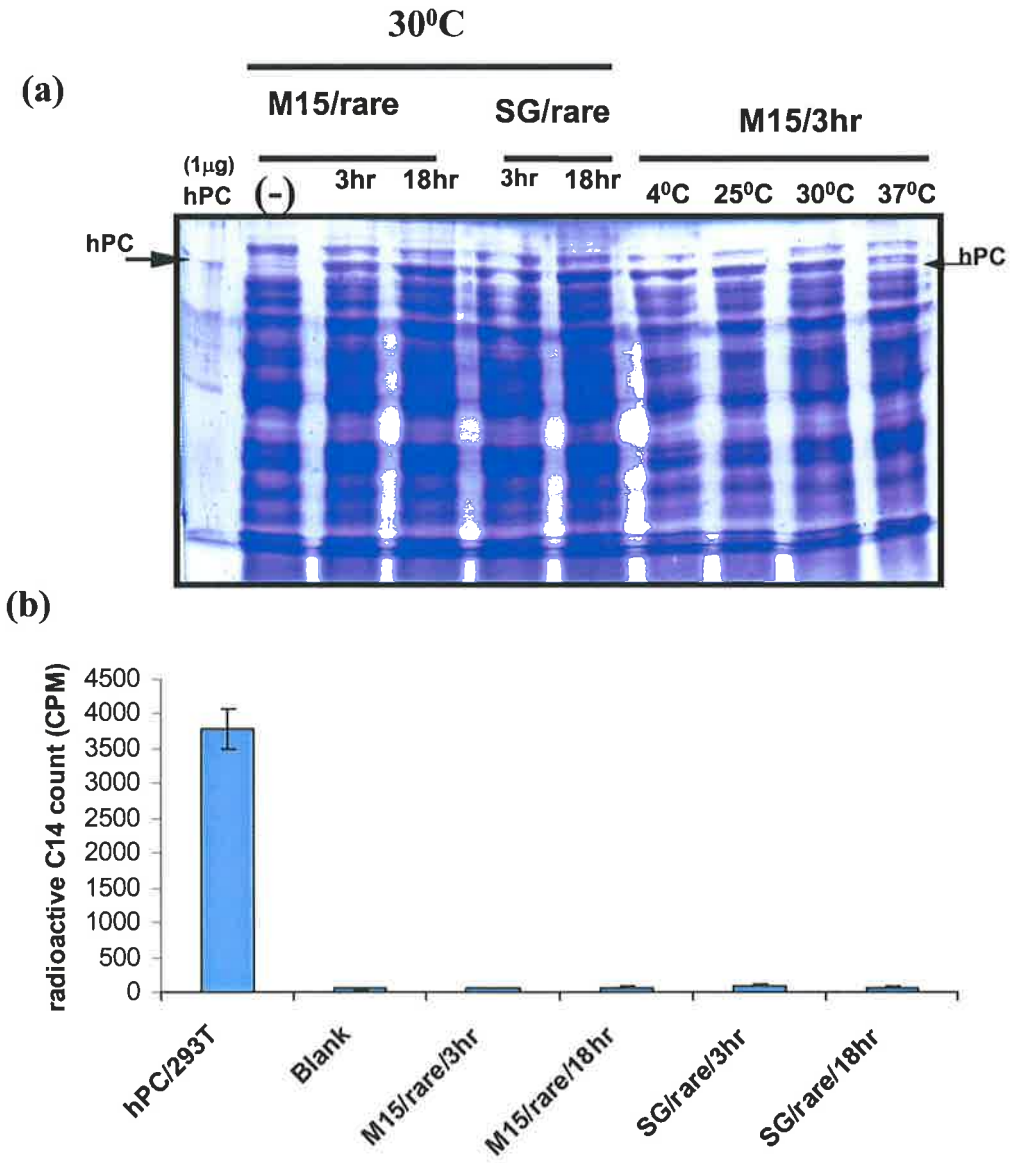

Figure 6.10 The effect of compensating for rare codons on expression of hPC (wild type pQE-hPC) in *E. coli* M15 and SG13009 cell. The bacteria M15 and SG13009 were co-transformed with plasmid pQE-hPC and pLysS/Rare codon (Section 6.3.2). The bacteria were incubated at 30°C with the induction of 2 mM IPTG for 3 hours and overnight. The cell lysates were prepared for SDS-PAGE analysis. (a) The level of expression of hPC was compared to bacteria M15 bearing only plasmid pQE-hPC on Coomassie gel. (b) The enzymatic activity (Section 6.2.5) of expressed hPC in 50 μg of whole cell lysate was analysed using a radiochemical assay, compared to 1 μg of hPC expressed in 293T.

yeast *Saccharomyces cerevisiae* is another possibility, since yeast genes are structurally and functionally related to genes in higher eukaryotes. Furthermore, yeasts are not only safe, easy to manipulate, but their cultivation is both inexpensive and can be easily be scaled up. Therefore, the expression of hPC in yeast was investigated by using the pVT100-U vector controlled by a constitutive alcohol dehydrogenase promoter to drive transcription (Vernet *et al.*, 1987). The vector pVT-hPC was constructed by Dr. S. Jitrapakdee and transformed into yeast strain W303 (Section 2.11.9). The whole cell lysate was prepared (Section 2.11.10) and analysed by SDS-PAGE followed by Western blot.

The expression of hPC in yeast *Saccharomyces cerevisiae* was achieved as shown in Figure 6.11a in six different clones of yeast containing plasmid pVT-hPC. The hPC band (expected molecular mass, 130 kDa) was hard to see because of the endogenous PC expressed in yeast. In addition, another protein also was expressed at the same size as hPC. However, the avidin blot showed the slightly increased expression levels of hPC from six different clones, compared to the background PC from yeast bearing just the parental vector (Figure 6.11b). This indicates that the level of expressed hPC in yeast was not sufficient to analyse the activity of hPC, due to the endogenous level of PC in yeast strain W303.

6.3.4 Expression from vector pVT-hPC without a mitochondrial targeting sequence (pVT-hPC-21) in yeast

It was shown that hPC was expressed at slightly elevated levels in yeast (Figure 6.11). In a study on the intracellular localisation of PC using an immunoelectron microscopy approach, rat PC was found to be located exclusively in the mitochondrial matrix and close to the inner mitochondrial membrane (Rohde *et al.*, 1991). Conversely, PC in *S. cerevisiae* was shown to be exclusively cytoplasmic (Rohde *et al.*, 1991). As yeast grown on glucose based media may have relatively few mitochondria

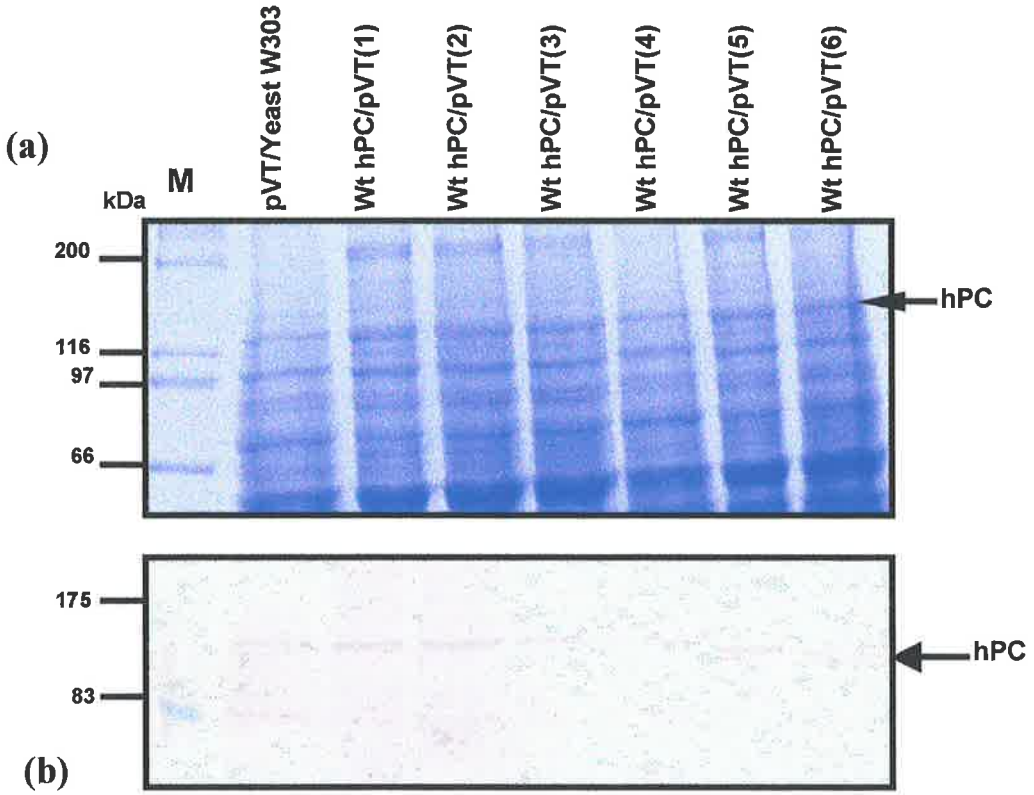

Figure 6.11 **The expression of hPC (pVT-hPC) in yeast *Saccharomyces cerevisiae.*** The plasmid pVT-hPC was constructed and transformed into yeast that were cultured at 30°C overnight (Section 2.11.9). Cell lysates were prepared (Section 2.11.10) for SDS-PAGE analysis. (a) The hPC expression from six different clones of yeast bearing plasmid pVT-hPC are shown on Coomassie gel. (b) The hPC was expressed at different levels compared to endogenous PC from the yeast strain W303 bearing the parent vector pVT100-U, shown by an avidin blot. M = Wide Range Protein Standard Marker (Mark12, Novex) for Coomassie stained gel and Prestained Protein Marker (New England Biolab) for the blots.

(Wallace *et al.*, 1968) this may lead to a problem in overexpressing a heterologous protein there. Therefore, the mitochondrial targeting sequence of hPC might not be advantageous for expression of hPC in yeast. To test this proposal, the vector pVT-hPC encoding cDNA of full-length hPC without the first 21 N-terminal residues of hPC (containing the mitochondrial targeting sequence) [pVT-hPC-21] was constructed (Section 6.2.3) and transformed into yeast (Section 2.11.9). The lysate was prepared (Section 2.11.10) and analysed by SDS-PAGE followed by Western blot.

As shown in Figure 6.12a the expression of hPC on Coomassie stained gel was not clearly seen in any of six different clones of yeast (wt hPC/pVT 3/1, 3/2, 3/3, 2/1, 2/2 and 2/3). However, expression of hPC in yeast was clearly seen on the avidin blot, but only the expression level from yeast clone wt hPC/pVT 2/1 was higher than other clones (Figure 6.12b). This result suggests that full-length hPC without mitochondrial targeting sequence was significantly expressed in *S. cerevisiae* but the amount of protein was still not enough for physical studies.

6.3.5 Expression of vector myc-tagged pVT-hPC without mitochondrial targeting sequence (myc pVT-hPC-21) in yeast

The hPC was expressed to some extent in yeast bearing vector pVT-hPC without mitochondrial targeting sequence, pVT-hPC-21 (Figure 6.12). Since the level of expression was not good compared to the level of endogenous PC in yeast, the addition of a myc tag to hPC might be useful for the purification of hPC. This would allow removal of endogenous PC during purification. To do this, the vector myc tagged pVT-hPC without mitochondrial targeting sequence (myc pVT-hPC-21) was constructed (Section 6.2.4) and transformed into yeast (Section 2.11.9). The lysate was prepared (Section 2.11.10) and analysed by SDS-PAGE followed by Western blot. The immunoblot was probed with monoclonal anti myc (dilution 1:1000) and goat anti mouse conjugated to horseradish peroxidase (dilution 1:4000).

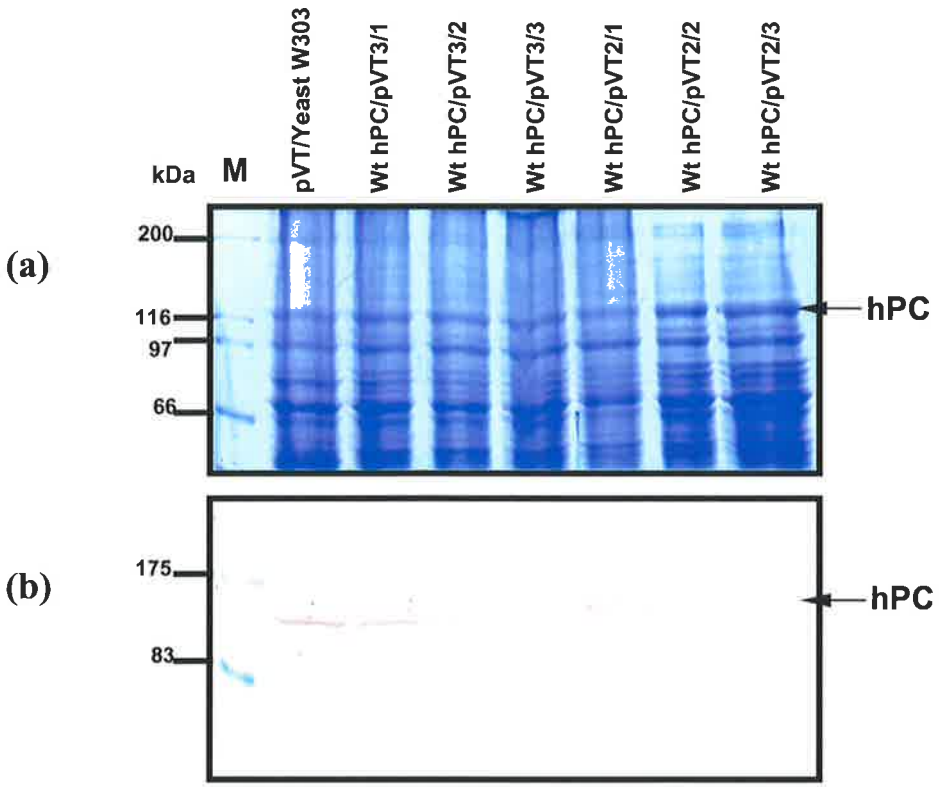

Figure 6.12 The expression from vector pVT-hPC without mitochondrial targeting sequence of hPC (pVT-hPC-21) in yeast *Saccharomyces cerevisiae.* The vector pVT-hPC-21 encoding cDNA of full-length hPC without the first 21 N-terminal residues of hPC (mitochondrial targeting sequence) was constructed (Section 6.2.3) and transformed into yeast (Section 2.11.9). The lysates were prepared (Section 2.11.10) and analysed by SDS-PAGE followed by Western blot. (a) The expression of hPC was hardly seen on Coomassie gel. (b) All six different clones of yeast bearing plasmid pVT-hPC without mitochondrial targeting sequence are shown to express hPC at different levels compared to the parent vector in yeast W303 on avidin blot. M = Wide Range Protein Standard Marker (Mark12, Novex) for Coomassie stained gel and Prestained Protein Marker (New England Biolab) for the blots.

As shown in Figure 6.13, three different clones of yeast W303 bearing vector myc pVT-hPC-21 generally produced insufficient hPC to detect on a Coomassie stained gel (Figure 6.13a). The avidin blot did not clearly show any improvement in the amount of expressed myc tag hPC compared to endogenous PC in parent yeast strain W303 bearing vector pVT100-U (Figure 6.13b). However, the anti myc blot analysis clearly showed that hPC in pVT100-U vector from three different clones were expressed in *S. cerevisiae* compared to the host strain yeastW303 (Figure 6.13c). This indicates that the level of expression of myc-tagged hPC was not sufficient for further steps of purification and enzymatic activity assay.

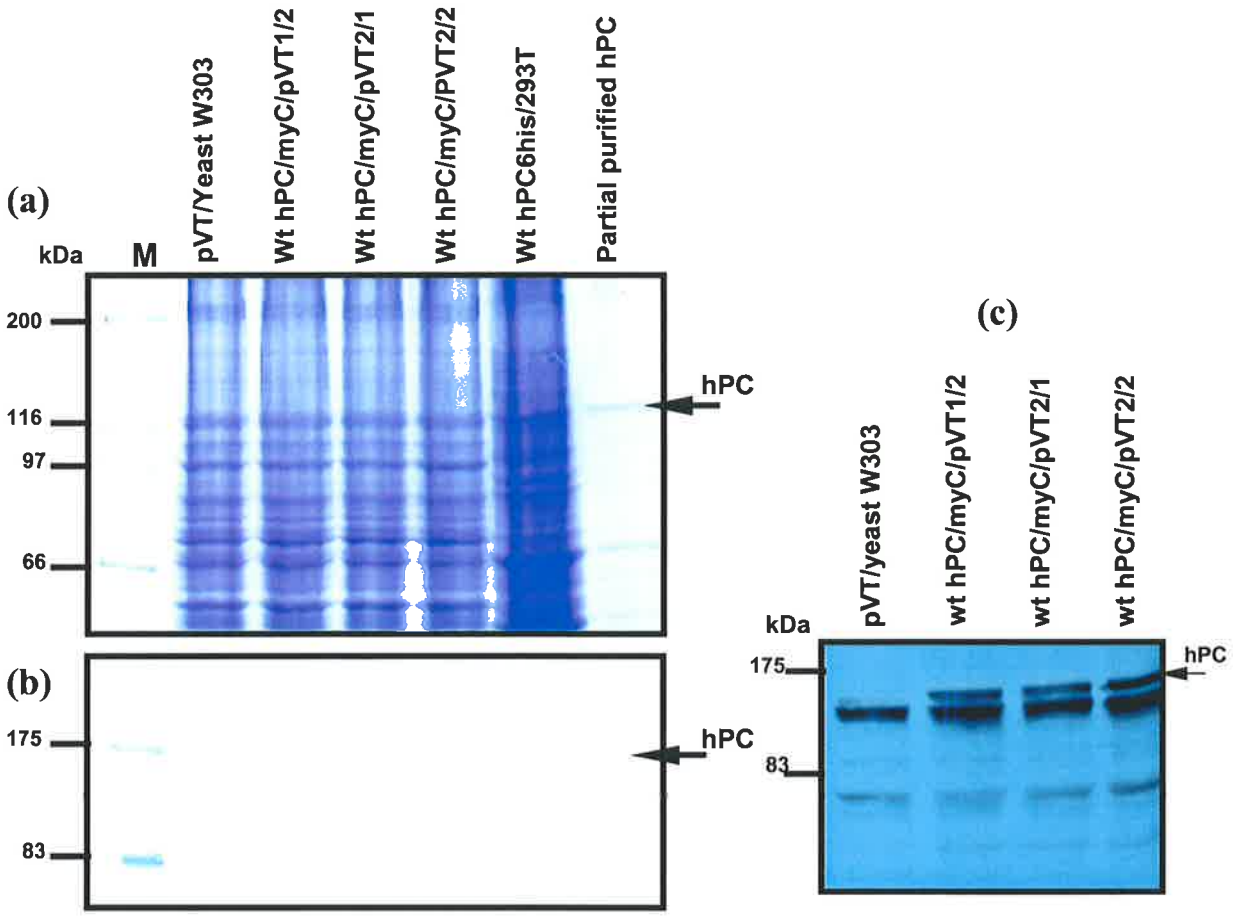

Figure 6.13 **The expression from vector myc tagged pVT-hPC without mitochondrial targeting sequence of hPC (myc pVT-hPC-21) in yeast *Saccharomyces cerevisiae.*** The vector myc tag pVT-hPC encoding cDNA of full-length hPC without the first 21 N-terminal residues of hPC as a mitochondrial targeting sequence was constructed (Section 6.2.4) and transformed into yeast (Section 2.11.9). The lysates were prepared (Section 2.11.10) and analysed by SDS-PAGE followed by Western blot. (a) The expression of hPC was not obvious on Coomassie gel. (b) Three different clones of yeast bearing plasmid myc pVT-hPC-21 were tested for PC expression and compared to the parent vector in yeast W303 (negative) and partially purified hPC (positive) on avidin blot. (c) The anti-myc blot showed the myc tag hPC expressed in three clones of yeast compared to yeast bearing parental vector, pVT100-U. M = Wide Range Protein Standard Marker (Mark12, Novex) for Coomassie stained gel and Prestained Protein Marker (New England Biolab) for the blots.

6.4 DISCUSSION

Until now, hPC has been successfully expressed in a mammalian cell line, 293T and active hPC purified from a mitochondrial extract (Jitrapakdee *et al.*, 1999). This procedure is well established but with only limited amounts of cultured cells available it leads normally to low production yields as a result of losses from the various purification steps. Such a procedure is expensive and time consuming.

In this study, we revealed that it is possible to obtain some hPC from *E. coli* by expressing hPC in the BL21 strain bearing plasmid pET-hPC (Figure 6.3). A study of *E. coli* codon usage analysis 2.0 by Morris Maduro (http://128.111.208.226/codonUsage/usage2.0c.html) revealed that 15% of codon usages in the hPC sequence are below the threshold 10% of *E. coli* for same amino acid (Appendix II).

A preferred codon is thought to optimise translation, and highly expressed genes usually have extreme codon bias (Ikemura, 1985; Sharp *et al.*, 1986). It has been shown that minor codons such as AGA, AGG, CUA, UCA, AGU, ACA, GGA, CCC and AUA are used preferentially within the first 25 codons in *E. coli* genes, termed as the minor codon modulator hypothesis (Chen & Inouye, 1990). When the cell growth reaches the stationary phase, the concentration of tRNA molecules for minor codons becomes extremely limited. This causes ribosome stalling at minor codon sites, inhibiting the effective entry of a ribosome at the initiation site, thereby resulting in a decrease in the rate of translation. The minor codons within this critical limit from the initiation codon are thought to play an important role in regulating gene expression (Chen & Inoue, 1994). In *E. coli* it has been shown that the codon usage bias is weaker and the synonymous substitution rate is lower in the initiation site than in the rest of the gene (Ohno *et al.*, 2001). Since even a single minor codon in the initiation site can reduce gene expression as a result of limited availability of tRNAs depending on the growth

phase (Chen & Inouye, 1990; Chen & Inoue, 1994) minor codons probably also have a negative effect on gene expression. However, the expression of hPC in T7 driven Rosetta (Novagen) and BL21 RIL (Stratagene) did not improve the level of expression. This indicates that the level of hPC expression is not greatly affected by codon preferences and may be affected by the coding sequence in other ways that are not yet well understood. It has been reported that not only the number of rare codons, but also their context and distribution within a given gene appear to influence expression levels (Kurland & Gallant, 1996).

In recent years, protein folding and assembly in living cells have been shown to be facilitated by molecular chaperones and catalysts of protein folding (Gething & Sambrook, 1992). Chaperones, with broad specificity capable of assisting the folding of a range of different proteins, have been identified in various cellular compartments, such as the cytoplasm, endoplasmic reticulum and in mitochondria and chloroplasts (Gething & Sambrook, 1992). I have attempted to determine whether the expression of hPC could require molecular chaperones to facilitate either subunit folding or assembly. The GroEL-GroES and DnaK-DnaJ were co-expressed in the Rosetta, BL21RIL, BL21 (DE3) and AD494 strains. Only BL21 RIL cells bearing the GroEL-GroES system expressed hPC in whole cell lysate and then only slightly, indicating that the GroEL-GroES and DnaK-DnaJ system also did not seem to play a major role in improving the *in vivo* folding or assembly of hPC in Rosetta, BL21RIL, BL21 (DE3) and AD494.

There is extensive evidence that co-overproduction of the GroEL-GroES and DnaK-DnaJ chaperones can greatly increase the soluble yields of aggregation–prone proteins (De Bernardez Clark *et al.*, 1999; Lilie *et al.*, 1998). The process does not involve dissolution of preformed recombinant inclusion bodies but is related to improving folding of newly synthesized protein chains (Thomas & Baneyx, 1996).

These authors also point out that "it is important, however, that the beneficial effect associated with an increase in the intracellular concentration of DnaK-DnaJ and GroEL-GroES is highly dependent on the nature of the overproduced protein, and that success is by no means guaranteed".

For this study, an alternative way to attempt the hPC expression in *E. coli* is to change the vector system using the pQE expression vector containing a 6 His affinity tag, which can be repressed by the presence of high levels of *lac* repressor. The thioredoxin fusion protein in the pET system did not improve the expression of hPC. Thus, pQE system with no fusion protein is another vector with which to attempt improving hPC expression. The hPC with its N-terminal 6-His tag expressed in 293T was found to be active (Chapter 4) thereby indicating that histidine would be unlikely to affect the activity of hPC expressed in bacteria. As shown in Figure 6.8, the K12 derived *E. coli* M15 and SG13009 bearing the plasmid pQE-hPC exhibited some increase in the hPC band around 116 kDa on SDS-PAGE analysis. The level of hPC expression with the T5 *lac*-driven expression (pQE system) was higher than using the T7-driven expression (pET system).

Initiation of translation of *E. coli* mRNAs requires a Shine Dalgarno (SD) sequence complementary to the 3' end of the 16s rRNA and of consensus 5'-UAAGGAGG-3', followed by an initiation codon, which is most commonly AUG. Because of the close coupling between transcription and translation in prokaryotes, engineering of the translation initiation region is a powerful tool for modulating gene expression in a promoter-independent fasion (Ringquist *et al.*, 1992). This also means that stable mRNA secondary structures encompassing the SD sequence and/or the initiation codon can dramatically reduce gene expression by interfering with ribosome binding. The pET and pQE vectors are commercial products which are both expected to

be good for SD sequence and initiation codon. Thus, the SD sequence is unlikely to cause the reduction of hPC expression.

In an attempt to explain my result with both expression systems, we propose that the sequences from the ribosome binding site (SD sequence) and the following 30-40 codons of the hPC gene might prevent mRNA from forming the correct secondary structure or stem-loops resulting in reduction of translation efficiency. This hypothesis assumes that the ribosomes are blocked by a number of stem-loops occurring with high free energy. This result (Figure 6.14) is based on the predicted mRNA structure by www.genebee.msu.su/cgi-bin/nph-rna2.pl. The results show that the numbers of stem-loops in sequences of pET/hPC (17 stems) with free energy of structure –105.5 kcal/mol were higher than in pQE/hPC (13 stems, -67 kcal/mol). It is likely that the protein expression in the pET system was less efficient because of the problem of secondary mRNA structure, resulting in reduced mRNA levels. Subsequent protein expression may be first reduced by the overall decrease in mRNA levels and secondly by the reduced efficiency of mRNA translation due to the mRNA secondary structure blocking ribosome binding. The expression of several genes in *E. coli* appeared inversely related to the stability of the secondary structure of their ribosome binding sites (de Smit & van Duin, 1990).

During the early days of recombinant DNA technology, it was thought that a strong promoter and a start codon at the beginning of the gene would be sufficient for good expression in *E. coli*. Since then it has been learned that the requirements for efficient translation are a good deal more complicated. In addition to a promoter and a start codon, good expression requires that the mRNA encoding the protein to be expressed contains a ribosome-binding site that is not blocked by mRNA secondary structure (de Smit & van Duin, 1990). These secondary structures can possibly be disrupted by RNA helicases such as the DEAD protein of *E. coli*. It was shown that

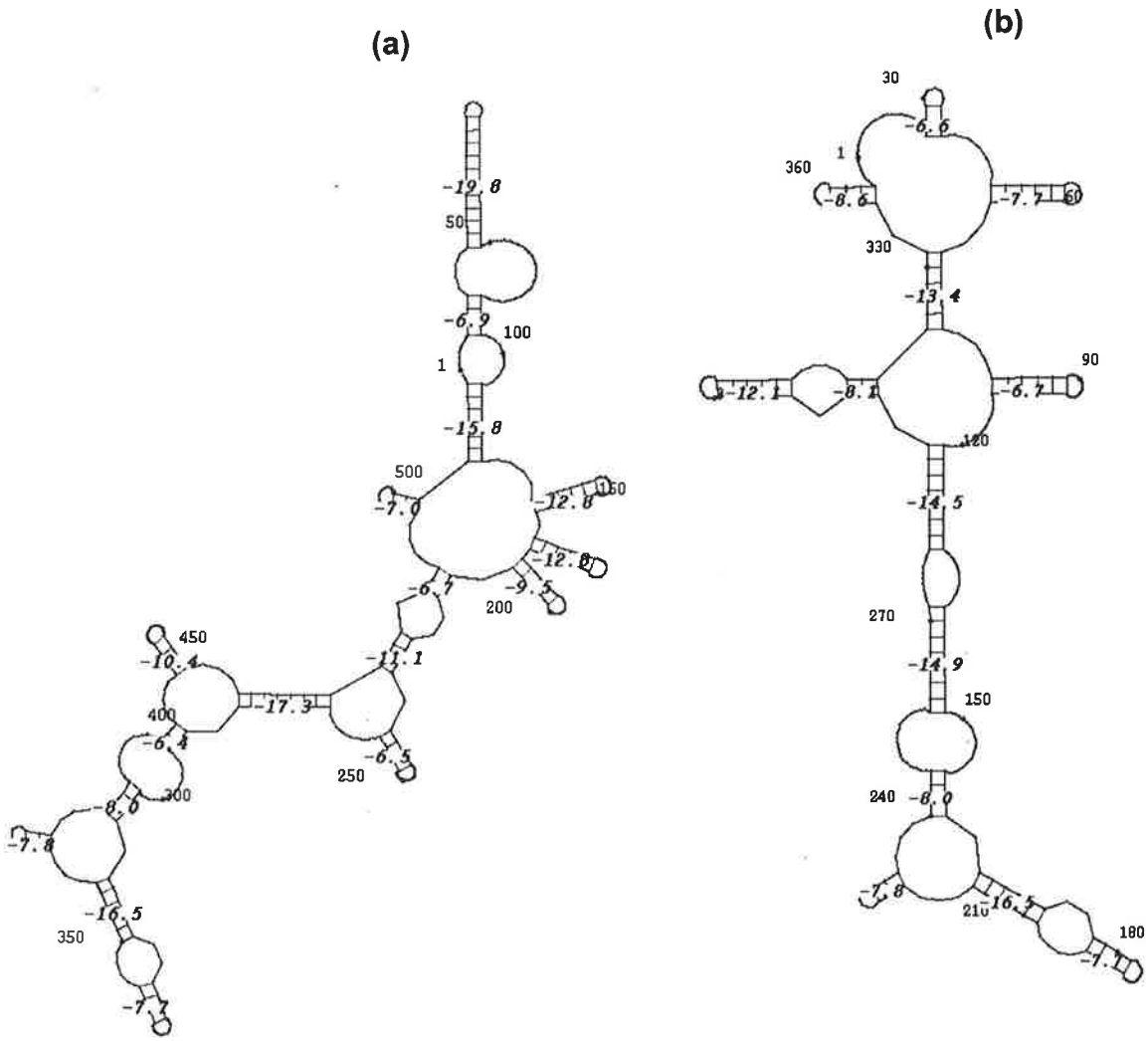

Figure 6.14 The predicted mRNA structure of human PC sequence expressed in pET and pQE vectors. The predicted secondary structure of first 75 amino acids from full-length hPC expressed in pET 32 a (+) vector, (pET-hPC) [a] was compared to that of pQE-hPC (b) using www.genebee.msu.su/cgi-bin/npb-rna2.pl. The free energy of structure of first 75 amino acids of hPC of pET-hPC (17 stems) and pQE-hPC (13 stems) were –105.5 and –67 kcal/mol respectively.

overexpression of the DEAD protein stimulated β-galactosidase expression 30 fold from the T7 promoter, but not from the *lac* promoter (Iost & Dreyfus, 1994).

Protein expression at reduced growth temperatures has been widely used to improve the folding of recombinant proteins (Baneyx, 1999). Because non-native polypeptides are a preferred substrate for cellular proteases, growth experiments were performed at different temperatures (4°C, 25°C, 30°C and 37°C). As expected, the level of hPC expression in pQE system was quite similar at the lower temperatures, but not at a higher temperature (37°C) [Figure 6.9]. Accumulation of intact hPC was favoured when T5 *lac*-driven expression was carried out at 4°C, 25°C or 30°C (Figure 6.9). The simplest explanation for this result is that protease cleavage sites become shielded owing to more efficient folding of the protein in the cytoplasm at low temperatures (Mujacic *et al.*, 1999).

The level of hPC expression in *E. coli* M15 and SG13009 bearing the plasmid encoding rare codons was similar to that in M15 (Figure 6.10). Moreover, there was no difference in the expression level of hPC when growth following the induction with IPTG was longer. The activity of hPC was negative for all expressed hPCs from both M15 and SG13009 (Figure 6.9c) including when there was co-expression of rare codons tRNAs (Figure 6.10b). These results suggest that the pQE system improved the level of hPC expression and also that the expressed hPC is biotinylated as shown on the avidin blot, but that these some degradation of the protein. The degradation of PC may occur due to its misfolding or to the assembly process resulting in inactive hPC. Together with protein misfolding, proteolytic degradation and toxicity can be serious impediments to the efficient production of recombinant gene products in *E. coli*.

Heterologous expression of proteins in *E. coli* and yeast has two great advantages over the mammalian expression systems, namely the speed of producing overexpressing strains and the ease and cheapness of large-scale production.

Expression of hPC in *E. coli* was a real possibility when the level of expression was improved by T5 *lac* promoter of pQE system. However, this system failed to produce functional hPC as assessed by radiochemical assay of hPC in the whole cell lysate. Proteins expressed in *E. coli* may also lack proper biological function and antigenicity because of the absence of eukaryotic post-translational modifications. However, except for biotinylation which did occur, post-translational modifications of PC including phosphorylation have not been reported (Leiter *et al.*, 1978) indicating that the failure of expressed hPC to be active in *E. coli* is likely to be due to an incorrect folding or assembly problem.

In this study, the expression of hPC in yeast *Saccharomyces cerevisiae* was attempted using the pVT-hPC vector containing cDNA of hPC and the pVT-hPC-21 vector containing cDNA of hPC without the mitochondrial targeting sequence. The level of hPC was slightly elevated compared to the endogenous yeast PC in yeast strain W303. The level of expression was slightly increased again from the plasmid pVT-hPC-21. Unfortunately, the low level of expression hPC compared to the background PC from yeast strain W303 indicating that this was not a useful source for hPC enzymatic activity. This suggests that the yeast system using the pVT100-U vector to express full-length hPC in *Saccharomyces cerevisiae* was unable to improve the expression and specific activity of hPC, as the mammalian system 293T cell line does (Jitrapakdee *et al.*, 1999). The level of expression of both full-length hPC and the version minus mitochondrial targeting sequence is not significantly different, indicating that the mitochondrial targeting sequence might not be important in transcriptional or translational efficiency of mRNA.

A similar result was obtained using the plasmid myc pVT-hPC-21 containing cDNA of hPC without the mitochondrial targeting sequence but with a myc tag. It was clearly shown that hPC with myc tag in pVT100-U vector was expressed in *S.*

cerevisiae compared to the host strain yeast W303 on the anti myc blot (Figure 6.13c). The expression level in *S. cerevisiae* was significantly lower than in the *E. coli* system using the pQE vector (Figure 6.10a). This result revealed that the yeast strain W303 might have been suboptimal for the expression of hPC. Because the expression of recombinant proteins can be highly strain and species-specific (Romanos *et al.*, 1992), hPC might express in other vectors and suitable strains of yeast or may express in the methylotrophic yeast *P. pastoris*.

"Some proteins, which cannot be expressed efficiently in bacteria, *S. cerevisiae* or baculovirus, have been successfully produced in functionally active form in *P. pastoris* (Cereghino *et al.*, 2002). There are many reasons for the popularity of the *P. pastoris* expression system, but two are most compelling. The first is an unusually efficient and tightly regulated promoter from the alcohol oxidase I gene (*AOX1*) that is used to drive the expression of the foreign gene (Hwang *et al.*, 2000). The *AOX1* promoter is strongly repressed in cells grown on glucose and most other carbon sources, the ability to repress expression of foreign proteins is advantageous if the protein is toxic to the cell. The second reason why this is such a popular system is that, physiologically, *P. pastoris* prefers a respiratory rather than a fermentative mode of growth in which ethanol and acetic acid quickly reach toxic levels in the high cell density environment of a fermenter"(Cereghino *et al.*, 2002; Cereghino & Cregg, 2000).

The low protein expression levels obtained in *S. cerevisiae* may also be due to low levels of transcription or translation efficiency. The translation efficiency may be influenced by the availability of tRNA subsets since *S. cerevisiae* uses predominantly only 25 out of 61 possible codons, and the restricted use of only these preferred codons might limit expression levels (Bennetzen & Hall, 1982). An analysis of codon usage in human PC was conducted using CUSP [http://bioweb.pasteur.fr/seqanal/interfaces/cusp.html] and compared with those

tabulated for 6,216 ORFs contained in the Saccharomyces Genome Database [http://genome-www.Stanford.edu/Saccharomyces] by J. Michael Cherry (cherry@genome.Stanford.edu) with the GCG program CodonFrequency. Of the 72 arginines in hPC only 8 are encoded by AGG which represents 48.3% of arginines in yeast, 3 by AGA (27.6%) while 32 are encoded by CGA, CGC and CGT which together account for only 9.7% of yeast preferred codons. Similarly, of the 104 leucines in hPC, only 6 are encoded by TTG and 0 by TTA which each represent 28% of yeast codons for leucine, while 21 are encoded by CTC and 73 by CTG which represent 6% and 11% (respectively) of leucine codons in yeast. These results, presented in Appendix III, suggest that a bias of codon usage in hPC may have adversely affected its expression in *Saccharomyces cerevisiae*.

In summary, attempts to express cDNA for full-length hPC clones in *E. coli* expression using a T7-driven vector and taking into account various effects such as codon usage, and the possible need for GroEL-GroES and DnaK-DnaJ chaperones achieved only very low levels of expression. However, we have succeeded in expressing the hPC protein in *E. coli* by changing the vector system to a T5 *lac*-driven vector (pQE system). Although the expression of hPC increased to detectable levels, the expressed hPC was catalytically inactive presumably because it was unfolded or unable to assemble in the *E. coli* system. We did not improve hPC expression in the *S. cerevisiae* system whether we tried to express hPC with or without the mitochondrial targeting sequence.

CHAPTER 7

Discussion

CHAPTER 7

Pyruvate carboxylase is a member of the biotin dependent family of enzymes found widely throughout nature. The comparison of primary structures has shown that with the exception of several bacterial species PC from a wide range of species contains three functional domains ie. the biotin carboxylation domain (N-terminal region), the transcarboxylation domain (central region) and the biotin carboxyl carrier domain (C-terminal region). Because of its importance in the intermediary metabolism of both prokaryotes and eukaryotes, PC has been of particular interest to our research laboratory with respect to its reaction mechanism, its subunit structure, the relationship between its structure and activity, and the regulation of its catalytic activity. With the advent of recombinant DNA technology, a boom in the availability of protein primary sequences has occurred. These, in combination with the availability of a human PC clone and a series of monoclonal antibodies against sheep PC developed in our laboratory, has led to this investigation of PC structure. The characterisation by epitope mapping of human PC along with studies on functional aspects of human PC may identify residues important in substrate binding, catalysis or for maintaining the correct conformation.

Epitope mapping of mAb6 on human PC

As described in Chapter 3, three of our monoclonal antibodies (mAb6, 12 and 42) strongly cross-reacted with human PC, and specifically and efficiently inhibited the acetylCoA-dependent activity of human PC.

The availability of cloned human PC cDNA has made it possible to successfully express human PC fragments and map the epitope of mAb6. By using monoclonal antibody 6 as a probe in cross-reactive binding measurements, its epitope on human PC was identified as LKDLPRV (amino acids 968-974), a continuous epitope in the proline

rich region of amino acids 951-1000, located between the central transcarboxylation domain and the C-terminal biotin carboxyl carrier domain (Chapter 3). Site-directed mutagenesis was used to introduce mutations into this epitope. Mutant D970A was found to completely abolish the binding of antibody and also to reduce the acetylCoA-dependent activity of human PC to 50% (Chapter 4).

The purification of this mutant protein would be essential for kinetic and physicochemical analysis to investigate the role of this critical residue in the context of full-length human PC to see if the defect in functional activity is not just a secondary consequence of defective domain folding. The mutation might also influence the assembly of human PC into active tetramer as a previous immunoelectron microscopy study (Rohde & Carey, unpublished work) localised mAb6 binding close to the intersubunit association region of the native tetramer. For example, it would be interesting to investigate the higher order assembly of the mutant and determine the ratio of active (tetramer) versus inactive (dimer or monomer) forms of this mutant using high-resolution gel permeation chromatography or ultracentrifugation.

The location of mAb6's epitope in the proline rich region at the junction between the transcarboxylation and the biotin carboxyl carrier domains is possibly associated with the mobility of this BCC domain in the catalytic reaction of PC. Structural analysis of complexes between a protein antigen and an antibody shows that typically between 14 and 21 residues are implicated in each epitope and most of the binding energy can be accounted for by only 3 to 10 side chains (Clackson & Wells, 1995). The blocking of enzyme activity by antibody 6 might occur at an area around the epitope containing 14-21 residues, which efficiently inhibits the activity of human PC. Thus, the deletion of the 7 amino acids of this epitope or up to 20 residues upstream or downstream from this epitope region might result in complete loss of PC

activity. This might be useful to further investigate the possible role of this epitope as a linker region of the BCC domain's movement in catalysis.

Studies of the deletion of four consecutive alanine residues adjacent to the lipoyl domain of pyruvate dehydrogenase (PDH) of *E. coli* showed that a small deletion of the PDH linker could result in complete loss of protein function *in vivo* (Cronan, 2002). This evidence supports the possibility that this epitope be further investigated as a potential linker in the BCC domain of human PC. Mobile linker and loop regions are of interest and have been studied extensively in *E. coli* BCCP and *E. coli* PDH (Cronan, 2002; Radford *et al.*, 1989a; Radford *et al.*, 1989b). The structure of such regions cannot be determined by the currently available techniques and is a major unsolved problem of structural biology (Cronan, 2002). The mAb6's epitope might be an alternative way to gain more structural insight into the critical residues close to this potential linker of the BCC domain's movement in the catalytic reaction of PC. Currently, the three dimensional structure and linker residues of PC in this region have not been studied, and knowledge of this would be advantageous in understanding its structural and functional role in PC's catalytic reaction mechanism.

Epitope mapping of mAb12 and 42 on human PC

As described in Chapter 3 and 5, the epitopes of mAb12 and 42 were revealed as discontinuous epitopes contained within the minimal C-terminal 80 residues of the biotin carboxyl carrier domain (BCC) of human PC. Studies with cross-reactive binding measurements (Western blot) and point mutations, based on not only the sequence alignment of human PC, yeast $PC_1$104 and BCCP of *E. coli* ACC but also on the predicted structure of human PC in this domain, showed that the alanine substitution of Met^{1116}, Met^{1143}, Leu^{1168} and Glu^{1169} results in reduction of the binding of mAb12. However, the most significant contributor to the binding of mAb12 is Met^{1143}. For

mAb42, the alanine substitutions of Ser^{1141}, Met^{1143} or Leu^{1168} most significantly account for reduction of this mAb's binding to human PC while $Lys^{1119}$and Asp^{1165} are likely to be modest contributors to mAb42's binding. Therefore, mAb42 appears to bind to the BCC domain of hPC at the surface area of the biotin-binding containing Met^{1143}, Asp^{1165}, Leu^{1168}, Lys^{1119} and Ser^{1141} which are close to the biotin moiety. However, the mAb12's epitope appears to be somewhat more centred on the opposite side of the biotin-binding and the Met^{1143} and Leu^{1168} might also be part of the overlap of these epitopes.

The reduction in binding affinities, which occurred as a result of the various mutations, was in most cases likely to be caused by changes in the direct interaction of the mAb with the altered residue. Alternatively, perhaps most likely in the case of Leu^{1168}, the mutation may have affected the secondary or tertiary structure of the biotin carboxyl carrier domain of human PC resulting in the secondary consequence of a conformational change in the epitope and hence reduction of the binding affinity. Therefore, in the future it would be valuable to measure the enzymatic activity of the eight mutant full-length hPC expressed in 293T cell lines, in order to specify the effects of critical residues of these epitopes on the catalytic activity of human PC. Furthermore, purification and kinetic analysis of these mutants compared to wild type in terms of the interaction of the substrates in the two partial reactions would further investigate the roles of these residues in the catalytic reaction.

Mutations in one of its subunits and expressed in the presence of endogenous PC could affect function in a variety of ways, including PC assembly, substrate binding, catalytic efficiency of the overall reaction, or catalytic efficiency in either of the partial reactions. For example, mutations in the subunits of PC could lead to loss of structure and hence the ability to assemble PC into tetramers. If the introduction of a mutation affects the ability of the mutant BCC of human PC to permit assembly, full-length

mutant PC might exhibit different ratios of monomer, dimer or tetramer. This could be assayed, if the overall catalytic activity of PC was affected. Chemical cross-linking of mutant subunits may promote the assembly of PC and increase the activity of the mutant compared to that of the wild type. This will imply that the introduced residues change the ability of mutant PC to assemble and affect the overall catalytic activity.

No structural information for this region is yet available from X-ray-crystallographic or NMR experiments with the BCC domain of human PC. Further work to investigate the epitope map of these two antibodies on the biotin carboxyl carrier domain using NMR or crystallography would be advantageous to precisely define the structural residues of these epitopes. The structure of the BCC domain once determined would be useful to provide more details of quaternary structure, which may allow us to solve the structure and function relation of PC.

As the size of PC appears to limit its suitability for detailed three-dimensional structure by NMR study, a further study would be to attempt expression of other domains of human PC, such as biotin carboxylation domain (residues 1-488) (Chapter 3), in sufficient quantities for analysis by crystallography. In addition, the functional significance of this region such as the first subsites could be tested in purified form after expression in a suitable system. With the knowledge of the three-dimensional structure of the domains of PC, together with site-directed mutagenesis to probe the role of specific amino acid residues in the catalytic reaction a model could be assembled to provide an overall structure and may allow us to understand the relationship of structure to function.

Expression of functional human PC in bacteria and yeast

The expression of full-length hPC in a bacterial system was attempted in many ways to obtain functional hPC which can be used for kinetic and physicochemical studies. The attempts to improve the level of expression and/or quality of the functional hPC in bacterial system were described in Chapter 6. Although the expression of hPC increased to detectable levels, the expressed hPC remained inactive.

It has long been clear that the codon preferences of *E. coli* are quite different from those of mammalian systems and that can lead to problems when trying to express a mammalian gene product in bacteria. The clustering of rare codons can lead to ribosomal pausing and frameshifting, which reduces the quantity of the desired gene product and leads to the production of truncated products (Shatzman, 1995). However, the expression of hPC in T7 driven Rosetta (Novagen) and BL21 RIL (Stratagene) *E. coli* strains did not improve the level of expression. The level of hPC expression in T7 driven system (pET vector) was not greatly affected by codon preferences and may be affected by the coding sequence in other ways that are not yet well understood. It has been reported that not only the number of rare codons, but also their context and distribution within a given gene appear to influence expression levels (Kurland & Gallant, 1996). Moreover, the thioredoxin fusion gene in pET vector did not enhance the level of hPC expression.

In *E. coli*, two molecular chaperone machines, GroEL-GroES and DnaK-DnaJ, a ubiquitous class of proteins, play important roles in protein folding by assisting other polypeptides to reach a proper conformation or cellular location without themselves becoming part of the final structure (Hartl *et al.*, 1994; Hendrick & Hartl, 1993). Currently, no definitive correlation has been established between amino acid sequence of a protein and its propensity to aggregate *in vivo*. Nevertheless, it has been shown that even small changes in primary structure can significantly affect solubility, presumably

by altering folding pathways (Thomas & Baneyx, 1996). For example, the insertion of a 30 amino acid segment from the S' region of Hepatitis B surface antigen (HbsAg) between the HbsAg preS2 sequence and β-galactosidase domains makes the resulting preS2-S'-β-galactosidase fusion protein highly susceptible to aggregation, while a fusion protein between these two domains is significantly soluble in wild type *E. coli* strains (Lee *et al.*, 1990). However, our results showed that production of components of either GroEL-GroES or DnaK-DnaJ molecular chaperone machines did not play a major role in improving the *in vivo* folding or assembly of hPC in Rosetta, BL21RIL, BL21 (DE3) and AD494. Other groups have also shown that the overexpression of some enzymes of the *E. coli* folding machinery such as GroES-GroEL chaperonins, disulfide-isomerase DsbA and proline-cis-trans-isomerase (PPIase) did not increase the yield of soluble antibody fragments (Duenas *et al.*, 1994). The degree of successful *in vivo* folding appears to depend very much on the primary sequence of the variable domains (Knappik & Pluckthun, 1995). It is now recognised that aggregation *in vivo* is not a function of the solubility and stability of the native state of the protein, but of those of its folding intermediates in their particular environment (Hockney, 1994).

Accumulation of expressed hPC was somewhat favoured when T5/*lac* driven expression (pQE vector) was carried out at lower temperatures in bacterial culture. The main difference between the T7 and T5/*lac* driven expression system is that the T7-driven (pET vector) is based on the thioredoxin fusion protein, while the T5/*lac*-driven expression system (pQE vector) consists of the *E. coli* phage T5 promoter, two *lac* operator sequences and a 6 His tag coding sequence. The special double operator system in this pQE system, in combination with the high levels of *lac* repressor provided by pREP4 from *E. coli* host cell, permits some control over the level of expression. Expression of hPC in *E. coli* was a real possibility when the level of expression was improved by T5 *lac* promoter of pQE system and also that the expressed

hPC was biotinylated, albeit with some degraded protein. However, the expressed hPC was not active in *E. coli*, and this is likely to be due to an incorrect folding or assembly problem.

Unlike many mammalian culture expression systems, yeast expression systems use completely synthetic growth media with no animal derived components in any part of the process. Yeast production is therefore relatively simple and can be more efficient than mammalian cell culture. Yeast is an excellent organism for the overproduction of multipolypeptide complexes, especially those of autologous origin (Burgers, 1999).

Unfortunately, the yeast system using pVT100-U vector controlled by a constitutive alcohol dehydrogenase promoter to express full-length hPC in *Saccharomyces cerevisiae* was unable to improve the expression and specific activity of hPC. The levels of expression of both full-length hPC and the version minus mitochondrial targeting sequence are not significantly different, indicating that the mitochondrial targeting sequence might not be important in transcriptional or translational efficiency of mRNA. The low protein expression levels obtained in *S. cerevisiae* may also be due to low levels of transcription or translation efficiency. Because the expression of recombinant proteins can be highly strain and species-specific (Romanos *et al.*, 1992), it may be worth trying to express hPC from the *GAL* promoter, which is an inducible promoter, and in different strains of yeast. An inducible expression system in yeast is very valuable as constitutive expression can be deleterious to cell growth (Burgers, 1999). For example, DNA polymerase is overexpressed constitutively, however, vigorous overproduction is observed when expression is induced after sufficient growth of the cells (Gerik *et al.*, 1997).

Other approaches could be employed for the expression of functional hPC. For instance, the yeast *RFC1* gene encoding the large subunit of the five subunit replication factor C cannot be expressed in *E. coli* at a detectable level (Burgers, 1999).

Overproduction of multisubunit factors in baculovirus has in general been successful (Roy & Jones, 1996). This evidence suggests the possibility that expression of tetrameric, functional hPC could be developed in a baculovirus system using insect cells. Recombinant baculoviruses can direct heterologous gene expression for longer periods of time during the infection process (Shatzman, 1995). Expression of a wide variety of mammalian gene products has been achieved using this system and shown to be stable for long periods of time, even in the absence of selection (Shatzman, 1995). The possibility of successful expression of PC in this system is also supported by the observation that a retroviral expression system for hPC was successfully used to analyse the effect of a hPC mutation found in the Ojibwa population (Amerindian pyruvate carboxylase deficiency). This mutant had decreased activity, decreased level of expression and inefficient import into the mitochondria (Carbone & Robinson, 2003).

Obviously, a suitable vector system to express functional hPC is essential for further study of the indirect role of the identified epitopes, in combination with the mutagenesis study. Information from structural studies may lead to further understanding of the catalytic reaction of PC and be helpful in understanding the mechanism of mutations which cause PC deficiency in humans. Ultimately, gene therapy might be developed as a method to treat these patients, based on this information.

REFERENCES

Alexander, H. (1996). Epitope mapping using an oligonucleotide replacement method. In *Methods in Molecular Biology : Epitope Mapping Protocols*, vol. 66 (ed. G. E. Morris), pp. 221-231. Humana Press, Totowa, New Jersey.

Alexeyev, M. F. and Winkler, H. H. (1999). Gene synthesis, bacterial expression and purification of the *Rickettsia prowazekii* ATP/ADP translocase. *Biochim Biophys Acta* **1419,** 299-306.

Al-ssum, R. M. and White, P. J. (1977). Activities of anaplerotic enzymes and acetyl coenzyme A carboxylase in biotin-deficient Bacillus megaterium. *J Gen Microbiol* **100,** 203-6.

Altschul, S. F. and Gish, W. (1996). Local alignment statistics. *Methods Enzymol* **266,** 460-80.

Amit, A. G., Mariuzza, R. A., Phillips, S. E. and Poljak, R. J. (1986). Three-dimensional structure of an antigen-antibody complex at 2.8 A resolution. *Science* **233,** 747-53.

Andersen, D. C. and Krummen, L. (2002). Recombinant protein expression for therapeutic applications. *Curr Opin Biotechnol* **13,** 117-23.

Anderson, O. D., Kuhl, J. C. and Tam, A. (1996). Construction and expression of a synthetic wheat storage protein gene. *Gene* **174,** 51-8.

Anglister, J., Levy, R. and Scherf, T. (1989). Interactions of antibody aromatic residues with a peptide of cholera toxin observed by two-dimensional transferred nuclear Overhauser effect difference spectroscopy. *Biochemistry* **28,** 3360-5.

Anglister, J., Scherf, T., Zilber, B., Levy, R., Zvi, A., Hiller, R. and Feigelson, D. (1993). Two-dimensional NMR investigations of the interactions of antibodies with peptide antigens. *FASEB J* **7,** 1154-62.

Aran, J. M., Gottesman, M. M. and Pastan, I. (1994). Drug-selected coexpression of human glucocerebrosidase and P-glycoprotein using a bicistronic vector. *Proc Natl Acad Sci U S A* **91,** 3176-80.

Arnold, G. L., Griebel, M. L., Porterfield, M. and Brewster, M. (2001). Pyruvate carboxylase deficiency. Report of a case and additional evidence for the "mild" phenotype. *Clin Pediatr (Phila)* **40,** 519-21.

Ashman, L. K. and Keech, D. B. (1975). Sheep kidney pyruvate carboxylase. Studies on the coupling of adenosine triphosphate hydrolysis and CO2 fixation. *J Biol Chem* **250,** 14-21.

Ashman, L. K., Keech, D. B., Wallace, J. C. and Nielsen, J. (1972). Sheep kidney pyruvate carboxylase. Studies on its activation by acetyl coenzyme A and

characteristics of its acetyl coenzyme A independent reaction. *J Biol Chem* **247,** 5818-24.

Ashman, L. K., Wallace, J. C. and Keech, D. B. (1973). Densitization of pyruvate carboxylase against acetyl-CoA stimulation by chemical modification. *Biochem Biophys Res Commun* **51,** 924-31.

Atassi, M. Z. (1975). Antigenic structure of myoglobin: the complete immunochemical anatomy of a protein and conclusions relating to antigenic structures of proteins. *Immunochemistry* **12,** 423-38.

Atassi, M. Z. (1978). Precise determination of the entire antigenic structure of lysozyme: molecular features of protein antigenic structures and potential of "surface-simulation" synthesis--a powerful new concept for protein binding sites. *Immunochemistry* **15,** 909-36.

Atassi, M. Z. (1984). Antigenic structures of proteins. Their determination has revealed important aspects of immune recognition and generated strategies for synthetic mimicking of protein binding sites. *Eur J Biochem* **145,** 1-20.

Athappilly, F. K. and Hendrickson, W. A. (1995). Structure of the biotinyl domain of acetyl-coenzyme A carboxylase determined by MAD phasing. *Structure* **3,** 1407-19.

Attwood, P. V. (1993). Locus of action of acetyl-CoA in the biotin-carboxylation reaction of pyruvate carboxylase. *Biochemistry* **32,** 12736-42.

Attwood, P. V. (1995). The structure and the mechanism of action of pyruvate carboxylase. *Int J Biochem Cell Biol* **27,** 231-249.

Attwood, P. V. and Cleland, W. W. (1986). Decarboxylation of oxalacetate by pyruvate carboxylase. *Biochemistry* **25,** 8191-6.

Attwood, P. V. and Geeves, M. A. (2002). Changes in catalytic activity and association state of pyruvate carboxylase which are dependent on enzyme concentration. *Arch Biochem Biophys* **1,** 63-72.

Attwood, P. V. and Graneri, B. D. (1991). Pyruvate carboxylase catalysis of phosphate transfer between carbamoyl phosphate and ADP. *Biochem J* **273,** 443-8.

Attwood, P. V. and Graneri, B. D. (1992). Bicarbonate-dependent ATP cleavage catalysed by pyruvate carboxylase in the absence of pyruvate. *Biochem J* **287,** 1011-7.

Attwood, P. V., Johannssen, W., Chapman-Smith, A. and Wallace, J. C. (1993). The existence of multiple tetrameric conformers of chicken liver pyruvate carboxylase and their roles in dilution inactivation. *Biochem J* **290,** 583-90.

Attwood, P. V., Tipton, P. A. and Cleland, W. W. (1986). Carbon-13 and deuterium isotope effects on oxalacetate decarboxylation by pyruvate carboxylase. *Biochemistry* **25,** 8197-205.

Attwood, P. V. and Wallace, J. C. (1986). The carboxybiotin complex of chicken liver pyruvate carboxylase. A kinetic analysis of the effects of acetyl-CoA, Mg2+ ions and temperature on its stability and on its reaction with 2-oxobutyrate. *Biochem J* **15,** 359-64.

Attwood, P. V. and Wallace, J. C. (2002). Chemical and catalytic mechanisms of carboxyl transfer reactions in biotin-dependent enzymes. *Acc Chem Res* **35,** 113-20.

Attwood, P. V., Wallace, J. C. and Keech, D. B. (1984). The carboxybiotin complex of pyruvate carboxylase. A kinetic analysis of the effects of Mg2+ ions on its stability and on its reaction with pyruvate. *Biochem J* **219,** 243-51.

Ausubel, F. M., Brent, R., Kingston, R. E., Moore, D. D., Seidman, J. G., Smith, J. A. and Struhl, K. (1998). Current protocols in molecular biology, vol. 3, pp. 16.1.1-16.1.3. Wiley interscience, Massachusetts.

Bais, R. and Keech, B. (1972). The magnesium ion (Mg^{2+}) activation of sheep kidney pyruvate carboxylase. *J Biol Chem* **247,** 3255-61.

Balass, M., Heldman, Y., Cabilly, S., Givol, D., Katchalski-Katzir, E. and Fuchs, S. (1993). Identification of a hexapeptide that mimics a conformation-dependent binding site of acetylcholine receptor by use of a phage-epitope library. *Proc Natl Acad Sci U S A* **90,** 10638-42.

Ballard, F. J. and Hanson, R. W. (1967). Phosphoenolpyruvate carboxykinase and pyruvate carboxylase in developing rat liver. *Biochem J* **104,** 866-871.

Ballard, F. J., Hanson, R. W. and Reshef, L. (1970). Immunochemical studies with soluble and mitochondrial pyruvate carboxylase activities from rat tissues. *Biochem J* **119,** 735-42.

Baneyx, F. (1999). Recombinant protein expression in Escherichia coli. *Curr Opin Biotechnol* **10,** 411-21.

Barlow, D. J., Edwards, M. S. and Thornton, J. M. (1986). Continuous and discontinuous protein antigenic determinants. *Nature* **322,** 747-8.

Barritt, G. J. (1985). Regulation of Enzymatic Activity. In *Pyruvate Carboxylase* (ed. D. B. Keech and J. C. Wallace), pp. 142-169. CRC Press, Boca Raton, Florida.

Bayer, E. A. and Wilchek, M. (1990). Biotin binding proteins: overview and prospects. *Methods Enzymol* **184**, 49-51.

Benjamin, A. M. and Quastel, J. H. (1974). Fate of L-glutamate in the brain. *J Neurochem* **23,** 457-64.

Benjamin, D. C., Berzofsky, J. A., East, I. J., Gurd, F. R., Hannum, C., Leach, S. J., Margoliash, E., Michael, J. G., Miller, A., Prager, E. M. and *et al.* (1984). The antigenic structure of proteins: a reappraisal. *Annu Rev Immunol* . **2,** 67-101.

Benjamin, D. C., Williams, D. C., Jr., Smith-Gill, S. J. and Rule, G. S. (1992). Long-range changes in a protein antigen due to antigen-antibody interaction. *Biochemistry* **31,** 9539-45.

Bennetzen, J. L. and Hall, B. D. (1982). Codon selection in yeast. *J Biol Chem* **257,** 3026-31.

Bessette, P. H., Qiu, J., Bardwell, J. C., Swartz, J. R. and Georgiou, G. (2001). Effect of sequences of the active-site dipeptides of DsbA and DsbC on in vivo folding of multidisulfide proteins in Escherichia coli. *J Bacteriol* **183,** 980-8.

Blackard, W. G. and Clore, J. N. (1988). Model to examine pathways of carbon flux from lactate to glucose at the first branch point in gluconeogenesis. *J Biol Chem* **263,** 16725-30.

Bordo, D. and Argos, P. (1991). Suggestions for "safe" residue substitutions in site-directed mutagenesis. *J Mol Biol* **217,** 721-9.

Bradford, M. M. (1976). A rapid and sensitive method for the quantitation of microgram quantities of protein utilizing the principle of protein-dye binding. *Anal Biochem* **72,** 248-54.

Branson, J. P. and Attwood, P. V. (2000). Effects of Mg(2+) on the pre-steady-state kinetics of the biotin carboxylation reaction of pyruvate carboxylase. *Biochemistry* **39,** 7480-91.

Branson, J. P., Nezic, M., Wallace, J. C. and Attwood, P. V. (2002). Kinetic characterization of yeast pyruvate carboxylase isozyme pyc1. *Biochemistry* **41,** 4459-66.

Brewster, N. K., Val, D. L., Walker, M. E. and Wallace, J. C. (1994). Regulation of pyruvate carboxylase isozyme (PYC1, PYC2) gene expression in

Saccharomyces cerevisiae during fermentative and nonfermentative growth. *Arch Biochem Biophys* **311,** 62-71.

Brooks, B. R., Bruccoleri, R. E., Olafson, B. D., States, D. J., Swaminathan, S. and Karplus, M. (1983). CHARMM: A Program for Macromolecular Energy, Minimization, and DynamicsCalculations. *J Comp Chem* **4,** 187-217.

Bukau, B. and Horwich, A. L. (1998). The Hsp70 and Hsp60 chaperone machines. *Cell* **92,** 351-66.

Burch, H. B., Nagy, E. V., Kain, K. C., Lanar, D. E., Carr, F. E., Wartofsky, L. and Burman, K. D. (1993). Expression polymerase chain reaction for the *in vitro* synthesis and epitope mapping of autoantigen. Application to the human thyrotropin receptor. *J Immunol Methods* **158,** 123-30.

Burgers, P. M. (1999). Overexpression of multisubunit replication factors in yeast. *Methods* **18,** 349-55.

Burrows, S. R., Gardner, J., Khanna, R., Steward, T., Moss, D. J., Rodda, S. and Suhrbier, A. (1994). Five new cytotoxic T cell epitopes identified within Epstein-Barr virus nuclear antigen 3. *J Gen Virol* **75,** 2489-93.

Calderone, T. L., Stevens, R. D. and Oas, T. G. (1996). High-level misincorporation of lysine for arginine at AGA codons in a fusion protein expressed in *Escherichia coli*. *J Mol Biol* **262,** 407-12.

Campbell, A. P., Wong, W. Y., Houston, M., Jr., Schweizer, F., Cachia, P. J., Irvin, R. T., Hindsgaul, O., Hodges, R. S. and Sykes, B. D. (1997). Interaction of the receptor binding domains of *Pseudomonas aeruginosa* pili strains PAK, PAO, KB7 and P1 to a cross-reactive antibody and receptor analog: implications for synthetic vaccine design. *J Mol Biol* **267,** 382-402.

Campeau, E. and Gravel, R. A. (2001). Expression in *Escherichia coli* of N- and C-terminally deleted human holocarboxylase synthetase. Influence of the N-terminus on biotinylation and identification of a minimum functional protein. *J Biol Chem* **276,** 12310-6.

Carbone, M. A., Applegarth, D. A. and Robinson, B. H. (2002). Intron retention and frameshift mutations result in severe pyruvate carboxylase deficiency in two male siblings. *Hum Mutat* **20,** 48-56.

Carbone, M. A., Mackay, N., Ling, M., Cole, D. E., Douglas, C., Rigat, B., Feigenbaum, A., Clarke, J. T., Haworth, J. C., Greenberg, C. R., Seargeant, L.

and Robinson, B. H. (1998). Amerindian pyruvate carboxylase deficiency is associated with two distinct missense mutations. *Am J Hum Genet* **62,** 1312-9.

Carbone, M. A. and Robinson, B. H. (2003). Expression and characterization of a human pyruvate carboxylase variant by retroviral gene transfer. *Biochem J* **370,** 275-82.

Carey, K. J. (1988). Pyruvate carboxylase: an immunological study. Ph.D. Thesis, University of Adelaide, South Australia.

Cazzulo, J. J. and Stoppani, A. O. (1968). The regulation of yeast pyruvate carboxylase by acetyl-coenzyme A and L-aspartate. *Arch Biochem Biophys* **127,** 563-7.

Cereghino, G. P., Cereghino, J. L., Ilgen, C. and Cregg, J. M. (2002). Production of recombinant proteins in fermenter cultures of the yeast *Pichia pastoris*. *Curr Opin Biotechnol* **13,** 329-32.

Cereghino, J. L. and Cregg, J. M. (2000). Heterologous protein expression in the methylotrophic yeast *Pichia pastoris*. *FEMS Microbiol Rev* **24,** 45-66.

Chapman-Smith, A., Booker, G. W., Clements, P. R., Wallace, J. C. and Keech, D. B. (1991). Further studies on the localization of the reactive lysyl residue of pyruvate carboxylase. *Biochem J* **276,** 759-64.

Chapman-Smith, A. and Cronan, J. E., Jr. (1999a). The enzymatic biotinylation of proteins: a post-translational modification of exceptional specificity. *Trends Biochem Sci* **24,** 359-63.

Chapman-Smith, A. and Cronan, J. E., Jr. (1999b). Molecular biology of biotin attachment to proteins. *J Nutr* **129,** 477S-484S.

Chapman-Smith, A., Morris, T. W., Wallace, J. C. and Cronan, J. E., Jr. (1999). Molecular recognition in a post-translational modification of exceptional specificity. Mutants of the biotinylated domain of acetyl-CoA carboxylase defective in recognition by biotin protein ligase. *J Biol Chem* **274,** 1449-57.

Chapman-Smith, A., Turner, D. L., Cronan, J. E., Morris, T. W. and Wallace, J. C. (1994). Expression, biotinylation and purification of a biotin-domain peptide from the biotin carboxy carrier protein of *Escherichia coli* acetyl-CoA carboxylase. *Biochem J* **302,** 881-887.

Chauhan, J. and Dakshinamurti, K. (1991). Transcriptional regulation of the glucokinase gene by biotin in starved rats. *J Biol Chem* **266,** 10035-8.

Chen, G. F. and Inouye, M. (1990). Suppression of the negative effect of minor arginine codons on gene expression; preferential usage of minor codons within the first 25 codons of the *Escherichia coli* genes. *Nucleic Acids Res* **18,** 1465-73.

Chen, G. T. and Inoue, M. (1994). Role of the AGA/AGG codons, the rarest codons in global gene expression in *Escherichia. Genes Dev* **8,** 2641-2652.

Cheng, T. H., Chang, C. R., Joy, P., Yablok, S. and Gartenberg, M. R. (2000). Controlling gene expression in yeast by inducible site-specific recombination. *Nucleic Acids Res* **28,** E108.

Chirinos-Rojas, C. L., Steward, M. W. and Partidos, C. D. (1997). Use of a solid-phase random peptide library to identify inhibitors of TNF-alpha mediated cytotoxicity *in vitro*. *Cytokine* **9,** 226-32.

Churchill, M. E., Stura, E. A., Pinilla, C., Appel, J. R., Houghten, R. A., Kono, D. H., Balderas, R. S., Fieser, G. G., Schulze-Gahmen, U. and Wilson, I. A. (1994). Crystal structure of a peptide complex of anti-influenza peptide antibody Fab 26/9. Comparison of two different antibodies bound to the same peptide antigen. *J Mol Biol* **241,** 534-56.

Clackson, T. and Wells, J. A. (1995). A hot spot of binding energy in a hormone-receptor interface. *Science* **267,** 383-6.

Colman, P. M. (1988). Structure of antibody-antigen complexes: implications for immune recognition. *Adv Immunol 1988.* **43,** 99-132.

Comte, B., Vincent, G., Bouchard, B., Jette, M., Cordeau, S. and Rosiers, C. D. (1997). A 13C mass isotopomer study of anaplerotic pyruvate carboxylation in perfused rat hearts. *J Biol Chem* **272,** 26125-31.

Connell, N. D. (2001). Expression systems for use in actinomycetes and related organisms. *Curr Opin Biotechnol* **12,** 446-9.

Cornelis, P. (2000). Expressing genes in different *Escherichia coli* compartments. *Curr Opin Biotechnol* **11,** 450-4.

Cortese, R., Monaci, P., Luzzago, A., Santini, C., Bartoli, F., Cortese, I., Fortugno, P., Galfre, G., Nicosia, A. and Felici, F. (1996). Selection of biologically active peptides by phage display of random peptide libraries. *Curr Opin Biotechnol* **7,** 616-21.

Cortese, R., Monaci, P., Nicosia, A., Luzzago, A., Felici, F., Galfre, G., Pessi, A., Tramontano, A. and Sollazzo, M. (1995). Identification of biologically active

peptides using random libraries displayed on phage. *Curr Opin Biotechnol* **6,** 73-80.

Crabtree, B., Higgins, S. J. and Newsholme, E. A. (1972). The activities of pyruvate carboxylase, phosphoenolpyruvate carboxylase and fructose diphosphatase in muscles from vertebrates and invertebrates. *Biochem J* **130,** 391-6.

Cronan, J. E., Jr. (1990). Biotination of proteins *in vivo*. A post-translational modification to label, purify, and study proteins. *J Biol Chem* **265,** 10327-33.

Cronan, J. E., Jr. (2002). Interchangeable enzyme modules. Functional replacement of the essential linker of the biotinylated subunit of acetyl-CoA carboxylase with a linker from the lipoylated subunit of pyruvate dehydrogenase. *J Biol Chem* **277,** 22520-7.

Cumme, G. A., Bublitz, R., Ehle, H. and Horn, A. (1990). Determination of rate constants of monoclonal antibodies to enzymes. *J Immunol Methods* **128,** 241-8.

Cumme, G. A., Walter, U., Bublitz, R., Hoppe, H., Rhode, H. and Horn, A. (1995). Characterization of the interaction of alkaline phosphatase with an activity inhibiting monoclonal antibody by progress curve analysis. *J Immunol Methods* **182,** 29-39.

Cunningham, B. C. and Wells, J. A. (1993). Comparison of a structural and a functional epitope. *J Mol Biol* **234,** 554-63.

Davies, D. R. and Cohen, G. H. (1996). Interactions of protein antigens with antibodies. *Proc Natl Acad Sci U S A* **93,** 7-12.

Davies, D. R., Padlan, E. A. and Sheriff, S. (1990). Antibody-antigen complexes. *Annu Rev Biochem* **59,** 439-73.

Dawson, R. M. C., Elliot, D. C., Elliot, W. H. and Jones, K. M. (1969). *Data for Biochemical Research*, 2 edition. Oxford University Press.

De Bernardez Clark, E., Schwarz, E. and Rudolph, R. (1999). Inhibition of aggregation side reactions during *in vitro* protein folding. *Methods Enzymol* **309,** 217-36.

De Smit, M. H. and Van Duin, J. (1990). Secondary structure of the ribosome binding site determines translational efficiency: a quantitative analysis. *Proc Natl Acad Sci U S A* **87,** 7668-72.

Del Tito, B. J., Jr., Ward, J. M., Hodgson, J., Gershater, C. J., Edwards, H., Wysocki, L. A., Watson, F. A., Sathe, G. and Kane, J. F. (1995). Effects of a minor isoleucyl tRNA on heterologous protein translation in *Escherichia coli*. *J Bacteriol* **177,** 7086-91.

Dimroth, P. and Thomer, A. (1992). The sodium ion pumping oxaloacetate decarboxylase of *Klebsiella pneumoniae*. Metal ion content, inhibitors and proteolytic degradation studies. *FEBS Lett* **300,** 67-70.

Dower, W. J. (1998). Targeting growth factor and cytokine receptors with recombinant peptide libraries. *Curr Opin Chem Biol* **2,** 328-34.

Du Plessis, D. H., Wang, L. F., Jordaan, F. A. and Eaton, B. T. (1994). Fine mapping of a continuous epitope on VP7 of bluetongue virus using overlapping synthetic peptides and a random epitope library. *Virology* **198,** 346-9.

Duenas, M., Vazquez, J., Ayala, M., Soderlind, E., Ohlin, M., Perez, L., Borrebaeck, C. A. and Gavilondo, J. V. (1994). Intra- and extracellular expression of an scFv antibody fragment in *E. coli*: effect of bacterial strains and pathway engineering using GroES/L chaperonins. *Biotechniques* **16,** 476-7, 480-3.

Duggleby, R. G., Attwood, P. V., Wallace, J. C. and Keech, D. B. (1982). Avidin is a slow-binding inhibitor of pyruvate carboxylase. *Biochemistry* **6,** 3364-70.

Dunn, M. F. (1998). Tricarboxylic acid cycle and anaplerotic enzymes in rhizobia. *FEMS Microbiol Rev* **22,** 105-23.

Dunn, M. F., Araiza, G., Cevallos, M. A. and Mora, J. (1997). Regulation of pyruvate carboxylase in *Rhizobium etli*. *FEMS Microbiol Lett* **157,** 301-6.

Dunn, M. F., Araiza, G. and Finan, T. M. (2001). Cloning and characterization of the pyruvate carboxylase from *Sinorhizobium meliloti* Rm1021. *Arch Microbiol* **176,** 355-63.

Dunn, M. F., Encarnacion, S., Araiza, G., Vargas, M. C., Davalos, A., Peralta, H., Mora, Y. and Mora, J. (1996). Pyruvate carboxylase from *Rhizobium etli*: mutant characterization, nucleotide sequence, and physiological role. *J Bacteriol* **178,** 5960-70.

Easterbrook-Smith, S. B., Hudson, P. J., Goss, N. H., Keech, D. B. and Wallace, J. C. (1976). Pyruvate carboxylase: mechanism of the second partial reaction. *Arch Biochem Biophys* **176,** 709-20.

Ehle, H., Godicke, C. and Horn, A. (1989). A new graphical method for determining the affinity constants of monoclonal antibodies to enzymes. *J Immunol Methods* **117,** 17-23.

Encarnacion, S., Dunn, M., Willms, K. and Mora, J. (1995). Fermentative and aerobic metabolism in *Rhizobium etli*. *J Bacteriol* **177,** 3058-66.

Eto, H., Yoon, S. S., Bode, B. P., Kamidono, S., Makino, K., Saya, H., Nakamura, H. and Tanabe, K. K. (2000). Mapping and regulation of the tumor-associated epitope recognized by monoclonal antibody RS-11. *J Biol Chem* **275,** 27075-83.

Fagerstam, L. G., Frostell, A., Karlsson, R., Kullman, M., Larsson, A., Malmqvist, M. and Butt, H. (1990). Detection of antigen-antibody interactions by surface plasmon resonance. Application to epitope mapping. *J Mol Recognit* **3,** 208-14.

Feldman, D. E. and Frydman, J. (2000). Protein folding *in vivo*: the importance of molecular chaperones. *Curr Opin Struct Biol* **10,** 26-33.

Freytag, S. O. and Collier, K. J. (1984). Molecular cloning of a cDNA for human pyruvate carboxylase. Structural relationship to other biotin-containing carboxylases and regulation of mRNA content in differentiating preadipocytes. *J Biol Chem* **259,** 12831-7.

Frillingos, S., Wu, J., Venkatesan, P. and Kaback, H. R. (1997). Binding of ligand or monoclonal antibody 4B1 induces discrete structural changes in the lactose permease of *Escherichia coli*. *Biochemistry* **36,** 6408-14.

Fujiwara, K., Okamura-Ikeda, K. and Motokawa, Y. (1991). Lipoylation of H-protein of the glycine cleavage system. The effect of site-directed mutagenesis of amino acid residues around the lipoyllysine residue on the lipoate attachment. *FEBS Lett* **293,** 115-8.

Gancedo, J. M. (1992). Carbon catabolite repression in yeast. *Eur J Biochem* **206,** 297-313.

Gerik, K. J., Gary, S. L. and Burgers, P. M. (1997). Overproduction and affinity purification of *Saccharomyces cerevisiae* replication factor C. *J Biol Chem* **272,** 1256-62.

Gershoni, J. M., Stern, B. and Denisova, G. (1997). Combinatorial libraries, epitope structure and the prediction of protein conformations. *Immunol Today* **18,** 108-10.

Gething, M. J. and Sambrook, J. (1992). Protein folding in the cell. *Nature* **355,** 33-45.

Getzoff, E. D., Geysen, H. M., Rodda, S. J., Alexander, H., Tainer, J. A. and Lerner, R. A. (1987). Mechanisms of antibody binding to a protein. *Science* **235,** 1191-6.

Getzoff, E. D., Tainer, J. A., Lerner, R. A. and Geysen, H. M. (1988). The chemistry and mechanism of antibody binding to protein antigens. *Adv Immunol* **43,** 1-98.

Geysen, H. M., Rodda, S. J. and Mason, T. J. (1986). A priori delineation of a peptide which mimics a discontinuous antigenic determinant. *Mol Immunol* **23,** 709-15.

Geysen, H. M., Rodda, S. J., Mason, T. J., Tribbick, G. and Schoofs, P. G. (1987). Strategies for epitope analysis using peptide synthesis. *J Immunol Methods* **102,** 259-74.

Goodall, G. J., Baldwin, G. S., Wallace, J. C. and Keech, D. B. (1981). Factors that influence the translocation of the N-carboxybiotin moiety between the two sub-sites of pyruvate carboxylase. *Biochem J* **199,** 603-9.

Goss, J. A., Cohen, N. D. and Utter, M. F. (1981). Characterization of the subunit structure of pyruvate carboxylase from *Pseudomonas citronellolis*. *J Biol Chem* **256,** 11819-25.

Gurtu, V., Yan, G. and Zhang, G. (1996). IRES bicistronic expression vectors for efficient creation of stable mammalian cell lines. *Biochem Biophys Res Commun* **229,** 295-8.

Hamilton, J., Rae, M. D., Logan, R. W. and Robinson, P. H. (1997). A case of benign pyruvate carboxylase deficiency with normal development. *J Inherit Metab Dis* **20,** 401-3.

Harlow, E. and Lane, D. (1989). *Antibodies: A Laboratory Manual*, 2 edition. Cold Spring Laboratory, Cold Spring Harbor, New York.

Hartl, F. U., Hlodan, R. and Langer, T. (1994). Molecular chaperones in protein folding: the art of avoiding sticky situations. *Trends Biochem Sci* **19,** 20-5.

Hawkins, R. E., Russell, S. J., Baier, M. and Winter, G. (1993). The contribution of contact and non-contact residues of antibody in the affinity of binding to antigen. The interaction of mutant D1.3 antibodies with lysozyme. *J Mol Biol* **234,** 958-64.

Hendrick, J. P. and Hartl, F. U. (1993). Molecular chaperone functions of heat-shock proteins. *Annu Rev Biochem* **62,** 349-84.

Henry, M., Zanelli, E., Piechaczyk, M., Pau, B. and Malthiery, Y. (1992). A major human thyroglobulin epitope defined with monoclonal antibodies is mainly recognized by human autoantibodies. *Eur J Immunol* **22,** 315-9.

Hobbs, S., Jitrapakdee, S. and Wallace, J. C. (1998). Development of a bicistronic vector driven by the human polypeptide chain elongation factor 1alpha promoter for creation of stable mammalian cell lines that express very high levels of recombinant proteins. *Biochem Biophys Res Commun* **18,** 368-72.

Hochleitner, E. O., Gorny, M. K., Zolla-Pazner, S. and Tomer, K. B. (2000). Mass spectrometric characterization of a discontinuous epitope of the HIV envelope

protein HIV-gp120 recognized by the human monoclonal antibody 1331A. *J Immunol* **164,** 4156-61.

Hockney, R. C. (1994). Recent developments in heterologous protein production in *Escherichia coli*. *Trends Biotechnol* **12,** 456-63.

Hoess, R. H. (1993). Phage display of peptides and protein domains. *Curr. Opin. Struct. Biol* **3,** 572-79.

Hoogenboom, H. R. and Winter, G. (1992). By-passing immunisation. Human antibodies from synthetic repertoires of germline VH gene segments rearranged in vitro. *J Mol Biol* **227,** 381-8.

Huang, X., Yang, X., Luft, B. J. and Koide, S. (1998). NMR identification of epitopes of Lyme disease antigen OspA to monoclonal antibodies. *J Mol Biol* **281,** 61-7.

Hwang, J. S., Yamada, K., Honda, A., Nakade, K. and Ishihama, A. (2000). Expression of functional influenza virus RNA polymerase in the methylotrophic yeast *Pichia pastoris*. *J Virol* **74,** 4074-84.

Ikemura, T. (1985). Codon usage and tRNA content in unicellular and multicellular organisms. *Mol Biol Evol* **2,** 13-34.

Iost, I. and Dreyfus, M. (1994). mRNAs can be stabilized by DEAD-box proteins. *Nature* **372,** 193-6.

Irias, J. J., Olmsted, M. R. and Utter, M. F. (1969). Pyruvate carboxylase. Reversible inactivation by cold. *Biochemistry* **8,** 5136-48.

Jelinek, R., Terry, T. D., Gesell, J. J., Malik, P., Perham, R. N. and Opella, S. J. (1997). NMR structure of the principal neutralizing determinant of HIV-1 displayed in filamentous bacteriophage coat protein. *J Mol Biol* **266,** 649-55.

Jerne, N. K. (1960). Immunological speculations. *Annu Rev Microbiol* **14,** 341-358.

Jin, L., Fendly, B. M. and Wells, J. A. (1992). High resolution functional analysis of antibody-antigen interactions. *J Mol Biol* **226,** 851-65.

Jitrapakdee, S., Booker, G. W., Cassady, A. I. and Wallace, J. C. (1996). Cloning, sequencing and expression of rat liver pyruvate carboxylase. *Biochem J* **316,** 631-7.

Jitrapakdee, S., Nezic, M. G., Cassady, A. I., Khew-Goodall, Y. and Wallace, J. C. (2002). Molecular cloning and domain structure of chicken pyruvate carboxylase. *Biochem Biophys Res Commun* **295,** 387-93.

Jitrapakdee, S., Petchamphai, N., Sunyakumthorn, P., Wallace, J. C. and Boonsaeng, V. (2001). Structural and promoter regions of the murine pyruvate carboxylase gene. *Biochem Biophys Res Commun* **287,** 411-7.

Jitrapakdee, S., Walker, M. E. and Wallace, J. C. (1999). Functional expression, purification, and characterization of recombinant human pyruvate carboxylase. *Biochem Biophys Res Commun* **266,** 512-7.

Jitrapakdee, S. and Wallace, J. C. (1999). Structure, function and regulation of pyruvate carboxylase. *Biochem J* **340,** 1-16.

Johannssen, W., Attwood, P. V., Wallace, J. C. and Keech, D. B. (1983). Localisation of the active site of pyruvate carboxylase by electron microscopic examination of avidin-enzyme complexes. *Eur J Biochem* **133,** 201-6.

Johne, B. (1996). Epitope mapping by surface plasmon resonance in the BIAcore. In *Methods in Molecular Biology : Epitope Mapping Protocols*, vol. 66 (ed. G. E. Morris), pp. 67-76. Humana Press, Totowa, New Jersy.

Johne, B., Gadnell, M. and Hansen, K. (1993). Epitope mapping and binding kinetics of monoclonal antibodies studied by real time biospecific interaction analysis using surface plasmon resonance. *J Immunol Methods* **160,** 191-8.

Johnson, V. G., Schlom, J., Paterson, A. J., Bennett, J., Magnani, J. L. and Colcher, D. (1986). Analysis of a human tumor-associated glycoprotein (TAG-72) identified by monoclonal antibody B72.3. *Cancer Res* **46,** 850-7.

Jonson, P. H. and Petersen, S. B. (2001). A critical view on conservative mutations. *Protein Eng* **14,** 397-402.

Jonsson, U., Fagerstam, L., Ivarsson, B., Johnsson, B., Karlsson, R., Lundh, K., Lofas, S., Persson, B., Roos, H., Ronnberg, I. and *et al.* (1991). Real-time biospecific interaction analysis using surface plasmon resonance and a sensor chip technology. *Biotechniques* **11,** 620-7.

Kazemi, M. and Finkelstein, R. A. (1991). Mapping epitopic regions of cholera toxin B-subunit protein. *Mol Immunol* **28,** 865-76.

Kaziro, Y., Hass, L. F., Boyer, P. D. and Ochoa, S. (1962). Mechanism of the propionyl carboxylase reaction II. Isotopic exchange and tracer experiments. *J. Biol. Chem.* **237,** 1460-1468.

Keech, D. B. and Attwood, P. V. (1985). The reaction mechanism. In *Pyruvate carboxylase* (ed. D. B. Keech and J. C. Wallace), pp. 109-140. CRC Press, Boca Raton, Florida.

Keech, D. B. and Utter, M. F. (1963). Pyruvate carboxylase II. Properties. *J. Biol. Chem.* **238,** 2609-2614.

Khew-Goodall, Y. S., Johannssen, W., Attwood, P. V., Wallace, J. C. and Keech, D. B. (1991). Studies on dilution inactivation of sheep liver pyruvate carboxylase. *Arch Biochem Biophys* **284,** 98-105.

Kim, S. W., Quinn-Allen, M. A., Camp, J. T., Macedo-Ribeiro, S., Fuentes-Prior, P., Bode, W. and Kane, W. H. (2000). Identification of functionally important amino acid residues within the C2-domain of human factor V using alanine-scanning mutagenesis. *Biochemistry* **39,** 1951-8.

Kiselar, J. G. and Downard, K. M. (1999). Direct identification of protein epitopes by mass spectrometry without immobilization of antibody and isolation of antibody-peptide complexes. *Anal Chem* **71,** 1792-801.

Kjeldsen, T., Clausen, H., Hirohashi, S., Ogawa, T., Iijima, H. and Hakomori, S. (1988). Preparation and characterization of monoclonal antibodies directed to the tumor-associated O-linked sialosyl-2-6 alpha-N-acetylgalactosaminyl (sialosyl-Tn) epitope. *Cancer Res* **48,** 2214-20.

Knappik, A. and Pluckthun, A. (1995). Engineered turns of a recombinant antibody improve its *in vivo* folding. *Protein Eng* **8,** 81-9.

Knowles, J. R. (1987). Tinkering with enzymes: what are we learning? *Science* **236,** 1252-8.

Knowles, J. R. (1989). The mechanism of biotin-dependent enzymes. *Annu Rev Biochem* **58,** 195-221.

Koffas, M. A., Ramamoorthi, R., Pine, W. A., Sinskey, A. J. and Stephanopoulos, G. (1998). Sequence of the *Corynebacterium glutamicum* pyruvate carboxylase gene. *Appl Microbiol Biotechnol* **50,** 346-52.

Kondo, H., Kazuta, Y., Saito, A. and Fuji, K. (1997). Cloning and nucleotide sequence of *Bacillus stearothermophilus* pyruvate carboxylase. *Gene* **20,** 47-50.

Kooistra, O., Herfurth, L., Luneberg, E., Frosch, M., Peters, T. and Zahringer, U. (2002). Epitope mapping of the O-chain polysaccharide of *Legionella pneumophila* serogroup 1 lipopolysaccharide by saturation-transfer-difference NMR spectroscopy. *Eur J Biochem* **269,** 573-82.

Kunst, F., Ogasawara, N., Moszer, I., Albertini, A. M., Alloni, G., Azevedo, V., Bertero, M. G., Bessieres, P., Bolotin, A., Borchert, S., Borriss, R., Boursier, L., Brans, A., Braun, M., Brignell, S. C., Bron, S., Brouillet, S., Bruschi, C. V.,

Caldwell, B., Capuano, V., Carter, N. M., Choi, S. K., Codani, J. J., Connerton, I. F., Danchin, A. and *et al.* (1997). The complete genome sequence of the gram-positive bacterium *Bacillus subtilis*. *Nature* **390,** 249-56.

Kurland, C. and Gallant, J. (1996). Errors of heterologous protein expression. *Curr Opin Biotechnol* **7,** 489-93.

Kuroki, M. (1996). A simple solid-phase competition assay with labelled antigen. In *Methods in Molecular Biology : Epitope Mapping Protocols*, vol. 66 (ed. G. E. Morris), pp. 47-53. Humana press, Totowa, New Jersey.

Kustanovich, I. and Zvi, A. (1996). Epitope mapping antibody-antigen complexes by Nuclear Magnetic Resonance spectroscopy. In *Methods in Molecular Biology : Epitope Mapping Protocols*, vol. 66 (ed. G. E. Morris), pp. 25-37. Humana Press, Totowa, New Jersey.

Laemmli, U. K. (1970). Cleavage of structural proteins during the assembly of the head of bacteriophage T4. *Nature* **227,** 680-5.

Lamhonwah, A. M., Quan, F. and Gravel, R. A. (1987). Sequence homology around the biotin-binding site of human propionyl-CoA carboxylase and pyruvate carboxylase. *Arch Biochem Biophys* **254,** 631-6.

Lane, D. P. and Stephen, C. W. (1993). Epitope mapping using bacteriophage peptide libraries. *Curr Opin Immunol* **5,** 268-71.

Lee, S. C., Choi, Y. C. and Yu, M. H. (1990). Effect of the N-terminal hydrophobic sequence of hepatitis B virus surface antigen on the folding and assembly of hybrid beta-galactosidase in *Escherichia coli*. *Eur J Biochem* **187,** 417-24.

Lee, S. C. and Olins, P. O. (1992). Effect of overproduction of heat shock chaperones GroESL and DnaK on human procollagenase production in *Escherichia coli*. *J Biol Chem* **267,** 2849-52.

Lee, S. H. and Davis, E. J. (1979). Carboxylation and decarboxylation reactions. Anaplerotic flux and removal of citrate cycle intermediates in skeletal muscle. *J Biol Chem* **254,** 420-30.

Lehn, D. A., Moran, S. M. and Macdonald, M. J. (1995). The sequence of the rat pyruvate carboxylase-encoding cDNA. *Gene* **165,** 331-2.

Leiter, A. B., Weinberg, M., Isohashi, F. and Utter, M. F. (1978). Relationshiop between phosphorylation and activity of pyruvate dehydrogenase in rat liver mitochondria and the absence of such a relationship for pyruvate carboxylase. *J Biol Chem* **253,** 2716-23.

Leon-Del-Rio, A. and Gravel, R. A. (1994). Sequence requirements for the biotinylation of carboxyl-terminal fragments of human propionyl-CoA carboxylase alpha subunit expressed in *Escherichia coli*. *J Biol Chem* **269,** 22964-8.

Levert, K. L., Lloyd, R. B. and Waldrop, G. L. (2000). Do cysteine 230 and lysine 238 of biotin carboxylase play a role in the activation of biotin? *Biochemistry* **11**.

Levy, R., Weiss, R., Chen, G., Iverson, B. L. and Georgiou, G. (2001). Production of correctly folded Fab antibody fragment in the cytoplasm of *Escherichia coli* trxB gor mutants via the coexpression of molecular chaperones. *Protein Expr Purif* **23,** 338-47.

Li, R. and Woodward, C. (1999). The hydrogen exchange core and protein folding. *Protein Sci* **8,** 1571-90.

Li, S. J. and Cronan, J. E., Jr. (1992). The gene encoding the biotin carboxylase subunit of *Escherichia coli* acetyl-CoA carboxylase. *J Biol Chem* **267,** 855-63.

Libor, S. M., Sundaram, T. K. and Scrutton, M. C. (1978). Pyruvate carboxylase from a thermophilic *Bacillus*. Studies on the specificity of activation by acyl derivatives of coenzyme A and on the properties of catalysis in the absence of activator. *Biochem J* **169,** 543-58.

Liedberg, B., Nylander, C. and Lundstrom, I. (1983). Surface plasmon resonance for gas detection and biosensoring. *Sensors Actuators* **4,** 299.

Lilie, H., Schwarz, E. and Rudolph, R. (1998). Advances in refolding of proteins produced in *E. coli*. *Curr Opin Biotechnol* **9,** 497-501.

Lim, F., Morris, C. P., Occhiodoro, F. and Wallace, J. C. (1988). Sequence and domain structure of yeast pyruvate carboxylase. *J Biol Chem* **263,** 11493-7.

Lim, F., Rohde, M., Morris, C. P. and Wallace, J. C. (1987). Pyruvate carboxylase in the yeast pyc mutant. *Arch Biochem Biophys* **258,** 259-64.

Lofas, S. and Johnsson, B. (1990). A novel hydrogel matrix on gold surfaces in surface plasmon resonance sensors for fast and efficient covalent immobilization of ligands. *J. Chem. Soc. Chem. Commun*, 1526.

Logan, A. J., Williamson, E. D., Titball, R. W., Percival, D. A., Shuttleworth, A. D., Conlan, J. W. and Kelly, D. C. (1991). Epitope mapping of the alpha-toxin of *Clostridium perfringens*. *Infect Immun* **59,** 4338-42.

Lorenzo, F., Jaulin, C., Vita, N., Froussard, P., Ferrara, P., Jankovic, D. L. and Theze, J. (1991). Structure-function study of the p55 subunit of murine IL-2 receptor by epitope mapping. *J Immunol* **147,** 2970-7.

Lu, D., Kussie, P., Pytowski, B., Persaud, K., Bohlen, P., Witte, L. and Zhu, Z. (2000). Identification of the residues in the extracellular region of KDR important for interaction with vascular endothelial growth factor and neutralizing anti-KDR antibodies. *J Biol Chem* **275,** 14321-30.

Lutomski, D., Joubert-Caron, R., Bourin, P., Bladier, D., and Caron, M. (1995). Use of thiophilic adsorption in the purification of biotinylated Fab fragments. *J Chromatogr B Biomed Appl* **664,** 79-82.

Luzzago, A., Felici, F., Tramontano, A., Pessi, A. and Cortese, R. (1993). Mimicking of discontinuous epitopes by phage-displayed peptides, I. Epitope mapping of human H ferritin using a phage library of constrained peptides. *Gene* **128,** 51-7.

Lynen, F. (1975). Structures of biotin enzymes in *Lipmann Symposium.* In *Energy, regulation & biosynthesis in Molecular Biology* (ed. D. Richter), pp. 671-698, W. de Gruyter, Berlin.

Maaheimo, H., Kosma, P., Brade, L., Brade, H. and Peters, T. (2000). Mapping the binding of synthetic disaccharides representing epitopes of chlamydial lipopolysaccharide to antibodies with NMR. *Biochemistry* **39,** 12778-88.

Macdonald, M. J. and Chang, C. M. (1985). Do pancreatic islets contain significant amounts of phosphoenolpyruvate carboxykinase or ferroactivator activity? *Diabetes* **34,** 246-50.

Macdonald, M. J., Kaysen, J. H., Moran, S. M. and Pomije, C. E. (1991). Pyruvate dehydrogenase and pyruvate carboxylase. Sites of pretranslational regulation by glucose of glucose-induced insulin release in pancreatic islets. *J Biol Chem* **266,** 22392-7.

Macdonald, M. J., McKenzie, D. I., Walker, T. M. and Kaysen, J. H. (1992). Lack of glyconeogenesis in pancreatic islets: expression of gluconeogenic enzyme genes in islets. *Horm Metab Res* **24,** 158-60.

Mackall, J. C. and Lane, M. D. (1977). Role of pyruvate carboxylase in fatty acid synthesis: alterations during preadipocyte differentiation. *Biochem Biophys Res Commun* **79,** 720-5.

Mackay, N., Rigat, B., Douglas, C., Chen, H. S. and Robinson, B. H. (1994). cDNA cloning of human kidney pyruvate carboxylase. *Biochem Biophys Res Commun* **202,** 1009-14.

Malmborg, A. C. and Borrebaeck, C. A. (1995). BIAcore as a tool in antibody engineering. *J Immunol Methods* **183,** 7-13.

Malthiery, Y., Henry, M. and Zanelli, E. (1991). Epitope mapping of human thyroglobulin reveals a central immunodominant region. *FEBS Lett* **279,** 190-2.

Martin, F., Toniatti, C., Salvati, A. L., Venturini, S., Ciliberto, G., Cortese, R. and Sollazzo, M. (1994). The affinity-selection of a minibody polypeptide inhibitor of human interleukin-6. *EMBO J* **13,** 5303-9.

Mayer, F., Wallace, J. C. and Keech, D. B. (1980). Further electron microscope studies on pyruvate carboxylase. *Eur J Biochem* **112,** 265-72.

Mayer, M. and Meyer, B. (1999). Characterisation of ligand binding by saturation transfer difference NMR spectroscopy. *Angew. Chem. International Ed.* **38,** 1784-1788.

McAlister, L. E., Evans, E. L. and Smith, T. E. (1981). Properties of a mutant *Escherichia coli* phosphoenolpyruvate carboxylase deficient in coregulation by intermediary metabolites. *J Bacteriol* **146,** 200-8.

McClure, W. R., Lardy, H. A. and Cleland, W. W. (1971). Rat liver pyruvate carboxylase. 3. Isotopic exchange studies of the first partial reaction. *J Biol Chem* **246,** 3584-90.

McNulty, D. E., Claffee, B. A., Huddleston, M. J. and Kane, J. F. (2003). Mistranslational errors associated with the rare arginine codon CGG in *Escherichia coli*. *Protein Expr Purif* **27,** 365-74.

Menendez, J., Delgado, J. and Gancedo, C. (1998). Isolation of the *Pichia pastoris* PYC1 gene encoding pyruvate carboxylase and identification of a suppressor of the pyc phenotype. *Yeast* **14,** 647-54.

Mian, I. S., Bradwell, A. R. and Olson, A. J. (1991). Structure, function and properties of antibody binding sites. *J Mol Biol* **217,** 133-51.

Mielke, C., Tummler, M., Schubeler, D., Von Hoegen, I. and Hauser, H. (2000). Stabilized, long-term expression of heterodimeric proteins from tricistronic mRNA. *Gene* **254,** 1-8.

Mink, M. A., Benichou, S., Madaule, P., Tiollais, P., Prince, A. M. and Inchauspe, G. (1994). Characterization and mapping of a B-cell immunogenic domain in hepatitis C virus E2 glycoprotein using a yeast peptide library. *Virology* **200,** 246-55.

Molina, F., Laune, D., Gougat, C., Pau, B. and Granier, C. (1996). Improved performances of spot multiple peptide synthesis. *Pept Res* **9,** 151-155.

Moller, H., Serttas, N., Paulsen, H., Burchell, J. M. and Taylor-Papadimitriou, J. (2002). NMR-based determination of the binding epitope and conformational analysis of MUC-1 glycopeptides and peptides bound to the breast cancer-selective monoclonal antibody SM3. *Eur J Biochem* **269,** 1444-55.

Moore, J. P., Sattentau, Q. J., Wyatt, R. and Sodroski, J. (1994). Probing the structure of the human immunodeficiency virus surface glycoprotein gp120 with a panel of monoclonal antibodies. *J Virol* **68,** 469-84.

Moradpour, D., Bieck, E., Hugle, T., Wels, W., Wu, J. Z., Hong, Z., Blum, H. E. and Bartenschlager, R. (2002). Functional properties of a monoclonal antibody inhibiting the hepatitis C virus RNA-dependent RNA polymerase. *J Biol Chem* **277,** 593-601.

Morris, G. E. (1996). *Epitope mapping protocols; Method in molecular biology.* Humana press, Totowa, New Jersey.

Morris, T. W. (1994). Lipoate-protein and Biotin-protein Ligase of *Escherichia coli.* Ph.D. Thesis, University of Illinois at Urbana-Champaign, Urbana.

Mueller, G. A., Smith, A. M., Chapman, M. D., Rule, G. S. and Benjamin, D. C. (2001). Hydrogen exchange nuclear magnetic resonance spectroscopy mapping of antibody epitopes on the house dust mite allergen Der p 2. *J Biol Chem* **276,** 9359-65.

Mujacic, M., Cooper, K. W. and Baneyx, F. (1999). Cold-inducible cloning vectors for low-temperature protein expression in *Escherichia coli*: application to the production of a toxic and proteolytically sensitive fusion protein. *Gene* **238,** 325-32.

Mukhopadhyay, B., Stoddard, S. F. and Wolfe, R. S. (1998). Purification, regulation, and molecular and biochemical characterization of pyruvate carboxylase from *Methanobacterium thermoautotrophicum* strain deltaH. *J Biol Chem* **273,** 5155-66.

Mumberg, D., Muller, R. and Funk, M. (1995). Yeast vectors for the controlled expression of heterologous proteins in different genetic backgrounds. *Gene* **156,** 119-22.

Murtif, V. L. and Samols, D. (1987). Mutagenesis affecting the carboxyl terminus of the biotinyl subunit of transcarboxylase. Effects on biotination. *J Biol Chem* **262,** 11813-6.

Nakamura, R. M., Kasahara, Y. and Rechnitz, G. A. (1992). Immunochemical Assays and Biosensor Technology for the 1990s, pp. 44-45. American Society for Microbiology, Washington, DC.

Ngo, T. H., Hoylaerts, M. F., Knockaert, I., Brouwers, E. and Declerck, P. J. (2001). Identification of a target site in plasminogen activator inhibitor-1 that allows neutralization of its inhibitor properties concomitant with an allosteric up-regulation of its antiadhesive properties. *J Biol Chem* **276,** 26243-8.

Nice, E., Layton, J., Fabri, L., Hellman, U., Engstrom, A., Persson, B. and Burgess, A. W. (1993). Mapping of the antibody- and receptor-binding domains of granulocyte colony-stimulating factor using an optical biosensor. Comparison with enzyme-linked immunosorbent assay competition studies. *J Chromatogr* **646,** 159-68.

Novotny, J., Bruccoleri, R. E., Carlson, W. D., Handschumacher, M. and Haber, E. (1987). Antigenicity of myohemerythrin. *Science* **238,** 1584-6.

Novy, R., Drott, D., Yaeger, K. and Mierendorf, R. (2001). Overcomimg the codon bias of *E. coli* for enhanced protein expression. *Innovations Newsletter of Novagen* **12,** 1-4.

O'Brien, R., Chuang, D. T., Taylor, B. L. and Utter, M. F. (1977). Novel enzymic machinery for the metabolism of oxalacetate, phosphoenolpyruvate, and pyruvate in *Pseudomonas citronellolis*. *J Biol Chem* **252,** 1257-63.

Oettinger, T. and Andersen, A. B. (1994). Cloning and B-cell-epitope mapping of MPT64 from *Mycobacterium tuberculosis* H37Rv. *Infect Immun* **62,** 2058-64.

Ohno, H., Sakai, H., Washio, T. and Tomita, M. (2001). Preferential usage of some minor codons in bacteria. *Gene* **276,** 107-15.

Owen, O. E., Patel, M. S., Block, B. S. B., Kreulen, T. H., Reichle, F. A. and Mozzoli, M. A. (1976). In *Gluconeogenesis* (ed. R. W. Hanson and M. A. Mehlman), pp. 533-558. John Wiley & Sons, New York.

Ozimek, P., Van Dijk, R., Latchev, K., Gancedo, C., Wang, D. Y., Van Der Klei, I. J. and Veenhuis, M. (2003). Pyruvate carboxylase is an essential protein in the assembly of yeast peroxisomal oligomeric alcohol oxidase. *Mol Biol Cell* **14,** 786-97.

Pacheco-Alvarez, D., Solorzano-Vargas, R. S. and Del Rio, A. L. (2002). Biotin in metabolism and its relationship to human disease. *Arch Med Res* **33,** 439-47.

Palmieri, L., Vozza, A., Agrimi, G., De Marco, V., Runswick, M. J., Palmieri, F. and Walker, J. E. (1999). Identification of the yeast mitochondrial transporter for oxaloacetate and sulfate. *J Biol Chem* **274,** 22184-90.

Papac, D. I., Hoyes, J. and Tomer, K. B. (1994). Epitope mapping of the gastrin-releasing peptide/anti-bombesin monoclonal antibody complex by proteolysis followed by matrix-assisted laser desorption ionization mass spectrometry. *Protein Sci* **3,** 1485-92.

Papadouli, I., Sakarellos, C. and Tzartos, S. J. (1993). High-resolution epitope mapping and fine antigenic characterization of the main immunogenic region of the acetylcholine receptor. Improving the binding activity of synthetic analogues of the region. *Eur J Biochem* **211,** 227-34.

Pappu, H. R., Pappu, S. S., Manjunath, K. L., Lee, R. F. and Niblett, C. L. (1993). Molecular characterization of a structural epitope that is largely conserved among severe isolates of a plant virus. *Proc Natl Acad Sci U S A* **90,** 3641-4.

Parker, C. E., Papac, D. I., Trojak, S. K. and Tomer, K. B. (1996). Epitope mapping by mass spectrometry: determination of an epitope on HIV-1 IIIB p26 recognized by a monoclonal antibody. *J Immunol* **157,** 198-206.

Parmley, S. F. and Smith, G. P. (1988). Antibody-selectable filamentous fd phage vectors: affinity purification of target genes. *Gene* **73,** 305-18.

Paterson, Y., Englander, S. W. and Roder, H. (1990). An antibody binding site on cytochrome c defined by hydrogen exchange and two-dimensional NMR. *Science* **249,** 755-9.

Perham, R. N. (2000). Swinging arms and swinging domains in multifunctional enzymes: catalytic machines for multistep reactions. *Annu Rev Biochem* **69,** 961-1004.

Perham, R. N., Duckworth, H. W. and Roberts, G. C. (1981). Mobility of polypeptide chain in the pyruvate dehydrogenase complex revealed by proton NMR. *Nature* **292,** 474-7.

Phillips, N. B., Keech, D. B. and Wallace, J. C. (1981). Pyruvate carboxylase: mechanism of the first partial reaction. *Proc. Aust. Biochem. Soc* **14,** 21.

Phillips, N. F., Snoswell, M. A., Chapman-Smith, A., Keech, D. B. and Wallace, J. C. (1992). Isolation of a carboxyphosphate intermediate and the locus of acetyl-CoA action in the pyruvate carboxylase reaction. *Biochemistry* **31,** 9445-50.

Pinilla, C., Appel, J. R. and Houghten, R. A. (1996). Tea bag synthesis of positional scanning synthetic combinatorial libraries and their use for mapping antigenic determinants. In *Methods in Molecular Biology : Epitope Mapping Protocols,* vol. 66 (ed. G.E. Morris), pp.171-9. Humana Press, Totowa, New Jersey.

Polakis, S. E., Guchhait, R. B. and Lane, M. D. (1972). On the possible involvement of a carbonyl phosphate intermediate in the adenosine triphosphate-dependent carboxylation of biotin. *J Biol Chem* **247,** 1335-7.

Polyak, S. W., Chapman-Smith, A., Mulhern, T. D., Cronan, J. E. J. and Wallace, J. C. (2001). Mutational analysis of protein substrate presentation in the post-translational attachment of biotin to biotin domains. *J Biol Chem* **276,** 3037-45.

Radford, S. E., Laue, E. D., Perham, R. N., Martin, S. R. and Appella, E. (1989a). Conformational flexibility and folding of synthetic peptides representing an interdomain segment of polypeptide chain in the pyruvate dehydrogenase multienzyme complex of *Escherichia coli*. *J Biol Chem* **264,** 767-75.

Radford, S. E., Laue, E. D., Perham, R. N., Miles, J. S. and Guest, J. R. (1987). Segmental structure and protein domains in the pyruvate dehydrogenase multienzyme complex of *Escherichia coli*. Genetic reconstruction *in vitro* and 1H-n.m.r. spectroscopy. *Biochem J* **247,** 641-9.

Radford, S. E., Perham, R. N., Ullrich, S. J. and Appella, E. (1989b). Antibodies against an inter-domain segment of polypeptide chain inhibit active-site coupling in the pyruvate dehydrogenase multienzyme complex. *FEBS Lett* **250,** 336-40.

Ramanathan, L., Ingram, R., Sullivan, L., Greenberg, R., Reim, R., Trotta, P. P. and Le, H. V. (1993). Immunochemical mapping of domains in human interleukin 4 recognized by neutralizing monoclonal antibodies. *Biochemistry* **32,** 3549-56.

Rao, L., Jones, D. P., Nguyen, L. H., Mcmahan, S. A. and Burgess, R. R. (1996). Epitope mapping using histidine-tagged protein fragments: application to *Escherichia coli* RNA polymerase sigma 70. *Anal Biochem* **241,** 173-9.

Raychaudhuri, G., McCool, D. and Painter, R. H. (1985). Human IgG1 and its Fc fragment bind with different affinities to the Fc receptors on the human U937, HL-60 and ML-1 cell lines. *Mol Immunol* **22,** 1009-1019.

Reche, P., Li, Y. L., Fuller, C., Eichhorn, K. and Perham, R. N. (1998). Selectivity of post-translational modification in biotinylated proteins: the carboxy carrier protein of the acetyl-CoA carboxylase of *Escherichia coli*. *Biochem J* **329,** 589-96.

Reddy, D. V., Rothemund, S., Shenoy, B. C., Carey, P. R. and Sonnichsen, F. D. (1998). Structural characterization of the entire 1.3S subunit of transcarboxylase from *Propionibacterium shermanii*. *Protein Sci* **7,** 2156-63.

Reed, K. E. and Cronan, J. E., Jr. (1991). *Escherichia coli* exports previously folded and biotinated protein domains. *J Biol Chem* **266,** 11425-8.

Rees, S., Coote, J., Stables, J., Goodson, S., Harris, S. and Lee, M. G. (1996). Bicistronic vector for the creation of stable mammalian cell lines that predisposes all antibiotic-resistant cells to express recombinant protein. *Biotechniques* **20,** 102-4, 106, 108-10.

Ringquist, S., Shinedling, S., Barrick, D., Green, L., Binkley, J., Stormo, G. D. and Gold, L. (1992). Translation initiation in *Escherichia coli*: sequences within the ribosome-binding site. *Mol Microbiol* **6,** 1219-29.

Roberts, E. L., Shu, N., Howard, M. J., Broadhurst, R. W., Chapman-Smith, A., Wallace, J. C., Morris, T., Cronan, J. E., Jr. and Perham, R. N. (1999). Solution structures of apo and holo biotinyl domains from acetyl coenzyme A carboxylase of *Escherichia coli* determined by triple-resonance nuclear magnetic resonance spectroscopy. *Biochemistry* **38,** 5045-53.

Robinson, B. H., Mackay, N., Chun, K. and Ling, M. (1996). Disorders of pyruvate carboxylase and the pyruvate dehydrogenase complex. *J Inherit Metab Dis* **19,** 452-62.

Robinson, B. H., Oei, J., Saudubray, J. M., Marsac, C., Bartlett, K., Quan, F. and Gravel, R. (1987). The French and North American phenotypes of pyruvate carboxylase deficiency, correlation with biotin containing protein by 3H-biotin incorporation, 35S-streptavidin labeling and Northern blotting with a cloned cDNA probe. *Am J Hum Genet* **40,** 50-9.

Robinson, M., Lilley, R., Little, S., Emtage, J. S., Yarranton, G., Stephens, P., Millican, A., Eaton, M. and Humphreys, G. (1984). Codon usage can affect efficiency of translation of genes in *Escherichia coli*. *Nucleic Acids Res* **12,** 6663-71.

Rohde, M., Lim, F. and Wallace, J. C. (1986). Pyruvate carboxylase from *Saccharomyces cerevisiae*. Quaternary structure, effects of allosteric ligands and binding of avidin. *Eur J Biochem* **156,** 15-22.

Rohde, M., Lim, F. and Wallace, J. C. (1991). Electron microscopic localization of pyruvate carboxylase in rat liver and *Saccharomyces cerevisiae* by immunogold procedures. *Arch Biochem Biophys* **290,** 197-201.

Romanos, M. A., Scorer, C. A. and Clare, J. J. (1992). Foreign gene expression in yeast: a review. *Yeast* **8,** 423-88.

Rosenberg, A. H., Goldman, E., Dunn, J. J., Studier, F. W. and Zubay, G. (1993). Effects of consecutive AGG codons on translation in *Escherichia coli*, demonstrated with a versatile codon test system. *J Bacteriol* **175,** 716-22.

Roy, P. and Jones, I. (1996). Assembly of macromolecular complexes in bacterial and baculovirus expression systems. *Curr Opin Struct Biol* **6,** 157-61.

Rylatt, D. B., Keech, D. B. and Wallace, J. C. (1977). Pyruvate carboxylase: isolation of the biotin-containing tryptic peptide and the determination of its primary sequence. *Arch Biochem Biophys* **183,** 113-22.

Saenko, E. L., Shima, M., Rajalakshmi, K. J. and Scandella, D. (1994). A role for the C2 domain of factor VIII in binding to von Willebrand factor. *J Biol Chem* **269,** 11601-5.

Sahu, A., Kay, B. K. and Lambris, J. D. (1996). Inhibition of human complement by a C3-binding peptide isolated from a phage-displayed random peptide library. *J Immunol* **157,** 884-91.

Saier, M. H., Jr. (1995). Differential codon usage: a safeguard against inappropriate expression of specialized genes? *FEBS Lett* **362,** 1-4.

Saint-Remy, J. M. (1997). Epitope mapping: a new method for biological evaluation and immunotoxicology. *Toxicology* **119,** 77-81.

Saito, N. G. and Paterson, Y. (1996). Nuclear Magnetic Resonance Spectroscopy for the Study of B-Cell Epitopes. *Methods* **9,** 516-24.

Sali, A., and Blundell, T.L. (1993). Comparative protein modelling by satisfaction of spatial restraints. *J Mol Biol* **234**, 779-815.

Sali, A., Overington, J. P., Johnson, M. S. and Blundell, T. L. (1990). From comparisons of protein sequences and structures to protein modelling and design. *Trends Biochem Sci* **15,** 235-40.

Samols, D., Thornton, C. G., Murtif, V. L., Kumar, G. K., Haase, F. C. and Wood, H. G. (1988). Evolutionary conservation among biotin enzymes. *J Biol Chem* **263,** 6461-4.

Sauers, C. K., Jencks, W. P. and Groh, S. (1975). The alcohol-bicarbonate-watwr system. Structure-reactivity studies on the equilibria for formation of alkyl monocarbonates and on rates of their decomposition in aqueous alkali. *J. Am. Chem. Soc* **97,** 5546-5553.

Saul, F. A. and Alzari, P. M. (1996). Crystallographic Studies of Antigen-Antibody Interactions. In *Methods in Molecular Biology : Epitope Mapping Protocols*, vol. 66 (ed. G. E. Morris), pp. 11-23. Humana Press, Totowa, New Jersey.

Schagger, H. and Von Jagow, G. (1987). Tricine-sodium dodecyl sulfate-polyacrylamide gel electrophoresis for the separation of proteins in the range from 1 to 100 kDa. *Anal Biochem* **166,** 368-79.

Scherf, T. and Anglister, J. (1993). A T1 rho-filtered two-dimensional transferred NOE spectrum for studying antibody interactions with peptide antigens. *Biophys J* **64,** 754-61.

Scott, J. K. and Craig, L. (1994). Random peptide libraries. *Curr Opin Biotechnol* **5,** 40-8.

Scott, J. K. and Smith, G. P. (1990). Searching for peptide ligands with an epitope library. *Science* **249,** 386-90.

Scrutton, M. C. and Taylor, B. L. (1974). Isolation and characterization of pyruvate carboxylase from *Azotobacter vinelandii* OP. *Arch Biochem Biophys* **164,** 641-54.

Scrutton, M. C. and Utter, M. F. (1965). Pyruvate carboxylase. V. Interaction of the enzyme with adenosine triphosphate. *J Biol Chem* **240,** 3714-23.

Scrutton, M. C. and White, M. D. (1973). Pyruvate carboxylase. Specific inactivation of acetyl coenzyme A-dependent oxaloacetate synthesis during modification of the enzyme by trinitrobenzene sulfonate. *J Biol Chem* **248,** 5541-4.

Scrutton, M. C., Keech, D. B. and Utter, M. F. (1964). Pyruvate carboxylase IV. partial reactions and the locus of activation by acetyl coenzyme A. *J Biol Chem* **240,** 574-581.

Seetharam, R., Heeren, R. A., Wong, E. Y., Braford, S. R., Klein, B. K., Aykent, S., Kotts, C. E., Mathis, K. J., Bishop, B. F., Jennings, M. J. and Et Al. (1988). Mistranslation in IGF-1 during over-expression of the protein in *Escherichia coli* using a synthetic gene containing low frequency codons. *Biochem Biophys Res Commun* **155,** 518-23.

Shank, R. P., Leo, G. C. and Zielke, H. R. (1993). Cerebral metabolic compartmentation as revealed by nuclear magnetic resonance analysis of D-[1-13C]glucose metabolism. *J Neurochem* **61,** 315-23.

Sharp, P. M., Cowe, E., Higgins, D. G., Shields, D. C., Wolfe, K. H. and Wright, F. (1988). Codon usage patterns in *Escherichia coli, Bacillus subtilis,*

Saccharomyces cerevisiae, *Schizosaccharomyces pombe*, *Drosophila melanogaster* and *Homo sapiens*; a review of the considerable within-species diversity. *Nucleic Acids Res* **16,** 8207-11.

Shatzman, A. R. (1995). Expression systems. *Current Opinion in Biotechnology* **6,** 491-493.

Shaw, W. V. (1987). Protein engineering. The design, synthesis and characterization of factitious proteins. *Biochem J* **246,** 1-17.

Shenoy, B. C., Xie, Y., Park, V. L., Kumar, G. K., Beegen, H., Wood, H. G. and Samols, D. (1992). The importance of methionine residues for the catalysis of the biotin enzyme, transcarboxylase. Analysis by site-directed mutagenesis. *J Biol Chem* **267,** 18407-12.

Sheriff, S., Silverton, E. W., Padlan, E. A., Cohen, G. H., Smith-Gill, S. J., Finzel, B. C. and Davies, D. R. (1987). Three-dimensional structure of an antibody-antigen complex. *Proc Natl Acad Sci U S A* **84,** 8075-9.

Simmons, L. C. and Yansura, D. G. (1996). Translational level is a critical factor for the secretion of heterologous proteins in *Escherichia coli*. *Nat Biotechnol* **14,** 629-34.

Smith-Gill, S. J., Wilson, A. C., Potter, M., Prager, E. M., Feldmann, R. J. and Mainhart, C. R. (1982). Mapping the antigenic epitope for a monoclonal antibody against lysozyme. *J Immunol* **128,** 314-22.

Smolke, C. D., Carrier, T. A. and Keasling, J. D. (2000). Coordinated, differential expression of two genes through directed mRNA cleavage and stabilization by secondary structures. *Appl Environ Microbiol* **66,** 5399-405.

Soos, M. A., Field, C. E., Lammers, R., Ullrich, A., Zhang, B., Roth, R. A., Andersen, A. S., Kjeldsen, T. and Siddle, K. (1992). A panel of monoclonal antibodies for the type I insulin-like growth factor receptor. Epitope mapping, effects on ligand binding, and biological activity. *J Biol Chem* **267,** 12955-63.

Spanjaard, R. A., Chen, K., Walker, J. R. and Van Duin, J. (1990). Frameshift suppression at tandem AGA and AGG codons by cloned tRNA genes: assigning a codon to argU tRNA and T4 tRNA(Arg). *Nucleic Acids Res* **18,** 5031-6.

Spence, J. T. and Koudelka, A. P. (1984). Effects of biotin upon the intracellular level of cGMP and the activity of glucokinase in cultured rat hepatocytes. *J Biol Chem* **259,** 6393-6.

Stephen, C. W., Helminen, P. and Lane, D. P. (1995). Characterisation of epitopes on human p53 using phage-displayed peptide libraries: insights into antibody-peptide interactions. *J Mol Biol* **248,** 58-78.

Stucka, R., Dequin, S., Salmon, J. M. and Gancedo, C. (1991). DNA sequences in chromosomes II and VII code for pyruvate carboxylase isoenzymes in *Saccharomyces cerevisiae*: analysis of pyruvate carboxylase-deficient strains. *Mol Gen Genet* **229,** 307-15.

Suckau, D., Kohl, J., Karwath, G., Schneider, K., Casaretto, M., Bitter-Suermann, D. and Przybylski, M. (1990). Molecular epitope identification by limited proteolysis of an immobilized antigen-antibody complex and mass spectrometric peptide mapping. *Proc Natl Acad Sci U S A* **87,** 9848-52.

Sutton, M. R., Fall, R. R., Nervi, A. M., Alberts, A. W., Vagelos, P. R. and Bradshaw, R. A. (1977). Amino acid sequence of *Escherichia coli* biotin carboxyl carrier protein (9100). *J Biol Chem* **252,** 3934-40.

Szewczuk, Z., Konishi, Y. and Goto, Y. (2001). A two-process model describes the hydrogen exchange behavior of cytochrome c in the molten globule state with various extents of acetylation. *Biochemistry* **40,** 9623-30.

Tashiro, M. and Montelione, G. T. (1995). Structures of bacterial immunoglobulin-binding domains and their complexes with immunoglobulins. *Curr Opin Struct Biol* **5,** 471-81.

Taylor, B. L., Frey, W. H., 2nd, Barden, R. E., Scrutton, M. C. and Utter, M. F. (1978). The use of the ultracentrifuge to determine the catalytically competent forms of enzymes with more than one oligomeric structure. Multiple reacting forms of pyruvate carboxylase from chicken and rat liver. *J Biol Chem* **253,** 3062-9.

Thomas, J. G., Ayling, A. and Baneyx, F. (1997). Molecular chaperones, folding catalysts, and the recovery of active recombinant proteins from *E. coli*. To fold or to refold. *Appl Biochem Biotechnol* **66,** 197-238.

Thomas, J. G. and Baneyx, F. (1996). Protein misfolding and inclusion body formation in recombinant *Escherichia coli* cells overexpressing Heat-shock proteins. *J Biol Chem* **271,** 11141-7.

Tipton, P. A. and Cleland, W. W. (1988 a). Carbon-13 and deuterium isotope effects on the catalytic reactions of biotin carboxylase. *Biochemistry* **27,** 4325-31.

Tipton, P. A. and Cleland, W. W. (1988 b). Catalytic mechanism of biotin carboxylase: steady-state kinetic investigations. *Biochemistry* **27,** 4317-25.

Towbin, H., Staehelin, T. and Gordon, J. (1979). Electrophoretic transfer of proteins from polyacrylamide gels to nitrocellulose sheets: procedure and some applications. *Proc Natl Acad Sci U S A* **76,** 4350-4.

Tribbick, G., Triantafyllou, B., Lauricella, R., Rodda, S. J., Mason, T. J. and Geysen, H. M. (1991). Systematic fractionation of serum antibodies using multiple antigen homologous peptides as affinity ligands. *J Immunol Methods* **139,** 155-66.

Trifilieff, E., Dubs, M. C. and Van Regenmortel, M. H. (1991). Antigenic cross-reactivity potential of synthetic peptides immobilized on polyethylene rods. *Mol Immunol* **28,** 889-96.

Tsang, P., Rance, M., Fieser, T. M., Ostresh, J. M., Houghten, R. A., Lerner, R. A. and Wright, P. E. (1992). Conformation and dynamics of an Fab'-bound peptide by isotope-edited NMR spectroscopy. *Biochemistry* **31,** 3862-71.

Tsang, P., Rance, M. and Wright, P. E. (1991). Isotope-edited nuclear magnetic resonance studies of Fab-peptide complexes. *Methods Enzymol* **203,** 241-61.

Tsuji, F. I., Davis, D. L. and Sowinski, R. (1960). Kinetics of the inhibition of Cypridina luciferase by specific antibody. *J. Immunol* **84,** 615.

Tu, Z. and Hagedorn, H. H. (1997). Biochemical, molecular, and phylogenetic analysis of pyruvate carboxylase in the yellow fever mosquito, *Aedes aegypti*. *Insect Biochem Mol Biol* **27,** 133-47.

Ujihara, N., Daw, K., Gianani, R., Boel, E., Yu, L. and Powers, A. C. (1994). Identification of glutamic acid decarboxylase autoantibody heterogeneity and epitope regions in type I diabetes. *Diabetes* **43,** 968-75.

Utter, M.F. and Keech, D.B. (1960) Formation of oxaloacetate from pyruvate and CO_2. *J. Biol. Chem.* **235**, 17-18.

Utter, M. F. and Keech, D. B. (1963). Pyruvate carboxylase Nature of the reaction. *J Biol Chem* **238,** 2603-2608.

Utter, M. F., Keech, D. B. and Scrutton, M. C. (1964). A possible role for acetyl CoA in the control of gluconeogenesis. *Adv Enzyme Regul* **2,** 49-68.

Val, D. L., Chapman-Smith, A., Walker, M. E., Cronan, J. E. J. and Wallace, J. C. (1995). Polymorphism of the yeast pyruvate carboxylase 2 gene and protein: effects on protein biotinylation. *Biochem J* **15,** 817-25.

Van Burik, J. A., Schreckhise, R. W., White, T. C., Bowden, R. A. and Myerson, D. (1998). Comparison of six extraction techniques for isolation of DNA from filamentous fungi. *Med Mycol* **36,** 299-303.

Van Regenmortel, M. H. (1989 a). The concept and operational definition of protein epitopes. *Philos Trans R Soc Lond B Biol Sci* **323,** 451-66.

Van Regenmortel, M. H. (1989 b). Structural and functional approaches to the study of protein antigenicity. *Immunol Today* **10,** 266-72.

Van Vliet, A. H., Jongejan, F., Van Kleef, M. and Van Der Zeijst, B. A. (1994). Molecular cloning, sequence analysis, and expression of the gene encoding the immunodominant 32-kilodalton protein of *Cowdria ruminantium*. *Infect Immun* **62,** 1451-6.

Van Zonneveld, A. J., Van Den Berg, B. M., Van Meijer, M. and Pannekoek, H. (1995). Identification of functional interaction sites on proteins using bacteriophage-displayed random epitope libraries. *Gene* **167,** 49-52.

Vernet, T., Dignard, D. and Thomas, D. Y. (1987). A family of yeast expression vectors containing the phage f1 intergenic region. *Gene* **52,** 225-233.

Waldrop, G. L., Rayment, I. and Holden, H. M. (1994). Three-dimensional structure of the biotin carboxylase subunit of acetyl-CoA carboxylase. *Biochemistry* **33,** 10249-56.

Walker, M. E., Baker, E., Wallace, J. C. and Sutherland, G. R. (1995). Assignment of the human pyruvate carboxylase gene (PC) to 11q13.4 by fluorescence in situ hybridisation. *Cytogenet Cell Genet* **69,** 187-9.

Walker, M. E., Val, D. L., Rohde, M., Devenish, R. J. and Wallace, J. C. (1991). Yeast pyruvate carboxylase: identification of two genes encoding isoenzymes. *Biochem Biophys Res Commun* **176,** 1210-7.

Wallace, J. C. (1985). Distribution and biological functions of pyruvate carboxylase in nature. In *Pyruvate carboxylase* (ed. D. B. Keech and J. C. Wallace). CRC Press, Boca Raton, Florida.

Wallace, J. C. and Easterbrook-Smith, S. B. (1985). The structure of pyruvate carboxylase. In *Pyruvate carboxylase* (ed. D. B. Keech and J. C. Wallace), pp. 66-108. CRC Press, Boca Raton, Florida.

Wallace, J. C., Jitrapakdee, S. And Chapman-Smith A. (1998). Pyruvate carboxylase. *Int J Biochem Cell Biol* **30,** 1-5.

Wallace, P. G., Huang, M. and Linnane, A. W. (1968). The biogenesis of mitochondria. II. The influence of medium composition on the cytology of anaerobically grown *Saccharomyces cerevisiae*. *J Cell Biol* **37,** 207-20.

Wallis, N. G. and Perham, R. N. (1994). Structural dependence of post-translational modification and reductive acetylation of the lipoyl domain of the pyruvate dehydrogenase multienzyme complex. *J Mol Biol* **236,** 209-16.

Wang, L., Black, C. G., Marshall, V. M. and Coppel, R. L. (1999). Structural and antigenic properties of merozoite surface protein 4 of *Plasmodium falciparum*. *Infect Immun* **67,** 2193-200.

Ware, J., Macdonald, M. J., Lo, M., De Graaf, S. and Fulcher, C. A. (1992). Epitope mapping of human factor VIII inhibitor antibodies by site-directed mutagenesis of a factor VIII polypeptide. *Blood Coagul Fibrinolysis* **3,** 703-16.

Wasserman, L., Doctor, B. P., Gentry, M. K. and Taylor, P. (1993). Epitope mapping of form-specific and nonspecific antibodies to acetylcholinesterase. *J Neurochem* **61,** 2124-32.

Weimar, T., Bukowski, R. and Young, N. M. (2000). The conformation of the T-antigen disaccharide bound to Maclura pomifera agglutinin in aqueous solution. *J Biol Chem* **275,** 37006-10.

Wells, J. A. (1996). Binding in the growth hormone receptor complex. *Proc Natl Acad Sci U S A* **93,** 1-6.

Werneburg, B. G. and Ash, D. E. (1997). VO^{2+}(IV) complexes with pyruvate carboxylase: activation of oxaloacetate decarboxylation and EPR properties of enzyme-VO^{2+}complexes. *Biochemistry* **36,** 14392-402.

Wexler, I. D., Du, Y., Lisgaris, M. V., Mandal, S. K., Freytag, S. O., Yang, B. S., Liu, T. C., Kwon, M., Patel, M. S. and Kerr, D. S. (1994). Primary amino acid sequence and structure of human pyruvate carboxylase. *Biochim Biophys Acta* **1227,** 46-52.

Wexler, I. D., Kerr., D. S., Du, Y., Kaung, M. M., Stephenson, W., Lusk, M. M., Wappner, R. S. and Higgins, J. J. (1998). Molecular characterization of pyruvate carboxylase deficiency in two consanguineous families. *Pediatr Res* **43,** 579-84.

Williams, D. C., Jr., Benjamin, D. C., Poljak, R. J. and Rule, G. S. (1996). Global changes in amide hydrogen exchange rates for a protein antigen in complex with three different antibodies. *J Mol Biol* **257,** 866-76.

Willison, J. C. (1988). Pyruvate and acetate metabolism in the photosynthetic bacterium *Rhodobacter capsulatus*. *J. Gen. Microbiol.* **134,** 2429-2439.

Wilson, I. A. and Stanfield, R. L. (1994). Antibody-antigen interactions: new structures and new conformational changes. *Curr Opin Struct Biol* **4,** 857-67.

Wilson, K. P., Shewchuk, L. M., Brennan, R. G., Otsuka, A. J. and Matthews, B. W. (1992). *Escherichia coli* biotin holoenzyme synthetase/bio repressor crystal structure delineates the biotin- and DNA-binding domains. *Proc Natl Acad Sci U S A* **89,** 9257-61.

Winter, G., Griffiths, A. D., Hawkins, R. E. and Hoogenboom, H. R. (1994). Making antibodies by phage display technology. *Annu Rev Immunol.* **12,** 433-55.

Wolf, B. (1995). The metabolic and molecular basis of inherited disease. In *Disorders of biotin metabolism*, pp. 7. McGraw-Hill, New York.

Wood, H. G. and Barden, R. E. (1977). Biotin enzymes. *Annu Rev Biochem* **46,** 385-413.

Wurtele, E. S. and Nikolau, B. J. (1990). Plants contain multiple biotin enzymes: discovery of 3-methylcrotonyl-CoA carboxylase, propionyl-CoA carboxylase and pyruvate carboxylase in the plant kingdom. *Arch Biochem Biophys* **278,** 179-86.

Yanisch-Perron, C., Vieira, J. and Messing, J. (1985). Improved M13 phage cloning vectors and host strains: nucleotide sequences of the M13mp18 and pUC19 vectors. *Gene* **33,** 103-19.

Yao, X., Wei, D., Soden, C., Jr., Summers, M. F. and Beckett, D. (1997). Structure of the carboxy-terminal fragment of the apo-biotin carboxyl carrier subunit of *Escherichia coli* acetyl-CoA carboxylase. *Biochemistry* **36,** 15089-100.

Yi, J. and Skalka, A. M. (2000). Mapping epitopes of monoclonal antibodies against HIV-1 integrase with limited proteolysis and matrix-assisted laser desorption ionization time-of-flight mass spectrometry. *Biopolymers* **55,** 308-18.

Young, N. M. and Oomen, R. P. (1996). Identification of Residues in Antigenic Determinants by Chemical Modification. In *Methods in Molecular Biology: Epitope Mapping Protocols*, vol. 66 (ed. G. E. Morris), pp. 77-83. Humana Press, Totowa, New Jersey.

Zahn, K. (1996). Overexpression of an mRNA dependent on rare codons inhibits protein synthesis and cell growth. *J Bacteriol* **178,** 2926-33.

Zaripov, M. M., Morenkov, O. S., Fodor, N., Braun, A., Schmatchenko, V. V., Fodor, I. and Brown, A. (1999). Distribution of B-cell epitopes on the pseudorabies virus glycoprotein B. *J Gen Virol* **80,** 537-41.

Zhang, J., Xia, W. L., Brew, K. and Ahmad, F. (1993). Adipose pyruvate carboxylase: amino acid sequence and domain structure deduced from cDNA sequencing. *Proc Natl Acad Sci U S A* **1,** 1766-70.

Zhao, Y. and Chalt, B. T. (1994). Protein epitope mapping by mass spectrometry. *Anal Chem* **66,** 3723-6.

APPENDIX I

All the work of producing and characterising of monoclonal antibodies against sheep PC presented in this Appendix was done by Carey (1988).

1.1 The effect of oxaloacetate on the inhibition of sPC activity by mAb6, 12 and 42 is summarised in Table 1.1.1 and Table 1.1.2.

sPC (3.6 mUnits, 23 units/ mg) was incubated with 350 ng, 600 ng and 2.8 µg of antibodies 6, 12 and 42 respectively in the presence of increasing concentrations of oxaloacetate (0, 1, 2, and 10 mM) for 1 hour at 30°C in 0.1 M Tris pH 7.2, 250 µM acetyl-CoA (incubation volume = 75 µl). After incubation the activity of the enzyme was determined by radiochemical assay. The values given are mean sPC activity expressed as mUnits/ml ± the standard deviation about the mean for three replicates. The percentage inhibition by the antibodies at each concentration of oxaloacetate tested (shown in brackets) is derived from the value where no antibody was present for that particular oxaloacetate concentration (ie. Zero inhibition).

Table 1.1.1 The effect of oxaloacetate on the inhibition of sPC activity by mAb6 and 12.

	Oxaloacetate mM			
Antibody	0	1	2	10
0	366 ± 11.5	319 ± 19.5	235 ±6.5	81 ± 3.0
	(0)	(0)	(0)	(0)
6	154 ± 27.5	38 ± 0	27 ± 5.0	12 ± 0.5
	(58)	(88)	(88)	(85)
12	154 ± 19.0	288 ± 1.0	232 ± 5.0	81 ± 9.5
	(58)	(10)	(1)	(0)

Table 1.1.2 The effect of oxaloacetate on the inhibition of sPC activity by mAb42.

	Oxaloacetate mM			
Antibody	0	1	2	10
0	173 ± 1.0	118 ± 3.5	109 ± 3.5	42 ± 4.0
	(0)	(0)	(0)	(0)
42	41 ± 2.5	219 ± 1.0	179 ± 0	64 ± 1.5
	(76)	(86)	(64)	(52)

1.2 The effect of pyruvate on the inhibition of sPC activity by mAb6, 12 and 42 is summarised in Table 1.2.1 and 1.2.2.

sPC (3.6 mUnits, 23 units/ mg) was incubated with 350 ng, 600 ng and 2.8 µg of antibodies 6, 12 and 42 respectively in the presence of increasing concentrations of pyruvate (0, 1, 2, and 10 mM) for 1 hour at 30°C in 0.1 M Tris pH 7.2, 250 µM acetyl-CoA (incubation volume = 75 µl). After incubation, the activity of the enzyme was determined by radiochemical assay. Since pyruvate was present in the samples being assayed, the concentration of pyruvate in the assay mix was adjusted to maintain a concentration of 10 mM during the assays. The values given are mean sPC activity expressed as mUnits/ml ± the standard deviation about the mean for three replicates. The percentage inhibition by the antibodies at each concentration of pyruvate tested (shown in brackets) is derived from the value where no antibody was present for that particular pyruvate concentration (ie. Zero inhibition).

Table 1.2.1 The effect of pyruvate on the inhibition of sPC activity by mAb6 and 12.

	Pyruvate mM			
Antibody	0	1	2	10
0	260 ± 12.5	301 ± 5.0	286 ± 16.5	293 ± 6.0
	(0)	(0)	(0)	(0)
6	88 ± 16.6	113 ± 1.5	97 ± 11.1	80 ± 19.5
	(66)	(64)	(66)	(73)
12	83 ± 6.0	64 ± 2.0	58 ± 10.5	59 ± 12.5
	(68)	(79)	(80)	(80)

Table 1.2.2 The effect of pyruvate on the inhibition of sPC activity by mAb42.

	Pyruvate mM			
Antibody	0	1	2	10
0	140 ± 24.5	154 ± 16.5	160 ± 5.5	150 ± 13.0
	(0)	(0)	(0)	(0)
42	37 ± 2.5	28 ± 3.5	26 ± 0.5	20 ± 0.5
	(74)	(82)	(84)	(87)

1.3 The effects of Mg^{2+} and $MgATP^{2-}$ on the inhibition of sPC activity by mAb6, 12 and 42 are summarised in Table 1.3.1 and 1.3.2.

sPC (1.83 mUnits, 23 units/ mg) was incubated with 350 ng, 600 ng and 2.8 μg of antibodies 6,12 and 42 respectively in the presence of either Mg^{2+} (7 mM) or both Mg^{2+} and ATP (sodium salt) of concentrations 7 mM and 2.5 mM respectively in 0.1 M Tris pH 7.2, 250 μM acetyl-CoA. After a one hour incubation at 30°C the activity of the enzyme was determined by radiochemical assay. Since either Mg^{2+} or $MgATP^{2-}$ was present in the samples being assayed, the concentrations of $MgCl_2$ and ATP (sodium salt) in the assay mix were adjusted to maintain a concentration of 7 mM $MgCl_2$ and 2.5 mM ATP during the assays. The values given are mean sPC activity expressed as mUnits/ml ± the standard deviation about the mean for three replicates. The percentage inhibition by the antibodies at each concentration of Mg^{2+} or $MgATP^{2-}$ tested (shown in brackets) is derived from the value where no antibody was present for that particular Mg^{2+} or $MgATP^{2-}$ concentration (ie. Zero inhibition).

Table 1.3.1 The effect of Mg2+ and $MgATP^{2-}$on the inhibition of sPC activity by mAb6 and 12.

Antibody	0	Mg^{2+}	$MgATP^{2-}$
0	183 ± 1.5	203 ± 12.0	136 ± 7.0
	(0)	(0)	(0)
6	52 ± 6.5	30 ± 3.0	20 ± 4.5
	(72)	(85)	(85)
12	50 ± 5.0	61 ± 1.5	52 ± 1.5
	(73)	(70)	(62)

Table 1.3.2 The effect of Mg2+ and $MgATP^{2-}$on the inhibition of sPC activity by mAb42. The effect of enzyme activity in the presence of Mg^{2+} or $MgATP^{2-}$ and antibody is indicated by asterisk.

Antibody	0	Mg^{2+}	$MgATP^{2-}$
0	117 ± 16.5	115 ± 12.5	99 ± 5.0
	(0)	(0)	(0)
42	33 ± 3.0	30 ± 1.4	109 ± 1.5
	(72)	(74)	(10)*

1.4 Competitive ELISA to determine the position of binding of monoclonal antibodies, anti-biotin and avidin relative to each other on sPC.

Competition ELISA was to determine whether antibodies shared the same area of binding on sPC. The microtiterplates were coated for 1 hour at 37°C with 50 µl of a 10 µg/ml of sPC (in the presence of 500 µM acetyl-CoA). The wells were subsequently blocked with 0.5% w/v gelatin for 1 hour at 37°C. After washing with PBS/0.05% Tween 20, dilutions of the challenge antibodies or tested antibodies being tested (indicated below) were added in 50 µl and incubated for 1 hour at room temperature. After incubation excess antibody was removed by washing with PBS/0.05% Tween 20. The second antibody conjugated to horseradish peroxidase was directed towards mouse and goat when mAbs or anti-biotin antibody respectively was used as test antibody. After incubation, washing and colour development of the reaction were determine at 450 nm.

Table 1.4 Competitive ELISA between mAbs, anti-biotin and avidin with sPC. The values presented in this table are the binding of test antibody to the antigen in the presence of challenging antibody or avidin, as a percentage of the binding of test antibody alone.

Challenge antibody	Goat anti-biotin (1:5000)	mAb6 (20 ng/ml)	mAb12 (20 ng/ml)	mAb42 (100 ng/ml)
None	100	100	100	100
Goat anti-biotin (1:100)	-	92	0*	33*
Avidin (11.8 µg/ml)	0	98	1*	3*
mAb6 (1 µg/ml)	112	-	nd	nd
mAb12 (1 µg/ml)	75*	nd	-	nd
mAb42 (1 µg/ml)	69*	nd	nd	nd

nd = not determined

* = competition with challenge antibody causes a significant change in the binding of test antibody

The following dilutions of serum and concentrations of antibodies and avidin were used:

	Test	Challenge
Goat anti biotin	1:5000	1:100
Avidin	-	11.8 µg/ml
MAb6, 12	20 ng/ml	1 µg/ml
MAb42	100 ng/ml	1 µg/ml

Avidin was used as challenge only.

1.5 The effect of biotin on the inhibition of sPC activity by mAb6, 12 and 42

Monoclonal antibodies (0-2 μg) were incubated in 0.1 M Tris-Cl pH 7.2 and 200 μM acetyl-CoA for 30 minutes at 30°C in the presence and absence of 5 nmoles (77 μM) of biotin for mAb6 and 12 or 25 nmoles (385 μM) of biotin for mAb42 (incubation volume = 65 μl). sPC (1.3 mUnits, 40 units/mg, 0.77nM) was added to the antibodies and incubated for a further 60 minutes at 30°C. After this time the enzyme activity was determined radiochemically. The activity of the enzyme was expressed as a percentage of the activity of sPC incubated without antibody or biotin.

Table 1.5 The effect of biotin on the inhibition of sPC activity by mAb6, 12 and 42.

μg of antibodies	0	0.25 μg	0.5 μg	0.75 μg	1 μg	1.5 μg	2 μg
Ab6-biotin	100	46	25	25	24	24	23
Ab6+biotin	112	50	37	26	25	24	24
Ab12-biotin	87	62	27	25	24	25	25
Ab12+biotin	110	75	54	27	25	25	25
Ab42-biotin	100	-	-	112	100	74	50
Ab42+biotin	105	-	-	110	100	75	48

1.6 Diagram of Binding Loci of Monoclonal Antibodies on SPC (Carey, 1988)

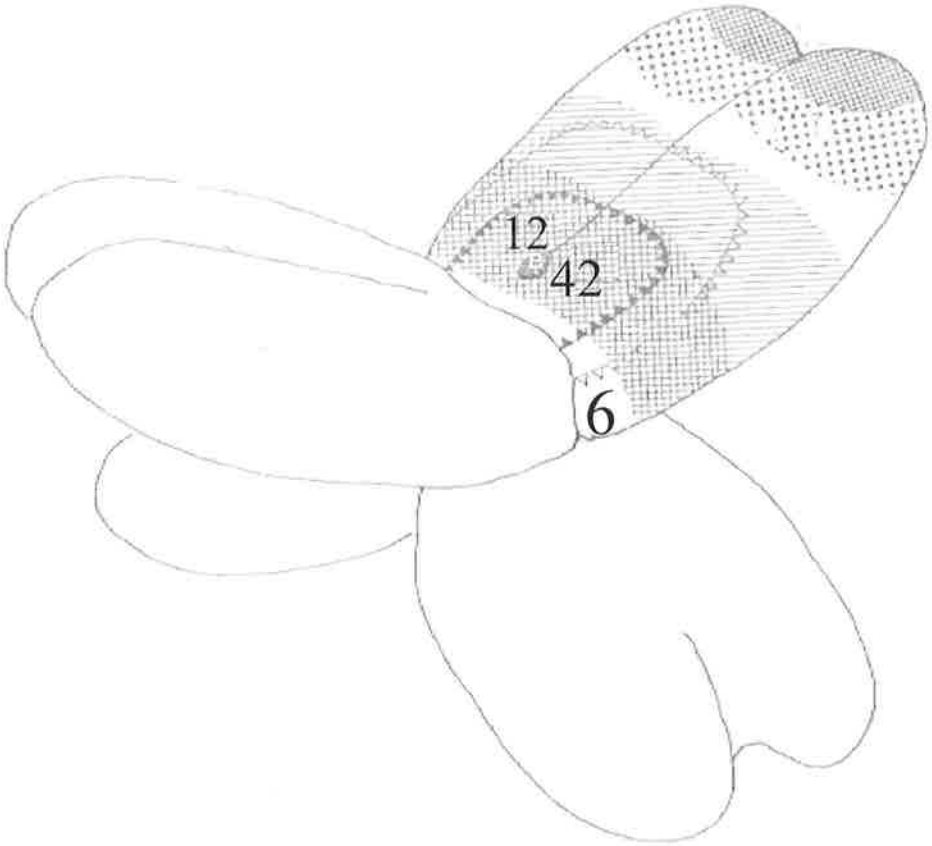

Figure 1.6 This diagram summarised the putative binding loci of the monoclonal antibodies 6, 12 and 42 on one subunit of sPC in relation to the biotin prosthetic group (B) and the regions occupied by anti-biotin IgG (△△△) and avidin (▼ ▼ ▼).

1.7 Localisation of the active site of pyruvate carboxylase by electron microscopic examination of avidin-enzyme complexes by Johannssen et al. (1983)

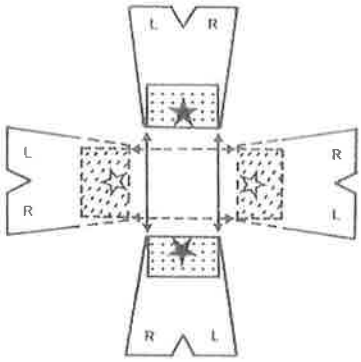

Figure 1.7 Exploded face-view of the enzyme tetramer [Mayer et al., (1980)] with an indication of the bound avidin molecule (shaded) with the sites of the biotin-binding areas indicated (★ on the avidin bound to the upper pair of pyruvate carboxylases subunits, ☆ on the avidin bound to the lower pair of pyruvate carboxylase subunits) [reproduced from Johannssen *et al.* (1983)].

APPENDIX II

Analysis of *E. coli* codon usage in human PC sequence by Morris Mauro using (http://128.111.208.226/codonUsage/usage2.0c.html) showed that 15% of codon usages in human PC sequence are below the threshold 10% of *E. coli* for same amino acids.
Colors: ■ = less than 10% of codons for same amino acid; ■ = at least 10%

Fraction of sense codons below threshold (10) = 185/1178 = 15%

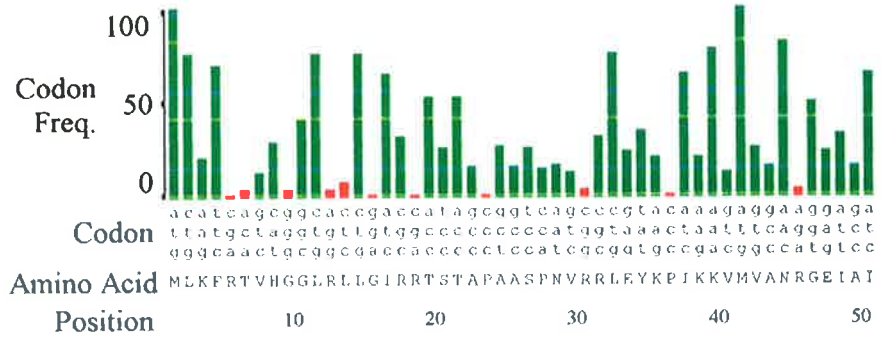

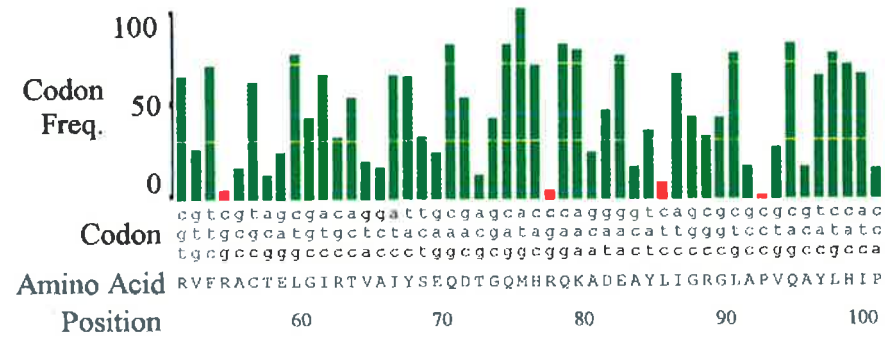

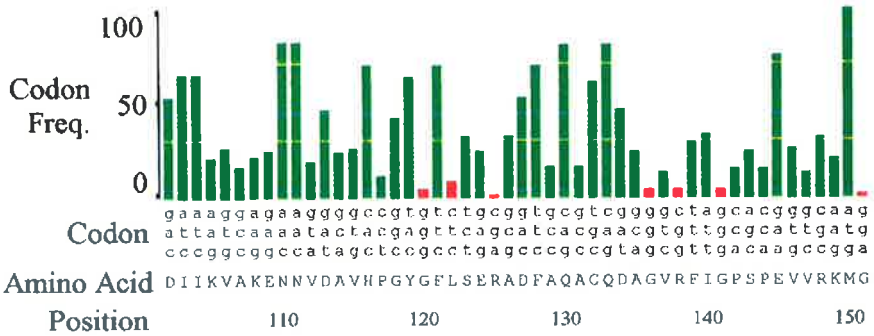

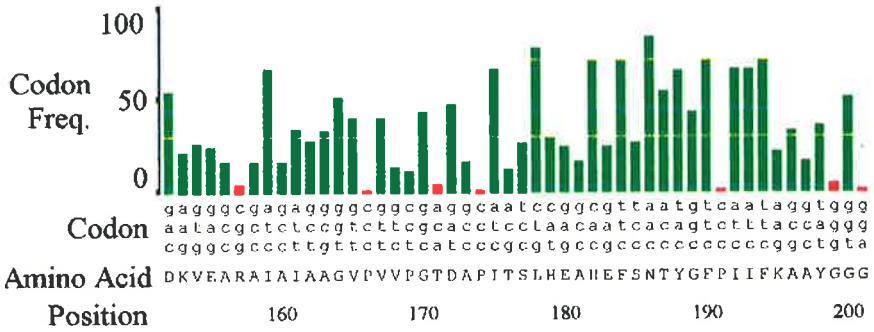

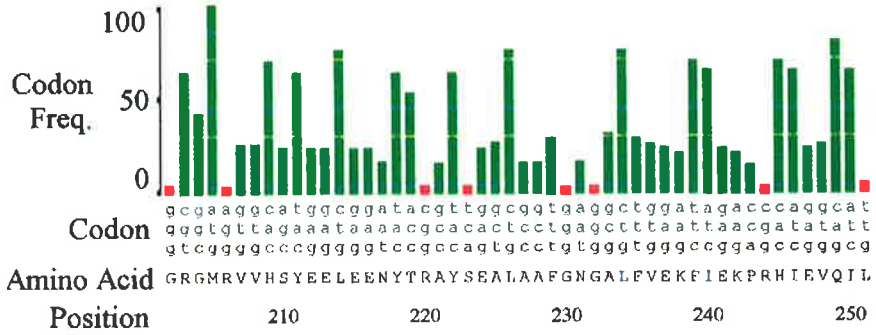
100
Codon
Freq.
50
0
Codon
Amino Acid
Position
210
220
230
240
250

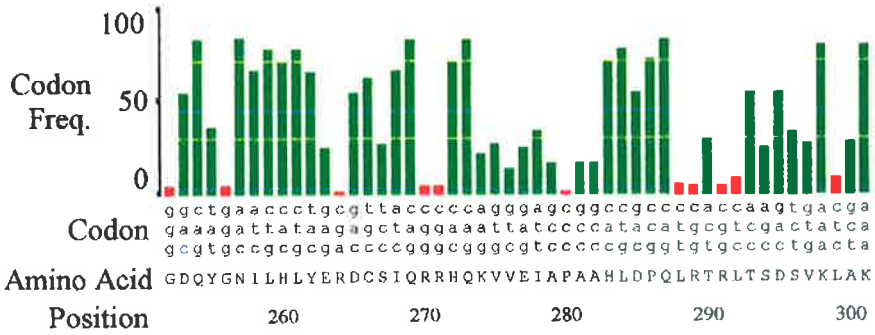
100
Codon
Freq.
50
0
Codon
Amino Acid
Position
260
270
280
290
300

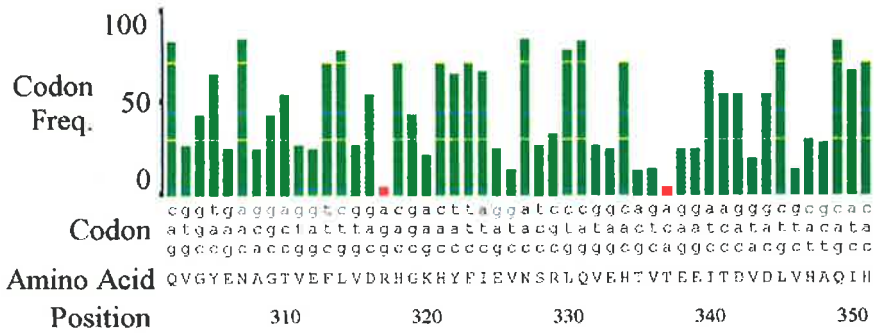
100
Codon
Freq.
50
0
Codon
Amino Acid
Position
310
320
330
340
350

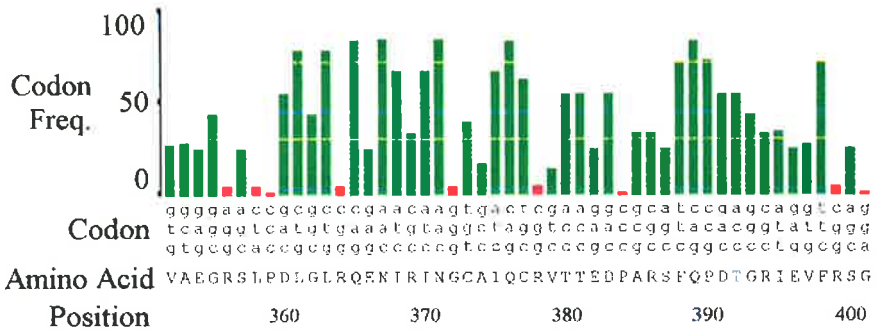
100
Codon
Freq.
50
0
Codon
Amino Acid
Position
360
370
380
390
400

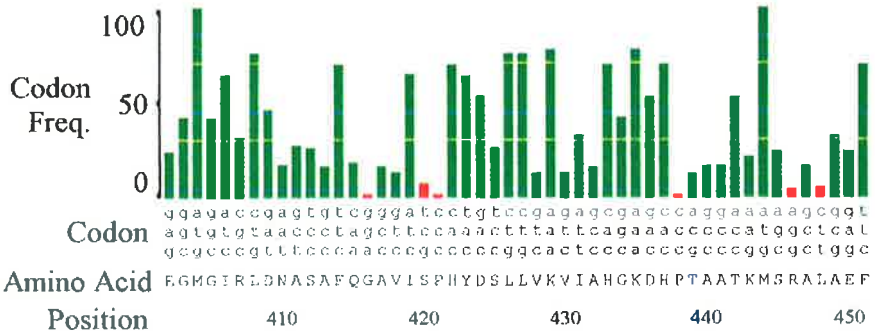
100
Codon
Freq.
50
0
Codon
Amino Acid
Position
410
420
430
440
450

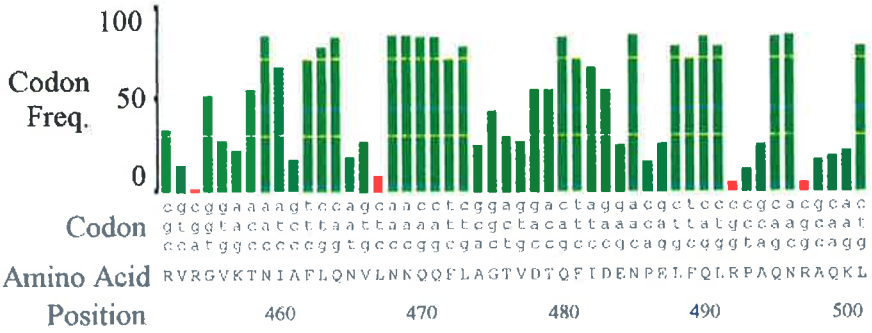
100
Codon Freq.
50
0
Codon
Amino Acid
RVRGVKTNIAFLQNVLNKQQFLAGTVDTQFIDENPELFQLRPAQNRAQKL
Position
460
470
480
490
500

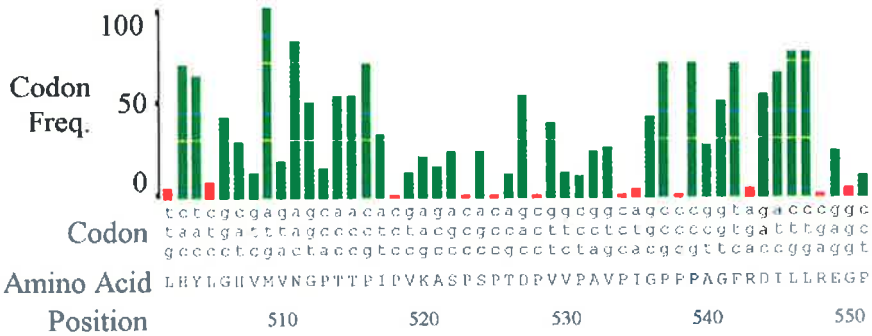
100
Codon Freq.
50
0
Codon
Amino Acid
LHYLGHVMVNGPTTPIPVKASPSPTDPVVPAVPIGPPPAGFRDILLREGP
Position
510
520
530
540
550

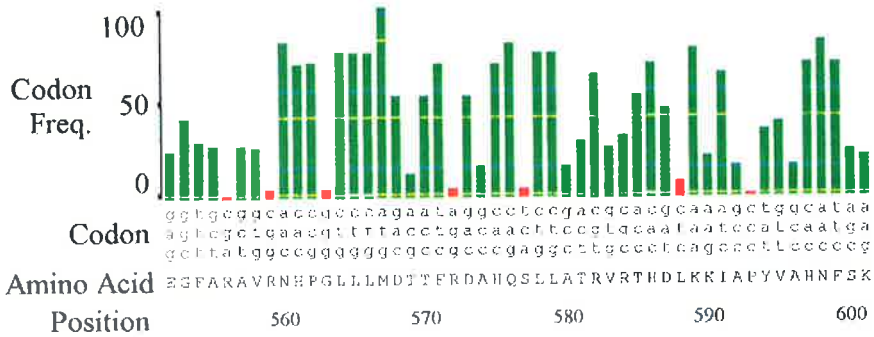
100
Codon Freq.
50
0
Codon
Amino Acid
EGFARAVRNHPGLLLMDTTFRDAHQSLLATRVRTHDLKKIAPYVAHNFSK
Position
560
570
580
590
600

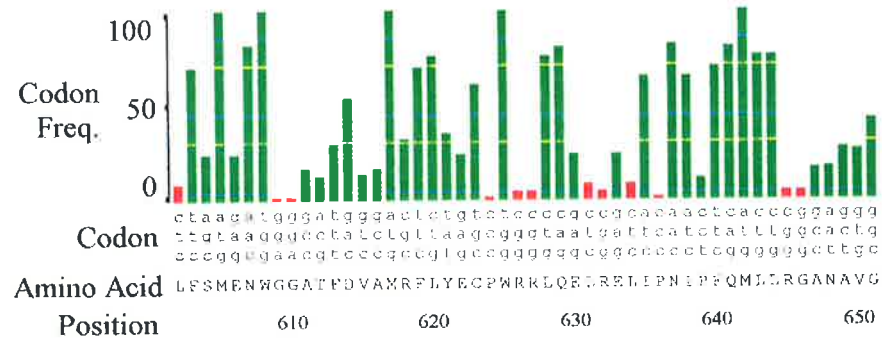
100
Codon Freq.
50
0
Codon
Amino Acid
LFSMENWGGATFDVAMRFLYECPWRRLQELRELIPNIPFQMLLRGANAVG
Position
610
620
630
640
650

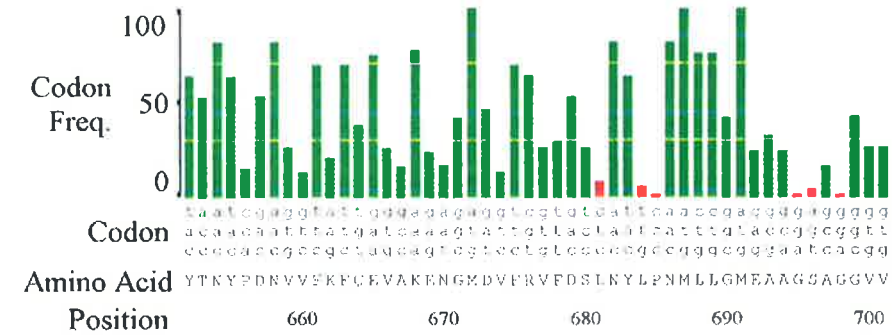
100
Codon Freq.
50
0
Codon
Amino Acid
YTKYPDNVVSKFCEVAKENGMDVFRVFDSLNYLPNMLLGMEAAGSAGGVV
Position
660
670
680
690
700

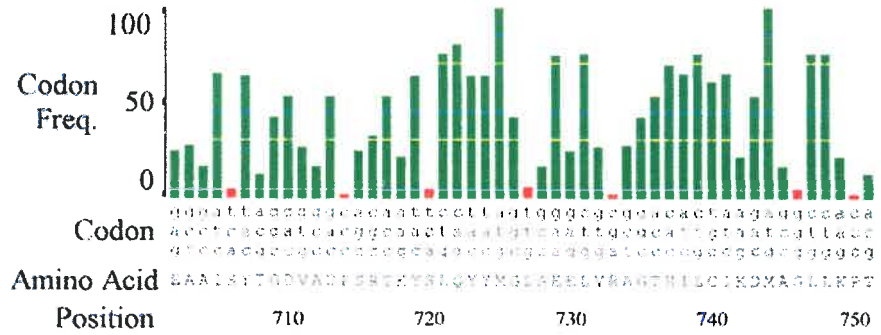
100
Codon
Freq.
50
0
Codon
Amino Acid
Position
710
720
730
740
750

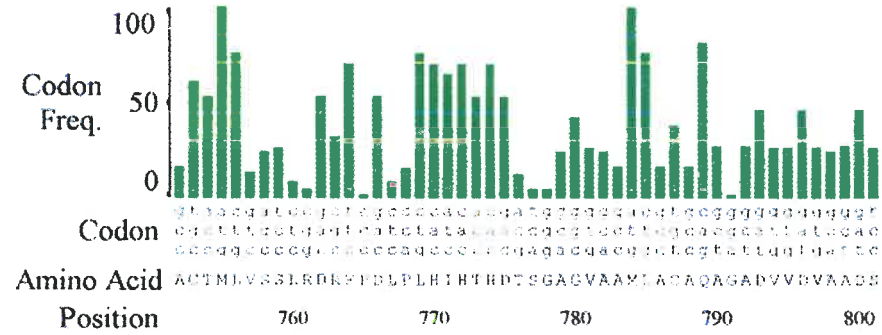
100
Codon
Freq.
50
0
Codon
Amino Acid
Position
760
770
780
790
800

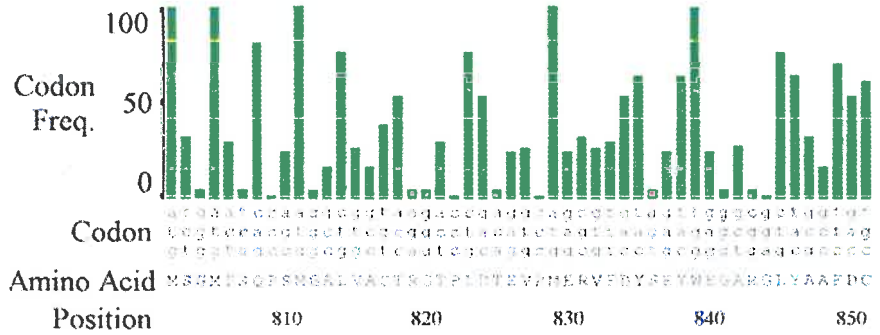
100
Codon
Freq.
50
0
Codon
Amino Acid
Position
810
820
830
840
850

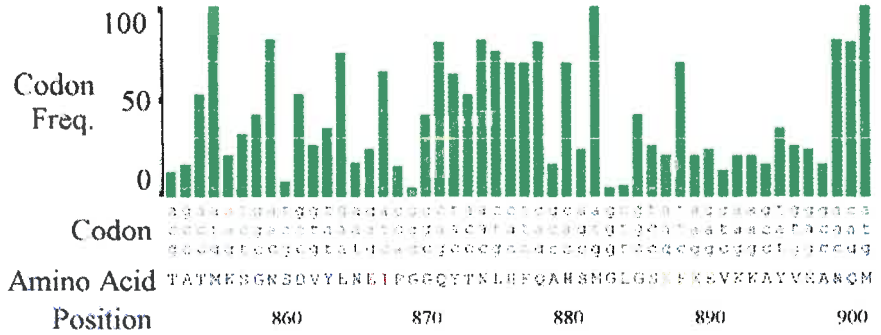
100
Codon
Freq.
50
0
Codon
Amino Acid
Position
860
870
880
890
900

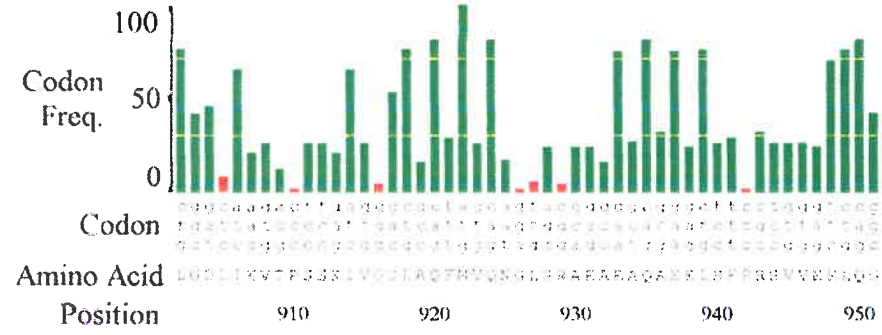
100
Codon
Freq.
50
0
Codon
Amino Acid
Position
910
920
930
940
950

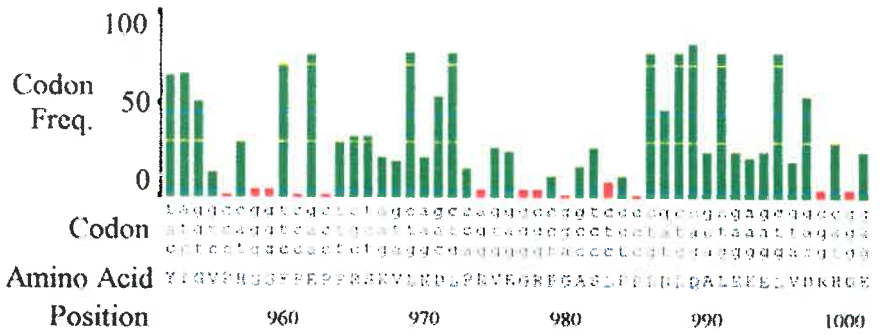
100
Codon
Freq.
50
0
Codon
Amino Acid
Position
960
970
980
990
1000

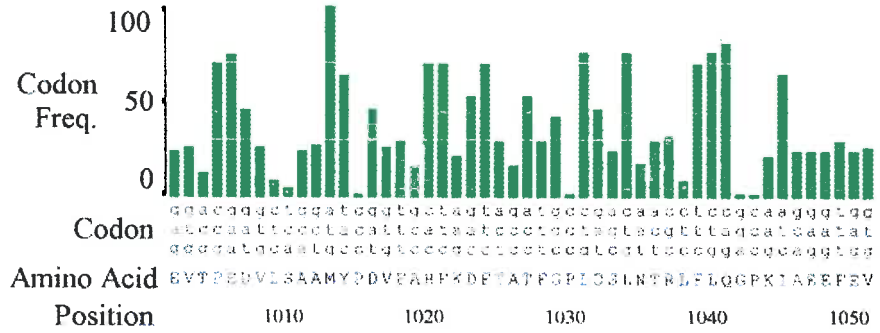
100
Codon
Freq.
50
0
Codon
Amino Acid
Position
1010
1020
1030
1040
1050

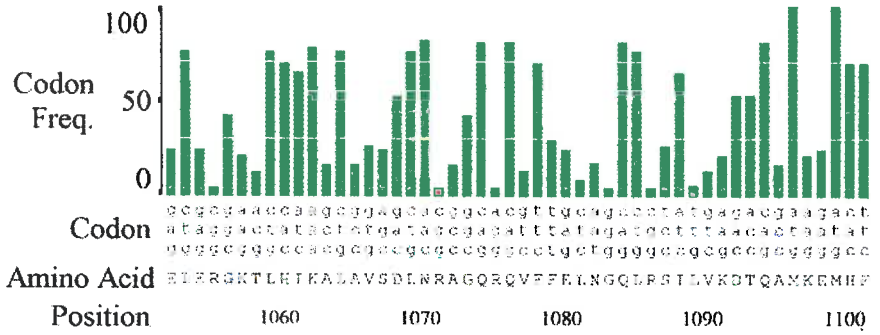
100
Codon
Freq.
50
0
Codon
Amino Acid
Position
1060
1070
1080
1090
1100

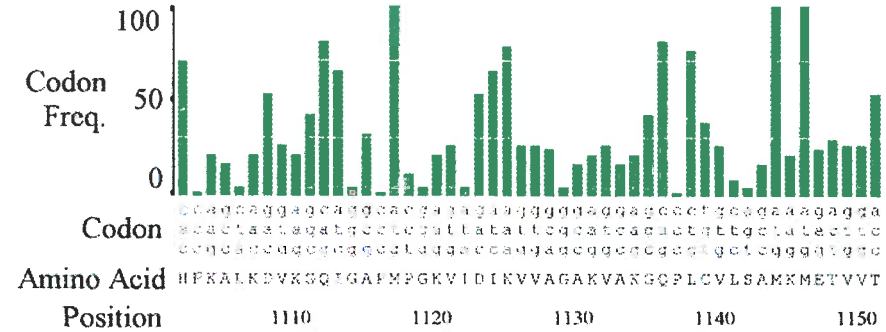
100
Codon
Freq.
50
0
Codon
Amino Acid
Position
1110
1120
1130
1140
1150

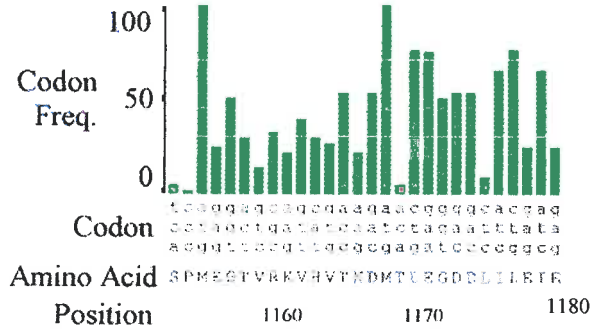
100
Codon
Freq.
50
0
Codon
Amino Acid
Position
1160
1170
1180

```
2341 gcagccatgctggcctgtgcccaggctggagctgatgtggtggat
      A  A  M  L  A  C  A  Q  A  G  A  D  V  V  D   795
2386 gtggcagctgattccatgtctgggatgacttcacagcccagcatg
      V  A  A  D  S  M  S  G  M  T  S  Q  P  S  M   810
2431 ggggccctggtggcctgtaccagagggactcccctggacacagag
      G  A  L  V  A  C  T  R  G  T  P  L  D  T  E   825
2476 gtgcccatggagcgcgtgtttgactacagtgagtactgggagggg
      V  P  M  E  R  V  F  D  Y  S  E  Y  W  E  G   840
2521 gctcgggggactgtacgcggccttcgactgcacggccaccatgaag
      A  R  G  L  Y  A  A  F  D  C  T  A  T  M  K   855
2566 tctggcaactcggacgtgtatgaaaatgagatcccaggggccag
      S  G  N  S  D  V  Y  E  N  E  I  P  G  G  Q   870
2611 tacaccaacctgcacttccaggcccacagcatggggcttggctcc
      Y  T  N  L  H  F  Q  A  H  S  M  G  L  G  S   885
2656 aagttcaaggaggtcaagaaggcctatgtggaggccaaccagatg
      K  F  K  E  V  K  K  A  Y  V  E  A  N  Q  M   900
2701 ctggcgatctcatcaaggtgacgccctcctccaagatcgtgggg
      L  G  D  L  I  K  V  T  P  S  S  K  I  V  G   915
2746 gacctggcccagtttatggtgcagaatggattgagcgggcagag
      D  L  A  Q  F  M  V  Q  N  G  L  S  R  A  E   930
2791 gccgaagctcaggcggaagagctgtcctttcccgctccgtggtg
      A  E  A  Q  A  E  E  L  S  F  P  R  S  V  V   945
2836 gagttcctgcagggctacatcggtgtcccccatgggggttcccc
      E  F  L  Q  G  Y  I  G  V  P  H  G  G  F  P   960
2881 gaacccttt cgctctaaggtactgaaggacctgccaagggtggag
      E  P  F  R  S  K  V  L  K  D  L  P  R  V  E   975
2926 gggcggcctggagcctccctcctcccctggatctgcaggcactg
      G  R  P  G  A  S  L  P  P  L  D  L  Q  A  L   990
2971 gagaaggagctggtagaccggcatggggaggaggtgacgccggaa
      E  K  E  L  V  D  R  H  G  E  E  V  T  P  E  1005
3016 gatgtgctctcagcagctatgtaccccgatgtgtttgcccacttc
      D  V  L  S  A  A  M  Y  P  D  V  F  A  H  F  1020
3061 aaggacttcactgccacctttggccccctggatagcctgaatact
      K  D  F  T  A  T  F  G  P  L  D  S  L  N  T  1035
3106 cgcctcttcctgcagggacccaagatcgcagaggagtttgaggtg
      R  L  F  L  Q  G  P  K  I  A  E  E  F  E  V  1050
3151 gagctggagcgggcaagacgctgcacatcaaagcctggccgtg
      E  L  E  R  G  K  T  L  H  I  K  A  L  A  V  1065
3196 agcgacctgaacggccggccagaggcaggtcttctttgagctc
      S  D  L  N  R  A  G  Q  R  Q  V  F  F  E  L  1080
3241 aatgggcagctgcggtccatcttggtcaaggacacccaggccatg
      N  G  Q  L  R  S  I  L  V  K  D  T  Q  A  M  1095
3286 aaggagatgcacttccaccccaaggccctaaaggacgtgaagggc
      K  E  M  H  F  H  P  K  A  L  K  D  V  K  G  1110
3331 cagatcggggcgcccatgcctgggaaggtgatagacatcaaagtg
      Q  I  G  A  P  M  P  G  K  V  I  D  I  K  V  1125
3376 gtggcaggggccaaggtggccaagggccagcccctgtgtgctc
      V  A  G  A  K  V  A  K  G  Q  P  L  C  V  L  1140
3421 agtgccatgaagatggagactgtggtgacctcacccatggagggt
      S  A  M  K  M  E  T  V  V  T  S  P  M  E  G  1155
3466 actgtccgcaaggttcatgtgaccaaggacatgacactggaaggt
      T  V  R  K  V  H  V  T  K  D  M  T  L  E  G  1170
3511 gacgacctcatcctggagatcgagtga
      D  D  L  I  L  E  I  E  *                    1178
```